ENGINEERING AN IMPROVED DENDRITIC CELL VACCINE EXPRESSING WHOLE ANTIGEN FOLLOWING NON-VIRAL TRANSFECTION

BY ANKIT ROHIT RAO

A thesis submitted to the University of Birmingham for the degree of DOCTOR OF PHILOSOPHY.

Institute for Cancer Studies

School of Cancer Sciences

University of Birmingham

September 2011

UNIVERSITY OF BIRMINGHAM

University of Birmingham Research Archive

e-theses repository

Abstract

Dendritic cells are efficient antigen-presenting-cells that can be used in tumour-antigen specific vaccination for malignant disease. Melanoma patients were recently treated with a dendritic cell vaccine expressing gp100 and Melan-A antigens after non-viral (CL22 peptide) transfection. Although clinical and immunological responses were noted, there was no correlation between responses and whole antigen expression levels in the vaccine cells that varied widely. Here, it is established that patient cells expressed detectable levels of Class I restricted epitopes from both antigens, although there was no correlation with whole antigen detection. CL22 transfected dendritic cells could simultaneously present a viral antigen (EBNA1) to CD8 and CD4 T-cells, which had not previously been demonstrated. Using RNA transfection, it was demonstrated that early after transfection cells are whole Melan-A positive yet negative for Class I epitopes and with time Melan-A antigen levels fall whilst Class I epitopes are generated. Loss of whole antigen expression seemed related to lysosomal function and, unlike the viral antigen EBNA1, Class I presentation from Melan-A was lysosome-dependent. For Class II presentation of EBNA1, cellular localisation seems to determine access to the Class II pathway although this depends on the time-scale over which epitope presentation is assessed.

Acknowledgements

Abbreviations

B-cell	B-lymphocyte
CD	cluster of differentiation
CTL	cytotoxic T-lymphocyte
CTLA4	cytotoxic T-lymphocyte antigen 4
DAMP	damage associated molecular pattern
DC	dendritic cells
DNA	deoxyribonucleic acid
ELISA	enzyme linked immunosorbent assay
ELISPOT	enzyme linked immunosport assay
GM-CSF	granulocyte-monocyte colony stimulating factor
HEK293	human embryonic kidney cell-293
HLA	human leucocyte antigen
IDO	indoleamine 2,3 dioxygenase
IFNγ	interferon gamma
IL	interleukin
LAMP1	lysosome associated protein 1
LCL	lymphocytoid cell lines
MHC	major histocompatibility complex
moDC	monocyte-derived dendritic cell
PAMP	pathogen associated molecular pattern
PBMC	peripheral blood mononuclear cells
p-MHC	peptide-MHC complex
PRR	pattern recognition receptor
RNA	ribonucleic acid
SEM	standard error of the mean
T-cell	T-lymphocyte
TCR	T-cell receptor
TGFβ	transforming growth factor beta

TIL   tumour infiltrating lymphocytes

TNFα   tumour necrosis factor alpha

Contents

Listing of figures and tables.

CHAPTER 1: INTRODUCTION

1.1. Antigen processing pathways .

T-lymphocytes recognise antigen differently to B-cells that recognise three-dimensional determinants of intact antigen. T-cells interact with pre-processed, digested forms of antigen (Gell and Benacerraf, 1959). APCs degrade protein antigens into constituent peptides that are presented to T-cells bound to Major Histocompatibility Complex (MHC) molecules at the cell surface (Groothuis and Neefjes, 2005 and Jensen, 2007).

Protein antigens are presented to T-cells expressing αβ T-cell receptor chains, and glycolipid antigen is presented via CD1a molecules expressed on DCs to either gamma-delta or alpha-beta T-cells or NK/T cells (Cohen at al., 2009).

1.2. The MHC Class I pathway.

The MHC Class I pathway is universally active and evolved as a rapid defense again intracellular, particularly, viral infection (Figure 1.1). It allows intracellular antigen, whether cytoplasmic or nuclear, to become visible to
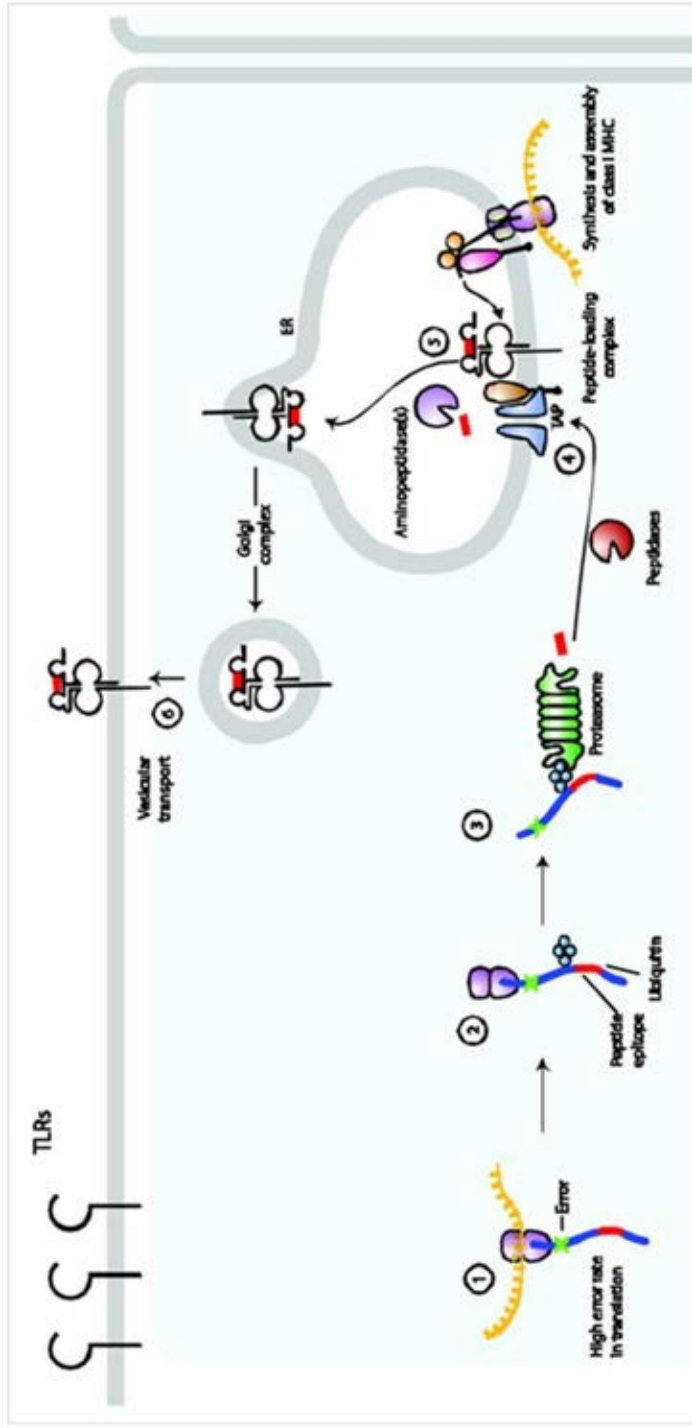
Figure 1.1. **The key steps in presentation of antigen via the MHC Class I pathway.** Error prone translation of mRNA leads to the formation of defective ribosomal products that rapidly becoming polyubiquitinated. These DRiPs are the substrate for proteasomal degradation into smaller polypeptides which compete for access to the endoplasmic reticulum via a large multi-subunit complex including the transporter associated with antigen processing (TAP). Here peptides associate with nascent MHC Class I molecules, although often further trimming of polypeptides by aminopeptidases is required. Binding of peptides to Class I molecules stabilises them and permits their export to the cell surface via vesicular transport. Although not shown here, mature full length proteins can also become polyubiquitinated and be a substrate for the proteasome:- approximately 30% of substrates are of this nature. Reproduced from Jensen (2007).

cytotoxic CD8 positive T-lymphocytes (Elliot and Neefjes, 2006).

Degradation of intracellular proteins for antigen presentation involves several cellular processes. Proteasomal processing is central (Baumeister et al., 1998). The proteasome is a large, multicatalytic, barrel-shaped complex found in nuclear and cytoplasmic compartments. Hydrolysis of polypeptide chains leads to the generation of peptides of 8-20 residues in length: longer than optimal for Class I binding. Processing of proteasomal substrates is non-selective: the majority of substrates are in fact newly synthesised proteins that are defective, misfolded or prematurely truncated (Yewdell et al., 2001) although correctly folded mature and senescent proteins are also degraded. Processing of newly-formed proteins couples viral infection with rapid and early presentation to cytotoxic T-lymphocytes. Aberrant protein manufacture is thought to primarily lead to DRiP (defective-ribosomal-product) formation, although specialised 'immuno-ribosomes' may produce faulty polypeptide chains for antigen presentation (Schwab et al., 2004).

The importance of DRiPs was suggested by the linkage between Class I presentation and protein synthesis and ribosomal function (Khan et al., 2001 and Qian et al., 2006), and by the fact that most newly-formed proteins were rapidly degraded (Schubert et al., 2000). Destabilisation of an influenza antigen by amino terminal modifications did not have any effect on generation of Class I peptides assessed by T-cell stimulation or presence of peptides in APC extracts (Goth, Nyugen and Shastri, 1996), suggesting that peptide supply did not directly relate to the stability of intact protein.

Khan et al (2001) showed that Class I presentation from the LCMV nucleoprotein ceased immediately when protein synthesis was terminated using a tetracycline-dependent promoter. This antigen is highly stable, yet CD8 T-lymphocytes specific for Class I epitopes within it are readily detectable in infected mice and epitope presentation is proteasome dependent (Schwarz et al., 2000 and Schubert et al., 2000).

Ubiquitination is tightly linked with proteasomal function. Ubiquitin is a highly conserved 76 amino acid polypeptide. Ubiquitin ligases covalently attach ubiquitin to the amino

terminus or to the amino group of an internal lysine residue of the protein marked for degradation. Ubiquitin 'tails' permit a stable interaction with the 26S, enzymatically active, subunit of the proteasome (Glickman and Ciechanover, 2002).

Polypeptides leaving the proteasome are further degraded by cytosolic aminopeptidases including tripeptidyl peptidase II (TPPII)(Reits et al., 2004) and others (York et al., 2003). There is a process of 'selection' where there is a limited opportunity for peptides to bind to the MHC Class I molecules – indeed of all proteins entering the proteasome only 0.1 to 1% will lead to the generation of Class I binding peptides. Due to the rapid action and efficiency of cytoplasmic peptidases, nascent peptides have only approximately 8 seconds to interact with the Class I machinery before becoming too small to do so.

During these eight seconds, peptides of approximately 8-16 residues must interact with either TAP or be sheltered from degradation by chaperone proteins. This is because their 'target', MHC Class I molecules, is found in a different compartment – the endoplasmic reticulum (ER) and peptides do not readily cross lipid bilayers. TAP is an ATP dependent

heterodimeric (TAP1 and 2) membrane pump spanning the ER membrane (Lankat-Buttgereit et al., 2002). TAP is selective for 8-12 residues peptides and excludes those with chemical modifications at the amino terminus or those with proline at position 2 or 3 as these have low binding affinities to Class I molecules (Momburg et al., 1994).

TAP is a component of a large multimeric complex in the ER membrane – the MHC Class I loading complex. The additional proteins are Class I molecules, chaperones Erp57 and calnexin and the peptide-editing molecule tapasin (Cresswell et al., 1999). Peptides transported into the ER interact with the heterodimers of beta-2-microglobulin and MHC Class I heavy chain and this releases them from the complex for subsequent transport to the cell surface. TAP substrates are often longer than ideal for Class I binding and the enzyme ERAAP may trim peptides to the optimal size – 8-10 residues (Saric et al., 2002).

The chaperone protein disulfide isomerase aids selection of high binding affinity peptides (Park et al., 2006).

TAP functions in a reasonably sequence independent fashion in order to supply peptides for binding to HLA molecules that are extremely polymorphic (Groothuis and Neefjes, 2005).

This process is inefficient and most proteins and peptides are immunologically irrelevant – 2×10^6 proteins are degraded yet only 2×10^4 Class I molecules are loaded with peptide (Yewdell et al., 2003). There is significant reserve within the system allowing responses to stress or viral infection. Rapid degradation of polypeptides means that only peptides binding with very high affinity to MHC Class I heavy chains are 'selected' – maintaining high levels of peptide-MHC complexes for several days on the surface of APCs to allow expansion of T-cell populations (Elliot and Neefjes, 2006).

1.3. MHC Class I pathway in dendritic cells.

Upon antigenic stimulation, IFNγ is produced and this causes upregulation of all components of the MHC Class I loading complex. It also has effects on the proteasome. In professional antigen presenting cells and when innate cytokines are being produced, there is substitution of the

three proteolytic subunits in each inner ring of the proteasome by alternative subunits known as LMP2 (for β1), LMP7 (for β5) and Mecl-1 (for β2) (Beninga and Goldberg, 1998). These are IFNγ inducible and when these are incorporated into proteasomes, they are termed 'immunoproteasomes' (Monaco and McDevitt, 1986). These are strongly enriched in activated dendritic cells and constitutively expressed in B-lymphocytes. LMP2 and 7 are encoded within the MHC super-complex (Goldberg and Rock, 1992) whereas Mecl-1 is not (Cruz et al., 1997).

These subunits have a specialised role in antigen presentation as LMP7 deficient mice had a marked reduction in surface MHC Class I density and were unable to present the minor histocompatibility antigen H-Y (Fehling et al., 1994).

However, epitopes more efficiently generated by immunoproteasomes are mainly viral, rather than tumour, derived. In fact, there is evidence that immunoproteasomes destroy epitopes from several melanoma associated antigens including gp100, tyrosinase and Melan-A and are less efficient than standard proteasomes at generating these epitopes (Van den Eynde, 2001).

The presence of Mecl-1, LMP2 and 7 favours cleavage after basic and hydrophobic amino acids rather than acidic ones (Gaczynska et al., 1993). However, production of peptides with basic and hydrophobic C-termini optimises binding stability with Class I molecules (Akiyama et al., 1994).

MoDC constitutively express all three inducible subunits, although prior to exposure to an activation stimulus roughly equal amounts of 'standard' and 'immuno' proteasomes were present, whereas after activation only immunoproteasomes were detected (Macagno et al., 1999).

The other unique features of Class I processing in DC is the existence of dendritic cell aggresome like induced structures (DALIS). It was first demonstrated (Lelouard et al., 2002) that in mouse Langerhans cells and CD34 derived human DCs that exposure to LPS causes an accumulation of peripheral 'aggregates' of ubiquitinated proteins. DALIS appear within 4 hours of LPS exposure and staining is maximal around 8 hours. By 36 hours of 'maturation', most aggregates have dispersed. Forced translational errors increased the number and size of DALIS, linking them tightly to translation and protein synthesis.

These structures may act as antigen depots, and by delaying the presentation of Class I restricted epitopes by 24-36 hours they allow coordination of the arrival of the DC in draining lymph nodes with the presentation of immunogenic epitopes. It would be wasteful for epitope display to begin immediately as time is required for the cells to migrate via lymphatics to secondary lymphoid tissue (Lelouard et al., 2004). This cellular 'sink' for ubiquitinated proteins in DCs may make room within the Class I loading compartments for peptides derived from the endocytic pathway destined for 'cross-presentation'.

Finally, in DC the Class I and II pathway are not mutually exclusive and cross-presentation can occur. This process is vital in the initiation of immune responses as most directly infected cells are poorly immunogenic and lack the necessary costimulation to drive the expansion of naive T-cells.

1.4. The MHC Class II pathway.

The Class II pathway is only constitutively active in B-lymphocytes, macrophages and DC. In the presence of IFNγ,

endothelial, epithelial and tumour cells can express Class II molecules (Watts, 2004).

It protects against extracellular pathogens unlike the Class I pathway. The extracellular environment is sampled by APCs and epitopes derived from internalised proteins are presented to CD4 positive (helper) T-cells (Vyas, Van den Veen and Ploegh, 2008). This is illustrated in Figure 1.2.

Extracellular material is taken up by macropinocytosis, receptor mediated endocytosis and enters the phagosome (Henry et al., 2004). This structure is formed from invagination of the plasma cell membrane and it eventually fuses with endo-lysosomes (Blander and Medzhitov, 2006).

Class II molecules consist of an αβ heterodimer (Janeway et al., 2005). Nascent Class II heterodimers in the ER interact with the chaperone invariant chain. The invariant chain molecule functions to block the peptide binding cleft of Class II molecules and prevents premature binding of peptides in the ER and also targets the molecules to late endosomal compartments (Cresswell, 1996). In late endosomes, cleavage of the cytoplasmic domain of invariant
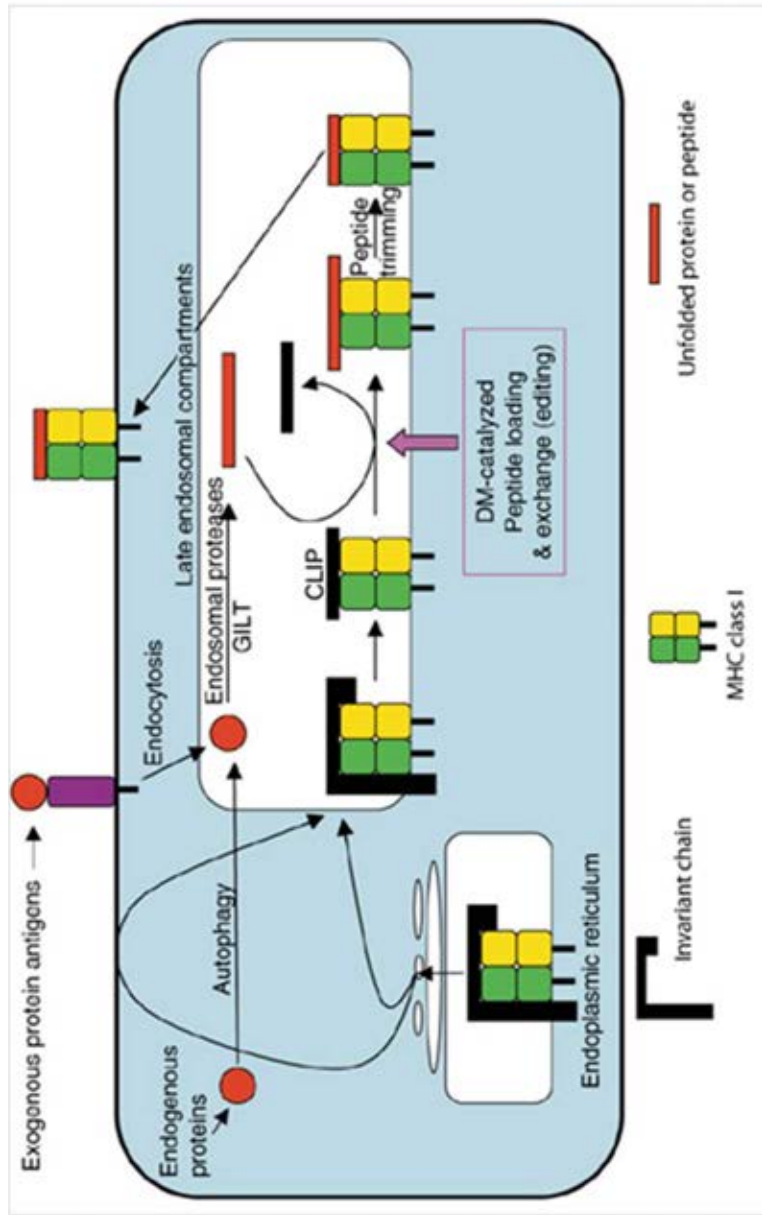
Figure 1.2. **The MHC Class II antigen presentation pathway.** Exogenously acquired protein antigens enter the cell by endocytosis and are digested to smaller polypeptdes by lysosomal hydrolases including Cathepsins. Newly sythesised MHC Class II molecules, bound to the invariant chain molecule, are transported into the MHC Class II loading compartments where they meet lysosome derived polypeptides. Sequential proteolytic cleavages occur, removing the invariant chain and then CLIP under the influence of the peptide-editing molecule HLA-DM which encourages the exchange of CLIP for high binding affinity peptides. There is likely to be further enzymatic 'trimming' of the ends of the peptides bound to MHC Class as it permits extended peptides to bind. Endogenous proteins can enter this pathway either directly (autophagic) or via the cell membrane.

12

chain occurs, leaving only CLIP (Class II invariant-chain associated peptide) in the peptide groove. The intersection between endolysosomes and phagosomes is known as the MHC Class II loading compartment.

The presence of CLIP stably bound to Class II molecules, means that many molecules do not acquire exogenous peptide before transport to the cell surface (Hiltbold and Roche, 2002). This problem is circumvented by the 'peptide-editing' molecule HLA-DM. Interactions between CLIP loaded Class II molecules and HLA-DM facilitate the release and subsequent binding of peptides (Zarutskie et al., 2001). HLA-DM favours removal of CLIP, protects the 'empty' Class II molecule from destruction and selects high binding affinity peptides that form long-lived complexes with MHC-II and are therefore highly immunogenic (Anderson and Gorski, 2003 and Carven and Stern, 2005). Typically Class II molecules bind stably with peptides 13-15 amino acids long. Most evidence suggests that long polypeptide chains bind to Class II molecules, endowing them with some degree of protection from the hostile environment of lysosomes. Further trimming by endo and aminopeptidases reduces the length of the chain to 13-15 residues (Dadaglio et al., 1997).

Peptide-loaded mature Class II molecules then traffic to the cell membrane, possibly through a direct route (Wubbolts et al. 1996) but more likely they are carried to the membrane by specific vesicles derived from early endosomes (Turley et al., 2000).

A negative regulator of the function of HLA-DM exists and in humans is known as HLA-DO (Liljedahl et al., 1996). It is encoded within the MHC super-cluster and like HLA-DM is non-polymorphic. It colocalises with HLA-DM in Class II loading compartments but its role in DC appears unclear. (Fallas et al., 2004).

The supply of peptides for Class II loading is dependent on lysosomal processing. Lysosomal proteases include cysteine, aspartate and serine proteasomes and metalloproteases. Cathepsin D is an aspartic protease and the cysteine proteases are Cathepsins B,F,H,L,S and Z (Riese and Chapman, 2000). Most enzymes have broad substrate specificity and include a mixture of those with endopeptidase and exopeptidase activity (Turk et al., 2001). Cathepsins S and L cleave and release the invariant chain (Shi et al., 1999).

A highly acidic pH in lysosomes compartments is vital for protein digestion. The acidic environment encourages breakage of disulfide bridges and unfolding of proteins, allowing access of proteolytic enzymes (Collins et al., 1991). There may also be active participation in this process by IFNγ inducible lysosomal thiol reductase (Arunachalam et al., 2000).

It is not uncommon for long polypeptide chains to interact with MHC II molecules and be trimmed at either end to the typical 13-15 amino acids length (Castellino et al., 1998).

Although most peptides bound to MHC Class II molecules are derived from exogenous proteins, senescent membrane proteins also contribute to the Class II peptide pool.

It was demonstrated that in human B-lymphoblastoid cell lines, peptides eluted from surface HLA-DR molecules were derived from over 170 core protein sequences and approximately 40% of these proteins were membrane bound, but 25% were intracellular proteins including cytoplasmic and nuclear ones. Macroautophagy was involved in mobilising

intracellular source proteins for MHC Class II presentation (Dorfel et al., 2005).

Autophagy is a bulk, non-selective process involving the degradation of senescent cellular organelles into their constituent amino acids for re-building of new structures (Klionsky and Emr, 2000). The best characterised is macroautophagy, although chaperone-mediated autophagy and microautophagy exist (Strawbridge and Blum, 2007). The rate of macroautophagy is low in resting cells and is upregulated in times of cellular stress and starvation (Crotzer and Blum, 2008). During amino acid deprivation, signalling via PI-3 kinase is decreased and this removes the break on macroautophagy inhibition by the mammalian target of rapamycin (mTOR) and increases autophagy (Klionsky, 2005).

There is now a body of convincing evidence that autophagy can supply substrate proteins into the endolysosomal pathway for subsequent MHC Class II restricted presentation (Crotzer and Blum, 2009) and that proteins from almost all cellular compartments can be processed via this route.

In macroautophagy, parts of the cytoplasm are gathered up within double membrane structures called autophagosomes that can eventually engulf whole organelles. Central to this process are a set of autophagy-related gene products (Atg) that are found in yeast and mammals. (Klionsky, 2005).

Several antigens found in the nucleus or cytoplasm have been shown to be presented via the MHC Class II pathway including neomycin resistance protein (Nimmerjahm et al., 2003), the Epstein Barr Virus Nuclear Antigen-1 (Paludan et al., 2005) and the tumour antigen mucin-1 (Dorfel et al., 2005). In all cases, an extracellular route has been excluded and inhibitors of autophagy such as 3-methyadenine or wortmannin or specific inhibition with Atg12 siRNA have reduced recognition by CD4 T-cells.

Macroautophagy is constitutively active in DC and B-lymphocytes, diverting some intracellular proteins into the Class II pathway (Schmid, Pypaert and Munz, 2007). In human DCs 40% of MHC Class II loading compartments were positive for autophagosome markers after chloroquine exposure to inhibit lysosomal acidification. Additionally, DCs expressing Flu-MP as a fusion protein with LC3 were more

strongly recognised by Flu specific CD4 T-cell clones than those expressing untagged Flu-MP.

These insights into 'novel' sources of Class II ligands are important in terms of DC vaccine design. As discussed in subsequent sections the generation of CD4 and CD8 T-cell responses simultaneously is a desired goal of vaccination and knowledge of how endogenously produced proteins may access the Class II machinery allows rational vaccine design.

1.4.1. The MHC Class II pathway in dendritic cells.

The key specialisation of the Class II pathway is that it is tightly regulated and this regulation is linked with the nature of activating, environmental stimuli received by the DC (Thery and Amigorena, 2001).

Activated DC possess an unusually high density of cell surface MHC Class II molecules. The strength of expression of costimulatory molecules such as CD86 is also exceptionally high.

In DC, newly formed Class II molecules associated with the invariant chain are exported to the cell surface where they are internalised into the lysosomal system for peptide loading.

Also, lateral clustering of peptide-MHC complexes on the surface of DCs leads to high local densities of p-MHC for interactions with cognate T-cells and a high likelihood of formation of a tight immunological synapse (Turley et al., 2000).

Prior to receipt of activating signals, the majority of MHC Class II molecules are found in intracellular vesicles that co-stain with lysosomal markers such as LAMP-1.

On receipt of TLR agonist stimulation or T-cell derived signals (such as CD40 ligation or IFNγ) and to a lesser extent proinflammatory cytokines such as TNFα, there is an initial further burst of macropinocytic activity followed by rapid downregulation. This makes sense, as it forms a positive feedback loop to allow maximal antigen uptake when pathogens are present. Transport of MHC Class II molecules from the Class II loading compartments to the cell surface

occurs and there is dramatic stabilisation of cell surface p-MHC-II complexes for several days. The rate of synthesis of Class II peptide complexes does not increase dramatically, and stabilisation of surface complexes is most important (Cella et al., 1997). DCs can present epitopes from antigens that have been captured up to several days before maturation.

There is also controlled and less complete degradation of antigens with the endocytic compartment in DCs as opposed to other phagocytic cells, preserving more information for antigen presentation. DC activation leads to an activation of lysosomal functions and there is an overall increase in proteolysis. The mechanism of upregulation of lysosomal processing is not straightforward however. There is no increase in expression of any lysosomal protease in the mature state. However, two cathepsins were found in a pro-enzyme (immature) state in immature DCs. The crucial step appears to be endolysosomal acidification with an intralysosomal pH of 5.4 in immature DCs falling to 4.6 after exposure to LPS. Acidification influences all key process of Class II loading including the activity of gamma interferon inducible lysosomal thiol reductase and HLA-DM (Trombetta et al., 2003).

An alternative Class II loading pathway may operate in some DC. DC express significant numbers of empty MHC Class II molecules at the cell surface (Santambrogio et al., 1999). Cell surface HLA-DM is present (Andersson et al., 1998) and immature DCs are able to secrete lysosomal proteases (Amoscato et al., 1998). This raises the possibility of extracellular peptide loading of Class II molecules (Santambrogio et al., 1999).

1.5. Human dendritic cell physiology

Langerhans cells were identified in the skin as a cell exhibiting extensive ramifications (Becker, 2003). They were considered neural cells (Bloch, 1929) and later senescent melanocytes (Billingham, 1948). With time, their central immune function has become apparent (Becker, 2003).

Human DC are found in the interstitium of almost all organs, in the blood and in secondary lymphoid tissues. Bronchial and gastrointestinal epithelia are especially DC rich. This makes sense as these are the areas where environmental antigens and pathogens come into contact with the immune system.

Within secondary lymphoid tissues, interdigitating DC, a miniscule fraction of the total cellular population, form a vast interconnected network with an enormous capability to survey lymphocytes trafficking between lymphoid tissues and the blood. This maximises the likelihood of the successful selection of individual antigen specific clones that are

extremely infrequent by activated DCs (Lindquist et al., 2004).

DC are the 'conductor' of the immune 'orchestra'. The DC network bridges innate and adaptive immunity and DC are able to interact with the full range of immune cells including granulocytes, T and B lymphocytes, natural killer and natural killer T cells and cells of monocyte-macrophage lineage.

When the immune system is challenged by antigen, whether a self-antigen such as a tumour-associated-antigen or an antigenic determinant of a foreign pathogen, the nature of the antigen itself and also the attendant innate immune response determine the characteristics of the ensuing adaptive immune response. DC are critical in ensuring that the information on the nature of antigenic challenge is relayed through to adaptive immunity to ensure a response that is appropriate and effective.

In the steady state DC mediate immune tolerance. The thymus produces naive T-lymphocytes and these cells have newly assembled T-cell receptors - some of which are self-

reactive. A process of negative selection occurs in which cells with high avidity receptors recognising self antigens are deleted. Both thymic epithelial cells and mature DC display self-peptides and are involved in this process – 'central' tolerance. However, whilst central tolerance is effective in removing high-avidity self-reactive T lymphocytes, it is an imperfect process and some escape into the periphery.

In the absence of infection, inflammation or cellular stress DC continually sample self tissues and present self-derived peptides in a tolerogenic fashion to T-cells. Antigen presentation in the absence of costimulatory molecules on the DC surface and in the presence of immunosuppressive cytokines leads to either functional unresponsiveness of specific T-cells or their deletion. Alternatively, it can generate T-cells with regulatory and suppressive capabilities that actively attenuate antigen specific T-cells. DC in this condition are described as tolerogenic, resting, or sometimes 'immature'.

However, when the immune system receives activating stimuli, the DC undergo a 'metamorphosis'. The activation programme involves a loss of adhesion and cytoskeletal

reconfiguration, increased motility, reduction in phagocytic and endocytic receptor expression (Steinman and Swanson, 1995), upregulation of costimulatory molecules, stabilisation of surface MHC Class II molecules (Mellman, 2005), secretion of T-cell polarising cytokines (Heufler et al., 1996) and induction of immunoproteasome subunits.

DC activation takes place either on direct recognition of foreign microbes or indirectly via the innate immune system. DC possess pattern-recognition-receptors (PRRs) that interact directly with conserved molecular patterns (PAMPs) that are shared between pathogens. There are ten toll-like receptor genes (TLRs) in humans. These have different ligands and cellular localisations. The particular TLR that is engaged by a pathogen can determine the nature of the adaptive response engendered (O'Neill et al., 2004).

C-type lectin receptors interact with the carbohydrate moiety of bacterial glycoproteins and include Blood dendritic cell antigen 2 (BDCA2) and DC-SIGN. They are found on many pathogens and ligation of the receptor leads to internalisation of the microbe. CLRs also function as adhesion molecules and the interactions between DC-SIGN and MAC-1 and CEACAM1 on neutrophils are important in innate

activation of DCs, between DC-SIGN and ICAM2 and ICAM3 play a role in endothelial egress and stabilisation of the DC-T cell interaction.

NOD like receptors sense intracellular microbial components and respond to proinflammatory cytokines. NOD1 and 2 and NALP3 interact with muropeptides that are fragments of peptidoglycans derived from bacterial cell walls.

DC can receive indirect signals of tissue damage and cellular stress – danger associated molecular patterns (DAMPs). DAMPs include heat-shock or stress proteins such as gp96 and HSP70 (Somersan et al., 2001) that encourage DC cross-presentation, high mobility group box protein-1 (HMGB1) that is a cytokine like molecule released from dying cells that induces macrophages to release IL-6 and TNFα, and β-defensins that are small peptides with antimicrobial activity released by neutrophils and epithelial cells in response to infection. Other DAMPS include endogenous molecules such as hyaluronic acid (Do et al. 2004) a component of the extracellular matrix and uric acid (Shi et al., 2003) that is increased in conditions of high cellular turnover and fibronectin (Jancic et al., 1998).

DC can conserve exogenously acquired antigens and present intact antigen to B-lymphocytes. They can initiate T-cell dependent antibody responses (Qi et al., 2006).

DC are the most professional of the professional APCs and, for several reasons, they are ideal candidates for cellular cancer vaccines.

First, DC have the near-unique ability to cross present antigen. In this process peptides derived from exogenous antigens are presented at the cell surface bound to MHC Class I molecules. This process was first observed in mice (Bevan, 1976), although DC involvement was only recently demonstrated (den Haan et al., 2000). The importance of cross priming is in the generation of immune responses against organisms that do not directly infect DCs, and also in tumour immunity where cancer cells are extremely poor antigen-presenting cells incapable of initiating T-cell expansion. In mice, only the CD8α^+ splenic DC subset has been shown to have cross-presenting ability (den Haan et al., 2000), although B-cells and macrophages may cross-present at low efficiencies in vitro (Reis e Sousa and Germain, 1995). DC are able cross-present at high efficiencies – DCs capturing apoptotic or necrotic vaccinia

virus infected cells in vitro were able to present Class I epitopes at an equivalent level to cells pulsed with 10^{-7} to 10^{-8} M exogenous peptide (Larsson et al., 2001). This is especially remarkable as it is thought that Class I presentation is often highly dependent on DRiPs and ongoing protein synthesis. The efficiency of the process is increased if DCs are activated by TLR agonists, immune complexes, dying cells or uptake via the DEC205 receptor. The efficiency of cross-presentation is far higher when antigen is delivered in particulate rather than soluble form (Rock et al., 1993). There are two putative mechanisms of cross-presentation that are not mutually exclusive and the relative importance of each depends on the DC subset and type of antigen (Rock and Shen, 2005). In one, there is phagosome to cytosol transport and then proteasomal processing and translocation of the peptides to the ER via TAP. In the other processing occurs in the phagosome followed by MHC Class I loading in the phagosome – MHC complexes recycling from the plasma membrane may intersect with phagosomes.

Second, DC are able to stimulate the expansion of naive T-lymphocytes. By virtue of interactions between CD86 and CD28 and DC-SIGN and ICAM3 (Bhardwaj, 2001) and the formation of a very tight immunologic synapse between T-lymphocyte and DC (Benvenuti et al., 2004), these cells are

28

responsible for priming the majority of cellular immune responses. However, suboptimally mature cells only promote 2 to 4 rounds of T-cell division. Mature DCs, in contrast to other APCs, have the ability to adhere to T-cells even in the absence of antigen.

Third, the efficiency of antigen processing in DC is greater than other APCs. This is not surprising as DC are the only APC whose exclusive function is antigen. DC in contrast to macrophages or B-cells are found in the naive T-cell zones of lymphoid organs. The extensive ramifications of DC increase the surface area for display of peptide-MHC complexes to T-cells and allow multiple simultaneous T-cell contacts. The number of peptide-MHC complexes generated per unit of antigen is also extremely high and surface MHC complexes, particularly Class II, are extremely stable and may persist for several days – greater than other APCs (Zehn et al., 2004).

Fourth, DC are distinguished by a very controlled and well regulated rate of lysosomal proteolysis and hydrolysis. In contrast to other cells types, DCs preserve a larger amount of antigenic 'information' for internalised proteins. The controlled lysosomal degradation increases the likelihood of

formation of small peptides for MHC loading (Delamarre et al., 2005). DC possess a range of cathepsin inhibitors for this purpose (Pierre and Mellman, 1998).

Fifth, the establishment of T cell memory depends on DC function. The development of cytotoxic T-cell memory/recall responses seem to be dependent on the presence of CD4 T-cells at the time of infectious challenge (Sun and Bevan, 2003). Zammit et al (2005) selectively depleted CD11c dendritic cells in transgenic mice and this attenuated the development of HSV specific CTL responses and recall responses.

Memory T-cell responses are characterised by their longevity, more rapid expansion and development of effector function and a greater frequency than naive T-cells. In terms of cancer immunotherapy the generation of a long-lived T-cell response is vital as complete eradication of the clone of cancerous cells by immune responses remains unlikely and so durable responses are needed to maximise progression-free survival times.

CTL memory responses are partly dependent of the recruitment of CD4 T-cell help (Bevan, 2004). There is evidence that initial CD8 priming can occur in the absence of CD4 T-cells, on subsequent re-encounter with antigen T-cells primed in the absence of CD4 cells die rather than proliferate in a TRAIL dependent fashion (Janssen et al., 2005). In fact, the continued presence of CD4 T-cells is vital in order for maintenance of CTL responses over time (Sun et al., 2004). During the CTL priming phase, exposure of CD8 T-cells to IL-2, the main source of which is activated CD4 T-cells, is vital in order to programme the cells to be able to respond to subsequent antigenic re-challenge (Williams et al., 2006). There are two main groups of theories of memory cell differentiation. The first suggests that the strength or quantitative differences in infectious stimuli determine memory polarisation – if high and prolonged antigen presentation occurs cells are driven towards an exhausted and fully differentiated 'effector' phenotype, whereas when antigen presentation is more restrained or controlled there is more of an opportunity for memory differentiation to occur. Alternatively, specific signals such as cytokines or subsets of DCs may encourage memory differentiation, and this possibility is supported by the fact that there is no difference in TCR specificity between effector and memory clones (Prlic et al., 2007). The maintenance of memory CTL populations in the absence of antigen requires IL15 and this

is produced by DCs upon CD40 ligation (Kennedy et al., 2000).

Memory CTL responses therefore depend upon the formation of a three-way immunological conjugate of antigen-presenting DC and cognate CD4 and CD8 T-cells. The consensus view has been that the requirement of CD4 augmentation of CTL responses varies according to the nature of the immune stimulus – in particular how 'inflammatory' it is.

However, numerous studies report that the expansion of memory CTLs to second and subsequent antigenic challenges is blunted or even abolished if the response was primed initially without CD4 'help' (Janssen et al., 2003 and Shedlock and Shen, 2003).

CD4 help is clearly antigen specific and CTL memory differentiation requires that the same antigen-presenting-cell interacts with cognate CD4 and CD8 T-cell (Cassell et al., 1988 and Bennett et al., 1997).

The critical cellular interaction in memory CTL priming is that between CD40 on the APC and CD40 ligand on CD4 T-cells.

The evidence for this was the loss of memory responses if either molecule was removed (Ridge et al., 1998).

Other downstream effector molecules that may amplify the effects of the CD40-CD40L interaction include IL2, IL12, IL15 and 4-1BBL.

DC are the ideal APC to participate in this process as their ability to cross-present allows them to simultaneously present Class I and II restricted epitopes, they strongly express CD40 on activation and controlled lysosomal hydrolysis (compared with, for example, macrophages) permits generation of Class II epitopes.

DC can programme T-cells to home to particular anatomic sites. Skin derived DCs 'imprint' the ability to home into cutaneous tissues on the induced effector T-cells, and Peyer's patch derived DCs generate DCs with the ability to migrate into inflamed gut (Mora et al., 2003).

1.6.   In vitro derived DC for vaccination.

DC are bone marrow derived antigen-presenting-cells. Their development is encouraged by granulocyte-monocyte colony stimulating factor (GM-CSF) and by the fms-like tyrosine-kinase 3 ligand (Flt3L) (O'Neill, Adams and Bhardwaj, 2004). Administration of synthetic Flt3L expands circulating DC populations at last 100 fold (Pulendran et al., 2000) and Flt3L double knockout transgenic mice are deficient in DCs (McKenna et al., 2000). All DCs are HLA DR positive and negative for other lineage markers (e.g. CD3, CD14, CD19, CD56).

Methods for generating cells with DC like properties in vitro are well established (Sallusto and Lanzavecchia, 1994) and this has spawned interest in the use of in vitro generated DC as vaccines in infectious and malignant disease and to downregulate T-cell responses in autoimmunity (Steinmann et al., 2000).

1.6.1. CD34 stem cell derived DCs

DCs can be produced from CD34 positive haematopoietic stem cells and peripheral blood monocytes.

The use of CD34 positive haematopoietic stem cells as a substrate for DC generation is well established. The frequency of stem cells in peripheral blood is extremely low - it is necessary to either use bone-marrow samples or to mobilise peripheral stem cells using G-CSF or GM-CSF injection. There are concerns regarding promotion of tumour growth with these drugs. The key advantage of using CD34 stem cells for DC culture is that there is abundant evidence suggesting that culture with GM-CSF, TNFα and Stem-cell factor or Flt3-L generates a population of cells recapitulating several characteristics of Langerhans cells (Ueno et al., 2007). This is ideal for immunotherapy as LCs drive powerfully cytotoxic CD8 T-cell responses. There is evidence of clinical efficacy of this approach in metastatic melanoma (Banchereau et al., 2001).

1.6.2. Monocyte derived DCs.

This has been the most used platform for DC generation. Culture of blood monocytes, easily obtainable either at low purity after plastic adherences or high-purity by immunomagnetic selection, with a cytokine-cocktail leads to cells with excellent antigen-presenting properties. Exposure of monocytes to GM-CSF and IL4 generates a

35

heterogeneous population of large, veiled cells that have lost CD14 expression and gained expression of CD1a. They are semi-mature or immature DCs as they express only low levels of costimulatory molecules, molecules involved in migration and MHC Class II molecules and when pulsed with peptides these cells tend to lead to the generation of regulatory T-cells or anergy of T-cell responses (de Vries et al., 2003 and Dhodapkar and Steinman, 2002).

However, exposure of cells to macrophage conditioned medium or to recombinant TNFα upregulates costimulatory molecules, class II molecules and receptors involved in lymphokine driven chemotaxis to lymph nodes and generates cells capable of priming effective T-cell responses (Sallusto and Lanzavecchia, 1994).

1.6.3. Activation and maturation of monocyte derived DCs.

DC are typically generated from monocytes by 5-7 days differentiation in GM-CSF and IL4 followed by 'activation' with TNFα, IL1β, IL6 and prostaglandin E2 (PGE2) (Jonuleit et al., 1997). Such DC have been convincingly shown, in proof-of-principle experiments, to be able to activate T-cell responses in healthy human volunteers. Dhodapkar et al

(2000) showed that intradermal administration of macrophage conditioned medium matured DCs loaded with either tetanus toxoid or keyhole-limpet haemocyanin led to the generation of durable (approximately 6 months durable) CD4 responses against these antigens in a specific fashion (i.e. no responses were seen in patients given tetanus toxoid or KLH alone or unloaded DCs). In addition, DCs loaded with an influenza matrix protein CD8 epitope were able to expand the epitope specific CTL population in vivo, and in fact in responding volunteers DC vaccination seems to increase the peptide sensitivity of these cells. However, the ability of MoDC to cross-present in less certain. The ability to cross-present is of paramount importance in cancer vaccination strategies when antigen is delivered as a tumour-lysate or recombinant protein. MoDCs ability to cross-present is critically dependent on the nature of the antigen presented. Certainly capture of apoptotic cells (Albert et al., 1998) and immune complexes (Dhodapkar et al., 2002) can lead to presentation of Class I restricted epitopes. Conjugation of antigens to the uptake receptor DEC205, expressed on moDCs, can ensure access to the Class I pathway for exogenous antigen (Bozzacco et al., 2007).

A major criticism has been that the phenotype of moDCs does not closely resemble any in-vivo subset and the cells seem

to be 'hybrids' with features of interstitial and dermal DCs, specialised for humoural rather than cellular response induction (Palucka, 2007).

The method of monocyte selection from peripheral blood mononuclear cells – elutriation, plastic adherence or immunomagnetic selection does not have a major effect on the function of the DCs.

The 7-9 day culture period is not ideal for clinical purposes and the yield and purity of DCs is higher and more highly avid CTL responses are induced by DCs differentiated in 24-48 hours (Tuyaerts et al., 2007).

Fast DC generated within 48 hours have a fully mature phenotype with MHC Class II, CCR7, CD40, and CD83 expression and are able to respond with migration to the lymphokine ligands. The minimal cytokines required for phenotypic maturation appear to be PGE2 and TNF (Dauer et al., 2005).

GM-CSF is essential to programme differentiation towards macrophage lineage cells but IL4 can be replaced by other cytokines. In a comparison of IL-4 and IL-15 moDCs loaded with Melan A 26-35 peptide, it was shown that comparable 26-

35 specific CD8 populations were induced but IL-15 DCs achieved this at lower peptide concentrations. Also, the induced CTL population had higher IFNγ release, stronger perforin and granzyme expression and crucially was able to lyse targets physiologically expressing antigen (Melan A positive melanoma cell line) – something that IL4 DC driven cultures were not capable of (Dubsky et al., 2007). IL15 DCs display some of the desirable features of Langerhans cells including Langherin, CCR6 and E-cadherin but not Birbeck granules (Mohamadzadeh et al., 2001).

A 'supplemented' cytokine cocktail includes T-cell derived signals and Type I interferons like IFNα (Lapenta et al., 2006). The impetus for such enhanced cocktails was the observation that cytokine matured moDC were deficient in IL12p70 production (Sporri and Reis e Sousa, 2005). This is the biologically active IL12 heterodimer that is essential for Th1 polarisation and development of long lived and avid T-cells (Trinchieri, 2003). Toll like receptor stimulation via MyD88 is important for IL12p70 secretion (Warger et al., 2006) and various compounds have been used including CpG oligodeoxynucleotides, Poly I:C (Rouas et al., 2004) and imiquimod. Adapting these compounds for clinical use is difficult, although a clinical study in metastatic breast cancer using IFNγ and LPS matured moDCs showed powerful

induction of CD4 and CD8 responses and reductions in disease volume (Czerniecki et al., 2007)

Addition of IFNα or T-cell derived signals - CD40 ligand and IFNγ - boosts the immunostimulatory properties of moDC in vitro (Dauer et al., 2008). This fits with the two-step model of T-cell activation. Activation begins on receipt of proinflammatory signals from bystander cells and direct pathogen recognition by DCs. Later, these activated DCs are 'licensed' to 'full' effector in the T-cell areas of lymph nodes by T-cell signals – this forms a positive feedback loop to amplify T-cell activation.

Although megacytokine cocktails seem optimal in in vitro assays of T-cell stimulation (Giermasz et al., 2009), a closer examination of the kinetics of the process in vivo raises questions about whether these findings will apply for clinical DC vaccination. Maturation stimuli including T-cell signals may lead to functionally exhausted DCs. The early release of IL12p70 is disadvantageous when the further 48 hour delay from administration to arrival in lymph nodes is considered. The more desirable property is to arrived 'licenced' and able to respond to T-cell signals in vivo with a further burst of IL12p70 secretion (Langenkamp et al., 2000).

Despite these advances, activation of monocyte derived DCs in-vitro attempts to model an extremely complex in-vivo process that has evolved over millions of years of the pathogen-host interaction (Gilboa, 2007)

1.6.4. Migration of monocyte derived DCs.

A critical property of DC vaccines is their ability to migrate from the injection site to secondary lymphoid tissue, as initiation of T-cell responses locally in the skin is unlikely. Only 5-10% of administered cells reach lymph nodes (Morse et al., 1999 and Adema et al., 2005). Although intralymphatic or intranodal injection of DCs should enhance migration, this has been difficult to demonstrate and there are concerns that intranodal injection could destroy the important micro-architecture of the node (Kyte et al., 2006).

An alternative perspective is that the low proportion of the vaccine reaching lymph nodes is advantageous as it may reflect a process of selection with only the most 'mature' DCs being capable of reaching T-cells.

Expression of the CCR7 chemokine receptor has dominated thought in this area. Most studies of DC vaccines have either not addressed the question of migration or simply used expression of surface CCR7 as a surrogate marker. Whilst the presence of CCR7 may be necessary for migration, it is not necessarily sufficient (Quillien et al., 2005).

Differential expression of chemokine receptors occurs in maturing DCs, with interactions between, for example, CCR1 and CCL3 and CXCR1 and CXCL8 in the early phase allowing DCs to home to sites of inflammation (Sallusto et al., 1998) and after activation these receptors are downregulated and interaction between the lymphokines CCL19 and CCL21 and their receptors CCR7 and CXCR4 becomes relevant (Cyster, 1999). CCR7 deficient mice show defective movement of skin DCs to draining superficial lymph nodes. However, movement of Langerhans cells can be CCR7 independent and may rely on the CCR6-CCL20 interaction instead (Ohl et al., 2004).

Important additional steps in this system downstream of either CCR7 or CXCR4 in particular leukotrienes LTD4 and LTDE4 (Randolph et al., 2005), expression of matrix metalloproteases 2 and 9 (Ratzinger et al., 2002) and lipid mediators including leukotriene C4 (Robbiani et al., 2000).

The rationale for inclusion of PGE2 in maturation cocktails has largely related to its effects on promoting CCR7 expression and migratory capacity on maturing DCs (Scandella et al., 2002 and Jonuleit et al., 1997). There was also some evidence that PGE2 in addition to TNFα in the maturation cocktail generated a high level of CD4 and CD8 stimulation than TNFα alone (Rubio et al., 2005).

However, IL12p70 production is attenuated by PGE2 (Kalinski et al., 2001) and induction of indoleamine 2,3 dioxygenase (IDO) is encouraged. It is suggested that the IL10:IL12p70 ratio and hence the balance between Th2 and Th1 responses is skewed in favour of humoural responses by PGE2 matured DCs (Jongmans et al., 2005). Other results suggest that the ability of PGE2 matured DCs to respond to subsequent CD40 ligation with IL12p70 secretion is compromised.

However, in the presence of powerful activating signals such as CD40L, IFNγ or Toll-like receptor ligands, the use of PGE2 in maturation cocktails may not have a profoundly negative effect on IL12p70 production.

However, more concerning is the recent realisation that inclusion of PGE2 in the maturation cocktail leads to generation of DCs that express the enzyme indoleamine 2,3

dioxgenase (IDO). IDO expression can also be linked to upregulation of CD25 (Von Bergweld-Baildon et al., 2006).

IDO catalyses the degradation of tryptophan to kyenurine and was discovered in the placenta (Munn et al., 1998). Here it plays a permissive role in the immunodeficiency of pregnancy and it suppresses T-cell responses against fetal allo-antigens (Mellor et al., 2001). T-cell activation and proliferation are dependent on adequate concentrations of tryptophan and are inhibited by kyenurines and IDO positive DCs constitute an immunoregulatory subset (Munn, 2002).

The coexistence of upregulation of CD25 and IDO on maturing DCs may also endue an immunosuppressive phenotype on the T-cell response as there is evidence that increased surface CD25 expression, once considered a marker of 'mature' DCs, correlates the secretion of soluble IL2 decoy receptors that can reduce local concentrations of IL2 and thus impair CD4 responses (Popov and Schultze, 2008).

Strategies for enhancing the migration of DC vaccines include pre-condition of the injection site with TLRs (Nair et al., 2003) and use of multiple, small DC inoculums (Gilboa, 2007).

1.6.5. Antigen transfer by vaccine-grade dendritic cells.

It is assumed that vaccine DC migrate to draining lymph nodes and form immunological synapses with T-cells to initiate expansion of T-cell populations. However in a mouse model of cutaneous HSV infection the cells responsible for presentation of a Class I restricted epitope did not originate from the infected epidermis (Allan et al., 2003).

It is currently thought that there is a lymph node resident, CD8α positive dendritic cell subset in mice that is entirely non-migratory and functions to acquire antigen from mobile DCs and cross-present it via the Class I pathway (Carbone, Belz and Heath, 2004).

Antigen likely accesses these cells either by direct carriage by the afferent lymph which may be relatively less immunogenic (Itano et al., 2003), or by active antigen transfer from migratory DC populations.

Clearly thse findings have implications for vaccine design. Monocyte derived DCs are known to be highly interactive cells forming gap junctions and transferring intact melanoma antigens to one another which amplifies the immune response (Mendoza-Naranjo et al., 2007). Alternatively exosomes

could be responsible for antigen transfer (Thery et al., 2002).

1.6.6. Antigen loading of vaccine-grade dendritic cells.

There are numerous methods for loading vaccine DCs with tumour associated antigens. These can be broadly divided into those in which antigen is produced endogenously within the cell and those where there is exogenous acquisition of antigen. The key disadvantages and benefits are summarised in Figure 1.3.

1.6.6.1. Peptide-pulsing

Most early studies, whether clinical or pre-clinical, utilised peptide pulsing of DCs with exogenous peptides. The advantages of this approach include the simplicity of peptide manufacture of peptides and their ease of use and stability. However, peptide based approaches require determination of patient HLA haplotypes and are often restricted to patients with common HLA alleles – typically HLA-A2 for Class I loading in Caucasian patients. Additionally, whilst the number of Class II binding peptides is expanding these are still relatively limited in number and induction of CD4 responses is vital to success of DC vaccination. Although epitope spreading may occur, single

Method	Advantages	Disadvantages
Peptide pulsing	Simple and rapid Long track record	Short-lived antigen presentation Optimal peptide 'dose' uncertain Few know Class II epitopes Need pre-knowledge of HLA haplotypes
Recombinant protein	No need for knowledge of HLA haplotypes Robust Class II epitope presentation	Difficult to produce at clinical grade Ability to access Class I pathway highly dependent on form of deliver
Tumour lysates	No need for knowledge of HLA haplotypes Robust Class II and possibly Class I presentation (due to presence of HSPs etc)	Not easy to prepare from inaccessible metastatic sites Risk of introducing immuno-suppressive proteins from tumour

Figure 1.3a.   Exogenous approaches for antigen loading of vaccine DC's.

Method	Advantages	Disadvantages
Viral transduction	Powerful transgene expression May have 'activating' effects on DCs via PRRs No need for knowledge of HLA haplotypes	May encourages immune responses against viral proteins Risk of integration into host genome (mutagenesis) Difficult and costly to prepare May be neutralised by pre-existing antibodies
DNA transfection	May activate DCs via TLRs Sustained antigen presentation No need for knowledge of HLA haplotypes Strong Class I presentation Plasmid DNA easy to prepare and store	Generally low transgene expression High cellular toxicity if electroporation used May need re-targeting sequences to ensure Class II presentation
RNA transfection	Electroporation leads to very high transgene expression Strong Class I (and sometimes II) presentation RNA labile and not easy to store	May need re-targeting sequences to ensure Class II presentation Less toxic if electroporation used Concerns about short intracellular half-life

Figure 1.3b.   Endogenous approaches to antigen loading of vaccine DCs.

peptide approaches are limited in the specificity of T-cells that they are likely to induce. Use of peptide pools is hindered by competition and inadequate T-cell stimulation (Dieckmann et al., 2005). It is difficult to determine the appropriate dose of peptide with which to pulse cells. Typically high doses are used in the micromolar range. However, there may be an inverse correlation between antigen dose and the T-cell receptor avidity of the induced T-cell populations. Using a model of latex beads coated with co-stimulatory molecules as artificial APCs, it was shown that Melan-A 26-35 specific T-cell populations induced with 10uM peptide were 1000 fold less avid than those induced with 10nM peptide (Walter et al., 2003). Finally, it is thought that peptide-MHC complexes formed by passive pulsing have a limited duration at the cell surface and it has been shown that protein loaded DCs cross-present a Class I restricted epitope for a longer period that peptide-pulsed cells (Schnurr et al., 2005). It is important to bear in mind the requirement for the peptide-loaded vaccine cells to migrate to lymph nodes. Despite all these concerns, meta-analyses of the clinical trials performed to date suggests that peptide-loaded DC vaccines give the highest objective response rates in metastatic melanoma (Nakai et al., 2010)

1.6.6.2. Protein loading.

Other exogenous approaches include co-incubating DC with recombinant proteins or tumour lysates. Most studies have been performed with tumour cell lysates rather than recombinant proteins as these are difficult to produce for clinical application. Additionally, the desired outcome – presentation of Class I and II restricted epitopes is highly dependent on the presence of 'danger signals' and often apoptotic or necrotic cell lysates will be rich in heat shock proteins and these have maturation enhancing effects on DCs (Somersan et al., 2001). However, all tumour associated proteins are transferred and whilst this has the advantage of including mutated tumour specific proteins, the possibility of exposing maturing DCs to tumour derived immunosuppressive substances remains. Also, obtaining sufficient quantities of tumour material for autologous lysates is not straightforward. Uptake of exogenous proteins by DCs is thought to favour the Class II pathway, particularly as the ability of monocyte derived DCs to cross-present is highly dependent on the activation stimulus used.

1.6.6.3. Endogenous antigen production.

Methods to endogenously produce within the DCs the antigen of interest have been developed. These include viral transduction and non-viral transfection. Viral vectors

typically encode specific pre-defined tumour antigens, whereas nucleic acid transfection can encompass either pre-defined antigens or bulk tumour-derived cDNA or mRNA.

Currently, favoured approaches centre on expression of full length, intact tumour-associated-antigen within the DC. Viral transduction with recombinant viruses, such as poxviruses (Kim et al., 1997) and adenoviruses (Butterfield et al., 1998) and is highly efficient in terms of transgene expression and leads to the robust generation of Class I, and in some cases Class II restricted epitopes. However, it can lead to non-specific immune effects, deleterious T cell responses to viral antigens expressed in the DC and is less easily applicable to clinical trials owing to regulatory issues. There are also safety concerns with regard to virally induced genomic mutagenesis. The preparation of plasmid cDNA or in-vitro transcribed RNA is more straightforward than generation of recombinant viruses which can take months.

1.6.6.4. Non-viral transfection: plasmid DNA.

Like other primary, non-dividing cells human dendritic cells were extremely resistant to transfection with plasmid cDNA constructs. Transfection techniques used have included

cationic lipids, nucleofection and electroporation. In the vast majority of studies, there was negligible transgene expression.

Rughetti et al (2000) demonstrated 10-20% transgene expression in human MoDC after cationic lipid transfection of Mucin-1 cDNA. However, cell viability was as low as 50% - although transfection appeared to have 'maturation-inducing' effects on the DCs and proliferative T-cell responses in the autologous system were observed despite low transfection efficiency. Landi et al (2007) showed transgene expression levels of 20% with cationic lipids.

Although transfection efficiency remained unassessed, Alijagic et al (1995) showed that MoDC transfected using lipofectamine with cDNA encoding tyrosinase were able to reactivate tyrosinase specific CD8 T-cells in autologous PBMCs.

A comprehensive analysis of various cationic lipids for transfection of human monocyte derived or CD34 stem cell derived DCs using eGFP as the reporter gene (Van Tendeloo et al., 1998) showed minimal transfection efficiency.

Electrical methods of cell transfection work by passing a current through the cells leading to the transient formation of membrane pores for entry of nucleic acids. Significant impairment of cell viability after 24 hours is usual.

Using GFP, it was shown that electroporation of plasmid DNA into stem cell derived DC did lead to expression levels of up to 15%, although 30% cell viability was typical. There was a wide range of fluorescence intensities in the transfected DC. It was also observed that moDC were relatively resistant to DNA electroporation (Van Tendeloo et al., 1998).

Although CD34 stem cell derived DC can be successfully electroporated with plasmid DNA, Melan A transfected HLA A2 positive CD34 DC were not recognised by a Melan A specific CD8 T cell clone by IFNγ ELISA due to non-specific stimulation in cells transfected with control plasmid (Van Tendeloo et al., 2001).

Amaxa nucleofection is a form of electroporation that uses buffer solutions and electrical parameters that are proprietary and vary according to the cell type being transfected. Expression levels of up to 50% can be achieved in human monocyte derived DC.

Nucleofection of immature human moDC with eGFP cDNA led to acceptable cell viability (37%) and good GFP expression (55%) at 24 hours. However, the cells' ability to upregulate co stimulatory molecules CD80 and CD83 in response to the lipopolysaccharide maturation stimulus was impaired after nucleofection. Production of inflammatory cytokines IL1B, TNFa and IL6 was diminished in nucleofected DC, although IL12 secretion was slightly enhanced. Nucleofection of mature DC, however, appeared to be the optimal approach as 39% of cells were GFP positive and retained their mature phenotype (Lenz et al., 2003).

As part of a systematic comparison of moDC generation protocols and transfection methodologies, Landi et al (2007) found that nucleofection of immature DC (differentiated from CD14 positive monocytes positively selected from PBMC) could be effectively utilised with transfection efficiency approaching 40%, but significant reduction in viability was seen after 24 hours. Ability of the DC vaccine to present antigenic epitopes was not assessed in this study.

In summary, T cell recognition of DC nucleofected with cDNA has not been demonstrated and negative effects on the ability of DC to functionally mature have been noted, despite easily detectable levels of antigen.

A novel technique uses a 35 amino acid cationic peptide (CL22) (rather than lipid) to condense the DNA into particles for cellular uptake. The presence of the lysosomal acidification inhibitor chloroquine during transfection maximises DNA delivery into the cytoplasm and nucleus by preventing lysosomal degradation. Percentages of cells expressing the transgene ranged from 80 to 20% for cell lines (monkey, human and mouse) and around 15% for the two primary cells tested (human DC and human umbilical vein endothelial cells).

An optimised procedure for human moDC was developed with transfection efficiencies ranging from 1-54% with an average of 17%. Transfection of human DC was shown to lead to the presentation of Class I restricted viral epitopes and, in mice, the development of a cellular (CD8 T cell) and humoural immune response. Presentation of Class II restricted epitopes to CD4 T cells was not specifically investigated (Irvine et al., 2000).

CL22 based transfection was taken forward into the clinical setting of metastatic melanoma (Steele et al., 2011) and this is discussed in detail in subsequent sections.

1.6.6.5.   Non-viral transfection – in-vitro transcribed RNA.

Endogenous production of whole antigen mainly directs the resultant epitope peptides into the Class I-CD8 pathway and in order to generate a complete cellular immune response presentation of Class II restricted peptides is crucial. For this reason, many antigens are expressed as fusion proteins alongside key components of the endolysosomal Class II pathway (e.g. invariant chain, LAMP) or autophagosomes (e.g. Atg8). A particularly interesting strategy to achieve this is co-transfection with antisense oligodeoxynucleotides directed again the invariant chain to increase the likelihood of endogenous produced peptides interacting with Class II molecules (Zhao et al., 2003).

The use of mRNA rather than cDNA for DC transfection has several putative advantages including a need for translation only and a requirement to only traverse one cell membrane. (Ponsaerts, 2003). RNA cannot be integrated into host genomes. However, RNA is highly prone to RNAase digestion ex vivo if not handled carefully and has a short intracellular half life which could lead to very transient protein expression. In vitro transcribed RNA must closely resemble physiologically produced mRNA and to bind stably to

ribosomes, and be translated efficiently it requires 5'
methylguanosine capping and the additional of a Poly A tail
(Colgan and Manley, 1997).

Van Tendeloo et al (2001) showed, using GFP, that
transfection efficiencies of 63% for immature moDC and 33%
for mature moDC could be achieved using electroporation of
in-vitro transcribed RNA at 24 hours post transfection. The
electroporated DC were able to upregulate CD80 and CD83 and
MHC Class II molecules in response to TNFα and
lipopolysaccharide (LPS), and stimulate IFNγ secretion from a
Melan A specific cytotoxic T lymphocyte (CTL) clone.

RNA electroporation of tumour and viral antigens, including
influenza matrix protein, Melan A, human telomerase reverse
transcriptase, HIV GAG, human papilloma virus E6 and E7 and
CEA, as well as whole tumour RNA into DC has been shown to
lead to T cell recognition and activation (Ponsaerts, 2003).

Generally the focus has been on Class I presentation to CTL
clones although CD4 T cell recognition of transfected cells
has also been demonstrated (Dorfel et al., 2005 and Su et
al., 2005).

In the work of Grunebach et al (2003), there was no apparent

correlation between transgene expression levels after RNA transfection and the ability of the DC to expand a specific CTL population in vitro – suggesting that even barely detectable antigen levels may be sufficient for epitope presentation.

RNA transfected DC stimulated up to 80% of maximal (i.e. peptide stimulated) IFNγ release, indicating the potential utility of RNA electroporation (Bonehill et al., 2004).

1.7. Malignancy as a target for immune responses.

1.7.1 Immune surveillance.

Administration of bacterial extracts to advanced sarcomas leads to transient tumour regressions – linking cancer and immunity (Coley, 1891). The tumour immunosurveillance hypothesis proposes that the adaptive immune system can recognise transformed cells as foreign antigenically and that immune function restrains the early stages of neoplasia (Burnet, 1967). This was based on the observation that irradiated cancer cell lines, derived from sarcomas in mice, when delivered to syngeneic mice as a vaccine, led to

protection from subsequent tumour challenge (Basombrio et al, 1970, Pellis et al, 1974).

There was also circumstantial evidence. Very occasionally spontaneous tumour regressions do occur and they are often accompanied by evidence of autoimmunity as in the case of melanoma and vitiligo (Cunha et al, 2009).

Necropsies suggest that the frequency of asymptomatic, microscopic foci of neoplasia far exceeds the frequency of known, symptomatic malignant disease (Ashley, 1965) and this raised the possibility that endogenous, perhaps immune, processes were able to prevent progression of premalignant lesions.

In paraneoplastic syndromes, neurological dysfunction occurs in the absence of demonstrable infiltration of neural tissue by tumour, and may happen even when tumours are completely undetectable clinically (Mathew et al, 2006). These syndromes are caused by cellular and humoral immune responses against antigens that are shared between tumours and neural tissues (Posner, 2003).

However, epidemiologic studies on cancer in immunosuppressed patients failed to provide evidence of increased incidence of non-virally driven malignancies (Penn and Brunson, 1988). The finding that nude, athymic mice did not have increased incidences of cancer questioned the tumour-immunosurveillance concept (Rygaard and Povlsen, 1974). Although experiments were performed using chemical carcinogens over a relatively short period of time – unlike the natural history of most cancers in humans, there was no difference in incidence of any cancer between the two groups (Stutman, 1974) and it was confirmed that the nude mice were severely immunodeficient and accepted allogeneic skin grafts.

Recent experiments have resurrected the tumour immuno-surveillance hypothesis. Transgenic mice lacking both copies of the recombinase-activating gene (RAG) were engineered. These animals lack all lymphocyte subsets that require somatic rearrangements of genes encoding antigen receptors – namely T cells, natural killer T cells and B cells. Such mice did show increases in incidence of spontaneous and induced cancers compared to littermates that were wild-type for the recombinase activating genes (Shankaran et al., 2001).

Nude, athymic mice do possess very low levels of specific lymphocytes. In particular, very low levels of alpha-beta T lymphocytes were present (Ikehara et al., 1984) and other subsets such as NK T cells and gamma-delta T-cells were replete in these mice. This allowed the two sets of results to be reconciled.

Modern epidemiologic studies reveal a two to five fold increase in non-viral malignancies in renal transplant recipients whose T-cell function is suppressed by drugs such as cyclosporine (Birkeland et al, 1995); although the majority of cancers in this population are sill associated with viral infection.

1.7.2. Efficacy of immune-based therapies for malignancy.

The efficacy of immune-based therapeutics for cancer implies an underlying immune control of malignancies. Intravesicular BCG is effective for superficial bladder cancer (Alexandroff et al, 1999). BCG is an attenuated form of Mycobacterium bovis and acts by inducing local non-specific immune stimulation. Non specific immune-stimulatory treatments, such as IL-2 (Atkins, 2002) and IFNα/β (Belardelli et al, 2002), are established therapies for advanced renal cell

carcinoma and malignant melanoma. The TLR7 agonist imiquimod is used for early skin cancers (Gaspari, 2007). In metastatic melanoma, an immunomodulatory drug – ipilimumab – has recently been shown to prolong overall survival (Hodi et al, 2010). The drug antagonises the function of CTLA4.

1.7.3. Tumour-infltrating lymphocytes

Histological studies of most tumours, including melanoma (Hom et al, 1991) show a T-cell infiltrate. This is unlikely to be an epiphenomenon as the density of the tumour-infiltrating-lymphocytes correlates with a favourable prognosis in a wide range of cancers:- head and neck squamous cell carcinoma (Pretscher et al., 2009), oesophageal cancer (Schumacher et al., 2001), squamous cervical carcinoma (Nedergaard et al., 2008), malignant melanoma (Taylor et al., 2007), ovarian cancer (Tomsova et al., 2008) and colorectal cancer (Katz et al., 2009).

The functionality of infiltrating lymphocytes is suggested by the observation that they only confer a better outcome if they are seen in an intratumoural rather than peritumoural location (Naito et al., 1998). Only TILs possessing activation markers (such as granzyme B (Van Houdt et al.,

2008) or CD69 expression (Badoual et al., 2006)) conferred a favourable prognosis. Analysis of TILs by gene expression profiling, in the setting of colorectal cancer, has proven to be more informative in terms of prognosis and need for adjuvant chemotherapy than the widely used TMN classification system (Galon et al., 2006).

1.7.4. Importance of the CD4 response in anti-tumour immunity

The anti-tumour immune response is an integrated and coordinated response that involves the full range of immune cells. The prime effector cell in immunosurveillance has been thought to be the cytotoxic CD8 T lymphocyte, as it possesses intracellular machinery that allows killing of target cells.

However, in the priming phase of the immune response the position of the CD4 helper T lymphocyte is a central one, and T_H cells may execute several effector functions of their own.

Mouse tumour vaccination-challenge models have demonstrated that depletion of the CD4 T lymphocyte subset at the time of

vaccination markedly attenuates the subsequent protection against tumour challenge.

Vaccination of B6 mice with autologous DC transfected with a gp100 plasmid using lipofectamine mediated protection against challenge with a gp100 transfected tumour (fibrosarcoma and plasmacytoma). However, CD4 depletion pre immunization abrogated protective responses. This suggests that CD4 cells may be involved in priming of the CD8 cytotoxic response (Yang et al., 1999).

The importance of CD4 T-cells is illustrated by findings that CD8 double knockout mice are able to mount a protective response to subcutaneous challenge with irradiated GM-CSF transduced B16 melanoma cells which,was significantly higher than that seen in CD4 $^{-/-}$ mice. Eosinophil recruitment requires CD4 help and the presence of tumour infiltrating eosinophils, and more specifically secretion of the toxic cationic basic protein, may be correlated with a less aggressive clinical course in several cancers including squamous cell carcinoma of the oral cavity (Falconieri et al., 2008).

Production of IFNγ from activated T_H cells leads to increased expression of inducible nitric oxide synthetase (iNOS) in tumour associated macrophages. NO has anti tumour effects in vivo and in vitro, some mediated by effects on the tumour vasculature. Secretion of highly toxic H_2O_2 or superoxide by macrophages is also T_H cell dependent and may have a role in antitumour immunity (Hung et al., 1998).

It is noted that many melanoma cells express very low levels of MHC Class I molecules but most do express MHC Class II molecules, at variable levels. This may make them more susceptible to Class II effectors.

The anti-tumour T helper response is interesting because, unlike the response to infectious pathogens which normally commits to either TH1 or TH2 pathways after 7-10 days post infection, it combines features of both (e.g. secretion of gamma interferon and IL4) for a prolonged period. This is sometimes known as the T_H0 response.

CD4 help also boosts opsonising antibody responses, and in DC, there is evidence that the unique ability to cross-present exogenously acquired antigen via the MHC Class I,

proteasomal pathway is dependent on the form of antigen that is available for uptake. Antigen as immune complexes is taken up more efficiently and leads to the generation of more Class I and II restricted peptide epitopes than free/soluble antigen (Schnurr et al., 2005).

It can also be envisaged that a humoural response against cell surface oncogenic proteins such as altered adhesion molecules or secreted molecules like matrix metalloproteases, involved in invasion and metastasis may limit tumour spread.

There is evidence that a subset of CD4 T helper cells may possess cytotoxic functions that are independent of CD8 T lymphocytes. Such cells have been detected in response to viral infections such as cytomegalovirus, human immunodeficiency virus and Epstein-Barr virus. The cytotoxic mechanism appears to be granule exocytosis of perforin and granzyme B. It is possible that cytotoxic CD4 cells represent a subset highly differentiated subset of frequently activated TH1 cells. Of particular relevance to

immunotherapy, EBV Latent Membrane Protein 1/2 specific CD4 T cell clones, with demonstrable cytotoxic activity in vitro, when administered to patients with EBV positive lymphomas resulted in durable disease remissions (Haigh et al., 2008 and Bollard et al., 2008).

Initiation of a cytotoxic T lymphocyte response requires the presence of CD4 helper T lymphocytes at the priming stage. There is a requirement for the CD4 T cell to recognise epitopes from the same antigen on the same antigen-presenting-cell as the CD8 cell receiving 'help'. However, the epitopes recognised are often different and CD4/CD8 recognition can be temporally and spatially distinct. Following dendritic cell capture of antigen, presentation of peptide-MHC complexes to CD4 T cells leads to enhanced CD40 ligand expression. Engagement of CD40 on DC stabilises and boosts the DC-CD8 interaction, allowing clonal expansion and development of effector functions.

1.7.5. Tumour promoting effects of chronic inflammatory cells

The presence of a chronic inflammatory infiltrate, characterised by cells of the innate immune system, is associated with a poorer outcome in cancer (Coussens and Werb, 2002). Tumour-associated macrophages secrete immunosuppressive cytokines (such as IL10 and IL4) that can inhibit tumour antigen specific Th1 responses, and proteases that aid tumour invasion and metastasis (Allavena et al., 2008). They also release pro-angiogenic factors. Myeloid derived suppressor cells also mediate a similar effect (Ostrand-Rosenberg and Sinha, 2009). MDSCs recruit regulatory T-lymphocytes and secrete soluble immunosuppressive cytokines. MDSCs also attenuate T-cell activation in the milieu of the tumour.

1.7.6. Tumour-associated antigens

A detailed analysis of TILs (in particular T-lymphocytes), circulating T-cells and of humoral responses to malignancy (often using the serological analysis of recombinant cDNA tissue libraries (Chen, 2000)) has led to the identification of numerous tumour-associated-antigens (Disis and Cheever, 1996). Despite the undeniable presence of T-cell responses to these tumour antigens, their overall efficacy must be modest, as eventually tumour escape and progression occurs in almost all cases.

One simple reason relates to the nature of the antigens. Viral tumour antigens (such as EBNA1 of Epstein-Barr Virus and human papillomavirus E6/E7 proteins) are foreign and therefore highly immunogenic, but other TAAs are self-proteins. A small proportion of these are oncogenic proteins by virtue of activating (e.g. k-RAS) or inactivating (e.g. p53) mutations. Mutated oncogenic proteins may also arise from chromosomal translocations Although the immune responses only occur in the presence of mutated proteins, the individual epitopes recognised are often from non-mutated, 'self' portions of the proteins.

However, most TAA are normal self-proteins that may be overexpressed or aberrantly expressed in malignancy; examples of these include differentiation antigens such as Melan-A, tyrosinase and gp100 in melanoma and cancer-testis antigens such as MAGEA1,2,3.

Thus, in view of immune tolerance, these TAAs are unlikely to elicit powerful immune responses. In fact, peripheral tolerance is mediated largely by regulatory T-cells. These cells, characterised by a CD4, CD25, FOXP3 positive immunophenotype, are able to actively suppress immune

responses against self-antigens in both contact dependent and independent manners (Waldmann and Cobbold, 2009). In the context of cancer, inverse correlations between T regulatory cell infiltrates and prognosis have been observed in numerous tumours – gastric cancer (Shen Z et al, 2010), chronic lymphocytic leukaemia (D'Arena et al, 2010), and colorectal cancer (Deng et al, 2010).

The categorisation of tumour-associated-antigens is summarised in Table 1.1.

1.7.7. Melanoma antigens

The melanoma differentiation antigens are present on both normal and malignant tissue (including retinal pigment epithelium) of the melanocytic lineage. CTL responses to these antigens recognise transformed and normal melanocytes (Anichini et al, 1993). The antigen group includes proteins with known enzymatic functions (tryosinase, tyrosinase-related-proteins 1 and 2), those with likely structural roles within melanosomes (gp100/PMEL17) and those without clearly defined functions (Mart1/Melan-A).

Table 1.1. Tumour associated antigens

Category	Examples	Immune responses
Viral	HPV E6 EBV EBNA1	CD4 Th1 helper cells (Welters, 2006) Decreased CD4 responses in EBV positive lymphomas (Heller et al., 2008)
Mutated	k-RAS p53 Bcl-Abl (fusion protein)	CD4 and CD8 T cell responses specific for point mutation (Gjertson et al., 1996) CD8 responses, HLA A2 restricted, some specific for point mutations (Ito et al., 2007) CD4 T cell responses specific for peptide spanning fusion region (Bosch et al., 1996)
Overexpressed	Her2Neu	CD8, HLA A2 restricted responses (Brossart, 1998)
Ectopically expressed (embryonic)	CT antigens MAGE family	CD8 HLA A2 restricted responses to MAGE-1 (Ottaviani, 2005)
Differentiation antigens	Tryosinase Gp100/PMEL17 Melan-A PSA	CD8 HLA A2 responses (Riley et al., 2001) and CD4 HLA DR15 (Kobayashi et al, 1998) HLA A2 CD8 responses (Bakker et al., 1995) and HLA DR7 and DR53 CD4 responses (Kobayashi et al., 2001) CD8 responses (HLA A2) (Kawakami et al., 1994) CD8 cytotoxic responses (HLA-A2) (Correale et al., 1997)
Abnormal post-translational modification	Mucin-1 (glycosylation)	HLA A2 CD8 response (Brossart, 1999).

Melan A is a small, type 1 transmembrane protein expressed in normal and malignant melanocytes. It is one of the most immunogenic melanocyte-differentiation antigens with T-cell responses being detectable in melanoma patients (Kawakami et al., 1994) and healthy donors (Pittet et al., 1999). The protein is found particularly in immature (Stages 1 and 2) melanosomes. It has no known enzymatic function, but may act as an escort or chaperone protein for other melanosomal protein including gp100 (Hoashi et al., 2005) and OA1 (Giordano et al., 2009).

A more detailed analysis of peptide epitope responses to this antigen in melanoma patients, using T2 cells pulsed with synthetic overlapping peptides as targets for CTL recognition, revealed that there was a highly immunodominant epitope spanning amino acids 26 to 35 of the protein sequence. Two HLA A-2 restricted epitopes 26-35 EAAGIGILTV and AAGIGILTV (27 to 35) are highly immunodominant (Kawakami et al, 1994). In direct ex-vivo analyses, Romero found that up to 30% of CD8 positive cells in tumour infiltrated lymph nodes (in metastatic melanoma) were Melan A 26-35 positive as assessed by tetramer staining. These cells were capable of in-vitro expansion upon cytokine exposure and the resultant cell lines were highly lytic against matched

targets including peptide-pulsed cells and autologous tumour cells (Romero et al., 1998).

Analysis of peptides that bind to HLA-A2 molecules (the commonest Class A haplotype in Caucasian populations) suggests that the optimum peptide length is 9 or 10 residues, and that important anchor residues are methionine or leucine at position 2 and valine at position 9 or 10. The 26-35 epitope (EAAGIGILTV) is therefore rather atypical, particularly with the negatively charged glutamic acid residue at position 1. Valmori et al (1998) demonstrated that HLA-A2 restricted TIL derived T cell clones specific for Melan A recognised the 27-35 epitope an order of magnitude less efficiently than the 26-35 epitope. Moreover, by making individual amino-acid substitutions it was shown than the 27 A→L peptide analogue had the highest HLA-A2 binding affinity in functional competition assays. The ELAGIGILTV analogue also had superior HLA binding kinetics and the peptide-HLA complex was stable over 6 hours as opposed to 1 hour for the unsubstituted 26/27-35 peptides. Functionally, the ability of Melan A specific TIL clones to recognise target cells pulsed with ELA was higher than when targets were pulsed with EAA, and the ability of the modified peptide to induce Melan A specific CTL in a PBMC population was also superior. Whilst the ELA analogue

may be useful for immunotherapeutic and vaccination purposes, it should be borne in mind that it does not exist in-vivo.

The immunodominance of the 26-35 epitope is striking and Melan A specific CD8 responses, whether in peripheral blood, metastatic lymph nodes or tumour itself are dominated by this epitope.

Gp100/PMEL17 is also a melanosome-associated protein. It is highly expressed in later stage melanosomes (Hoashi et al., 2005), where it forms a structural, fibrillar framework for the subsequent deposition of melanin pigment. In contrast to the immunodominance of Melan A 26-35, several HLA A2 restricted epitopes have been discovered. Although T-cell responses to gp100 are common in melanoma patients, they are very rare in healthy donors. Sequences within gp100 that lead to the melanosomal or endolysosomal localisation of the protein have been identified (Lepage and Lapointe, 2006). MHC Class II restricted presentation of gp100 epitopes is also dependent on these sequences (Robila et al., 2008).

1.7.8. Tumour-mediated immunosuppression.

Active tumour-driven immunosuppressive mechanisms do exist. The tumour microenvironment, which encompasses endothelial, vascular, immune and stromal cells as well as malignant cells themselves, actively produces immunomodulatory substances that can have negative effects on both infiltrating T lymphocytes and on local dendritic cells (Gajewski et al., 2006).

An important mediator of immunosuppressive effects in the tumour microenvironment is transforming growth factor beta (TGFβ) (Disis, 2009). It favours the generation of regulatory T cell responses over cytotoxic T cell responses (Li and Flavell, 2008) and may blunt high avidity CTL responses by reducing IL12 and 15 production (Sanjabi et al, 2009).

In antigen-specific vaccination for cancer, it is often observed that an expansion of CD4 or CD8 T cells specific for the antigen can be achieved in blood. However, the frequency of clinical responses is much lower. This may relate to suboptimal recruitment and movement of T lymphocytes from the circulation or lymphatic system into

tumour masses (Lee et al, 1999). Aberrant patterns of expression of chemokines and adhesion molecules may be responsible (Adams et al., 1997).

Despite these numerous impediments to T-cell recruitment to tumour sites, Tumour-Infiltrating-Lymphocytes are readily detected in almost all tumour types. However, the cells generally show multiple functional deficits compared to circulating lymphocytes and are blunted in effector function (Appay et al., 2006).

In the same context of metastatic melanoma, Zippelius et al (2004) show appreciable frequencies of Melan A $_{26-35}$ specific CD8 T cells in three locations – in increasing order – peripheral blood, metastatic lymph nodes and visceral metastases. The majority of cells were antigen experienced, in contrast to the naive cells found in PBMC of healthy donors. T-cell clones derived from metastatic lymph nodes demonstrated high T-cell receptor avidity. However, crucially, in both metastatic lymph nodes and visceral metastases specific T-cells showed reduced IFNγ release in short term stimulation assays compared with circulating cells, even though the response to non-specific stimulation

was preserved. Cells from metastatic lymph nodes additionally displayed deficient perforin expression. When cells were cultured in the presence of IL2 or IL7 in-vitro, cytolytic capacity was rapidly restored.

The widespread expression of programmed death ligand-1 (PD-L1) on various cancer cells leads to engagement of the PD-1 receptor on T-lymphocytes (Dong et al, 2003). This receptor is upregulated on activated T-cells and functions as a brake on immune responses (Latchman et al, 2001)

The enzyme IDO is overexpressed in the tumour microenvironment, although the cell of origin remains unclear and malignant, vascular, stromal, myeloid-derived suppressor (Meisel et al, 2004) and immature dendritic cells (Munn et al, 2002) may all make a contribution. IDO catalyses the degradation of the amino acid tryptophan to catabolites including quinolinic acid, L-kynurenine and picolinic acid. These metabolites have a pro-apoptotic effect on T-cells and tryptophan depletion places a proliferative block on activated T-cells (Frumento et al, 2002). In colorectal cancer, high IDO expression by tumour cells correlated inversely with overall survival and density

of CD3 positive T-cell infiltrate and positively with likelihood of metastatic disease (Brandacher et al, 2006).

Most tumours are poorly immunogenic by virtue of downregulation of surface HLA molecules and lack of co-stimulation (Gilboa, 1999). Epigenetic changes, for example in promoter methylation state, may drive HLA downregulation (Nie et al., 2001). Aside from HLA molecules themselves, loss of the Class I associated protein β2M and mutations of LMP2/7 and TAP can be associated with tumour immune escape (Restifo et al., 1996 and Marincola et al., 2000).

Other important tumour derived substances that have suppressive effects on DC maturation or T-cell activation include Suppressor-of-Cytokine signalling-1 (SOCS-1) (Evel-Kabler et al., 2006), STAT3 (Cheng et al., 2003) and L-galectin (Perillo et al., 1995).

In summary, as discussed above, tumour antigen specific T-cell responses are detectable ex-vivo from the blood of cancer patients. However, due to tumour driven immunosuppressive mechanisms (illustrated in Figure 1.4),
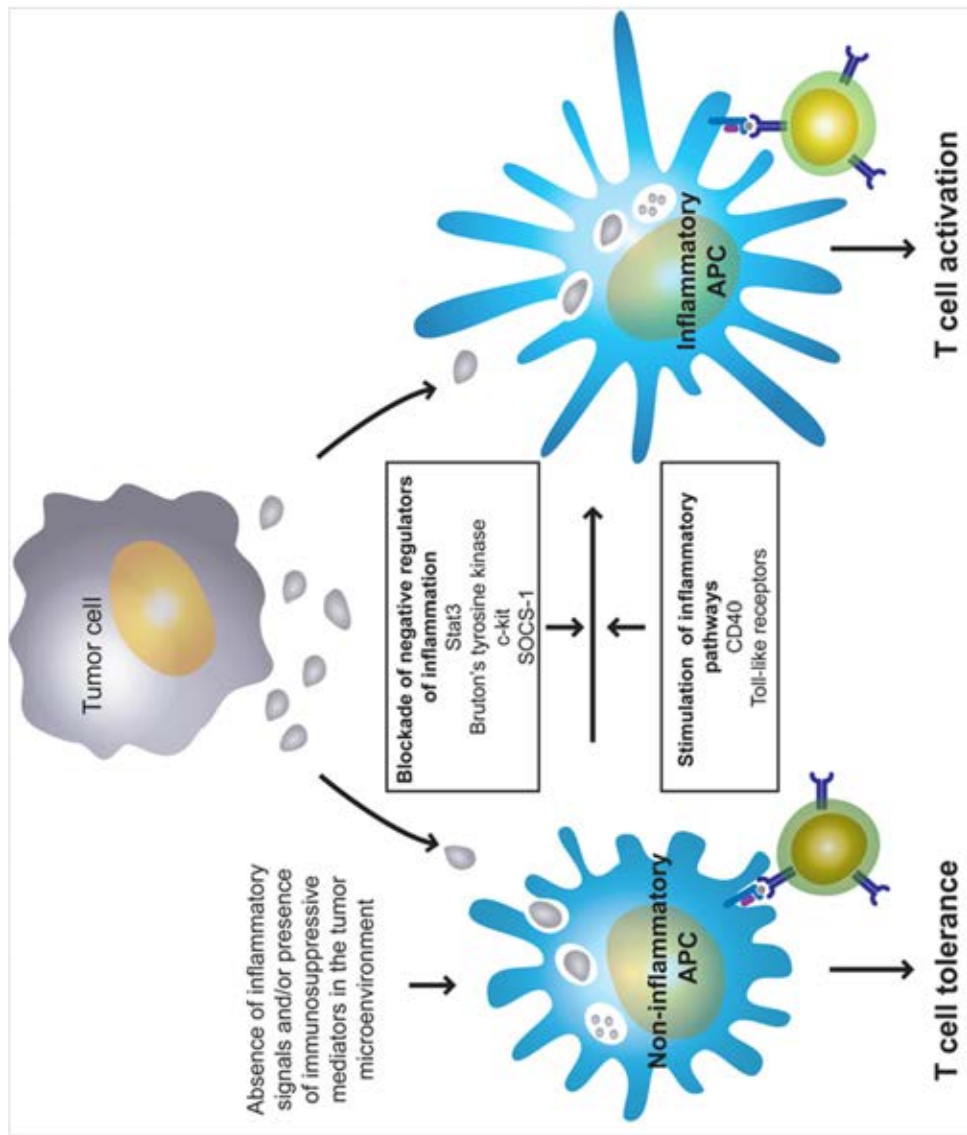
Figure 1.4a. **Tumour mediated immunosuppression: role of DCs.** This figure illustrates the crucial role played by the interaction between tumour cell derived factors and dendritic cells. Factors such as Stat3 and SOCS1 encourage recruitment of immunosuppressive/tolerogenic DCs whereas CD40 ligation and toll-like receptor stimulation drive immunogenic DCs that lead to anti tumour T-cell responses. Reproduced from Rabinovich et al (2007)

Figure 1.4b. **Tumour driven immunosuppression – summary.** This figure illustrates the innumerable mechanisms by which tumour cells actively suppress and evade immune responses. These include soluble factors such as IL10 and TGFβ that impair DC activation as well as alterations in tryptophan metabolism, MHC Class I processing and costimulatory activity. Reproduced from Rabinovich et al (2007).

these responses are not highly efficacious in eradication of established malignancy. The partial and incomplete activation of tumour infiltrating DC plays a key role in this. This forms the rationale behind the development of immunotherapeutic approaches to cancer that attempt to enhance and augment tumour-specific immune responses. These specific immunotherapies include: adoptive transfer of T-lymphocyte clones and antigen specific vaccination.

1.7.9. Clinical studies of DC vaccination

As discussed earlier, in-vitro derived DC can be loaded with antigens in many ways. Here, the focus is on clinical use of nucleic acid transfection with defined, rather than bulk, tumour antigens.

A summary of clinical trials of DC vaccination for cancer with vaccine cells transfected with nucleic acid encoding whole antigen is presented in Tables 1.2 A and B.

Table 1.2A. Summary of clinical trials of RNA transfected DC vaccines for cancer

Patients	DC generation	Maturation stimulus	Vaccine properties	Antigen expression	Immune effects	Clinical effects	Reference
Single case of IIIB ovarian cancer (heavily pre-treated)	MoDC (adherence) RNA electro-poration – FRα	IL1β, TNFα, IL6, PGE2	Not described	80-85% FR-α positive	30 and 15 fold induction of FR-α specific CD8 and CD4 T-cells	Durable partial response on imaging and Ca125	Hernando (2007)
Metastatic prostate cancer	MoDC (adherence, leukapheresis) Coincubation with PSA RNA	No maturation stimulus	Not assessed	Not assessed	Increase in frequency of PSA specific T-cells related to DC dose	1/7 – ↓PSA, 6/7 – ↓PSA velocity, 2/3 – transient ↓ circulating tumour cells	Heiser (2002)
Metastatic prostate cancer	MoDC (adherence), electroporation of hTERT±LAMP1 RNA	TNFα, IL1β, PGE2, IL6	MHC I and II high, CD83 and 86 high	Not assessed	↑hTERT specific CD8 cells, ↑CD4 cells (LAMP1), ↑T cell sensitivity	No objective responses, ↓ PSA velocity, transient ↓ circulating tumour cells	Su (2005)
CEA expressing cancers	MoDC (leukapheresis, adherence), co-incubation with CEA RNA	No maturation stimulus	CD14 low, CD86 high, HLA DR high	Not assessed	Not assessed	3/24 – disease response, 3/24 stable disease	Morse (2003)
Resected pancreatic cancer (post chemo-RT and surgery)	MoDC (leukapheresis, adherence), co-incubation with CEA RNA	No maturation stimulus	CD14 low, DR high, CD86 high	Not assessed	Increased DTH reactions to CEA in all patients	Prolonged disease free survival (>4 years)	Morse (2002)

Patients and route of administration	DC generation	Maturation stimulus	Vaccine properties	Antigen expression	Immune effects	Clinical effects	Reference
Stage IIIB (irresectable)/IV melanoma. Intravenous and intradermal administration of DC	CD14 selection of leukopharesis products, mRNA transfection of CD70, CD40L and caTLR4 and TAA with li tag	TNFa, IL1b, PGE2 and IL6	CD40, CD80, CD86 and Class I/II high, CD83 moderate	Not formally measured (Class II targeting sequence)	12/21 had antigen specific T-cells in DTH sites	0/17 clinical responses with DC alone, 1 PR and 5 SD (of 18) with IFNa SC after vaccination	Wilgenhof et al (2011)
Colorectal cancer with resectable liver metastasis	Monocyte adherence, electroporation with RNA in mature state vs peptide-loading	TNFa, IL1b, PGE2 and IL6	Not assessed	Not measured	8/11 patients had peptide specific T-cell response in DTH sites, 0/5 had CEA specific responses after RNA transfection	Not assessed (resectable metastases)	Lesterhuis et al (2010)
Acute myeloid leukaemia with response to chemotherapy but high risk of relapse. Intradermal administration	Leucopharesis, CD14 selection, electroporated with WT1 RNA as mature cells	TNFa, IL1b, PGE2, IL6	CD80, CD86, HLA 1 and 2 high	Not assessed	↑plasma IL2, ↑activated NK cells, no change in WT1 IgG levels, 2/5 ↑ WT1 specific CD8 by tetramer	2/10 patients from partial to complete remission, 4/10 from complete to molecular remission (transient)	Van Tendeloo (2010)
Hormone refractory prostate cancer. Intradermal and nodal administration	Negative selection from PBMC, electroporated with RNA from 3 prostate ca cell lines.	PGE2, IL1b, IL6, TNFa	CD83 variable, CD86, HLA II high, CD14 low	Assessed using in-parralel experiments with eGFP	↑ frequency IFNg secreting T-cells post vaccination (ELISPOT with mock/transfected DC)	No objective response on bone scan, 13/19 had reduced PSA velocity	Mu 2005

Table 1.2B. Summary of clinical trials of DNA transfected DC vaccines for cancer.

Patients	DC generation	Maturation stimulus	Vaccine properties	Antigen expression	Immune effects	Clinical effects	Reference
Ampullary, breast and pancreatic cancer	MoDC (adherence), Cationic lipids transfection of cDNA – MUC1	No exogenous maturation stimulus	Prior to administration, CD1a, 80, 83, 86, HLA DR positive	Variable % MUC1 positive cells – 2-52% - no relation to response	↑ MUC1 specific CD8 cells, DTH response to MUC1	1/10 patients – stable disease, 9/10 – disease progression	Pecher (2002)
Metastatic melanoma (Stage IV)	MoDC (adherence), CL22 peptide transfection of cDNA – Melan-A and gp100	TNFα and IL1β, no IL6 or PGE₂ were used	CD1a high, CD83 and 86 high, CD14 low, CCR7 intermediate	Flow cytometry – Melan A <10% , gp100 1-96% positive cells – highly variable	Consistent ↑ frequency of CD8 and CD4 T-cells to both antigens relative to viral responses, ↑ T-cell response to whole antigen	4/22 patients – clinical response by RECIST criteria	Steele (2011)

Several observations can be drawn from these studies. First, these are all exploratory Phase I and II trials and the absence of a matched, untreated control group makes it impossible to draw definite conclusions regarding clinical efficacy. Second, immunologic responses to vaccination have been more impressive than clinical responses. Third, in terms of vaccine characterisation, all studies report the immunophenotype, yield and viability of cells prior to re-administration. However, only two of the studies measure the level of transgene expression in transfected DCs and the importance of this parameter in determining vaccine immunogenicity remains unexplored. Fourth, not all studies specifically address the enhancement of CD4, MHC Class II restricted responses. Finally, a plethora of different transfection strategies have been employed and there is no consensus over which method is the most effective, although most recent in-vitro studies of DC vaccination focus on RNA electroporation.

There was a recent breakthrough in the field of ex-vivo generated DC vaccines for cancer with the approval by regulatory authories in the United States of 'Sipuleucel-T' for prostate cancer. This is an autologous cellular product designed to stimulate protective T-cell immunity against prostatic acid phosphatise, an enzyme only expressed in prostatic tissue. It is a vaccine approach although the

85

nature of the vaccine is essentially uncharacterised. It is prepared from autologous PBMCs co-incubated with a fusion protein of GM-CSF with prostatic acid phosphatise, making it likely that the differentiation of antigen-presenting-cells is encouraged (Small et al., 2000). These may be DC like cells. Unlike other vaccination approaches, randomised Phase III trials have been carried out and meaningful endpoints including progression free and overall survival have been studied, rather than surrogates such as PSA velocity (Higano et al., 2009). Sipuleucel-T treatment is associated with an overall extension of survival of 4-5 months (Small et al., 2006). There was an 8 fold amplification of T-cell responses to PAP, although only a small subset of patients were analysed. Whilst not strictly speaking a DC vaccine, this approach paves the way for the expansion of DC vaccination and testing in randomised trials.

1.8. Rationale and Aims

Methods for in-vitro generation of DCs from peripheral blood monocytes have been available for well over a decade (Sallusto and Lanzavecchia, 1994). During this time, DCs have been used in the clinical context as cellular vaccines for many, usually advanced, malignancies (Nestle et al., 2005).

The outcome of clinical trials of DC vaccination has not been overwhelmingly encouraging. On the one hand, monitoring of immune responses against vaccinated antigen has generally shown upregulation of responses and sometimes epitope spreading. In contrast, long-lived, durable objective tumour regressions have been very rare (Rosenberg et al., 2004). This may reflect the advanced stage of tumour growth, where the balance is heavily in favour of the tumour cells in tumour immunosurveillance. Also, in these trials DC vaccination has been used in isolation, and combination with other immunomodulatory strategies such as CTLA-4 blockade (Hodi et al., 2010 and Phan et al., 2003) or selective depletion of regulatory T-cells may improve response rates.

Individual clinical-grade DC vaccines have been highly variable in terms of DC generation method, selection of antigen and antigen loading strategy, maturation stimulus used and route of administration; perhaps contributing to the heterogeneity of observed outcomes (Figdor et al, 2004). Quality control of DC vaccines is therefore a crucial aspect of the development pathway and for transfected DC vaccines expressing whole antigen the importance of whole antigen detection remains uncertain.

1.8.1 Phase I/II trial of a dendritic cell vaccine transfected with DNA encoding melan A and gp100 for patients with metastatic melanoma

Recently, metastatic (Stage IV) melanoma patients were treated with an autologous DC vaccine expressing whole antigen following transfection of plasmid DNA using a novel cationic peptide – CL22 (Steele et al., 2011). Clinical responses were observed in a small subset (approximately 15%) of patients. Overall, T-cell responses to a range of Class I and Class II restricted epitopes from the two antigens (Melan A/MART-1 and gp100/PMEL17) increased in frequency across vaccination cycles. This was antigen-specific as IFNγ responses to viral recall epitopes remained

static in comparison. The DC vaccine was characterised by assessment of surface markers of maturation and intracellular antibody staining for Melan A and gp100 protein 48 hours after transfection (just prior to re-administration).

The proportion of DCs expressing either antigen was highly variable both between and within patients as shown in Figure 1.5 for gp100 and Melan-A. The key observation was that, on a patient-by-patient basis, there was no evidence of correlation between antigen-positivity of DCs and subsequent clinical or immunological outcomes. The question therefore arises whether whole antigen detection at 48 hours after transfection is a surrogate marker of DC immunogenicity or not, and if not, what other possible markers might be of use.

As mentioned above, IFNγ ELISPOT assays demonstrated an overall increase in frequency of responses to Class II restricted epitopes from both antigens. It should be noted that the number of know Class II restricted peptide epitopes was relatively modest. Pre-clinical work using the transfection system used in this trial had only formally demonstrated presentation of Class I restricted viral
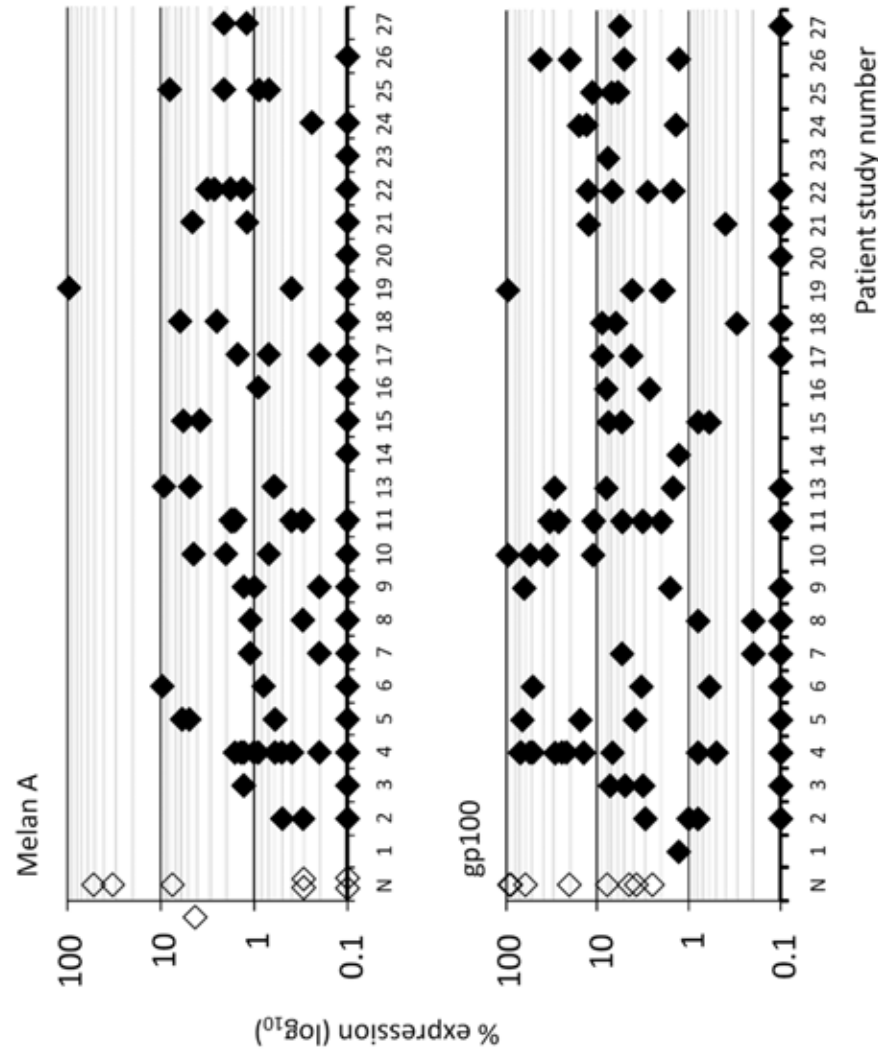
Figure 1.5. **Whole antigen expression in CL22 transfected dendritic cells in the melanoma clinical trial and in normal healthy volunteers (N).** 48 hours after CL22 transfection and maturation dendritic cells were fixed, permeabilised and stained with mouse monoclonal antibodies directed against Melan A and gp100 folllowed by goat anti mouse phycoerythrin conjugated secondary antibodies. PE fluorescence was analysed by flow cytometry. Background (non-specific) fluorescence was set using negative control antibodies. Reproduced from Steele et al (2011).

epitopes by DCs in-vitro. There was circumstantial, indirect evidence for Class II presentation however as mice immunised with transfected DCs mounted IgG responses to the antigens, suggesting T helper cell involvement (Irvine et al., 2000).

1.8.2. Aims

The aims of the project were as follows:-

1. **To investigate antigen presentation in DC using CL22 peptide mediated transfection of plasmid DNA**

    a. Determine whether or not vaccination as part of the clinical trial led to upregulation of IgG responses against gp100 and Melan-A

    b. Determine the presence and level of Melan A $_{26-35}$ and gp100 $_{280-288}$ HLA A2 restricted peptide display on patients' transfected DC preparations

    c. To demonstrate whether or not simultaneous presentation of Class I and II restricted epitopes from endogenously produced antigen in CL22 transfected DCs occurs

    d. To ascertain whether or not plasmid transfection into DCs using CL22 peptide leads to activating or maturation-enhancing effects on DCs.

e. To determine the relative immunogenicity of CL22 peptide transfected in comparison with other nucleic acid transfection methods.

2. **To investigate the relationship beween epitope presentation focussing on Class I restricted epitopes and whole antigen detection in transfected vaccine DCs.**

   a. To determine the importance of whole antigen detection in immunogenicity and antigenicity

   b. To determine, if whole antigen detection seems irrelevant, what other measurements might be suitable surrogate markers of immunogenicity

   c. To determine whether or not this relationship between antigen detection and epitope presentation is a general feature of DC biology or is antigen-specific

3. **To investigate the relationship between the properties of antigen and its ability to be presented via the MHC class II pathway in transfected vaccine DC**

   a. To determine if the nature of antigen – viral (EBNA1) or self antigen (Melan-A, gp100) affects Class II presentation

b. To determine whether or not cellular localisation of antigen (EBNA1) affects the ability to access the Class II pathway

c. If Class II presentation of endogenously synthesised antigen is detectable – determine the mechanism (secretion and reuptake, autophagy)

d. To determine whether the kinetics of Class II restricted epitope presentation differ from those of Class I presentation

e. To determine whether mode of transfection or antigen dose affect Class II restricted presentation.

CHAPTER 2: METHODS

2.1. Generation of immature dendritic cells

Blood was drawn from laboratory volunteers into heparinised syringes (10 units unfractionated heparin per ml). Donors had previously had HLA haplotyping performed by PCR. Blood was mixed in a 1:1 (v/v) ratio with warm RPMI 1640 medium (Invitrogen). After thorough mixing, diluted blood (30ml per tube) was carefully layered on top of 15mls of Ficoll-lymphoprep (Axis-Shield) in 50ml centrifuge tubes. Tubes were centrifuged at 300G rpm with the brake off for 30 minutes. Using Pasteur pipettes, the interface cells were aspirated and transferred to new tubes. PBMC were washed three times with RPMI 1640 medium. PBMC were resuspended in a small volume of standard medium (RPMI 1640 supplemented with 10% v/v fetal calf serum, 1% v/v penicillin-streptomycin and 1% L-glutamine (both Invitrogen), filter-sterilised before use). Viability counts were performed using Trypan blue exclusion. Typically, 0.75-1.5 x 10^6 PBMC were obtained per ml of whole blood. Up to 6 x 10^7 PBMC were resuspended in 20 mls of standard medium, mixed well by pipetting and added to 75cm^2 tissue culture flasks which were incubated flat for 2 hours at 37°C and 5% CO_2. Flasks were removed from the incubator and loosely adherent cells were gently removed by gentle pipetting and collected in a

separate 50ml tube. The base of the flask was rinsed gently with 10ml warm standard medium twice to minimise contamination of adherent monocytes with lymphocytes. The non-adherent cell fraction was either discarded or cryoperserved . 20ml of cytokine supplemented standard medium (500 IU/ml recombinant human IL4 (R and D systems) and GM-CSF (Queen Elizabeth Hospital Pharmacy)) was added to each 75 cm^2 flask and these were then returned to the incubator for 5 days.

Buffy-coat samples from the National Blood Service were occasionally used for DC generation, particularly when knowledge of HLA haplotypes was unnecessary and larger DC yields were required. PBMC isolation was performed as described above with the addition of sterile filtering (0.33 μM) to remove clumps of cellular debris.

On day 5, cells were harvested thoroughly. Viability counts were performed and an estimate was made of the relative proportion of dendritic cells and contaminating lymphocytes by morphology. The percentage of lymphocytes ranged from 20-40%. At this point, cells were used for nucleic acid transfection. However, in most experiments, a small proportion of immature DCs were transferred directly to DC maturation medium (standard medium supplemented with GM-CSF

and IL4 (500 IU/ml) and TNFa and IL1b). After transfection, all DC were transferred into maturation medium before incubation for 24-48 hours prior to further assays.

2.2. Dendritic cell transfections

2.2.1. CL22 mediated transfection

This technique was identical to Steele et al (2011), except that fewer DC were used per transfection. Transfection reagents were unused clinical grade products and had been stored at -80°C. Immature DCs were washed twice with RPMI 1640 and resuspended in RPMI medium at 1.2 x10^6 cells/ml. Hepes Buffered saline (HBS) was used dilute the CL22 peptide to a concentration of 92 μg/ml and plasmid DNA was diluted to 40 μg/ml. Concentrations were verified by spectrophotometry (Nanodrop). Diluted DNA and CL22 peptide were gently mixed by pipetting and DNA:peptide complexes were allowed to form for 1 hour at room temperature. Depending on the number of DCs available for transfection, the DNA:peptide mixture was added to multiwell plates: 1.5 x 10^6 DC/transfection – 12 well plate – 250ul DNA:peptide and 1.25ml of cellular suspension, 7.5 x 10^5 DC/transfection – 24 well plate – 125 ul DNA:peptide and 750ul cellular suspension. Cells were added dropwise to DNA:peptide mix. Chloroquine (QE Hospital Pharmacy) was added to each well at

a final concentration of 40μM. Plates were gently agitated before being centrifuged at 150G for 5 minutes. Plates were transferred to the incubator for 90 minutes post transfection. Transfection medium was gently removed and maturation medium (see above) was added (1.5ml for 12 well plates, and 750 ul for 24 well plates), and plates were incubated until further analysis.

2.2.2. Nucleofection of plasmid DNA or RNA.

This was performed as per the manufacturer's instructions. DC (mature or immature) were counted and $0.5-2 \times 10^6$ DCs per nucleofection were centrifuged and the supernatant was completely removed. Human DC nucleofector solution was mixed with nucleofector supplement (18μl supplement and 82 microlitres nucleofector solution per nucleofection) and left to warm to room temperature for at 30 minutes. The DC pellet was resuspended in supplemented nucleofector solution and plasmid DNA or in-vitro transcribed RNA (1μg nucleic acid per 0.5×10^6 cells) was added. Cells and nucleic acid were mixed and transferred to the Amaxa cuvettes. Cells were nucleofected using the U-02 programme on the Nucleofector I device. After nucleofection, cuvettes were very gently removed and 500 μl prewarmed maturation medium was gently added on top of the cell pellet. Cells were then

carefully transferred to either 12 or 24 well plates pre-filled with warm maturation medium (500ul for 24 well plate, 1ml for 12 well plates).   Cells were transferred to the incubator prior to further analysis.

2.2.3. Electroporation of in-vitro transcribed RNA.

In vitro transcribed RNA was stored in 2 µg aliquots at -80°C. For each RNA transfection, a single aliquot was thawed at room temperature immediately before use. Concentration of RNA was re-checked by spectrophotometry. DC for transfection (typically 0.5-2 x 10^6 cells) were washed once with warm sterile phosphate-buffered-saline (PBS) and then with warm serum free medium (OPTImem, Invitrogen). Cells were resuspended in 300µl OPTImem and RNA was added (2µg per 10^6 DC). After mixing, DCs and RNA were transferred to 4mm electroporation cuvettes (Cell Projects). Cuvettes were placed into a Genepulser electroporation machine (Biorad) and electroporated (square wave) at 300V and 500µF. The typical time constant obtained for DCs was 15-20 milliseconds. These electrical settings were obtained from the methods of Landi (2007) and did not require further optimisation as initial experiments with GFP encoding RNA showed high GFP expression and excellent cellular viability (>90%). After electroporation, 300 µl prewarmed maturation

medium was added to cuvettes dropwise and cells were gently transferred to wells prefilled with maturation medium (total volume 1.6ml in 24 well plates). Transfected DC were incubated until further analysis was performed.

2.3. Peptide loading of dendritic cells

Alongside transfection of DCs, loading of mature DC with exogenous peptide was performed as a positive control for DC integrity and T-cell functionality. DC were washed twice with RPMI 1640 (serum free) and resuspended in 100µl of RPMI. Previous work at this institution had suggested that peptide loading is most efficient in serum-free conditions (G.Taylor, personal communication). Synthetic peptide epitopes (dissolved in dimethylsulphoxide (DMSO)) were available in-house. They were stored at -20°C. Peptides were added to cells at a final concentration of 5µg/ml (≈5µM). As a negative control, an equivalent volume of DMSO was added. DCs were returned to the incubator for 90 minutes, during which time, tubes were agitated every 30 minutes. At 90 minutes, cells were washed with standard medium twice to remove unbound peptide before use in assays.

2.4. Cryopreservation and thawing of cells

Cells were frozen at a maximum density of 2×10^7 cells/vial. Cells were centrifuged and resuspended in 500μl fetal bovine serum per vial. They were then placed on ice for 10 minutes alongside freezing mix (20% DMSO in FCS (v/v)). An equivalent volume of freezing mix was added dropwise and cells were transferred to cryotubes (Nunc, Denmark) – 1ml cell suspension per tube. Tubes were transferred to isopropanol filled containers and then to a -80°C freezer for short-term storage. If long-term cryopreservation was needed, tubes were moved to liquid nitrogen storage (-180°C).

Cells were thawed as follows. Vials were placed in a 37° waterbath for 2-3 minutes. Just before the last ice crystal melted, they were removed and warmed standard medium was added dropwise with continual agitation. Cells were washed twice with standard medium to remove excess DMSO before use.

2.5. Generation of in vitro transcribed RNA.

2.5.1. Linearisation of plasmid DNA

Plasmid DNA was the substrate for RNA synthesis. Plasmid maps were inspected for unique restriction sites just distal to the inserted DNA coding sequence. Plasmid DNA was then digested with the appropriate enzyme. Typically, digests were set up in 100μl microcentrifuge tubes as follows: 4μg

plasmid DNA, 20 units of restriction enzyme, 4μl buffer (x10) and sufficient ultrapure water to make a total reaction volume of 40μl. Reagents were mixed and incubated in a 37°C waterbath for 90 minutes. Control digests (lacking enzyme) were set up in parallel. Approximately 8μl was used for analysis.   The reaction products were separated by electrophoresis on an agarose gel (0.8%) and were stained with ethidium bromide for visualisation.   If a clear difference in electrophoretic mobility (reflecting linearised versus circular plasmid) was observed, DNA was purified with the use of a PCR clean up kit (Roche) according to manufacturer's instructions. DNA was eluted in 100μl elution buffer (DNAase and RNAase free). DNA was quantitated on a Nanodrop spectrophotometer. Typically, the yield was 75%.

2.5.2. RNA synthesis

10μl 3M sodium acetate (pH 5.5 – RNAase free, Ambion) was added to DNA.   250μl absolute ethanol (pre-cooled at -20°C) was added and the solution mixed well.   The tubes were centrifuged at 13,000 rpm for 15 minutes at 4°C. Supernatant was very carefully removed and 500μl 70% v/v ethanol (with DEPC-treated water) was added.   Tubes were centrifuged at 13,000 rpm for 3 minutes, supernatant were removed and

pellets were allowed to air dry. DNA pellets were resuspended in 18μl RNAase-free water. The in-vitro transcription reaction was set up as follows:

Reagent	Volume (μl)
DNA	18
NTP/CAP (nucleotides, capped)	30
10x reaction buffer	6
RNA polymerase enzyme mix	6

All in-vitro transcription reagents were part of the mMessagemMachine kit from Ambion. Kits had been stored at -20°C. After reactions had been set up and mixed, tubes were incubated at 37°C for 60 minutes. 3μl TURBO DNAase enzyme was then added to destroy template DNA and tubes were incubated for a further 15 minutes. RNA was purified from the reaction using the RNEasy Mini Kit (Qiagen). At the RNA elution stage, to maximise RNA concentration, RNA was eluted twice in the same 30μl of elution buffer. RNA yield and purity were determined by spectrophotometry. Typical yields of RNA from 4ug of plasmid DNA ranged from 20-80μg.

2.5.3. Polyadenylation of in-vitro transcribed RNA

RNAs were polyadenylated using the USB Yeast Poly (A) polymerase kit, as per manufacturer's instructions. The reaction was carried out for 20 minutes at 37°C. 275μl DEPC-

treated water were added to the 25µl polyadenylated RNA. An equivalent volume of phenol-chloroform was added and after brief vortexing to mix, tubes were centrifuged at 13,000 rpm for 10 minutes at 4°C. The aqueous layer was aspirated off into a new tube. 10% (v/v) 3M sodium acetate was added, followed by 250% (v/v) absolute ethanol (pre-cooled to -20°C). After mixing, samples were cooled for 30 minutes at -80°C. They were centrifuged at 13,000 rpm for 20 minutes at 4°C, pellets were washed with 500µl 70% (v/v) ethanol and then air-dried. RNA was resuspended in 20µl of DEPC-treated water and quantitated on a spectrophotometer, before being stored in small aliquots. As a check on polyadenylation and integrity of RNA, pre and post polyadenylation RNAs were separated by electrophoresis on 0.75% agarose gels. In all cases, there was a difference in mobility after polyadenylation and discrete bands were seen.

2.6 Surface and intraceullar staining of dendritic cells – flow cytometry

For surface staining, 10^4-10^5 DC were used per stain. The DC were washed once with FACS buffer (PBS with 1% BSA and 0.05% sodium azide). The pellet was resuspended in 480ul FACS buffer and mixed with 120ul purified polyclonal mouse IgG (Serotec). Cells were then left on ice for 30 minutes to block surface Fc receptors. 50µl cell suspension was

transferred to each well on a V-bottomed 96 well plate. 5ul
of antibody solution was added per well and cells and
antibody were mixed by pipetting. Antibodies used are
summarised below:

Specificity	Conjugate	Isotype	Supplier
Human CD1a	Phycoerythrin	IgG1	BD Pharmingen
Non-specific	Phycoerythrin	IgG1	BD Pharmingen
Human CCR7	Phycoerythrin	IgG2a	R and D systems
Non-specific	Phycoerythrin	IgG2a	R and D systems
Human CD14	Phycoerythrin	IgG1	Serotec
Human CD83	Phycoerythrin	IgG1	Serotec
Human CD86	Phycoerythrin	IgG1	Serotec
Human CD25	Phycoerythrin	IgG1	Serotec
Non-specific	Phycoerythrin	IgG1	Serotec

Cells and antibodies were incubated for 30 minutes at room
temperature. Cells were washed twice with cold FACS buffer
and resuspended in 150 μl sterile PBS. Cells were
transferred into 7ml tubes containing 350μl sterile PBS and
500ul samples were used for flow cytometric analysis.
Phycoerythrin fluorescence was measured on the FL1 channel
and background fluorescence was set as 1-2% PE positive
cells on DCs stained with isotype-matched non-specific
antibodies. At least 5000 gated events were counted. For
intracellular staining, after incubation with purified mouse
IgG, cells were resuspended in 50ul FACS buffer and 100ul of
Reagent 1 (IntraPrep permeabilisation kit, Beckman Coulter)
before immediate vigorous mixing and incubation for 15

minutes at room temperature. Cells were washed with sterile

PBS before 100ul reagent 2 was gently added on top of cell

pellets. After 5 minutes, tubes were gently agitated and

stained proceeded as above.

2.7. Intracellular staining of dendritic cells – fluorescence microscopy

$2-3x10^5$ DC were used per stain. DC were washed with PBS

twice to remove medium. Cells were resuspended in 50μl PBS

and incubated on ice for 15 minutes. The DC suspension was

added to warm (37C) polyethylene coated microscopy slides;

these were returned to 37C for 15 minutes. This maximises

DC adherence. Cells were fixed with 4% v/v paraformaldehyde

for 10 minutes at room temperature, washed once with PBS and

then permeabilised with 0.1% v/v Triton X100 for 5 minutes.

Non-specific reactivity was blocked with 50μl 20% HINGS

(heat-inactivated-normal-goat-serum) per spot for 15 minutes

at room temperature. HINGS was removed by pipetting and

primary antibody (EBNA1 – R4 rabbit polyclonal antibody at

1/1000 dilution, Melan-A and gp100 – A103 and HMB45 mouse

monoclonal antibodies at 1/100 dilutions) was added at 30μl

per spot. Primary antibody incubation was for 1 hours in

humidified chambers at 37C as was secondary antibody

incubation (EBNA1 – 1/1000 goat anti rabbit Alexa 594,

Melan-A and gp100 – goat anti mouse Alexa 488). After extensive washes, cell nuclei were stained with DAPI (4',6-diamidino-2-phenylindole) and single drops of 90% v/v glycerol were added to spots before viewing under a fluorescence microscope (Nikon E600). Representative images are presented for red/green (antibody) and blue (DAPI) fluorescence filters.

2.8. Measurement of IFNγ release: ELISPOT assays.

The human IFNγ ELIspot kit (Mabtech, Denmark) was used according to manufacturer's instructions. PBS was syringe filtered. ELISPOT plates (Mabtech, Denmark) were filled with 50 µl/well of 70% ethanol for 1 minute at room temperature and then washed twice with 200µl per well filtered PBS. Diluted capture antibody (human IFNγ specific, 1D1K) at 7.5µg/ml in PBS was then added - 50µl per well. Plates were incubated at 4C overnight. Primary antibody was removed and wells were washed with pre-warmed RPMI 1640 medium 6 times. Wells were filled with 200µl complete medium (10% FCS) and incubated for 3 hours at 37C to minimise non-specific binding. During this time, target and effector cells were prepared in complete medium at the required cell density (typically 10^3-10^4 cells/well) and added to ELISPOT plates. Plates were incubated overnight at

37C. Cells were removed and wells were washed 6 times with PBS-Tween (PBS with 0.005% Tween-20). Second antibody 7B61-biotin was diluted to 1μg/ml and 50μl per well was added. After 3 hours at room temperature, second antibody was removed and wells were washed again. 50μl per well diluted alkaline-phosphatase-streptavidin conjugate (1:1000) was added for 90 minutes at room temperature. Colour reagent A and B were mixed in a 1:1 (v/v) ratio and AP colour development buffer was diluted 1:25 (v/v) with sterile water. These two were mixed and were added at plates at 100μl/well. After 15 minutes, colour reagents were removed and the reaction was stopped with tap water. Plates were fully dried. Spot counts were enumerated on an automated ELISpot reader (AID). Results are presented as individual spot counts per well.

2.9. Measurement of IFNγ release: ELISA assay.

IFNγ in culture supernatants was quantified by ELISA. Assays were assembled in triplicate with effectors being T-cells and targets were either DC or LCLs/B-cell blasts. 96 well Maxisorp plates (Nunc) were coated with 50ul/well mouse anti-human IFNγ antibody at 0.75ug/ml in coating buffer (0.1M Na_2HPO_4, adjusted to pH 9 with 0.1M NaH_2PO_4) and were incubated at 4C overnight. Primary antibody was removed and

non-specific binding was blocked with 200ul/well of blocking buffer (PBS with 1% w/v bovine serum albumen and 0.05% v/v Tween 20) for 1 hour at room temperature. After six washes, 50ul culture supernatant or diluted recombinant human IFNγ (doubling dilutions from 2000pg/ml to 31.25 pg/ml) were added to wells for 3 hours at room temperature. After six hours, 50ul per well of biotinylated anti-human IFNy antibody was added per well at 0.75ug/ml and incubation was at room temperature for 90 minutes. After 6 further washes, 50ul per well of ExtrAvidin peroxidise (Sigma) was added at 1:1000 in blocking buffer for 30 minutes. After 8 washes, 80ul per well of substrate (3',5,5'-tetramethylbenzidine solution containing peroxide – TebuBiotech) was added; after 15 minutes the reaction and colour development was stopped with 1M HCl. Absorbance was measured at 450nm using an automated plate reader (Bio-Rad). IFNy release was determined using a linear equation derived from the standard curve of recombinant IFNy concentration and absorbance.

2.10. Measurement of cytokine release by dendritic cells: ELISA

The Ebioscience 'Ready-Set-Go' cytokine ELISA kits – IL12p70, IL12p40 and IL10 were used as per manufacturer's instructions. Plates were 96 well NUNC (Denmark) Maxisorp plates. Coating antibody (IL10, IL12p40 or IL12p70) was

diluted according to the Certificate of Analysis in coating buffer and was added at 100µl per well. Plates were incubated overnight at 4C. Wells were washed 5 times with wash buffer and were then blocked with assay diluent (diluted 1:5 in sterile water) . Assay diluent was removed and 50µl/well of dendritic cell supernatant (directly removed from culture wells, spun at 10,000 rpm for 5 minutes to pellet any cellular material) was added to wells for 2 hours at room temperature. After 5 washes with wash buffer, diluted capture antibody was added at 100µl/well for 1 hour at room temperature. Diluted Avidin-horseradish peroxidase conjugate was added at 100µl per well for 30 minutes at room temperature. After further washes, substrate solution was added at 50µl per well for 15 minutes and the reaction was stopped with 50µl/well stopping solution. Absorbance was measured at 450nm wavelength on a multiplate spectrophotometer. To determine cytokine levels, a standard curve was constructed for these assays using recombinant cytokines provided. A best-fit line was determined using Microsoft Excel and the equation for this line was used to calculate cytokine levels in unknown samples. The standard curves generated for IL10, IL12p40 and IL12p70 are presented in Figures 2.1 A-C.
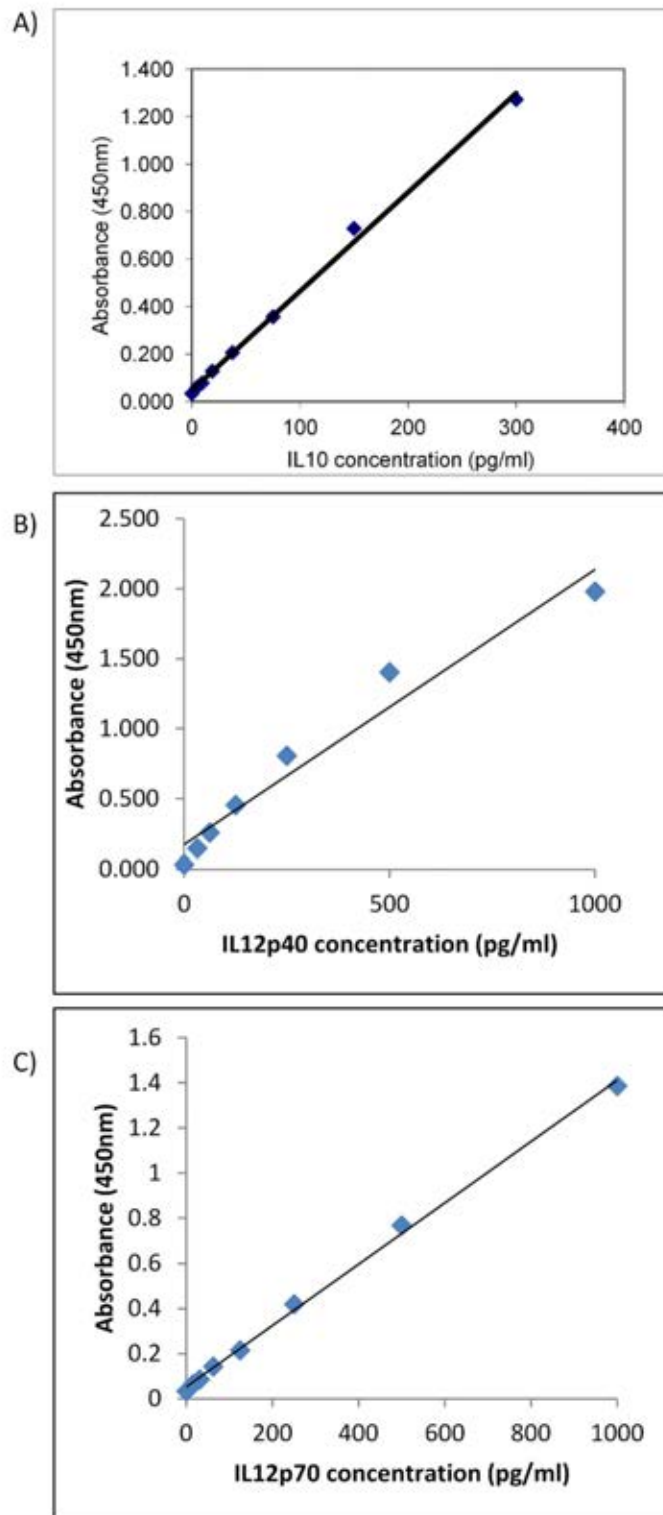
Figure 2.1 A-C. Standard curves for quantification of cytokine release by two-step ELISA (sandwich). The indicated concentrations of recombinant cytokine were prepared by serial dilutions. The diluted cytokines were added to test wells and the ELISA was performed as described. The Y axis presents the absorbance obtained at 450nm by absorbance spectrophotometry. Results are means of triplicate wells and linear trend-lines have been added using Microsoft Excel. The derived equations were used to calculate cytokine concentrations in test samples.

109

2.11. ELISA for anti Melan-A IgG.

96 well flat bottomed ELISA plates (Falcon) were coated with recombinant Melan-A protein (ProSpecTany Technogene, Israel) at 5µg/ml in coating buffer (Na_2CO_3/$NaHCO_3$ buffered at pH 9.6) overnight at 4C. Wells were washed with PBS three times before being blocked with PBS containing 5% (w/v) non-fat dried milk for 2 hours at 37C. Wells were washed thrice with PBS containing 0.05% (v/v) Tween-20 (Sigma) and samples were added. Plasma samples were either used fresh (lab donors) or gently thawed at 37C for 5-10 minutes followed by gentle mixing by pipetting. They were diluted to 1:50, 1:250 and 1:500 (v/v) in PBS-Tween-5% milk and were added to wells at 50µl/well for 1 hour at room temperature. After further washing of wells with PBS-Tween, the detection antibody (goat anti human IgG-alkaline phosphatase, Sigma) was added at 50µl per well at a dilution of 1:1000 in PBS-Tween-5% milk for 1 hour at room temperature. After further washes, the substrate (p-nitrophenyl-phosphate, Sigma) was added at 100µl per well and after 30 minutes the reaction was stopped with 0.1M H_2SO_4 and the absorbance was determined on a spectrophotometer at 450nm. Assays were set up in triplicate, and in initial optimisation assays, the plasma samples were replaced with primary Melan-A specific antibodies (mouse anti-human Melan-A, A103). In experiments to determine the effect of preincubation of plasma with

recombinant Melan-A, plasma samples were pre-incubated with either bovine serum albumen (Sigma) or Melan-A protein prior to analysis as above.

2.12. Staining with HLA 35-HPV tetramer

This tetramer (Khan et al., 2004) was a kind gift from Dr Andrew Hislop, Institute for Cancer Studies. It is conjugated with a phycoerythrin tag. Cells (at least 105 per stain) were washed twice and suspended in PBS containing 2% fetal calf serum and 1:50 (v/v) HPV specific tetramer. Cells and tetramer were mixed well and left at room temperature for 15 minutes. Cells were washed twice with 10ml 2% FCS/PBS and pellets were suspended in 500ul PBS before flow cytometric analysis on the FL2 channel. Negative control was unstained cells and cells lacking the HLA B35 epitope; background fluorescence was set at 1-2%.

2.13. Western blotting – EBNA1 and Melan-A.

Transfected HEK293 cells were approximately 70% confluent and culture medium was removed followed by two washes with sterile PBS. Lipofectamine 2000 (24ul) was diluted in OptiMEM (800ul). 1.6µg plasmid DNA (encoding Melan-A ELA variant) was diluted in 100ul of OptiMEM. As a control pcDNA3.1 (empty plasmid) and the Melan-A WT plasmid were

also used. DNA and lipofectamine 2000 were combined and 200ul per well was added. Cells and DNA were incubated for 1 hour. Transfection was terminated by adding 2ml DMEM containing 10% FCS per well. After 72 hours, cells were harvested. 140μl of 9M urea were added per tube and cells were resuspended by pipetting. From this point samples were maintained on ice. Urea lysates were sonicated briefly for 5 seconds and samples were centrifuged at 13,000 rpm for 5 minutes at 4C. Protein containing supernatants were aspirated carefully and cellular debris was discarded. Protein content was determined using a Biorad Bradford assay. After protein determination, 15ug protein was added to sterile distilled water for a total volume of 20ul and an equivalent volume of Laemelli sample buffer was added (950ul buffer with 50ul B-mercaptoethanol). Samples were boiled at 98C for 3 minutes and cooled rapidly on ice. Running buffer was made – 100ml Tris-Bicine at 1M was added to 10ml 20% SDS and made up to 1 litre with sterile distilled water. The gel for electrophoresis was prepared – 13.3ml of 30% polyacrylamide contain 0.4ml 20% SDS and 4ml 1M Tris-Bicine made up to 40ml with sterile distilled water. Polymerisation was induced with Tetramethylethylenediamine and ammonium persulphate. 35ul of each sample and adjacent protein ladders were loaded and electrophoresis was performed for 2.5 hours at 40mA. Proteins were electro-blotted onto a nitrocellulose membrane overnight at 13V.

Blotting buffer was 43g glycine and 9g Tris dissolved in 600ml methanol and made up to 3l with distilled water. Proteins were stained with Ponceau S. Non specific antibody binding was blocked with PBS containing 5% non-fat milk and 0.1% Tween (20ml) for 90 minutes at room temperature. Mouse anti Melan-A monoclonal antibody (Dako, A103) was diluted to 1ug/ml in 20ml of blocking buffer and blots were stained with regular tilting for 2 hours at room temperatures. Blots were washed three times with 50ml PBS for 10 minutes and then stained with goat anti-mouse IgG-HRP (1:1000 in blocking buffer). After three further washes, chemiluminescent substrate was added and films were developed and exposed.

For EBNA1, transfection of HEK293 cells was performed exactly as above, with approximately 75,000 cells per transfection at confluency of 70-80%. The pcDNA3.1 plasmid (Invitrogen) containing inserts encoding EBNA1 (full length), EBNA1ΔGAr, EBNA1ΔGAr-NLS mutation and pcDNA3.1 with no insert and no DNA controls were used. After 48 hours, some cells were removed for immunofluorescence microscopy studies and the remainder were left for 24 hours for use in Western blotting. The only differences in method were that urea lysates were sonicated twice for 10 seconds and 50ug of protein was loaded per lane and electrophoresis was

performed for 3 hours at 40mA. As a positive control, lysates of EBV transformed B-LCLs were also used. Primary antibody was anti EBNA1 rat monoclonal (1H4) at 1/50 and secondary antibody was goat anti rat IgG-HRP conjugate at 1/1000.

2.14. Immunofluorescence staining of EBNA1 in transfected HEK293 cells

This was performed as for dendritic cells with some modifications. HEK293 cells were plated onto microscopy slides at 30,000 cells per spot and were allowed to adhere for 4 hours at 37C. After fixation and permeabilisation, antigen retrieval was performed. Citric acid buffer was made up with 2.1g citric acid in 100ml of distilled water, the pH was adjusted to 5.8 with 1M NaOH and the total volume made up to 1L with water. Slides were placed in a plastic container and covered with citric acid buffer, and were heated in a microwave for 30 minutes. After cooling at room temperature, slides were gently washed with tap water and staining proceeded as above. The 1H4 antibody was used at 1:50 dilution and secondary antibody was goat anti rat Alexa 594 conjugate at 1/500 dilution.

2.15. Generation of Melan-A ELA variant plasmid DNA.

The starting point for these experiments was the Melan-A wildtype (EAA) plasmid (Plasmid Factory). The strategy used was PCR based site-directed mutagenesis. Mutagenesis primers were designed flanking the site of the EAA→ELA mutation and included a single mutated codon which encodes leucine rather than alanine. Two sequencing primers flanking the entire Melan-A coding sequence were also purchased. Melan-A plasmid DNA was diluted to 1ng/ul in distilled water and mutagenesis primers 1 and 2 were diluted to 10uM concentrations in water. Polymerase chain reactions were set up with 12ul of Phusion HF buffer, 1.2ul of dinucleotidetriphosphates at 10mM, 3ul primer 1 and 2 and 37.2ul of distilled water with 0.6ul of Taq DNA polymerase enzyme. 19ul of reaction mix were added to 1ul of diluted plasmid DNA. Thermal cycling conditions were as follows – 98C for 1 minute and then 35 cycles of 98C for 20 seconds, 60C for 20 seconds and 72C for 150 seconds followed by 5 minutes at 72C and reaction products were held at 4C. PCR products were analysed by gel electrophoresis - 9ul of reaction product were added to 2ul loading buffer (x5) and a 1.5% agarose gel was poured. 10ul samples were loaded into each lane alongside DNA markers and electrophoresis was performed for 45 minutes at 110V. This result is illustrated in Figure 2.2. The reactions showing a strong band at approximately 4kb were taken forward. Appropriate bands were cut from the gel and extraction of DNA from the

gel was undertaken using the Qiagen gel extraction DNA purification kit according to manufacturer's instructions. DNA was eluted in 30ul buffer and DNA concentrations were 4.9ng/ul for reaction 1 and 10.1ng/ul for reaction 3. The ends of linear DNA produced were ligated – 50ug DNA with 10ul ligation buffer (x2) and 1ul DNA ligase enzyme. Reactions were mixed and left at room temperature for 25 minutes. As a control, reactions lacking ligase enzyme were also assembled. 2ul of each reaction was transferred to eppendorf microtubes and 50ul of XL1Blu bacterial cells were added per tube. As a control for the transformation process, circular plasmid DNA (encoding Melan-A WT) was also used. Bacteria and DNA were left together on ice for 30 minutes and were rapidly heated to 45C for 45 seconds before being returned to ice. At this point, 200ul warm super optimal broth medium was added per tube. Transformed bacteria were shaken at 2000 rpm at 37C for 90 minutes. Bacterial suspensions were spread onto agar plates at either 50 or 150ul per plate. Plates were incubated overnight at 37C and individual colonies were selected with a pipette. There were over 200 colonies per plate with the Melan-A plasmid DNA, at least 50 with the ligation reactions and less than 10 with 'no ligase' controls. In total, 16 colonies from Melan-A ELA ligation DNA were selected and 5ml LB medium was added to each before overnight incubation at 37C. DNA was purified from bacteria using the QIAprep Spin

MiniKit (QIAGEN) according to manufacturer's instructions and DNA was eluted in 50ul buffer. Resultant plasmid DNA was analysed by Sanger dideoxy sequencing as described here. Per reaction, 1ul 'Big-Dye' enzyme mix (ABI PRISM), 4ul buffer (x5), 1ul sequencing primer at 3.2uM and 10ul of distilled water were combined. 16ul of reaction mix was added to 4ul of DNA and the PCR was performed overnight using the following cycles: 95C for 15 seconds, 50C for 15 seconds, 60C for 150 seconds for 25 cycles. 2ul 0.25M EDTA was added to 18ul reaction products. 60ul absolute ethanol was added and reactions were left at room temperature for 15 minutes. After centrifugation at 13,000 rpm for 30 minutes at 4C, supernatants were carefully removed leaving 1-2ul. 100ul 70% v/v ethanol were added and further centrifugation at 13,000 rpm for 10 minutes was performed. Supernatants were removed as completely as possible and pellets were air-dried before being resuspended in 10ul formamide. After brief vortexing, they were heated for 2 minutes at 96C and rapidly cooled on ice. 10ul was loaded onto an ABI PRISM machine for sequencing. Sequencing data were analysed using the Chromas software package. In-silico translation was performed in all three reading frames. Results indicated that several clones had alterations around the ELA encoding codons. 4 clones containing DNA encoding the ELA sequence were sequenced again using a reverse sequencing primer and fidelity of the sequence was confirmed. These plasmids were

introduced into HEK293 cells and Melan-A protein detection was performed by Western blotting (see above).

2.16. Generation of EBNA1 encoding plasmid DNA.

Plasmids encoding EBNA1 were a gift from Dr Graham Taylor, Institute for Cancer Studies. However, different EBNA1 isoforms were available in varying plasmid backbones. For comparative experiments, all isoforms were required in the same vector. The starting point was pCGC vector containing an EBNA1ΔGAr and EBNA1ΔGAr-NLS mutation insert, alongside rat CD2 cytoplasmic domain and eGFP sequences. The EBNA1 insert sequence is flanked by Not1 and Xho1 restriction sites. These are also present in the pcDNA3 cloning site. Reactions were assembled:

pcDNA3 (360 ng/ml)	pcGC-EBNA1 (1.5mg/ml)
Plasmid DNA – 6ul	Plasmid DNA – 2ul
2ul buffer H	2ul buffer H
11ul distilled water	15ul distilled water
0.5ul (5 units) Not1 enzyme	0.5ul (5 units) Not1 enzyme
0.5ul (5 units) Xba1 enzyme	0.5ul (5 units) Xba1 enzyme

Reactions were performed overnight at 37C. 1μl of shrimp alkaline phosphatase was added per reaction for 5 minutes at 37C and it was then inactivated at 65C for 20 minutes. Gel electrophoresis of reaction products revealed an approximately 4kb band for linearised pcDNA3 and a 4kb and 1.2kb band for pCGC-EBNA1. The 4kb pcDNA3 band and 1.2kb EBNA1 insert band were excised from the gel and DNA extraction was performed using the QIAGEN Gel extraction kit. DNA concentrations were: pcDNA3 – 43 ng/ul, EBNA1ΔGA – 16.6 ng/ul, EBNA1ΔGA-NLS mutation – 25.5 ng/ul. DNA ligation was performed – A)pcDNA3 alone 1ul with 9ul water B)pcDNA3 (1ul) and EBNA1ΔGA (3ul) with 6ul water C)pcDNA3 (1ul) and EBNA1ΔGA-NLS (2ul) with 7ul water. 10ul ligation buffer (x2) was added to each tube and 1ul fast DNA ligase was added. After 15 minutes, reactions were cooled on ice. Agar plates containing 100mg/ml ampicillin were poured and XL1Blu bacterial cells were thawed. 2ul of each ligation reaction was added to 50ul XL1Blu cells and these were incubated on ice for 45 minutes. Bacterial transformation, selection of colonies and DNA extraction were performed as above. Restriction digest with Not1 and XhoI confirmed the presence of the EBNA1 inserts in these plasmids.

The puc19 vector containing a full length EBNA1 encoding sequence was a gift from Dr Graham Taylor. The pcDNA3-

EBNA1ΔGA and puc19-EBNA1 vectors were digested with Not1 and Xcm1 enzymes and the linearised pcDNA3 vector was treated with shrimp phosphatase. Successful DNA cleavage was confirmed by gel electrophoresis and the bands representing full length EBNA1 insert and linearised pcDNA3 were excised and DNA extraction was performed. Ligation and transformation of XL1Blu were performed as above. There were no bacterial colonies from reactions lacking ligase enzyme. 5 colonies were selected and these were digested with Not1 and Xho to confirm correct insert sizes (approximately 1.8kb). For final checks, digests were performed with an enzyme that does not cut the full length but does cut the ΔGA sequence, and it was also verified that the insert size was greater for full-length EBNA than ΔGA. However, all plasmids were sequenced for final confirmation of correct coding sequence. Results revealed correct sequence alignments with long open reading frames encoding the known sequences of EBNA1.

For the EBNA1ΔGAr-invariant chain fusion protein the starting point was pcDNA-invariant chain plasmid, a kind gift from Dr Graham Taylor. This encodes the cytoplasmic domain of the human invariant chain (Ii) – approximately 80 amino acids. Primers flanking the Ii sequence were designed and sequences are given in Appendix 1. PCR was assembled as

follows (per reaction): 1ul template DNA (at 10ng/ul), 2.5ul magnesium containing PCR buffer, 1.25ul of each primer (at 10uM), 0.5ul dNTPs and 0.2ul HiFi DNA polymerase. Thermal cycling was as follows: 94C for 2 minutes, then 40 cycles of 94C 20 seconds, 55C for 20 seconds, 72C for 30 seconds, followed by 7 minutes at 72C and a hold a 4C. The results of PCR with and without template DNA were analysed by gel electrophoresis: reactions without template showed faint bands at 150bp (primer-dimers) but reactions with template showed a strong band at 250bp. This is the expected size of the Ii fragment. PCR product was purified using the Roche PCR clean up kit as per manufacturer's instructions. The concentration of invariant chain PCR product was 4000ng/ul. 4ug of DNA (pcDNA3.1-EBNA1ΔGA and Ii DNA were used for a Not1 digest. After gel electrophoresis, relevant bands were excised and DNA was purified. The EBNA1 digest was dephosphorylated with shrimp alkaline phosphatase. DNA was diluted to 10.4ng/ul (EBNA1ΔGAr) and 5.2 ng/ul Ii. 50ng of vector was combined with 10ng of insert DNA. The total reaction volume was 20ul – 5ul vector, 2ul insert, 3ul water, 10ul 2x buffer and 1ul ligase enzyme. After 20 minutes at room temperature, XL1Blu bacteria were transformed with ligation and control reaction products by heat-shock. Individual colonies (10) were selected and expanded, followed by DNA purification with the QIAGEN MiniPrep kit. DNA from these colonies was analysed by

digestion with Not1 enzyme. 6 of 10 DNA preparations contained an approximately 250bp fragment on gel electrophoresis. As the cloning process was bi-directional, these six clones were taken forward to DNA sequencing to ascertain the orientation of the insert. DNA concentrations ranged from 130 to 240 ng/ul. Sequencing PCR reaction utilised a T7 primer and a total of 400-50-ng DNA was used per reaction. Per reaction – 1ul BigDye, 4ul 5x BigDye buffer, 1ul T7 primer (3.2uM) and 12ul distilled water with 2ul template DNA. Thermal cycling was as per BigDye protocol. Reaction products were added to 2ul 0.25M EDTA and 60ul absolute ethanol. After centrifugation (13000 rpm for 30 minutes at 4C), supernatants were aspirated and after a wash with 70% ethanol, pellets were air-dried and suspended in 10ul formamide. One plasmid contained the Ii insert in the correct orientation.

2.17. Staining of cells with recombinant T-cell receptors – flow cytometry.

Cells were washed with PBS-0.5% FCS and were resuspended at 10^5 cells/ml. 90ul cell suspension was added to each FACS tube ($9x10^4$ cells). Soluble TCR (Immunocore Ltd, Abingdon) was diluted in PBS/FCS and added at 100nM. Cells and TCR were mixed by gentle 'flicking' and left at room temperature for 10 minutes. After 1 wash, supernatants were fully removed and cells were resuspended in 90ul of buffer.

Streptavidin-phycoerythrin conjugate (Promega) was prepared and added at 10µg/ml. After 10 minutes at room temperature, cells were washed twice and resuspended in 500ul PBS before immediate analysis by flow cytometry. The negative control was streptavidin-PE only (i.e. no TCR). PE fluorescence was measured by flow cytometry and background fluorescence was set at 1-2%.

2.18. Staining of cells with recombinant T-cell receptors – fluorescence microscopy.

Staining was performed on cryopreserved DC. DC were thawed and kept on ice during transport. Cells were resuspended in imaging medium (RPMI medium without Phenol red, 10% FCS 1% glutamine and 1% penicillin/streptomycin). 5×10^4 to 10^5 cells were used per stain and viability as ranged from 50-75%. Cellular pellet was suspended in 200ul recombinant TCR (at 10µg/ml in BSA/PBS) for 30 min at 4°C. Cells were washed twice with PBS and the pellet was resuspended in 200ul of Streptavidin/PE (at 10µg/ml) for 20min at room temperature in the dark. Cells were washed twice with 10ml PBS, with complete removal of media. Pellets were resuspended in 50ul imaging medium and were transferred to 8 well chamber coverslips for analysis. Single-molecule wide field fluorescence microscopy was performed on a Zeiss 200M/Universal Imaging system with a 63x objective. PE

fluorescence was detected using a 535/50 excitation, 610/75 emission,and 565LP dichroic filter set (Chroma). Given that staining of cell surface-bound biotinylated complexes with an excess of streptavidin-PE has been shown to result in monomeric association of streptavidin-PE with target protein (Purbhoo et al., 2004), a single detected PE signal corresponds to a single TCR-peptide-HLA complex. To cover the entire three-dimensional surface of the cell, z-stack fluorescent images were taken (21 individual planes, 1 μm apart). Data were evaluated for at least 30 cells in each experimental condition. Spot counts were enumerated manually. This work was performed in close collaboration with Dr Giovanna Bossi, Immunocore Ltd at Abingdon.

2.19. Epitope detection using soluble TCR-anti CD3 fusion protein.

A fusion protein comprising the gp100 $_{280-288}$ (YLE) specific T-cell receptor and an anti human CD3 antibody was a kind gift from Dr Rebecca Ashfield (Immunocore Ltd). Engagement of the TCR with the epitope leads to CD3 ligation and T-cell activation. Only effector memory cells becomed rapidly activated (R.Ashfield, personal communication). T-cell activation was detected by IFNγ ELISPOT assay. Patient DC were thawed, washed twice and resuspended in 10% FCS/RPMI and were added to ELISPOT wells at 5 x 10^3 cells/well. HLA

A2 positive LCLs were loaded with GLC (BMLF-1, negative control), and YLE peptide as described above and were also used as targets at 5×10^3 per well. Effector cells were the EBNA1 HPV specific clone c47. DC are EBV negative cells and should not display this epitope, minimising background recognition. Targets and effectors were combined and the fusion protein was added in 10%FCS/RPMI at 10^{-8}, 10^{-9} and 10^{-10}M. These concentrations were recommended by the manufacturer with the caveat that the highest and lowest concentrations may lead to non-specific and low signals respectively. Since the strongest specific signal was obtained with 10^{-9}M fusion protein on peptide-loaded LCL target cells, patient data from 10^{-9}M concentration is presented.

2.20. Cytotoxicity assays.

Cytolytic ability of T-cells (clones or polyclonal populations) was assessed by the 51Chromium release assay. Target cells were labelled with 15ul of 51Cr sodium chromate solution (Amersham) – 50-100 uCi – for 90 minutes at 37C in serum-free medium. If peptide-loaded targets were required, peptide-loading was performed simultaneously. After washing to remove unbound peptide/sodium chromate, cells were used as targets. Targets were plated at 10^5 cells per well into V-bottomed 96 well plates. Effector cells were added (at

various E:T ratios) and plates were centrifuged at 500rpm for 5 minutes to increase cell-cell contact. After 6 hours at 37C, plates were centrifuged at 600G for 5 minutes and 50ul supernatant was transferred to mini-tubes for gamma counting. Positive control was targets lysed with 1% SDS in water and negative control was targets alone (background release). Percentage specific lysis was calculated as specific lysis/maximal lysis x 100.

2.21. Proliferation assays.

Cellular proliferation was measured by determination of thymidine incorporation, a well-established technique (Kern et al., 1987). For proliferation assays with bulk populations of T-cells, U-bottomed 96 well plates were used, whereas for T-cell clones, flat bottomed 96 well plates were utilised. For allogeneic mixed lymphocyte reactions (effect of plasmid DNA on DC maturation) – 4 x 10^4 DCs (irradiated at 4000 rad) were plated per well in 10% FCS/RPMI without cytokines with responder cells – 2 x 10^5 allogeneic PBMCs per well. Total volumes were 200ul per well. Negative control was stimulator cells alone and assays were set up in quadruplicate. After 6 days incubation at 37C, 1µCi 3H methyl thymidine solution (Amersham) – 10ul per well – was added. 16 hours after this, cells were harvested using sterile distilled water and were passed through glass fibre

filters under suction. The filters were removed and allowed to fully air-dry at room temperature. Liquid scintillation cocktail was added (30μl per well) by pipetting and filters were loaded into cassettes for counting. Radioactivity was measured (counts per minute) on a liquid scintillation counter. Plate temperature was monitored. For assays using T-cell clones (Melan-A specific) as responders, 104 T-cells per well were used with equivalent numbers of stimulator DCs (non-irradiated). After 72 hours, 1μCi 3H thymidine was added per well and assays were completed as above.

2.22. Generation of B-cell blasts.

The starting point for this work were L-cells. These were a kind gift from Dr Heather Long, Institute for Cancer Studies. They are mouse fibroblasts that are transfected with human CD40 ligand cDNA (Van Kooten et al., 1994). L-cells were cultured in DMEM (Gibco) containing 10% heating inactivated fetal calf serum and 1% penicillin-streptomycin and 1% L-glutamine. They are adherent cells and were sub-cultured by detachment with 2% trypsin-EDTA and re-plating. After trypsinisation, cells were irradiated at 4000 rad, counted and plated into 6 well plates. Freshly isolated non-adherent PBMCs were resuspended at 1.5 x 10^6 in IMDM containing 5% pooled human serum with 0.7 ug/ml cyclosporin

A (Queen Elizabeth Hospital Pharmacy) and 5ng/ml recombinant human IL4 (R and D systems). Medium was aspirated from L-cells, and 3ml PBMC suspension was added per well. After 2-3 days, when medium was yellow, non-adherent cells were stripped off by vigorous pipetting, resuspended and counted and re-plated onto fresh irradiated adherent L-cells. This process was repeated 6-7 times and at that point B-cell blasts were frozen for immediate use subsequently.

2.23. Statistical analysis

Where indicated, the Student's T-test was used to assess the significance of the difference of mean values of experimental groups. The paired t-test was performed using the statistical package GraphPad Prism for Windows. P-values are shown to 3 decimal places. For correlation coefficients, again GraphPad Prism software was used and the Pearson correlation coefficient (R2) is given to 3 decimal places.

3. Melanoma DC vaccine trial and CL22 mediated DC transfection.

3.1 Humoral responses to DC vaccination in melanoma clinical trial.

In the melanoma trial (Steele et al., 2011), although the frequency of Class II restricted T-cell responses increased with vaccination, there were few Class II epitopes known. Hence, a more broadly applicable method of assessing CD4 responses was sought.

Since IgM to IgG isotype switching is dependent on helper T-lymphocyte responses (Parker, 1993), IgG responses are an indirect marker of CD4 responses.   Therefore, these experiments aimed to measure IgG responses against Melan-A in patients.

A two-step ELISA was developed.   Initial experiments determined the optimal concentration of recombinant Melan-A protein to coat wells within the 'capture' stage. As shown in Figure 3.1A, the optimum signal was achieved with 5μg/ml Melan A protein for primary antibody concentrations of 1 in 1600 and 1 in 6400. When primary antibody was used at 1 in 400, the best protein concentration appeared to be 2.5μg/ml. However, since the expected concentrations of antibody in

B)

Absorbance (405nm)

1.2 · 1 · 0.8 · 0.6 · 0.4 · 0.2 · 0

1 in 500 1 in 1000 1 in 2000 1 in 4000 1 in 8000 1 in 16000 1 in 32000 negative

Primary antibody dilution

◆ 5 μg/ml protein
■ No protein

A)

Absorbance (405nm)

1 · 0.8 · 0.6 · 0.4 · 0.2 · 0

5 2.5 1.25 0.625 0.3125 0.15625 0.078125 negative

Melan A protein concentration (mcg/ml)

1 in 400
1 in 1600
1 in 6400
No antibody

C)

Absorbance (405nm)

1 · 0.8 · 0.6 · 0.4 · 0.2 · 0

■ no MART1
■ MART1 protein (5 ug/ml)

Plasma	+	+	+	+	+	+
Melan-A preincubation	-	-	+	+	-	+
BSA preincubation	-	-	+	+	+	+

Figure 3.1. Development of ELISA to measure anti Melan A IgG antibodies.

A) Effect of Melan A protein concentration on performance of anti Melan A IgG ELISA across a range of primary antibody concentrations. ELISA plate wells were coated with Melan A protein (0-5μg/ml) and mouse monoclonal anti Melan-A antibody was added (1/400-6400), absorbance was measured.

B) Relationship between absorbance and primary antibody concentration. ELISA plate was coated with 5μg/ml Melan-A protein or buffer alone, and monoclonal mouse anti Melan-A antibody was added (1/500-32000). Absorbance was measured.

C) Assessment of specificity of ELISA. Plasma from a laboratory donor was applied to ELISA wells coated with Melan-A protein or not. Beforehand, samples were incubated with Melan-A or irrelevant control protein (BSA). Absorbance was measured in the presence and absence of plasma.
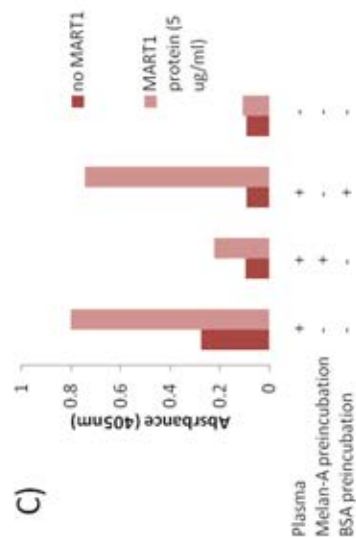
plasma samples were expected to be very low, 5µg/ml was taken forward in further experiments.

Using a mouse antibody, the ability of the assay to quantify a range of antibody concentrations was determined. There was an approximately linear relationship between the measured absorbance and antibody concentration (Figure 3.1B).

Having detected mouse monoclonal antibodies against Melan-A, experiments moved onto the use of donor plasma samples. To verify the specificity of the assay, plasma samples were pre-incubated with Melan-A and an irrelevant protein (BSA). The Melan-A specific signal (i.e. absorbance in the presence - absence of Melan-A protein) was diminished after pre-incubation with Melan-A but not BSA (Figure 3.1C): suggesting specificity.

This assay was then used to measure anti Melan-A IgG responses in clinical trial plasma samples (pre vaccination and post Cycle 4). Since it was not possible to determine the exact relationship between observed absorbance and

antibody concentration, trial patient plasma was diluted to three different concentrations for the assay.

As shown in Figure 3.2, there were detectable levels of anti-Melan-A IgG in most patients and levels were widely variable. However, there was no overall change in antibody levels after vaccination.

Two of twenty patients analysed demonstrated an increase in Melan-A specific absorbance at all dilutions tested after vaccination (Figure 3.3). One of these had a prolonged clinical response to vaccination.
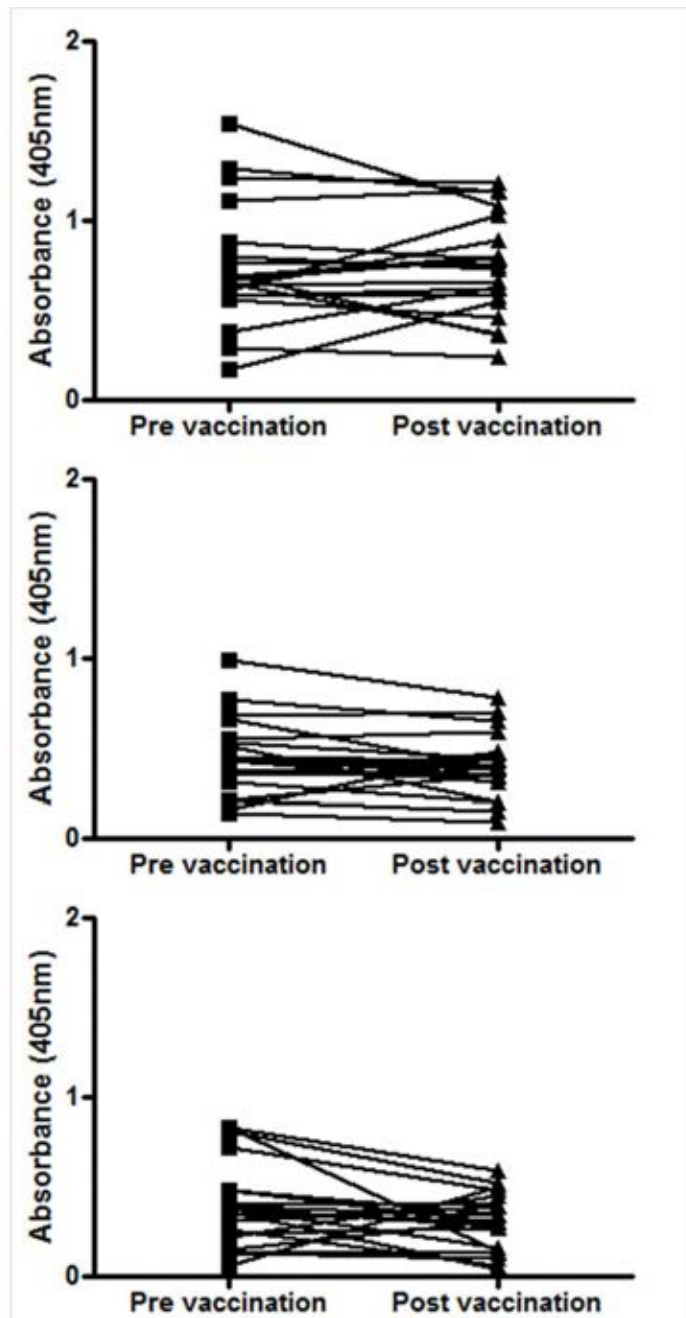
Figure 3.2. Measurement of anti Melan A IgG in patient plasma samples. Plasma samples were diluted to the indicated concentrations. Plates were coated with 5μg/ml recombinant Melan A protein or PBS alone. Results are presented as absorbance (at 405nm) in the presence minus the absence of Melan A protein for pre and post vaccination samples.
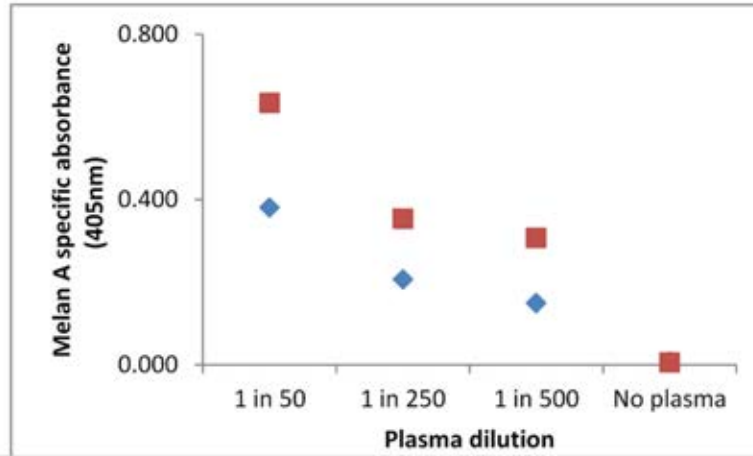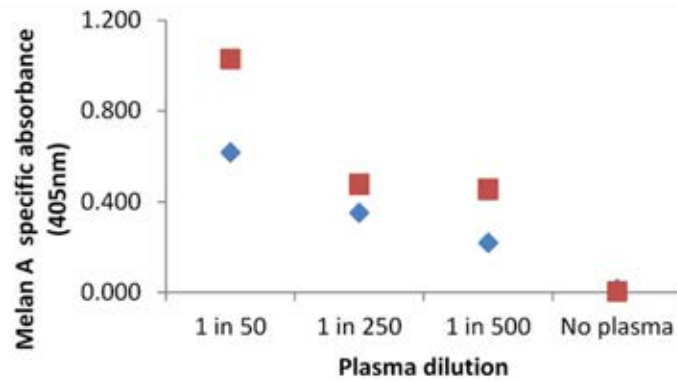
Figure 3.3. Melanoma DC trial patients with increases in anti Melan A IgG levels after vaccination. Plasma samples were used at 1 in 50, 1 in 250 and 1 in 500. Melan A IgG specific absorbance is calculated as the difference between absorbance values in wells precoated with Melan A or not (PBS alone). Blue diamonds(◆) are pre vaccination and red squares (■) are post vaccination plasma samples. A)Patient 1 B)Patient 2

3.2. Presentation of HLA-A2 restricted gp100 and Melan A epitopes by patient DCs from the melanoma vaccine trial.

The antigenic epitopes studied here are summarised in Table 3.1 below:

Table 3.1. MHC Class I restricted peptide epitopes from Melan-A and gp100

Antigen	Epitope	Amino acid position	HLA restriction
Melan A/MART-1	EEAGIGILTV (Kawakami et al., 1994)	26-35	A2
	ELAGIGILTV (Valmori et al., 1998)	26-35	A2
gp100/PMEL17	YLEPGPVTA (Cox et al., 1994)	280-288	A2
	KTWGQYWQV (Bakker et al., 1995)	154-162	A2

3.2.1. Clinical material

In the trial, a maximum of 5×10^{6} DC were administered per cycle. If DC culture was particularly efficient, there were

excess DC for cryopreservation. There were 18 HLA-A2 positive patients with excess transfected DC. These were used for analysis of HLA A2 restricted epitope presentation.

3.2.2. Presentation of Melan A $_{26-35}$ epitope by patient DCs.

For the Melan-A $_{26-35}$ epitope, a CD8 positive T-cell clone was used as a cellular readout of epitope presentation. This T cell clone specific for the Melan-A $_{26-35}$ epitope (**E(A→L)A**GIGILTV) was a kind gift from Immunocore Ltd. This clone, Mel c5, was generated from PBMC of a laboratory donor. Melan A specific CD8 T cells were initially selected using IFNγ capture and cells were expanded using autologous APC pulsed with ELA peptide (R.Ashfield, Immunocore Ltd, Abingdon, personal communication).

The peptide-sensitivity and specificity of the clone are shown in Figure 3.4. Target cells were HLA A2 positive B-cell blasts loaded with ELA, EAA and GLC (A2, BMLF1,control) peptides. There is clearly recognition of A2 positive B-cell blasts loaded with ELA peptide. This appears to be a bi-phasic response: there is recognition above background levels (GLC peptide) down to 10^{-7} M, this reappears at 10^{-11} and 10^{-12}M albeit at a much reduced level. There may be a
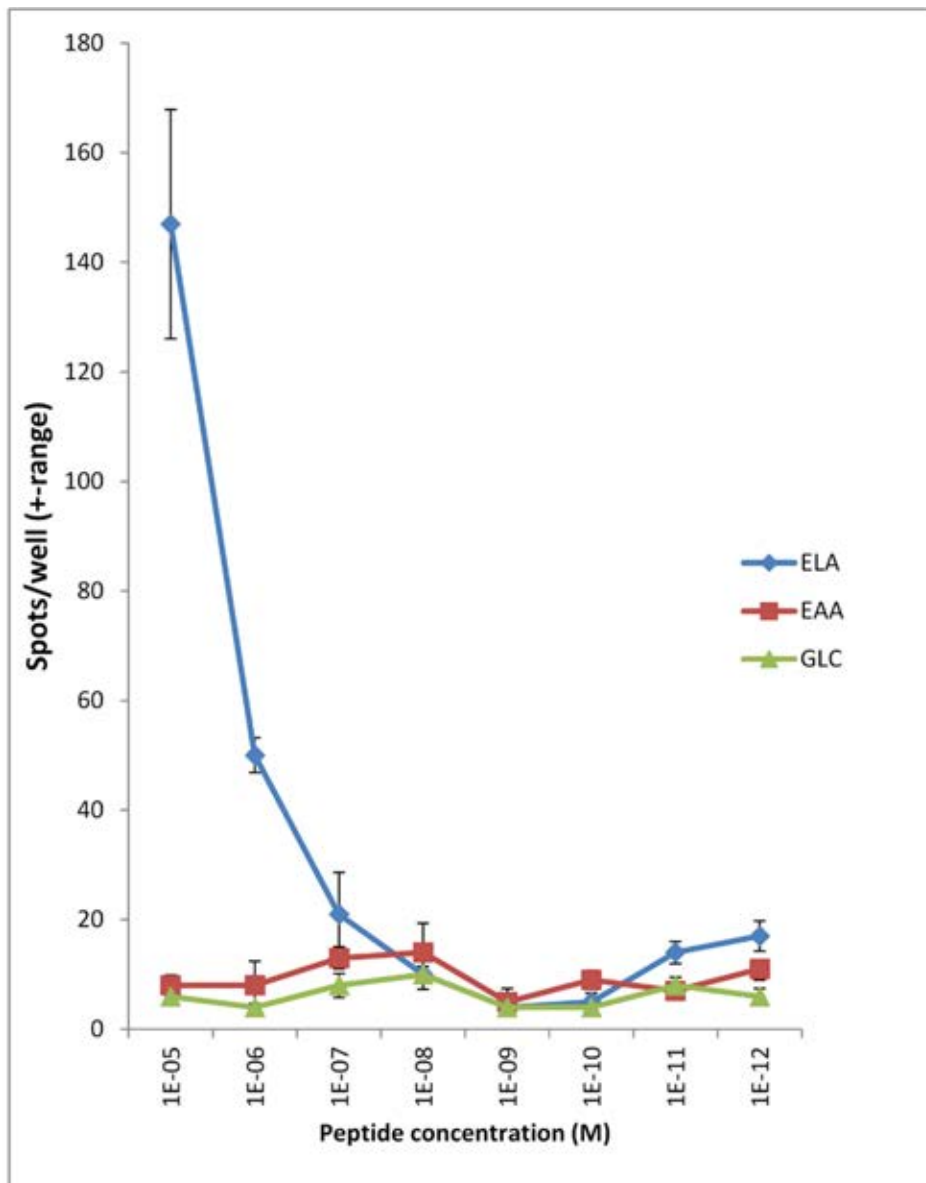
Figure 3.4. Characterisation of Mel c5 clone. HLA A2 positive B-cell blasts were loaded with the indicated concentration of exogenous peptide (ELA – **ELA**GIGILTV, EAA – **EAA**GIGILTV, GLC - **GLC**TLVAML (A2 restricted control epitope from EBV lytic protein BMLF1)) in serum-free medium for 90 minutes at 37°C. After unbound peptide was washed off twice, B-blasts (10^4) were coincubated with T-cells (10^3) in triplicate in overnight IFNγ ELISPOT assays. Results are presented as mean values of triplicate wells and error bars represent the range (highest and lowest value).

very low level of recognition of EAA peptide – at 6 of 8 peptide concentrations tested, spot counts with EAA loaded B-blasts are slightly higher than with GLC. Thus, this appears to be a T-cell clone with relatively low avidity for ELA peptide and barely detectable activity against the native peptide.

The plasmid DNA (CTL901) used in the clinical trial encodes the wild-type Melan A protein (i.e. 26-36: EAAGIGILTV), and the ability of the T-cell clone to recognise EAA peptide was very limited. However, it was decided to proceed with the use of the clone as a cellular readout as in vivo the ELA epitope does not exist and there may well be differences between the passive process of coating surface HLA molecules with exogenous peptide at high concentrations and the physiologic, active process of proteolysis and HLA loading intracellularly. Thus, the fact that responses to exogenous EAA peptide are very weak does not necessarily mean that the same will hold true for intracellularly generated epitopes. In fact, work presented in Chapter 5 strongly suggests that this is indeed the case.

Since the aim of the clinical trial was to generate the most effective cellular vaccine possible, all immature dendritic

cells were transfected with plasmid DNA. Therefore, there were no cryopreserved untransfected DCs available. These would, as antigen negative cells, have been ideal control cells in the ELISPOT assays using the Melc5 clone. However, their absence does not preclude a comparative analysis between patients.

Patient DC preparations were used as targets in overnight IFNγ ELISPOT assays with Mel c5 effector cells. As a control HLA A2 positive LCLs were loaded with GLC (negative control) and ELA (positive control) peptides at 5μM. The viability of DC preparations ranged from 50-80% after thawing. One cryopreserved sample had compromised viability (10%) and was therefore not used for cellular assays.

There was an unequivocal recognition of ELA-coated LCLs (mean 164 v 3 spots/well for ELA v GLC loaded targets); indicating functionality and specificity of the Mel c5 clone.

The Melan A $_{26-35}$ specific spot count (representing presentation of the 26-35 epitope) was calculated as IFNγ secreting cells in the presence of T-cell effectors and

their absence (i.e. dendritic cells alone). The relationship between epitope presentation and whole antigen detection (% of DCs positive for Melan A) is presented in Figure 3.5A. There is no apparent relation between epitope presentation and the percentage of cells that are positive for whole Melan A.

When the one patient DC preparation with an unusually high percentage of Melan A positive cells (96%) is removed from the analysis, a modest negative correlation of -0.29 emerges (Figure 3.5B). The excluded sample is highly atypical, in that over 90% of all DC preparations in the trial were less than 10% Melan A positive. This inverse correlation is in full agreement with the conclusions from experiments using laboratory donor DCs. These experiments, presented in subsequent chapters, showed that Melan-A negative DCs could in fact present Class I restricted epitopes and that at early time-points after transfection when whole antigen positive cells were seen, epitope presentation was minimal.

Additionally, in general the level of epitope presentation, certainly in comparison to peptide-loaded target cells, is low. Even the patient DC sample with the strongest evidence
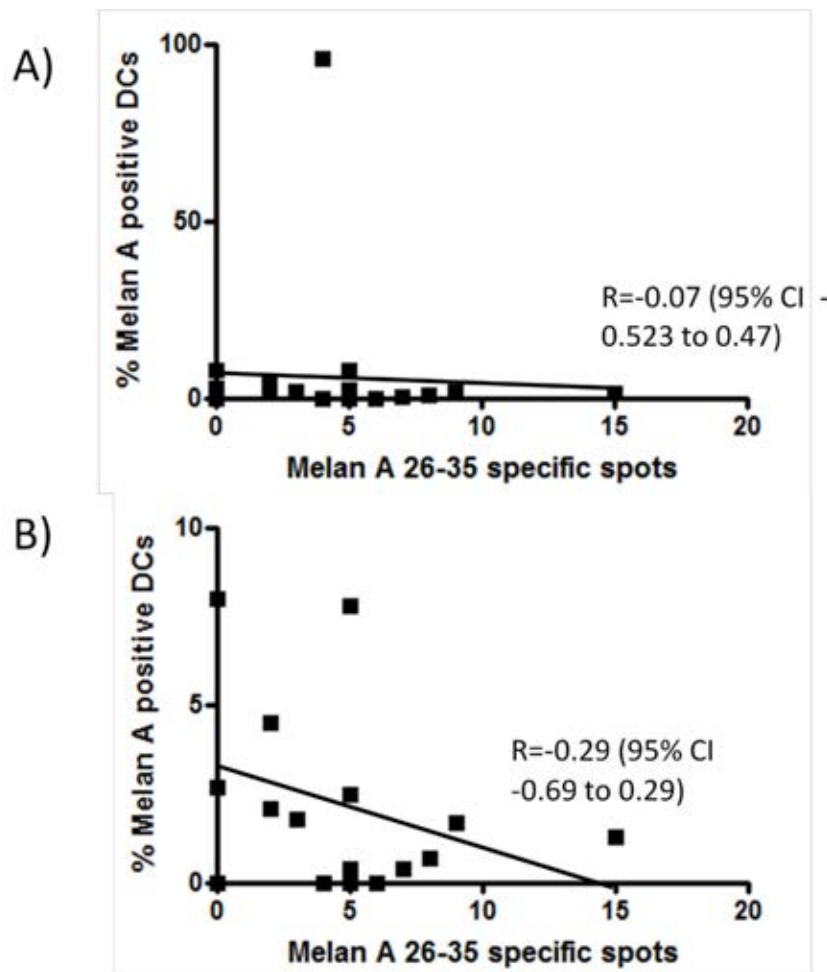
Figure 3.5. Relationship between whole Melan A positivity and Melan-A $_{26-35}$ epitope presentation by DCs from melanoma clinical trial. Patient DCs (10^4/well) were co-incubated with Melan-A 26-35 specific T-cell effectors (10^3/well) in triplicate in overnight IFNγ ELISPOT assays. Wells containing only DCs (no effectors) were also set up in parallel. The percentage of Melan A positive DCs had been previously determined by antibody staining and flow cytometry. Upper panels – all available DC samples. Lower panel – exclusion of patient DC sample with 96% Melan-A positive cells. Melan A 26-35 specific spots are calculated as: spot counts in the presence of effectors – spot counts in the absence of effectors (DCs only). Trendlines indicate Pearson's correlation coefficient (R).

of epitope presentation is only approximately 10% of maximum (i.e peptide-driven responses).

3.2.3. Presentation of gp100 $_{280-288}$ epitope by patient DCs.

Experiments then moved on to assess the presentation of the gp100 $_{280-288}$ epitope (YLE) by patient DC preparations. Unfortunately, a T-cell clone specific for this epitope was not available. However, epitope presentation was measured using a recombinant human T-cell receptor-anti CD3 fusion protein that specifically binds to HLA A2-YLE complexes. This was a kind gift from ImmunoCore Ltd (Abingdon, Oxon, UK).

3.2.4. Characterisation of gp100 $_{280-288}$ specific recombinant T-cell receptor

The ability of this reagent to detect the YLE epitope bound to HLA-A2 molecules in a specific fashion is demonstrated in Figure 3.6. The principle of these assays was as follows – interaction of the peptide-HLA complex (on target cells) with the recombinant T-cell receptor leads to cross-linking of CD3 on effector cells. The effectors can be either allogeneic PBMC or a CD8 T-cell clone of unrelated specificity. CD3 cross-linking leads to activation of the
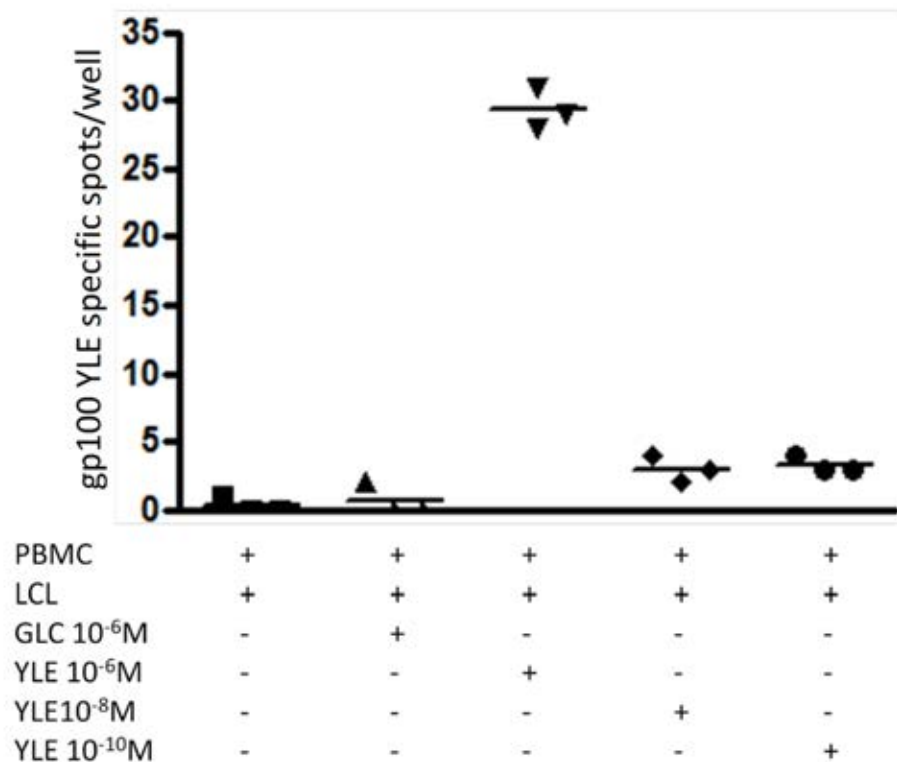
Figure 3.6. Detection of the HLA-A2-YLE complex on B-LCL loaded with exogenous peptides. EBV transformed B-LCL from an HLA-A2 positive laboratory donor were loaded with decreasing concentrations of YLE peptide and an irrelevant peptide (GLC, BMLF1). These LCLs were used as target cells in overnight IFNγ ELISPOT assays. Targets were used at 500 cells/well and effector cells were allogeneic PBMCs (1000 cells/well). Assays were assembled in triplicate. YLE specific TCR-anti CD3 fusion protein was added at a final concentration of 10^{-9}M. Results are presented as spot counts in the presence − absence of TCR fusion protein: triplicates and mean values.

effector memory subset of T-cells and subsequent secretion of cytokines, including IFN-γ. This is quantified using an ELISPOT assay. It is likely that use of a T-cell clone is more efficient than PBMCs as all the cells are effector memory, allowing the use of lower numbers of effectors per well (R.Ashfield, ImmunoCore Ltd, personal communication).

As shown in Figure 3.6, there is recognition of HLA A2 positive targets loaded with YLE peptide at the high concentration of 10^{-6} M (mean 2 spots with GLC-loaded targets v 29 spots with YLE-loaded targets). Even when target cells are loaded with very low concentrations of YLE peptide (down to 10^{-10}M) the spot count is still slightly higher than that obtained with the control (GLC) peptide at 10^{-6}M (mean spots – 3 versus 1). Encouraged by the sensitivity of the reagent, the next question was whether it could be used to detect epitope presentation from endogenous gp100 protein. The actual spot counts in this experiment are low in comparison to those presented in Figure 3.7. This reflects the lower number of effector T-cells (PBMC) used in this assay – 1000/well.

The aim of the next experiment was to determine whether or not the T-cell receptor fusion protein was a sufficiently

sensitive reagent to be able to detect presentation of the YLE epitope when it is derived from intracellular source protein rather than exogenous peptide. LCLs from an HLA-A2 positive donor were transfected with gp100 and control (GFP) DNA using electroporation. To assess transfection efficiency, the cells were subjected to flow cytometric analysis for GFP expression. Approximately 25% of cells were GFP positive. Transfected LCLs were used as target cells with allogeneic PBMC as responder cells. As shown in Figure 3.7, there is evidence that epitope presentation is detectable on these cells above background levels in GFP expressing cells. There is, however, a higher level of non-specific PBMC activation with GFP-transfected targets compared to targets loaded with irrelevant peptide. This reflects the lower viability of LCLs that have been electroporated with DNA ($\approx$50% versus 90%).

3.2.5. Assessment of gp100 280-288 presentation by patient DCs

Having established the utility of the fusion protein in detecting YLE epitopes from transfected cells, the reagent was used to measure levels of epitope presentation on patient cryopreserved DC preparations.

PBMC	+	+	+	+
LCL-GFP DNA	+	+	-	-
LCL-gp100 DNA	-	-	+	+
YLE-anti CD3 protein (10^{-9}M)	-	+	-	+
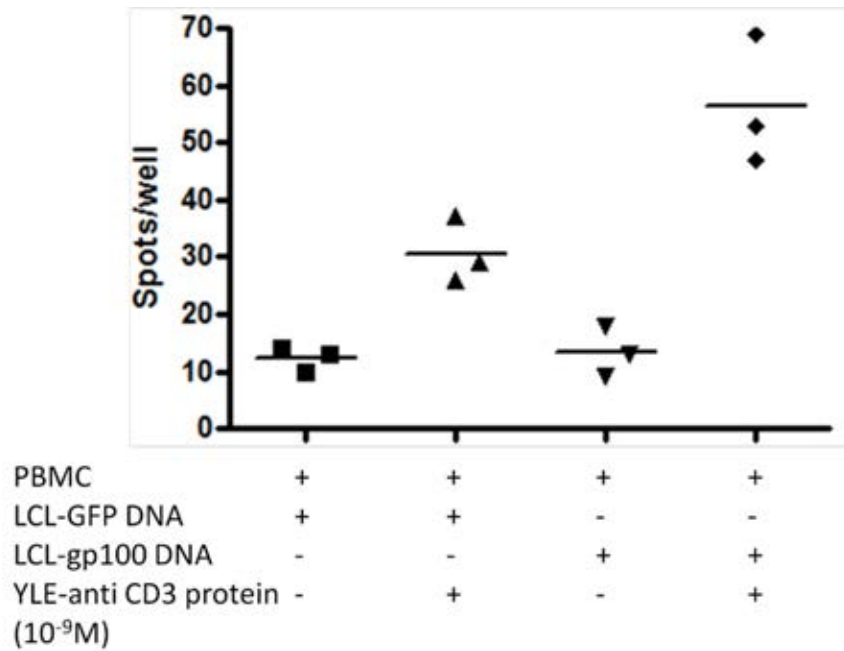
Figure 3.7. Detection of HLA A2-YLE complexes on transfected B-LCLs. The YLE specific TCR-anti CD3 fusion protein was used to measure levels of YLE epitope presentation. Target cells were HLA A2 positive B-LCLs that had been electroporated with either GFP or gp100 encoding plasmid DNA. After 24 hours in culture, LCLs were harvested and used as targets in overnight IFNγ ELISPOT assays. 10^3 LCL were coincubated with 10^4 allogeneic PBMCs per well in triplicate, in the presence or absence of the fusion protein (at 10^{-9}M). Results are presenting as numbers of IFNγ secreting cells per well – individual triplicates and mean values (horizontal bars).

In this experiment, responder/effector T-cells were a CD8 T-cell clone specific for the EBNA1 HPV epitope. The use of an antigen-experienced clone means that all cells will be effector-memory in phenotype and able to secrete IFNγ on CD3 ligation. Importantly, monocyte-derived DCs are EBV (and therefore EBNA1) negative cells – minimising background levels of recognition by the HPV specific clone.

To confirm functionality of the T-cell receptor fusion protein, HLA-A2 positive B-LCLs were loaded with 10^{-6}M YLE (and GLC, control) peptide and also used as targets in the assay. The YLE loaded cells led to strong, specific IFNγ responses (mean spots/well = 190 with YLE v 3 with GLC (control)). In terms of patient DC preparations, a proportion of samples displayed a clear increase in spot count, in the presence of 10^{-9}M fusion protein, over counts with GLC-loaded LCLs. This is highly suggestive that the epitope is being presented by patient DCs.

These results are presented in Figure 3.8A and B. In Figure 3.8A, the relationship between gp100 YLE specific spots (i.e. epitope presentation) and the percentage of DCs positive for whole antigen is illustrated. There is no apparent correlation between the two variables; the
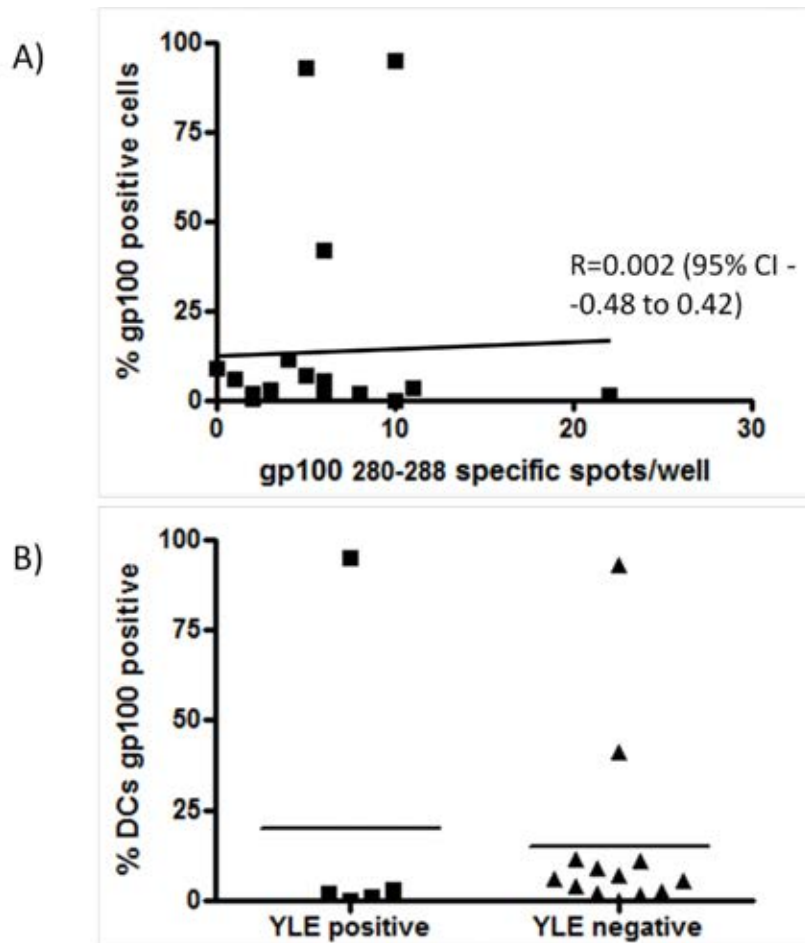
Figure 3.8A and B. **Detection of HLA-A2-YLE complexes on the surface of DCs from patients in the melanoma clinical trial.** The YLE specific TCR-anti CD3 fusion protein was used to measure levels of YLE epitope presentation. Target cells were patient DCs (1000 cells/well) and effectors were an HPV (EBNA1 $_{409-419}$) specific T-cell clone restricted through HLA-B35 (5000 cells/well). Cells were coincubated in the presence or absence of the fusion protein at 10^{-9}M final concentration. Assay were set up in triplicate. A)Relationship between whole Melan A positivity (previously determined) and YLE specific spots (spot count in presence of fusion protein – absence of fusion protein). B)Whole Melan A positivity in YLE epitope positive and negative DCs. Positive is defined (arbitrarily) as greater than or equal to twice the spot count obtained with GLC loaded LCLs as target cells. A)Trendline indicates Pearson's correlation coefficient.

correlation co-efficient is -0.05. In Figure 3.8B, patient
DC are divided into two groups – epitope positive and
negative. Positivity is arbitrarily defined as having spot
counts over twice those obtained with GLC peptide loaded
target cells. Here, there is no difference in whole gp100
positivity between the two groups. In fact, the only DC
preparation with over 10% maximal responses was only 1.3%
whole gp100 positive.

These results, for both gp100 and Melan-A epitopes, strongly
suggest low-level epitope presentation that is unrelated to
the percentage of whole antigen expressing cells.   This
means that whole antigen measurement is unlikely to reflect
the immunogenicity of the DC vaccine.

3.4. Assessment of immune-stimulatory effects of CL22 transfection of plasmid DNA on immature dendritic cells.

The aim of this set of experiments was to determine whether
DC expressed TLR9, and if so, could transfection of plasmid

DNA using CL22 have immune-enhancing effects. It was suspected that the non-electrical nature of CL22 transfection might be associated with fewer negative effects on DC function and CL22 has been used in the clinical setting.

DC generated from adherent monocytes after exposure to GM-CSF and IL4 do express TLR9 (Figure 3.9). The proportion of positive cells falls after exposure to TNFα and IL1β. This makes physiologic sense as recognition of pathogens is important at the activation phase rather than T-cell priming phase of DC function. The proportions of positive cells vary between different donors. Since TLR9 is thought to be expressed on a subset of PBMCs, (particularly monocytes and B-lymphocytes) these cells were also included in the analysis.

The percentages of TLR9 positive cells are tabulated in Table 3.2.

Table 3.2. TLR9 expression in dendritic cells and PBMCs assessed by flow cytometry.

	% TLR9 positive		
Donor	Immature DCs	Mature DCs	PBMCs
1	65.8	25.6	20.3
2	28.8	10	1.6
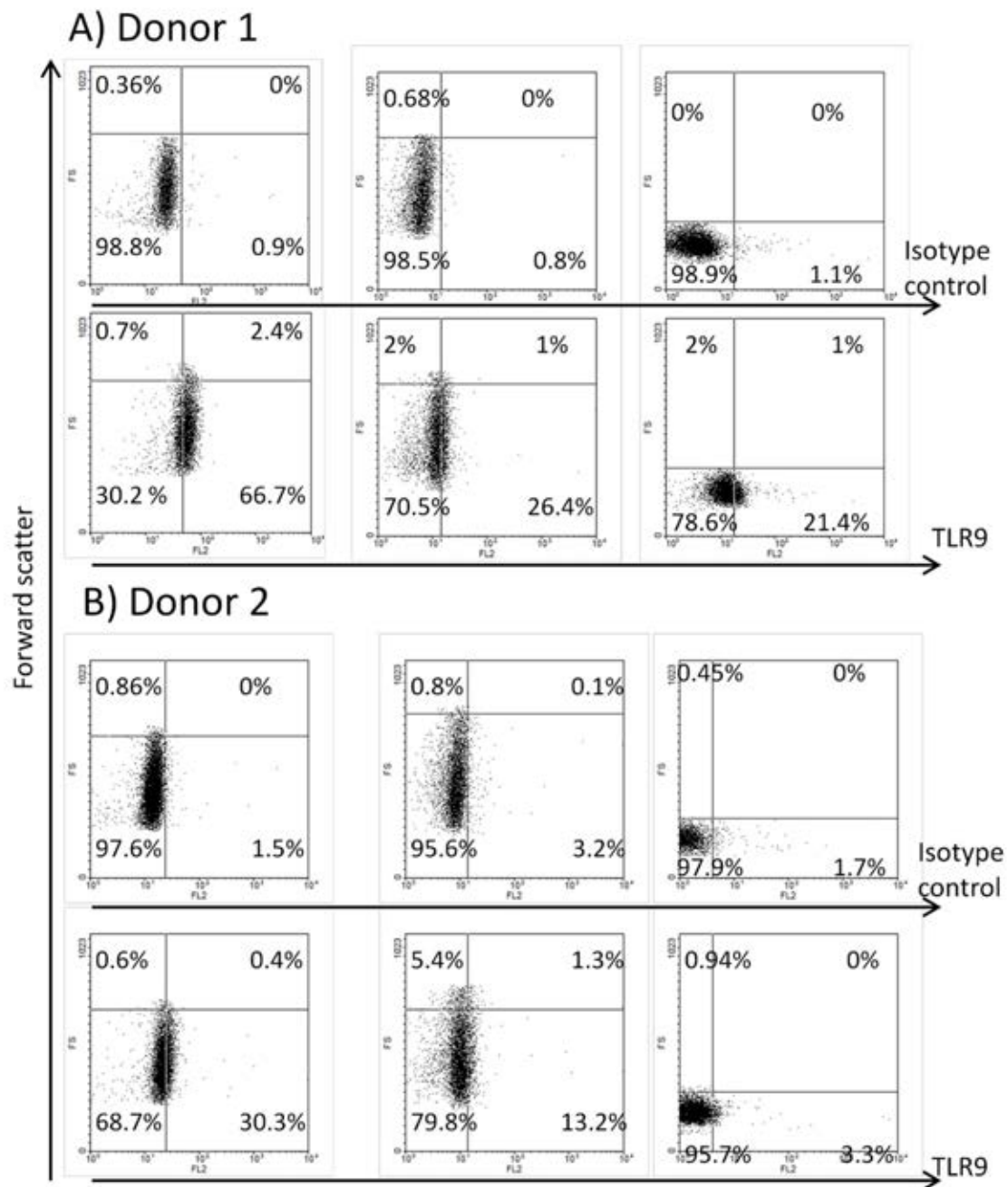
Figure 3.9. **Assessment of TLR9 expression on dendritic cells and lymphocyte from two anonymous blood donors**. Dendritic cells were prepared as in methods. Cells were fixed, permeabilised and stained with anti-TLR9 antibody and matched isotype control antibody (both mouse), followed by goat anti-mouse phycoerythrin conjugate. Fluorescence was analysed by flow cytometry on the FL2 channel, and 10,000 gated events were collected. Left panels – Immature DCs. Centre panels – mature DCs. Right panels – Lymphocytes. Y axis – Forward scatter, X axis – PE fluorescence (FL2). Percentages refer to % all gated cells in each quadrant.

This result, that moDCs appear to be TLR9 positive, raised the possibility that they may be responsive to plasmid DNA in terms of maturation and function. To determine whether this was the case, immature DC were prepared from blood donors. These cells were either transfected with GFP plasmid DNA or underwent the transfection procedure (i.e. exposure to CL22 and chloroquine) in the absence of DNA. Cells were also either exposed to proinflammatory cytokines or not. This experimental design, summarised in Figure 3.10, would allow detection of effects of DNA in the presence or absence of cytokines and any possible synergistic effects.

Each of the four groups of DCs (and pre-transfection DCs – Day 4) was assessed for three parameters of DC function. The expression of maturation markers CD83, CD86 and CD25, the lymphokine receptor CCR7, and lineage specific markers CD1a (dendritic cells) and CD14 (monocytes) was measured by antibody staining. GFP expression was also measured in this way. The ability of these DC to stimulate allo-specific proliferative responses in allogeneic PBMCs was determined by thymidine incorporation assays. The secretion of IL12p70, Il12p40 and IL10 were also determined by ELISA on culture supernatants. These assays were repeated on DC from three donors.
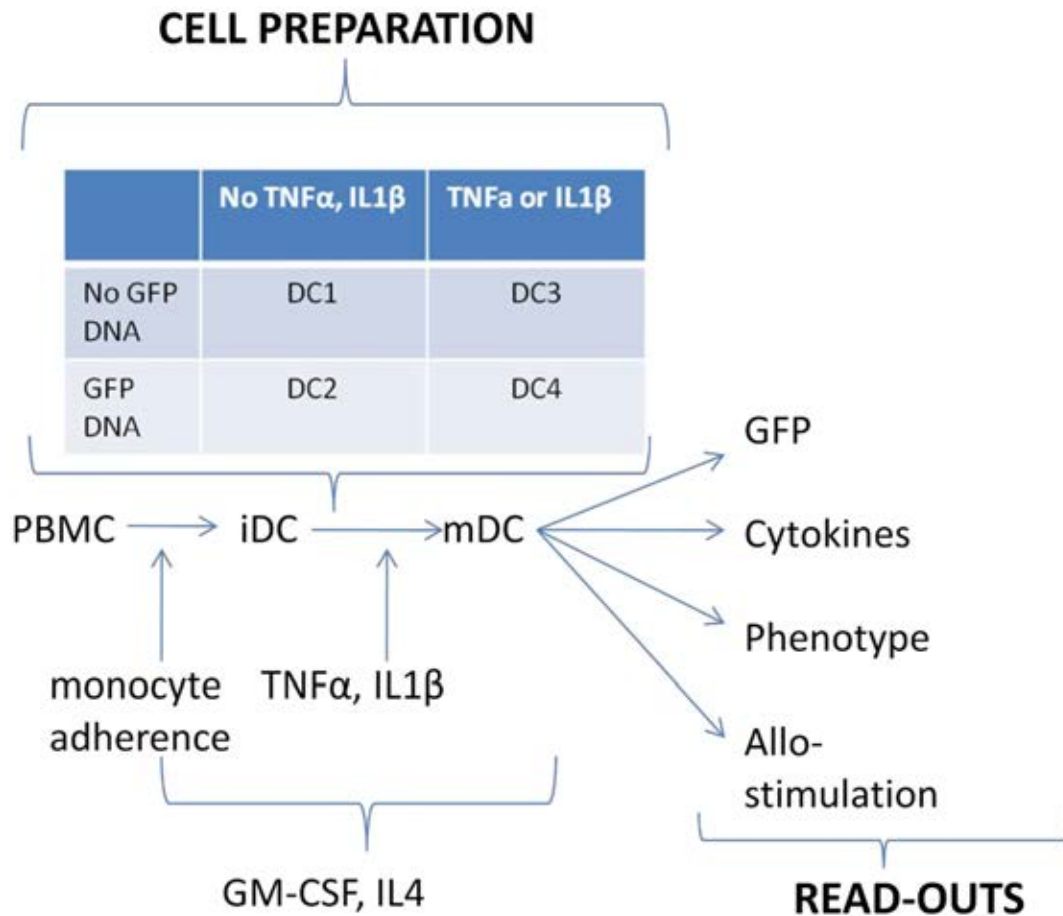
Figure 3.10. **Effect of plasmid DNA transfection using the CL22 peptide on DC maturation.** The diagram indicates the experimental process – from preparation of dendritic cells, through transfection and maturation. On the right of the diagram the outcome measurements are stated. Abbreviations - iDC: immature dendritic cell, mDC: mature dendritic cell, PBMC: peripheral blood mononuclear cells, GFP: green fluorescence protein, TNF: tumour necrosis factor, IL1b – interleukin 1b, IL4 – interleukin 4, GM-CSF: granulocyte-monocyte colony stimulating factor. This experimental process was repeated for three different blood donors.

Transgene expression varied from donor to donor, as found in pre-clinical work prior to the melanoma clinical trial (Irvine et al., 2000 and Haines et al., 2000). GFP expression is shown in Table 3.3.

Table 3.3. GFP expression assessed by flow cytometry on DCs transfected with GFP DNA using the CL22 peptide

Donor	TNFα, IL1β	GFP DNA	% GFP positive cells
1	−	−	0.09
1	−	+	0.78
1	+	−	0.06
1	+	+	0.29
2	−	−	3.06
2	−	+	8.31
2	+	−	2.4
2	+	+	10.8
3	−	−	0.19
3	−	+	1.54
3	+	−	0.17
3	+	+	0.58

One donor shows clearly detectable GFP expression, whereas in the other two it is barely detectable (<1% of DCs). It is also evident that the percentage of positive cells is lower in those DCs exposed to maturation-inducing cytokines, perhaps implying active processing of GFP.

As shown in Figure 3.11, there are donor-to-donor variations in the expression of the DC marker CD1a and monocyte marker CD14. Donors 2 and 3 display a 'typical' DC phenotype with almost total loss of CD14 expression and high CD1a

Figure 3.11. Phenotypic analysis of dendritic cells derived from three anonymous donors. Cells were analysed just before and 48 hours after transfection with the CL22 peptide and GFP DNA. At transfection, as summarised in Figure 3.7, cells were split into 4 experimental groups (no DNA, no cytokines, DNA no cytokines, DNA no cytokines and DNA cytokines). Cells were blocked with polyclonal mouse IgG, then stained with phycoerythrin conjugated mouse monoclonal antibodies against CD1a, CD14, CCR7, CD25, CD83 and CD86 or appropriate isotype matched controls. After washing, live cells were analysed by flow cytometry. At least 10,000 gated events (i.e. DCs) were collected each time. Results are presented as the percentage of DCs exhibiting specific fluorescence for each marker (% positive with specific antibody - % positive with isotype control) on the Y axis. Background fluorescence was always set <2%.

156

expression. However, in donor 1 CD14 is retained and only about a third of cells express CD1a. This suggests that these DC may have retained some features of monocytes, supported by the finding of low CD83 expression on these cells.

In terms of phenotypic maturation, there is no consistent change in expression after exposure to GFP DNA regardless of the presence of cytokines. CCR7 levels are generally low which is expected in the absence of PGE_2 (Scandella et al., 2002). CD25 expression is higher in DNA-exposed cells in all three donors. CD86 expression is generally very high, and in fact it increases even on cells not exposed to DNA or a cytokine stimulus.

The allo-stimulatory capacity of these DC is illustrated in Figure 3.12. DC were irradiated prior to use, to ensure that measured thymidine incorporation reflected allogenic PBMC proliferation. In donors 1 and 3, there are clear-cut increases in proliferation when stimulator DCs have been exposed to GFP DNA. In donor 1 only, there are synergistic effects of DNA and cytokines. In donor 2, however, this effect is not seen. Additionally, in terms of fold-increase in proliferation (i.e. proliferation index), DCs from donors
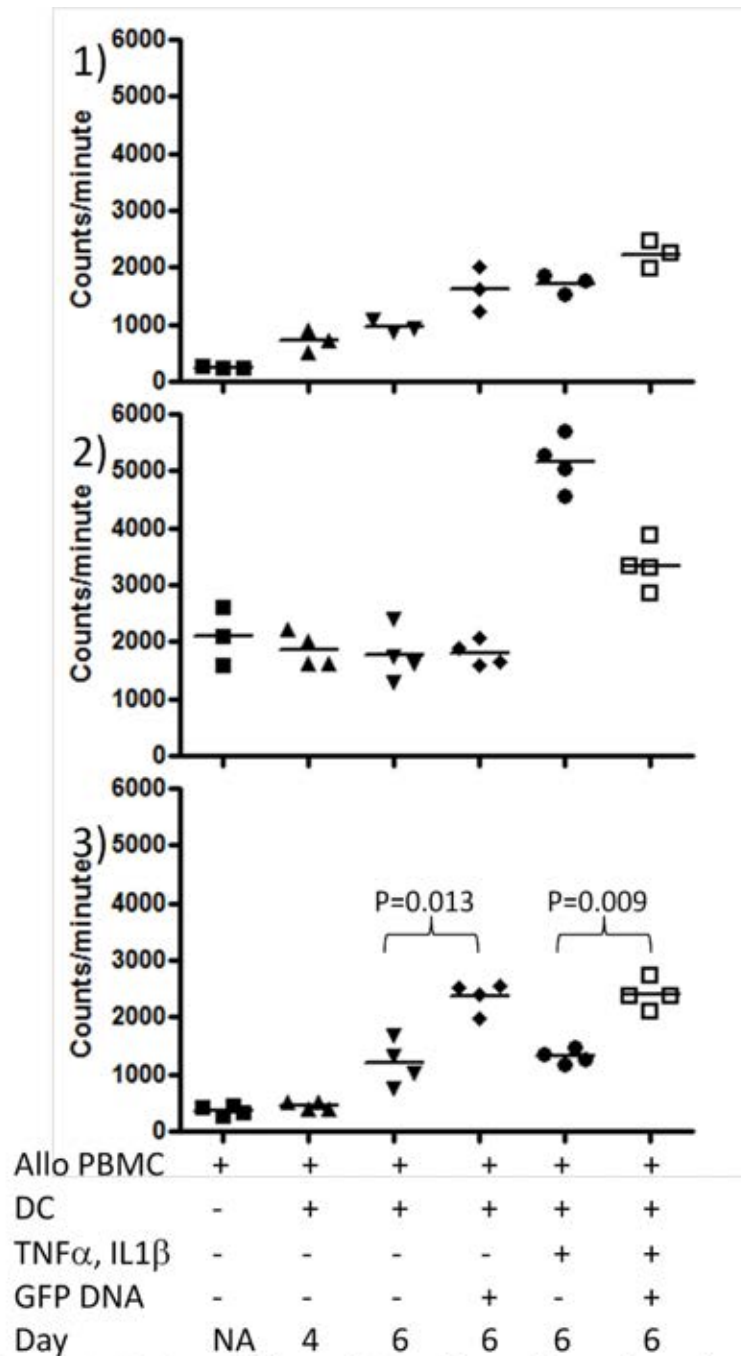
Figure 3.12 A. **Ability of DCs (from three donors) to stimulate proliferative responses in allogeneic PBMCs.** $4x10^4$ DCs were irradiated at 4000 rad and then co-incubated with $2x10^5$ allogeneic PBMCs in quadruplicate in 96 well plates. As a negative control, wells were set-up with responder PBMC alone. After 5 days culture, 1μCi of ^{3}H thymidine was added to each well, and 20 hours later, cells were harvested. Incorporated radioactivity was measured on liquid scintillation counter. Results are presented as individual replicates and mean values (horizontal bars). Students' T-test was used to determine significance of differences between mean values of experimental groups as indicated.

1 and 3 are more immunogenic than those of donor 2. However, in terms of absolute levels of proliferation, the highest levels are achieved with donor 2 DCs.

Finally, cytokine secretion was measured by ELISA. The concentrations of IL12p40, IL12p70 and IL10 measured are illustrated in Figure 3.13. Interleukin-12 p40 levels are two to three-fold lower in DCs from donor 1. This is not unexpected as it has been found that only CD1a expressing DCs secrete IL-12 (Cernadas et al., 2009). However, there is an effect of exposure to GFP DNA in two of three donors. In donor 1 this is seen in the presence or absence of exogenous cytokines, whereas in donor 3 it is only apparent in the absence of cytokines. However, in donor 3 exposure to DNA in the absence of cytokines leads to almost equivalent IL12p40 production as exogenous cytokines. There is no evidence of IL12p70 production by DCs from donor 1, as expected from low CD1a expression. In donor two, there is evidence of IL12p70 secretion at a low level, but only in cells exposed to DNA and cytokines. In donor 3, exposure to DNA seems to slightly increase IL12p70 release. IL10 release is highest in donor 1, where exposure to DNA is associated with increased secretion. In donor 2, IL10 is secreted by cells exposed to inflammatory cytokines. In donor 3, there is barely detectable IL10 secretion by DCs.
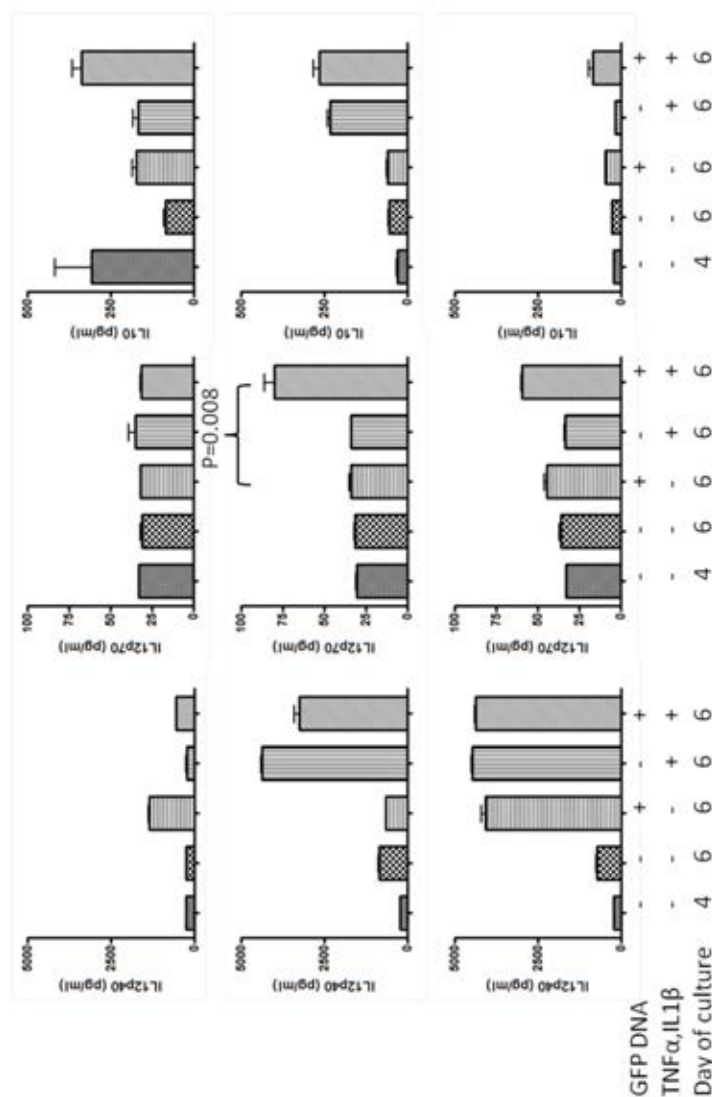
Figure 3.13. Measurement of cytokine secretion by DCs (from three donors). 500µl (of 2ml) supernatant was carefully removed from DC cultures without disturbing the cells, 48 hours after transfection or cytokine exposure. Supernatants were assayed for the presence of cytokines – IL12p40 (left panels), IL12p70 (middle panels) and IL10 (right panels) by sandwich/capture ELISA. Top panels – Donor 1, middle panels – Donor 2, bottom panels – Donor 3. Results are presented as mean values and ranges. Comparison of means was made using Students' T-test as indicated.

The critical observation is probably that biologically active IL12 (p70) is only released by DCs exposed to a stimulus via TLRs (i.e. DNA) and inflammatory cytokines. However, the absolute levels of bioactive (i.e. p70) IL12 release from these DCs is very low.

These experiments suggest that introduction of DNA into immature DCs using the CL22 peptide may lead to maturation, particularly in terms of allostimulatory capacity and cytokine release. Effects are, however, variable from donor to donor. It is noted that in the donor with the highest transgene expression, effects are the least impressive. In view of the demonstrable TLR9 expression in DCs, this may reflect the proposed endosomal localisation of TLR9.

3.5. Simultaneous Class I and Class II restricted epitope presentation by CL22 peptide transfected DCs.

Transfection of moDC using CL22 peptide and plasmid DNA has been shown to lead to presentation of Class I restricted epitopes using viral antigens in vitro (Haines et al., 2000). In a mouse model, vaccination with transfected DC led to production of opsonising antibodies against the antigens, suggesting helper T-cell involvement (Irvine et al., 2000). This transfection methodology has been taken forward into the clinical arena in the setting of metastatic melanoma (Steele et al., 2011). Although Class II restricted T-cell responses increased with vaccination, it has not been formally demonstrated in vitro that human DC transfected using this system present Class II restricted epitopes.

The aim of this experiment was therefore two-fold. The primary objective was to determine whether or not CL22 transfected DCs present MHC Class II restricted epitopes from endogenous antigen. The secondary objective was to determine whether or not the previously demonstrated lack of correlation between whole antigen detection and epitope

presentation held true for other (i.e. non-melanoma) antigens.

3.5.1. Antigens and epitopes.

The antigens and epitopes studied in this set of experiments is summarised in tabular form below (Table 3.4)

Table 3.4. EBNA1 epitopes studied

Antigen	Epitope	Amino acid position	HLA restriction
Epstein Barr Virus Nuclear Antigen 1	TSLYNLRRGTALAI (Long et al., 2005)	515-528	DR1 (DR103)
Epstein Barr Virus Nuclear Antigen 1	HPVGEADFYEY (Leen et al., 2001)	407-417	B35

The Epstein Barr virus EBNA1 antigen is vital for episomal maintenance of the viral genome in host cells and is expressed in all forms of latent viral infection (Leight and Sugden, 2000). More pertinent to DC vaccines for cancer, it

163

is the only EBV protein expressed in all EBV driven malignancies including nasopharyngeal carcinoma (Young et al., 1988), Hodgkin's lymphoma (Grasser et al., 1994) and post-transplant lymphoproliferative disease (Hopwood and Crawford, 2000). Antigen processing and presentation of EBNA1 are relatively well-characterised. The protein contains a long repetitive sequence (Glycine-Alanine repeat) that inhibits presentation of MHC Class I restricted epitopes (Levitskaya et al., 1995). This is due to slower rate of translation and decreased DRiP generation (Tellam et al., 2007) and also resistance to proteasomal degradation (Tellam et al., 2001). The natural nuclear localisation of EBNA1 depends upon a signal sequence. Alteration of this sequence can artificially re-localise the protein into cytoplasmic compartments (Kitamura et al., 2006). In order to get a comprehensive picture of Class II restricted epitope presentation from EBNA1, all three forms of the protein were expressed: full length EBNA1, GA repeat deleted EBNA1 and cytoplasmic GA repeat deleted EBNA1. As a positive control for MHC Class II restricted presentation, a fourth EBNA1 variant was included – EBNA1ΔGA-invariant chain.

3.5.2. Tools: T-cell clones.

A CD8 T cell clone specific for the EBNA1 $_{407-417}$ epitope (**HPV**GEADFYEY) was a kind gift from Dr. Jill Brooks. The HPV epitope is restricted through HLA B35, and the clone recognises B35 matched LCL (autologous and allogeneic) in IFNγ ELISPOT assays. These cells endogenously express EBNA1 from the resident Epstein-Barr virus genome. Recognition of B35 positive, but not B35 negative, LCL is enhanced by addition of exogenous HPV peptide. This is shown in Figure 3.14.

A CD4 positive T cell clone specific for the EBNA1 $_{515-528}$ epitope (**TSL**YNLRRGTALAI) was generated from a DR1 positive EBV seropositive donor previously demonstrated to make responses to this epitope, using limiting dilution cloning. The functional avidity and MHC restriction of clones was assessed using autologous B-cell blasts as target cells. Targets were pulsed with reducing concentrations of cognate peptide, in the presence or absence of anti MHC antibodies, in IFNγ ELISA assays. The results of these assays are shown in Figure 3.15A and B. There is evidence of HLA-DR restriction and a response to B-cell blasts pulsed with 1nM exogenous peptide. However, it was also important to assess their ability to recognise cells endogenously expressing EBNA1 rather than merely exogenously added peptide, to gauge the sensitivity of the clone. As shown in Figure 3.15C, the

T cell clone	+	+	+	+	+	+	+
LCL	-	+	+	+	+	+	+
Autologous	-	+	+	-	-	-	-
HLA-B35 match	-	-	-	+	+	-	-
HLA-B35 mismatch	-	-	-	-	-	+	+
HPV peptide 10^{-5}M	-	-	+	-	+	-	+
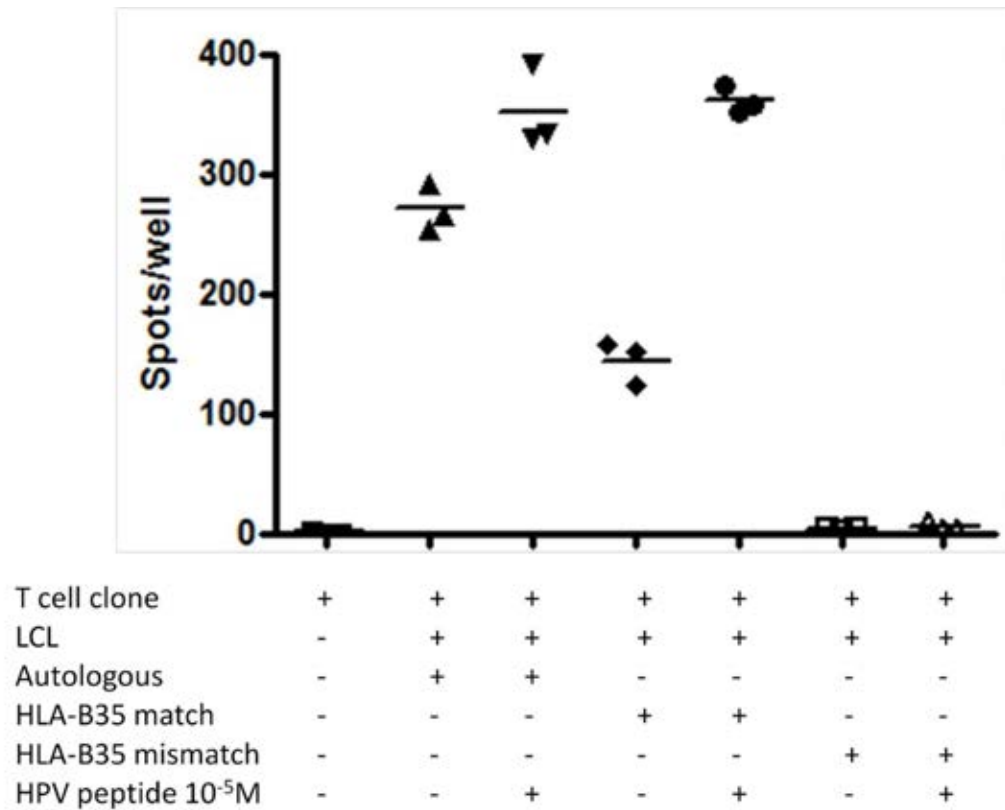
Figure 3.14. Characterisation of EBNA1 HPV specific clone. EBNA1 $_{407-417}$ specific clone c41 (10^3 cells/well) was co-incubated with EBV transformed LCLs (autologous, HLA B35 match and mis-match) (10^4 cells/well) in triplicate overnight IFNγ ELISPOT assays. Additionally, target LCLs were either pulsed with HPV peptide at 10^{-5}M or not. Results are presented as spot counts/well – triplicate and mean (horizontal bars) values.
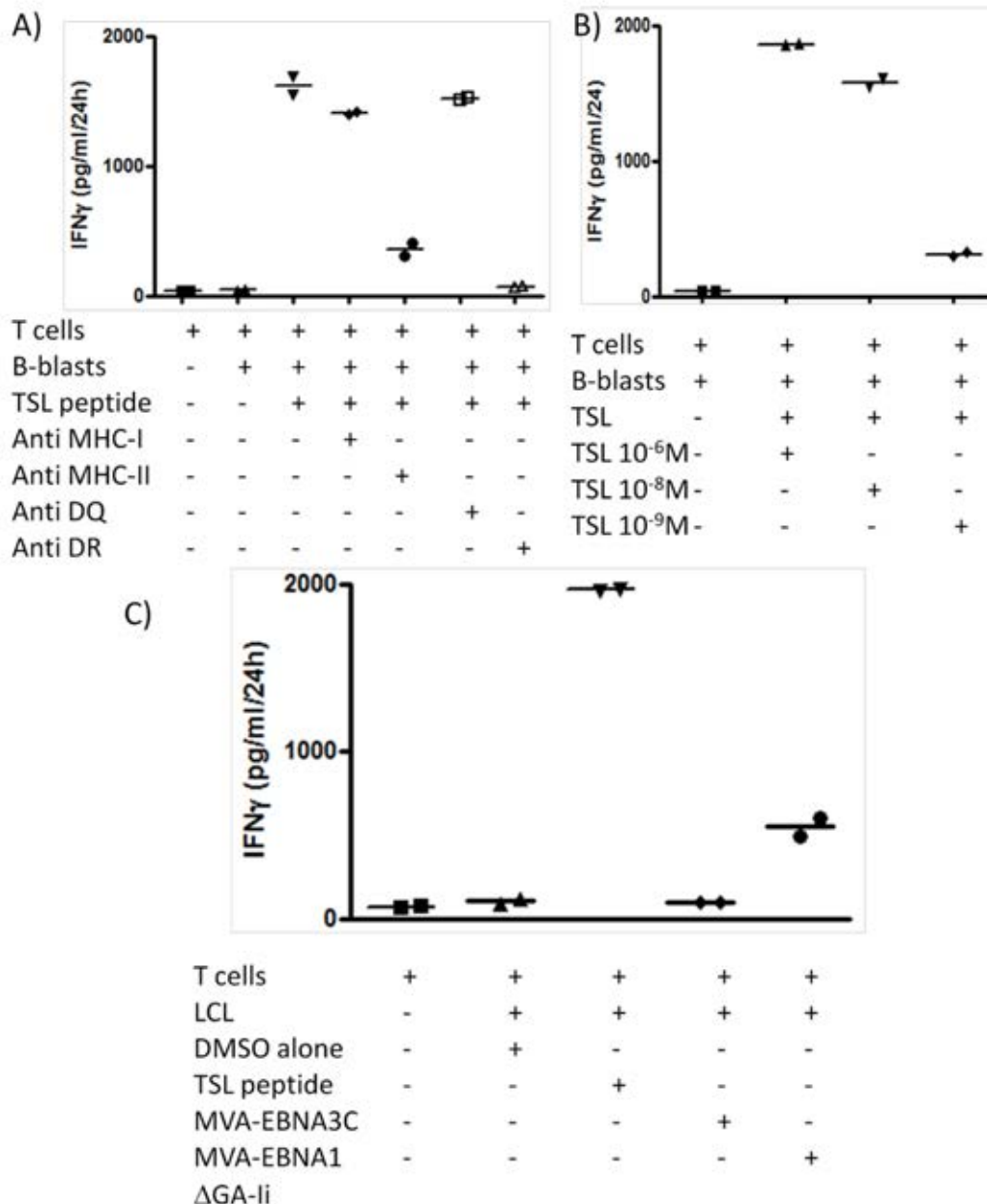
Figure 3.15A-C. Characterisation of EBNA1 TSL specific T cell clone B5. A)MHC Restriction. Effector cells were TSL clone B5 at 5×10^3/well and target cells were autologous B-cell blasts loaded with 10^{-6}M TSL peptide at 10^4/well. Anti-MHC antibodies were added to co-cultures as indicated. Assays were set up in duplicate. After 24 hours, supernatants were collected and IFNγ was measured by ELISA. Results are presented as duplicate and mean values. **B)Functional avidity.** Target cells were autologous B-cell blasts pulsed with exogenous TSL peptide at concentrations of 10^{-6}, 10^{-7} and 10^{-9}M, or DMSO alone (5×10^3 effectors, 10^4 targets/well). **C)Recognition of cells expressing whole EBNA1.** Target cells were autologous B-LCL either pulsed with TSL peptide at 10^{-6}M or DMSO alone, or infected with MVA-EBNA1ΔGA-invariant chain or MVA-EBNA3c virus. 5×10^3 effectors, 10^4 targets/well.

clone is able to recognise DR1 positive target cells endogenously expressing EBNA1. Autologous LCL were transduced with a modified vaccinia Ankara (MVA) virus expressing EBNA1ΔGAr-invariant chain (or EBNA3C negative control) at a multiplicity of infection of 1 and these were clearly recognised, at approximately 1/3 to 1/4 of peptide-stimulated levels.

The EBNA1ΔGAr-invariant chain MVA virus expresses a fusion protein of EBNA1 and the cytoplasmic tail and transmembrane domain of the human invariant chain polypeptide (amino acids 1-80, NH_2 terminus))(Chaux et al., 1999). This invariant chain sequence causes the EBNA1 protein to be ectopically localised in the endolysosomal system with resultant improved MHC Class II restricted presentation.

3.5.3. Tools: EBNA1 plasmid DNA.

To confirm functionality of EBNA1 plasmids (EBNA1 full length, EBNA1ΔGAr, EBNAΔGAr cytoplasmic) they were introduced into HEK293 cells using Lipofectamine 2000. After 72 hours, cells were harvested and EBNA1 expression was assessed by immunocytochemistry and immunoblotting. As

shown in Figure 3.16, all three plasmids lead to the production of EBNA1 species of the correct molecular weights. Immunofluorescence staining of transfected cells, shown in Figure 3.17, indicates that EBNA1 protein is produced from these plasmids and that the nuclear localisation signal mutation does indeed relocalise the protein from the nucleus to the cytoplasm.

In contrast to Figures 3.16 and 3.17, where functionality of EBNA1 plasmid DNA constructs was confirmed by expression in HEK293 cells followed by antibody staining, an alternative approach was required in the case of the EBNA1ΔGAr-invariant chain construct. A plasmid encoding EBNA1ΔGAr-invariant chain in the pcDNA3.2 vector that other EBNA1 constructs are in was generated. Being ectopically expressed in the endo-lysosomal compartment, the antigen is expected to be rapidly degraded and in the B-cell system is barely detectable by Western blot (G.Taylor, University of Birmingham, personal communication). Therefore, its functionality was assessed in T-cell recognition assays. HLA DR11 positive LCL were transfected (by electroporation) with the plasmid and recognition by VYG specific CD4 positive T-cells (EBNA1 $_{509-528}$) was measured in IFNγ ELISA. As shown in Figure 3.18, there is a clear increase in IFNγ release by a VYG specific

Figure 3.16. Expression of EBNA1 plasmid DNA (pcDNA3.2 backbone) in HEK293 cells. 293 cells were transfected using Lipofectamine 2000, and after 72hours cell lysates were prepared. Lysates were also prepared from LCLs which express EBNA1 from the resident EBV genome. 20µg protein was separated by SDS-PAGE and transferred to a nitrocellulose membrane. Membranes were blocked with 5% milk in PBS, and probed with anti EBNA1 antibody (1H4) (1/50), followed by rabbit anti rat-HRP secondary antibody (1/1000). After extensive washes, enhanced chemiluminescent substrate was applied and x-ray film exposed for 15 seconds. Abbreviations – LCL: EBV transformed B lymphocytoid cell line, ΔGA: gly-ala repeat deleted, NLS – nuclear localisation sequence mutated (cytoplasmic), GA+ - gly-ala repeat containing (full-length).

PLASMID DNA

pcDNA3.1

EBNA1ΔGAr

EBNA1ΔGAr
cytoplasmic
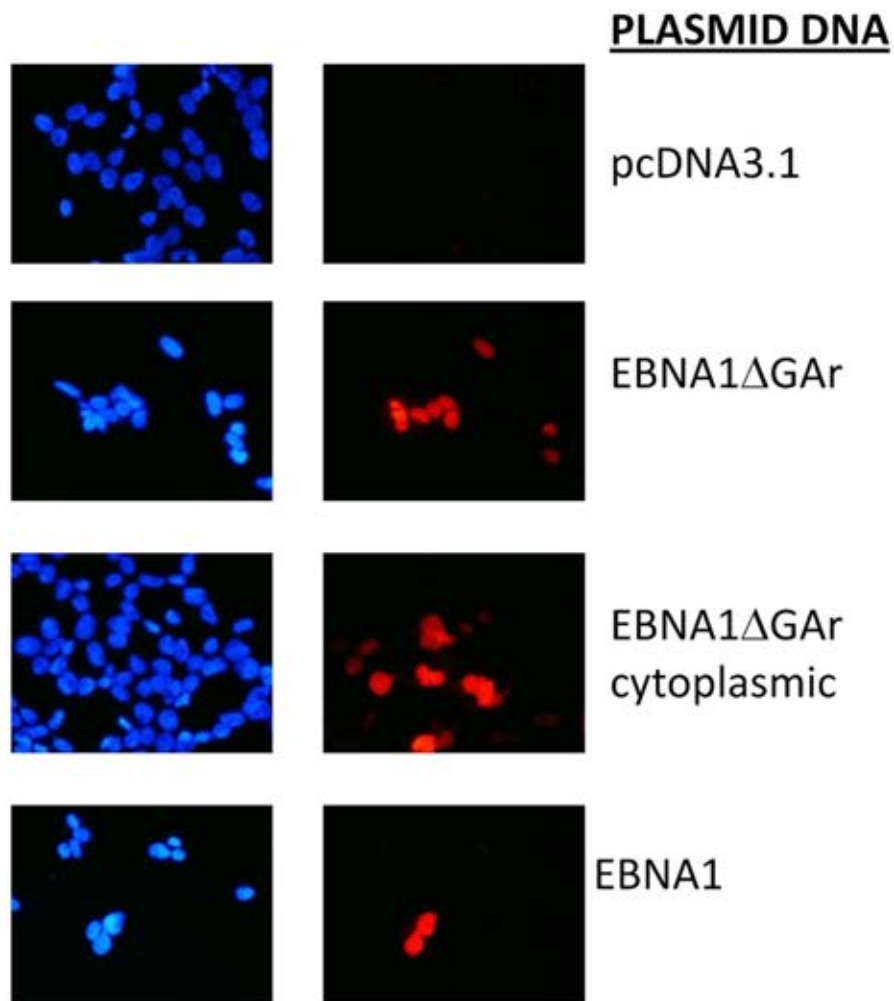
EBNA1

Figure 3.17. Expression of EBNA1 in transfected HEK293 cells by immunocytochemistry. 293 cells were transfected with the indicated DNA constructs using Lipofectamine 2000 and analysed after 72 hours. Cells were fixed with 4% paraformaldehyde, permeabilised with 0.5% Triton X100. Antigen retrieval was performed by boiling slides in 1M citric acid for 30 minutes. Non-specific binding was blocked with 20% HINGS. Primary antibody was rat anti EBNA1 (1H4) at 1:50, followed by goat anti rat Alexa 594 (1/500). After extensive washes, cells were stained with DAPI and viewed on a fluorescence microscope. Left panels show nuclear staining with DAPI, right panels show red fluorescence (indicative of EBNA1 staining).

VYG specific T cells	+	+	+	+	+
HLA DR11 LCL	-	+	+	+	+
GFP DNA	-	+	-	-	-
pcDNA3.2	-	-	+	-	-
EBNA1ΔGA DNA	-	-	-	+	-
EBNA1ΔGA-Ii DNA	-	-	-	-	+
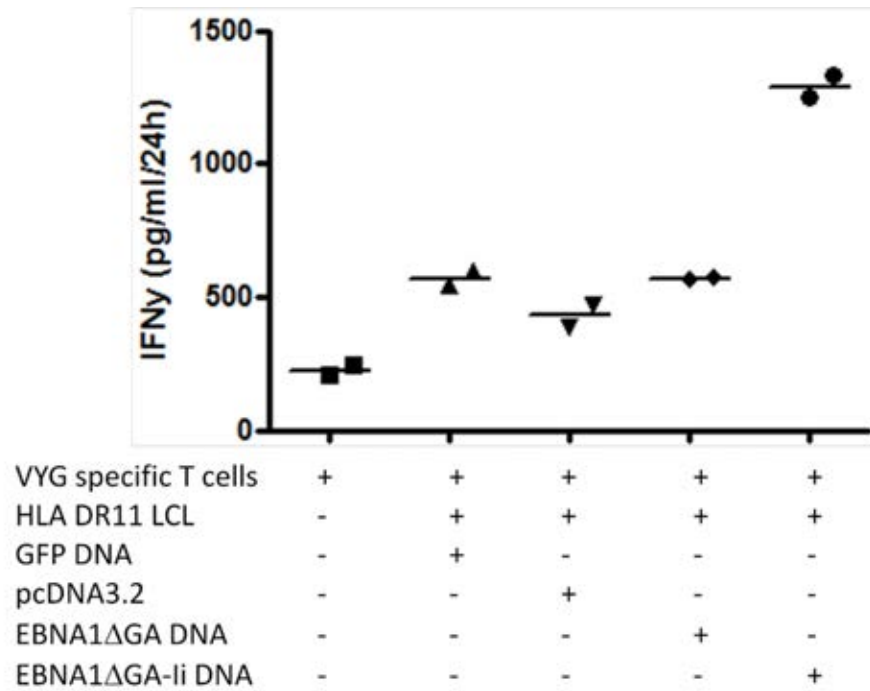
Figure 3.18. Functional assessment of EBNA1dGA-Ii plasmid DNA.
Recognition of HLA DR11 positive LCL electroporated with plasmid DNA: negative controls (GFP, pcDNA3.2), EBNA1ΔGAr, EBNA1ΔGAr-Invariant chain (Ii) by VYG (EBNA1 $_{509-528}$) specific CD4 T-cell clone. 5 x 10^4 LCL were coincubated with 10^4 T-cells per well. Duplicate and mean values are shown.

clone in response to LCL transfected with this plasmid. This indicates that EBNA1 is expressed from this construct and it is able to gain access to the MHC Class II pathway, as expected.

EBNA1 was chosen as a model antigen for these experiments. The protein's glycine-alanine repeat (GAr) provides a degree of protection from CTL recognition but has not been reported to have any inhibitory effect on MHC Class II restricted epitope presentation. In vivo, CD4 T-cell responses against EBNA1 epitopes are particularly abundant, in constrast to the CD8 response. Plasmid DNA encoding four different forms of EBNA1 was used: EBNA1ΔGAr, EBNA1ΔGAr cytoplasmic, full length EBNA1 and EBNA1ΔGAr-invariant chain (Ii). The EBNA1ΔGAr cytoplasmic plasmid contains a mutation within the EBNA1 nuclear localisation sequence and the protein is therefore redistributed in nuclear and cytoplasmic compartments rather than being exclusively nuclear. The EBNA1ΔGAr-invariant chain construct encodes a fusion protein of EBNA1ΔGAr and the cytoplasmic tail and transmembrane domain of the human invariant chain. This protein is ectopically expressed in the endolysosomal system where MHC Class II restricted epitopes are generated.

Use of the full range of EBNA1 constructs allows determination of the role of cellular localisation (nuclear versus cytoplasmic versus endolysosomal) and protein stability and rate of translation in generation of Class II restricted epitopes (full length versus GAr deleted).

The aim of these experiments (Figures 3.19 to 3.21) was to determine whether CL22 transfection of mo-DCs with EBNA1 encoding DNA led to presentation of MHC Class II restricted epitopes; and to determine the relation between whole antigen expression and Class I and II epitope presentation.

3.5.4. Whole antigen expression in EBNA1 transfected DCs.

DC were prepared from a B35 and DR1 positive donor. These DC were CL22 transfected with plasmid DNA encoding EBNA1: EBNA1ΔGA, EBNA1ΔGA cytoplasmic, full length EBNA1 and EBNA1ΔGAr-invariant chain (Ii). All these EBNA1 constructs were in the pcDNA3.2 plasmid vector (Invitrogen). After 48 hours TNFα and IL1β exposure, cells were stained for EBNA1 by immunocytochemistry and their recognition by EBNA1 $_{407-417}$ (HPV, Class I) and EBNA1 $_{515-529}$ (TSL, Class II) specific T-cell clones was assayed by overnight IFNγ ELISPOT assays. Cell viability was over 95%.
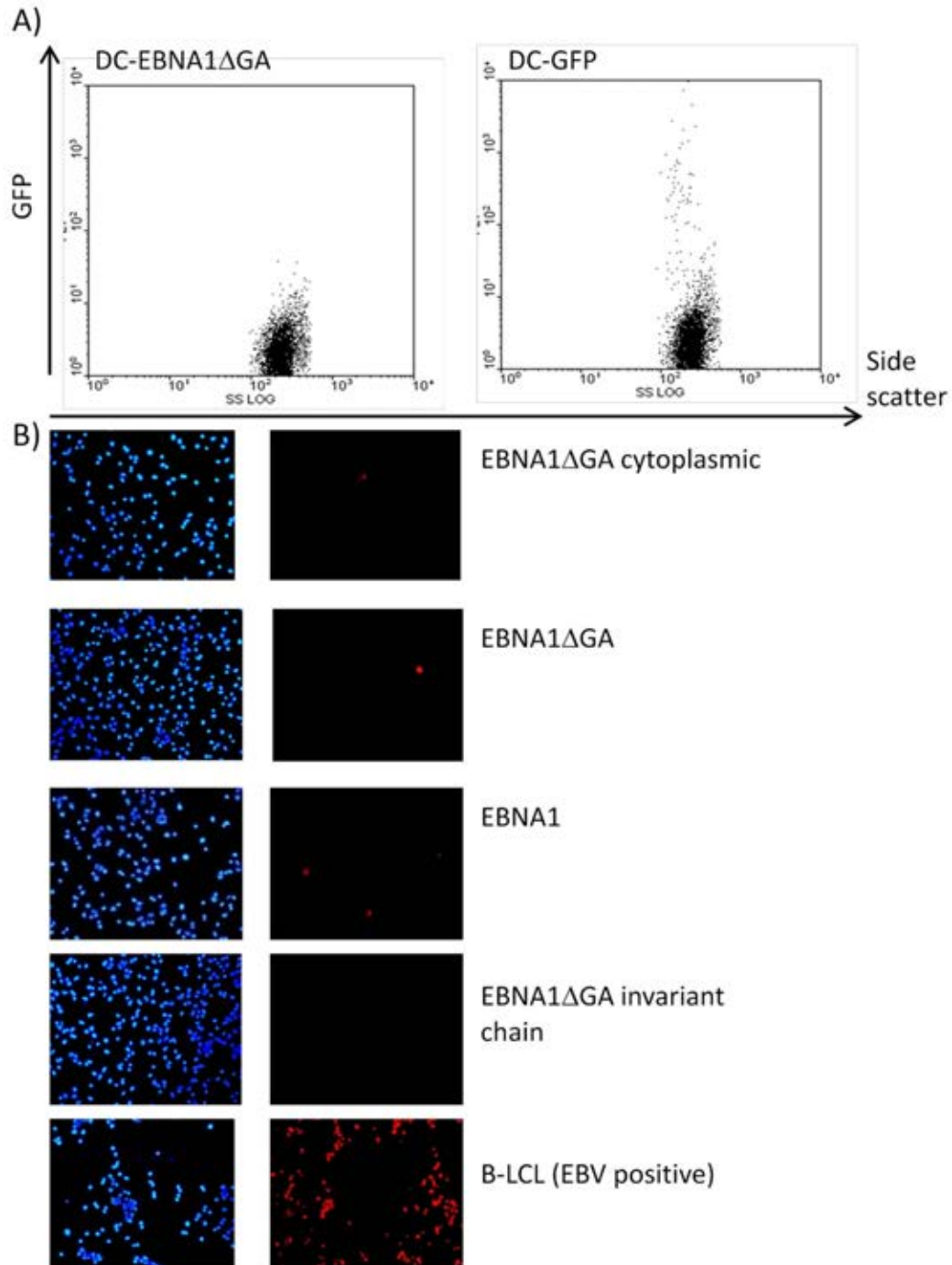
Figure 3.19. EBNA1 expression in CL22 transfected DCs. A)DC transfected with GFP DNA or EBNA1ΔGAr DNA were analysed by flow cytometry for green fluorescence. DC were gated based on typical side scatter and forward scatter characteristics. 10000 gated events were counted. B)EBNA1 transfected DC were stained with EBNA1 rabbit polyclonal antibody followed by goat anti rabbit Alexa 594 secondary antibody and analysed by fluorescence microscopy. Nuclear staining with DAPI is shown on the left and red fluorescence (EBNA1 staining) on the right panels.

DC	+	-	+	+	+	+	+	+	+
T cells	-	+	+	+	+	+	+	+	+
DMSO	-	-	+	-	-	-	-	-	-
HPV/TSL 10^{-6}M	-	-	-	+	-	-	-	-	-
GFP DNA	-	-	-	-	+	-	-	-	-
E1ΔGA DNA	-	-	-	-	-	+	-	-	-
E1GA NLS DNA	-	-	-	-	-	-	+	-	-
E1 DNA	-	-	-	-	-	-	-	+	-
E1ΔGA-Ii DNA	-	-	-	-	-	-	-	-	+
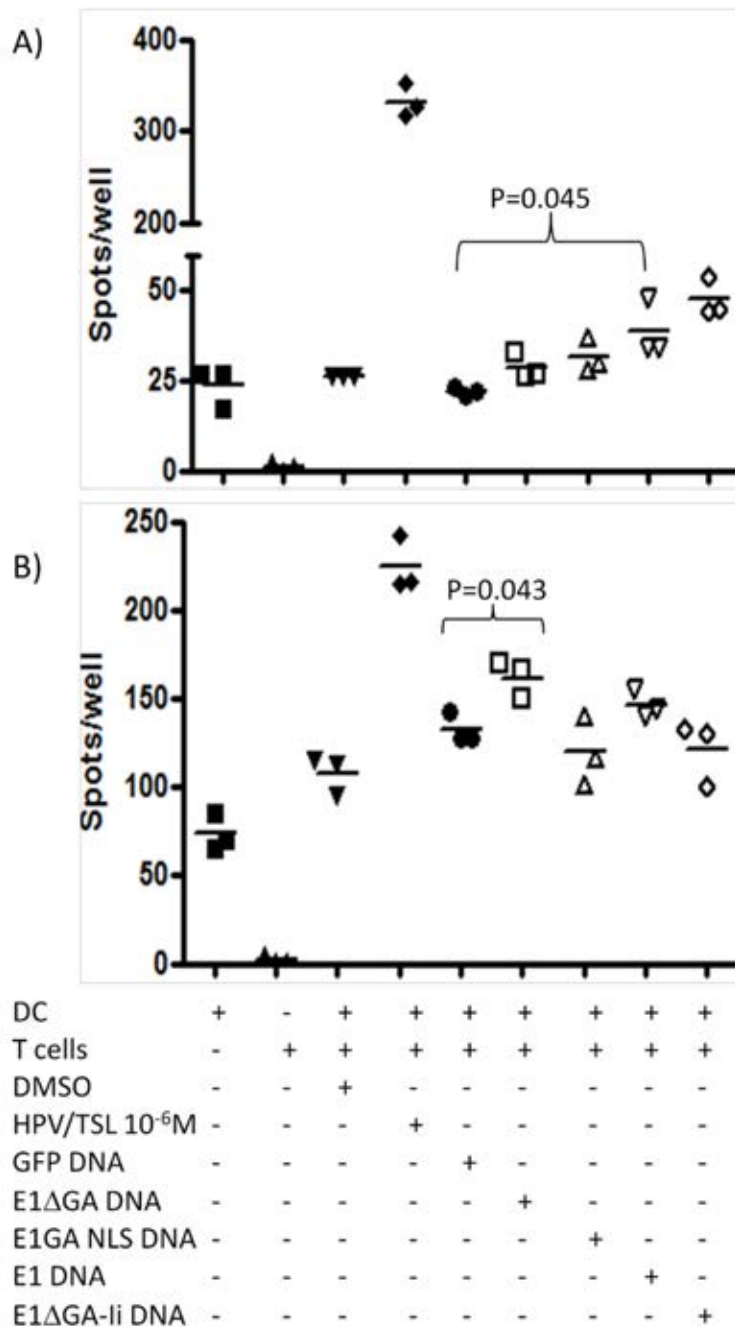
Figures 3.20A and B   Recognition of transfected and peptide-loaded DC by TSL (A) and HPV (B) specific T-cell clones. DC were either loaded with cognate peptide (1μM) or DMSO (control), or transfected with plasmid DNA encoding EBNA1 (E1), EBNA1-GAr deleted (ΔGA), EBNA1ΔGA cytoplasmic (NLS), EBNA1ΔGA-invariant chain (Ii) or GFP (control). 10^4 DC were coincubated with 10^3 T cells in overnight IFNγ ELISPOT assays. Results are shown as triplicate and mean values. Significance of the difference between means of experimental groups are calculated using Students' T-test as indicated.
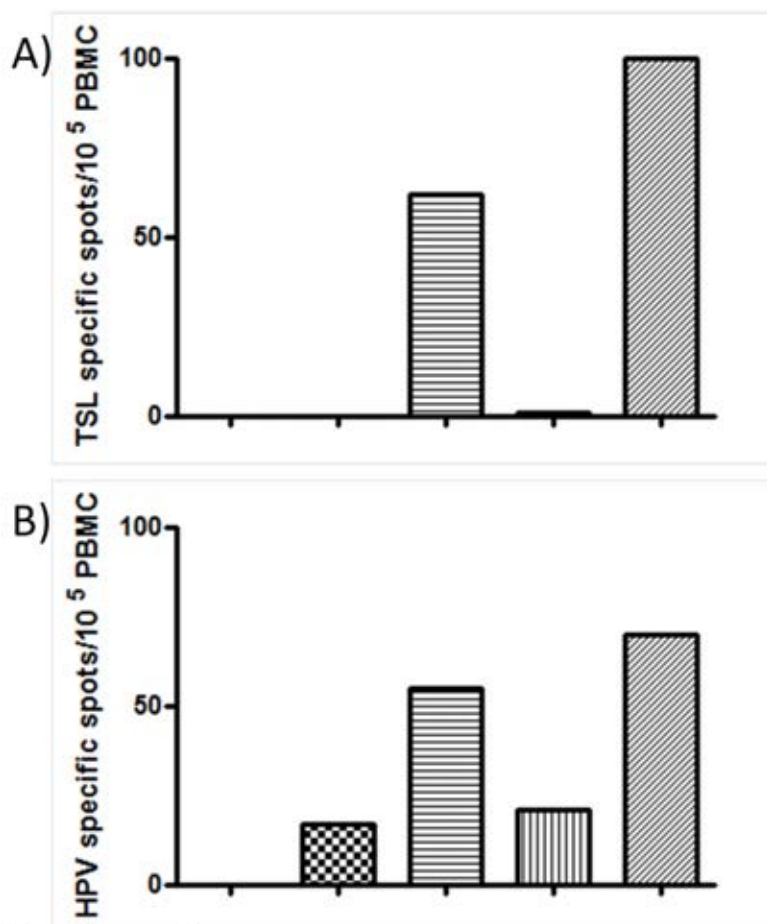
Stimulator cells:

EBNA1ΔGA	+	-	-	-	-
EBNA1ΔGA-NLS	-	+	-	-	-
EBNA1	-	-	+	-	-
EBNA1ΔGA-li	-	-	-	+	-
TSL/HPV peptide	-	-	-	-	+

Figures 3.21A and B. Immunogenicity of CL22 EBNA1 transfected DCs
Transfected (GFP control and EBNA1) and peptide loaded (DMSO control, TSL/HPV peptide) DC (1.5×10^5/well) were coincubated with autologous non-adherent PBMC (1.5×10^6/well). After 7 days, a further 1.5×10^5 DC were added to cultures, as was 25 u/ml IL2. On day 14, cells were harvested and used as responder cells (1.5×10^5/well) in IFNγ ELISPOT assays using autologous B-cell blasts (3×10^4/well) loaded with DMSO or TSL/HPV peptides (10μM) as stimulator cells. Results are presented as TSL (A) or HPV (B) specific spot counts (spot count in the presence of peptide loaded – DMSO only B-blasts). Y-axis displays the spot count obtained with antigen loaded stimulator cells minus antigen negative (i.e. GFP expressing) stimulator cells.

GFP expression in transfected DC was 1.5% by flow cytometry (Figure 3.19A). Preliminary experiments, comparing transfection methods, had shown that CL22 transfection was highly variable in efficiency (range 0 to 11% GFP positive cells) in contrast to RNA electroporation that was highly efficient (consistently >90% GFP positive cells). EBNA1 staining revealed occasional EBNA1 positive cells, with an frequency of 1/100-1/150 in all transfections except the EBNA1ΔGAr-invariant chain (Figure 3.19B). This is of the same order of magnitude as the GFP expression. There is strong staining on EBNA1 positive EBV transformed B-LCL. The antibody used for EBNA1 detection (R4) has been shown to recognise EBNA1 expressed from these DNA constructs in HEK293 cells. Additionally, DCs expressing EBNA1 from RNA generated using these constructs as the template, are also clearly stained by the R4 antibody. This confirms that the antibody recognises artificially and naturally (i.e. from the resident EBV genome) expressed EBNA1 protein.

3.5.5. Antigenicity of EBNA1 transfected DCs.

In terms of antigen presentation, there was evidence of recognition of EBNA1 expressing DC compared to GFP transfected (control) DC for Class I and II restricted clones in IFNγ ELISPOT assays. There was a hierarchy of

recognition - invariant chain tagged EBNA, then full length EBNA1 followed by cytoplasmic EBNA1ΔGAr expressing DC - by the TSL specific clone as shown in Figure 3.20A. Although the level of recognition was modest in comparison to peptide-stimulated responses (approximately 5%), these data show that the Class II restricted TSL epitope is presented to specific CD4 T cells after CL22 transfection. Full-length EBNA1 appears most likely to give rise to Class II epitope presentation, perhaps as a result of reduced proteasomal processing and therefore increased availability for endolysosomal processing. As expected, the TSL epitope is presented most efficiently by DCs expressing invariant chain tagged EBNA1.

In parallel with these experiments, presentation of a Class I restricted epitope (HPV) by these same DCs was also examined. The HPV specific clone recognised DC expressing full length EBNA1 and EBNA1ΔGAr (Figure 3.20B) in IFNγ ELISPOT assays. Again, levels of recognition were relatively low in comparison to peptide-driven responses. Particularly in view of the low level of EBNA1 expression in these DC preparations, this result is important in confirming that successful transfection and gene expression was achieved. The level of HPV epitope display from full-length EBNA is similar to GA repeat deleted EBNA1. This is

in accordance with reports that GA repeat mediated protection from Class I presentation is not absolute.

T-cell recognition assays demonstrate that presentation of a Class II restricted epitope from endogenously expressed EBNA1 occurs. Additionally, Class I and II epitope presentation takes place simulataneously despite relatively low proportions of DCs expressing whole antigen at 48 hours.

3.5.6. Immunogenicity of EBNA1 transfected DCs

However, in these experiments epitope presentation is measured only at a specific time-point (between 48 and 72) hours after transfection. In vivo, DC migration from the administration site to T-cell zones of secondary lymphoid tissue takes 24-48 hours (Adema et al., 2005), so persistent epitope presentation may be more physiologically relevant.

Experiments were therefore extended in scope. Their aim was to determine whether or not DC transfected with EBNA1 encoding DNA using the CL22 peptide can expand TSL and HPV specific T-cell populations within PBMC.

This question was answered by using the same transfected DCs as stimulator cells and autologous non-adherent PBMC as responder cells in polyclonal cultures. This method mirrors the clinical use of DC vaccines to stimulate T-cell responses in cancer patients and is therefore pertinent. Also, unlike T-cell recognition assays, in-vitro reactivation experiments gauge epitope display over a far longer period (7-14 days). Once again, for transfected cells the negative control transfection was with GFP encoding DNA, and negative control for peptide (HPV or TSL) loaded DCs was DMSO without peptide. An initial stimulation was performed, and excess transfected (and mature untransfected) DCs were cryopreserved. Seven days later, these DCs were thawed (and untranfected DC were loaded with peptides) and added to polyclonal lines. Low dose IL-2 was added at this time.

The polyclonal T-cell lines thus generated were analysed for the presence of either HPV or TSL specific IFNγ secreting T-cells by overnight ELISPOT assays on day 14. In these, stimulator cells were previously cryopreserved autologous B-cell blasts loaded with exogenous peptide (HPV, TSL) at 5μM and responders were polyclonal PBMC.

Quantification of TSL and HPV specific responses is illustrated in Figures 3.21A and B. Peptide-specific spot counts were calculated as number of spots in the presence of peptide-loaded versus DMSO only B-blasts. Results are presented as spot count with antigen loaded DC – spot count with antigen negative DC (GFP or DMSO). Peptide-loaded DC are able to expand the epitope specific T-cell populations, and in terms of absolute numbers TSL specific responses are increased to a greater extent than HPV (≈100 spots/well v 70 spots/well). In terms of transfected DCs expressing whole EBNA1, only full-length EBNA1 expressing cells lead to expansion of both HPV and TSL responses. In both cases, responses with full length EBNA1 are comparable to peptide-driven responses. This is in marked contrast to the results obtained with T-cell clones as readouts. This difference could reflect the importance of persistent antigen presentation: possibly several days with transfected DC as compared to 12-16 hours with peptide-loaded cells. For HPV specific responses, EBNA1ΔGA cytoplasmic and EBNA1ΔGA-invariant chain expressing DCs are also immunogenic, but not to the same extent as full-length EBNA1. The superiority of full-length EBNA1 in these assays of DC immunogenicity could reflect the stability and long-lived nature of the protein in comparison to other isoforms. Overall, these results are consistent with those obtained using T-cell clones in

showing that CL22 transfection can lead to presentation of MHC Class II restricted epitopes and that epitope presentation (Class I or II) does not depend upon high levels of whole antigen expression.

3.6. Systematic comparison of dendritic cell transfection methodologies.

In general, CL22 transfection of DC is relatively inefficient in terms of transgene expression, although it can be variable. Therefore, alternative DC transfection methodologies were investigated.

Three transfection methods were used in this set of experiments. In brief, CL22 based transfection utilises a 35 amino acid cationic peptide (CL22) to condense plasmid DNA for cellular uptake (Haines et al., 2000). Transient exposure to the lysosomal acidification inhibitor chloroquine minimises endolysosomal degradation of DNA. This system has been shown to lead to reliable transfection of immature human monocyte-derived DCs (Irvine et al., 2000). Nucleofection is a proprietary technique using individual electroporation settings and solutions according to the cell type being transfected. The human dendritic cell nucleofector kit was used (Lonza Bio). Electroporation of in-vitro transcribed RNA is widely considered the most efficient method of transfection for human monocyte DCs and immunogenicity of these DCs has been demonstrated in preclinical and clinic settings (Ponsaerts et al., 2003).

3.6.1. GFP expression, cellular viability and phenotypic maturation.

Thus, a systematic comparison was made between CL221 transfection, DNA nucleofection and RNA electroporation using GFP in DCs. Nucleofection can be used to transfer DNA or RNA into DCs, however, preliminary experiments had indicated that RNA nucleofection of DCs was not particularly efficient and was poorly-sustained. On theoretical grounds, nucleofection is optimised to deliver nucleic acid to the nucleus, which would be unnecessary for RNA that only needs access to the cytoplasm.

Immature DC were prepared from a single donor, the yield of immature DC was 12×10^6 cells from 250×10^6 PBMC ($\approx 5\%$). The phenotypic profile of these iDC was typical and is shown in Figure 3.22A. 24 hours after transfection, cells were harvested and cellular viability and GFP expression was measured. GFP expression is presented in Figure 3.22B (i-iii).

Cellular viability, as assessed by trypan blue exclusion and light microscopy, and GFP expression is presented in Table 3.5.
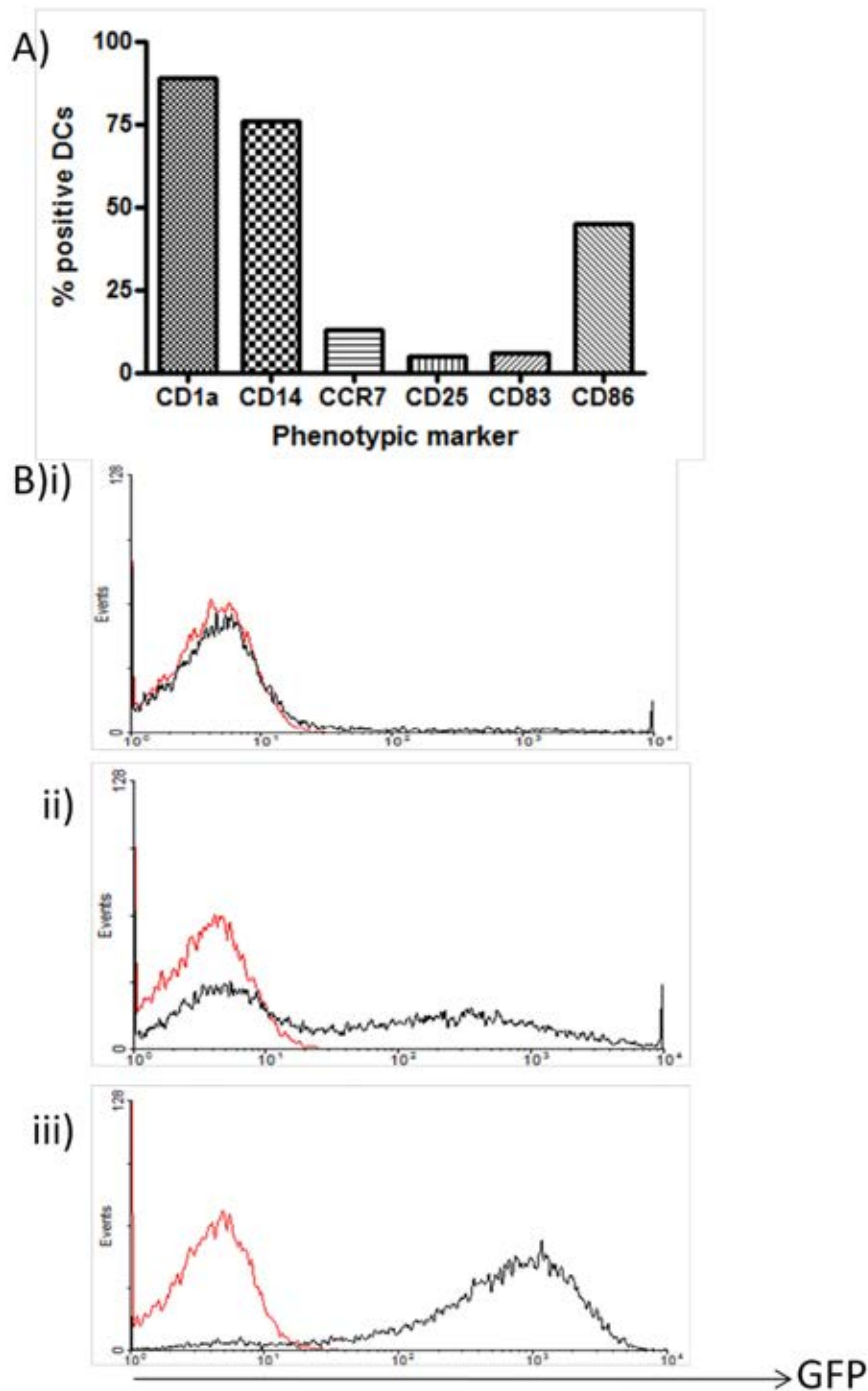
Figures 3.22A-B. Comparison of transfection methods in DC. Immature DC were transfected with nucleic acid encoding GFP or control (empty plasmid/no RNA) by CL22, DNA nucleofection and RNA electroporation. Cells were stained with a panel of antibodies (and isotype controls) and analysed by flow cytometry – A. After 24 hours exposure to TNFα and IL1β, DC were harvested and viability and GFP expression were measured - B. i)CL22 transfection ii)Nucleofection of DNA iii)RNA electroporation. 10^4 gated events (DCs) were collected. Red line – control. Black line – GFP.

Table 3.5. Comparison of DC transfection methods – transgene expression and viability at 24 hours.

	% viable DC		% DC GFP positive	
Transfection method	mock	GFP DNA/RNA	mock	GFP DNA/RNA
CL22	44.7	49.3	1.03	8.1
Nucleofection DNA	36.5	36.9	0.46	48.8
Electroporation RNA	44.7	43.7	0.55	93.1

These data demonstrate that CL22 transfection leads to good cell viability but low levels of transgene expression, nucleofection of DNA has a transfection efficiency approaching 50% with significant impairment of viability whereas RNA electroporation leads to high levels of transgene expression with excellent viability.

The ability of immature dendritic cells to upregulate markers of maturation (such as CD25, CD83 and CD86) in response to the proinflammatory cytokines TNFα and IL1β was demonstrated in the DC vaccine clinical trial after CTL901 transfection (Steele et al., 2011).

However, this has not been established for the other two transfection methods. Therefore, the phenotype of RNA electroporated DC was determined and this is compared to the pre electroporation (immature) phenotype in Figure 3.23. There is no evidence that the electroporation of RNA into immature DC impairs their subsequent ability to respond to proinflammatory cytokines by upregulating CD25, CD83 or CD86. GFP expression was 93% in these DCs, and phenotypic assessment of maturation markers was performed after 24 hours.

Nucleofection of DC led to approximately half of the cells expressing GFP, and this provided the opportunity for further investigation of the effect of the nucleofection process on the ability of immature DC to display phenotypic maturation. To separate the effect of the nucleofection process and the introduction of plasmid DNA into the DC, immature DC were nucleofected in the absence of DNA. These cells showed normal maturation in response to proinflammatory cytokines.

24 hours after nucleofection with GFP DNA, DC were approximately 50% GFP positive and cells were sorted on GFP into GFP negative and positive fractions. These two

populations were then stained with antibodies against three key DC surface markers (CD25, CD83 and CD86) and analysed by flow cytometry. The GFP negative fraction showed clear increases in CD25, CD83 and CD86. In contrast, the GFP positive fraction failed to show upregulation of these markers (Figure 3.24). This suggests that DNA nucleofection impairs the ability of immature DC to respond to a maturation stimulus. Similar findings have been reported previously (Lenz et al., 2003).

3.6.2. Epitope presentation by EBNA1 expressing dendritic cells.

The experiments discussed above show that all three transfection methods lead to detectable transgene expression using GFP, albeit at very different levels (7%, 48% and 93% GFP positive cells). Nucleofection is distinguished by lower cellular viability and possible impairment of DC 'maturation'.

These experiments were extended to determine whether or not differences in transgene expression, viability and 'maturation' between the three transfection methods translated to differences in presentation of MHC Class I and II restricted epitopes to T lymphocytes. Epitope
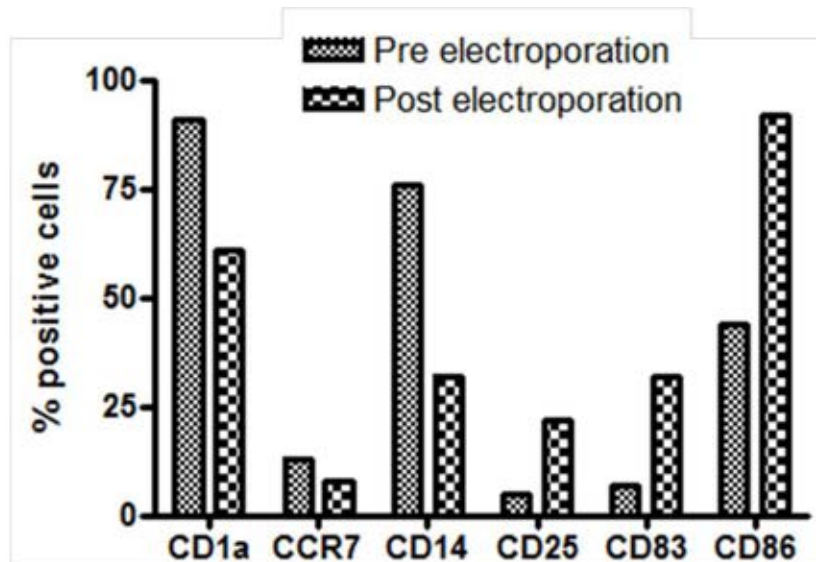
Figure 3.23. Phenotypic maturation of DCs electroporated with GFP RNA. Phenotypic analysis of immature DC and DC after RNA electroporation and 24 hours exposure to TNF and IL1β. % positive cells is calculated as % positive with specific antibody - % positive with matched isotype control antibody. Cells were analysed by flow cytometry and at least 10^4 events in the DC gate were counted.
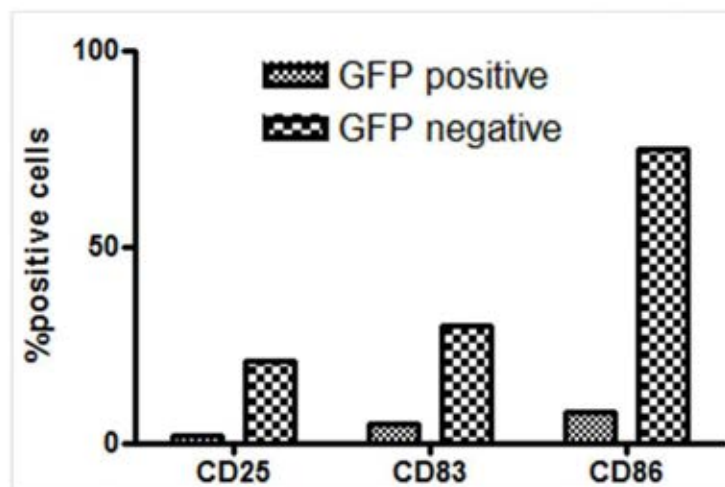
Figure 3.24. Phenotypic maturation of DCs nucleofected with GFP DNA. Immature DC were nucleofected with GFP DNA. After 24 hours culture with TNFa and IL1b, cells were sorted on GFP and the GFP positive and negative fractions were stained separately with anti CD25, CD83 and CD86 antibodies. Cells were analysed by flow cytometry and 5 x10^3 events in the DC gate were collected. % positive cells refers to % positive with specific antibody - % positive with matched isotype control antibody.

presentation is essential for an effective DC vaccine. The EBV antigen EBNA1 was used for this experiment.

HLA B35 and DR1 positive immature DCs were transfected with nucleic acid encoding EBNA1ΔGA, EBNA1ΔGA-invariant chain or GFP (negative control). These isoforms of EBNA1 were chosen for study as glycine-alanine repeat deleted EBNA1 is efficiently processed via the proteasome for Class I presentation (Levitskaya et al., 1995) and co-expression with the human invariant chain reroutes the protein into the MHC Class II loading compartments (Chaux et al., 1999). Both antigenicity (i.e. ability to be recognised by a T-cell clone) and immunogenicity (i.e. ability to expand the epitope specific T-cell population in peripheral blood lymphocytes) were assessed in these transfected DCs, along with measurement of whole antigen expression by immunofluorescence microscopy.

GFP expression was measured by fluorescence microscopy on transfected DCs:- proportion and percentage of GFP positive cells was 2/50 (4%), 4/58 (7%) and 80/122 (66%) for CL22 transfection, DNA nucleofection and RNA electroporation respectively.

Immunofluorescence microscopy for EBNA1 expression showed the following proportion and percentages of EBNA1 positive cells:- EBNA1ΔGA – 0/77 (0%), 6/85 (7%) and 35/110 (32%) EBNAΔGA-invariant chain – 0/80 (0%), 2/80 (2.5%) and 30/115 (26%) for CL22 transfection, DNA nucleofection and RNA electroporation respectively. These data are shown in Figures 3.25A-C. It is also clear that in RNA electroporated DCs, the EBNA1 staining intensity is clearly lower in cells transfected with the invariant chain tagged EBNA1 compared with EBNA1ΔGA transfected cells.

These data, concerning whole antigen expression, are in line with the results presented in Figure 3.22B, with a hierarchy of transfection efficiency with RNA electroporation being superior to DNA nucleofection which is superior to CL22 transfection.

3.6.2.1. Antigenicity of EBNA1 transfected DCs.

These cells (EBNA1 expressing) were then used as targets in overnight IFNγ ELISPOT assays with the EBNA1 TSL specific CD4 T cell clone (17B) and EBNA1 HPV specific CD8 T cell clone (17A) as effectors. Results of these T cell recognition assays are presented in Figures 3.26 A and B.
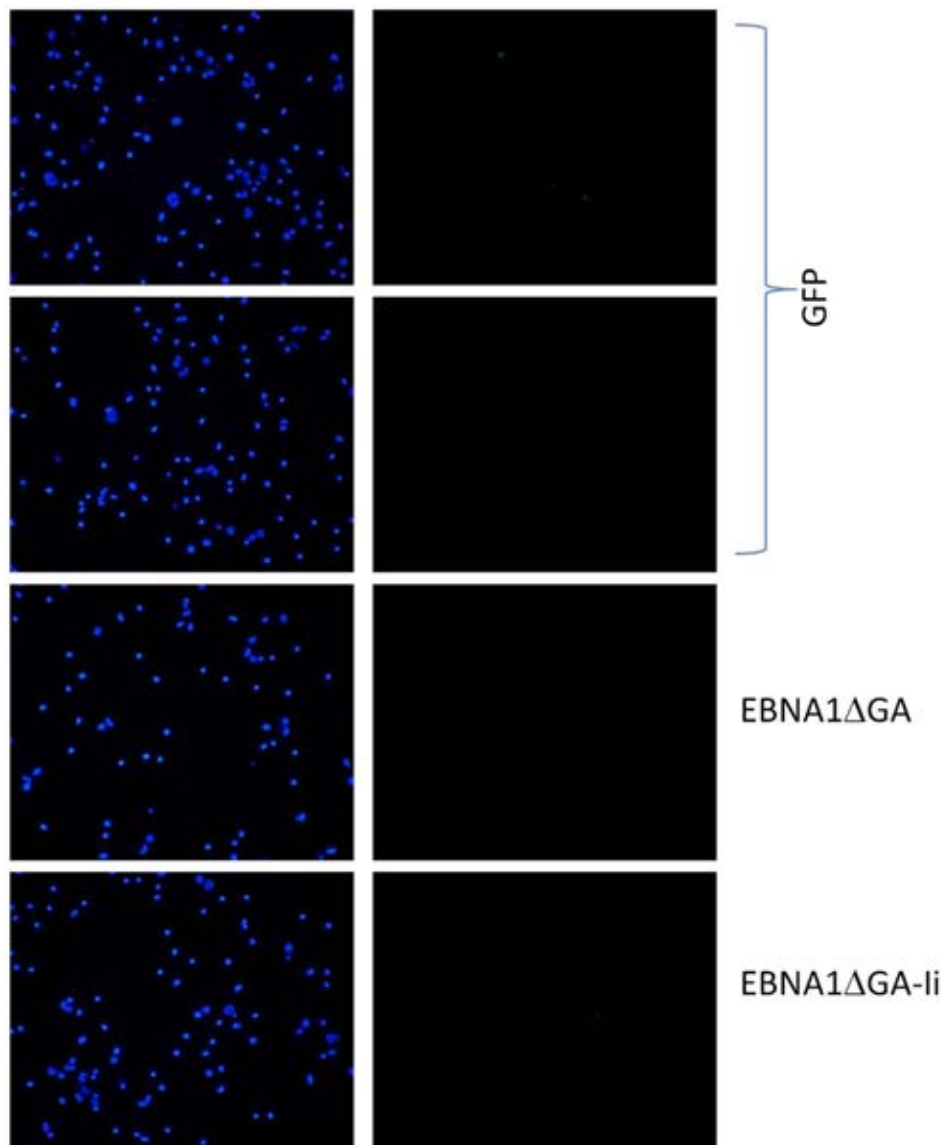
Figure 3.25A. Comparison of transfection methods in DCs: EBNA1 expression by immunofluorescence microscopy in cells transfected using CL22 peptide. 24 hours after transfection, DCs were fixed, permeabilised and stained with rabbit polyclonal anti EBNA1 antibody (R4), followed by goat anti rabbit-Alexa 594 secondary antibody. Left panels show nuclear staining with DAPI. Right hand panels show red fluorescence indicative of EBNA1 staining or green fluorescence in GFP expressing cells. The lower three panels show cells stained with EBNA1 antibody.
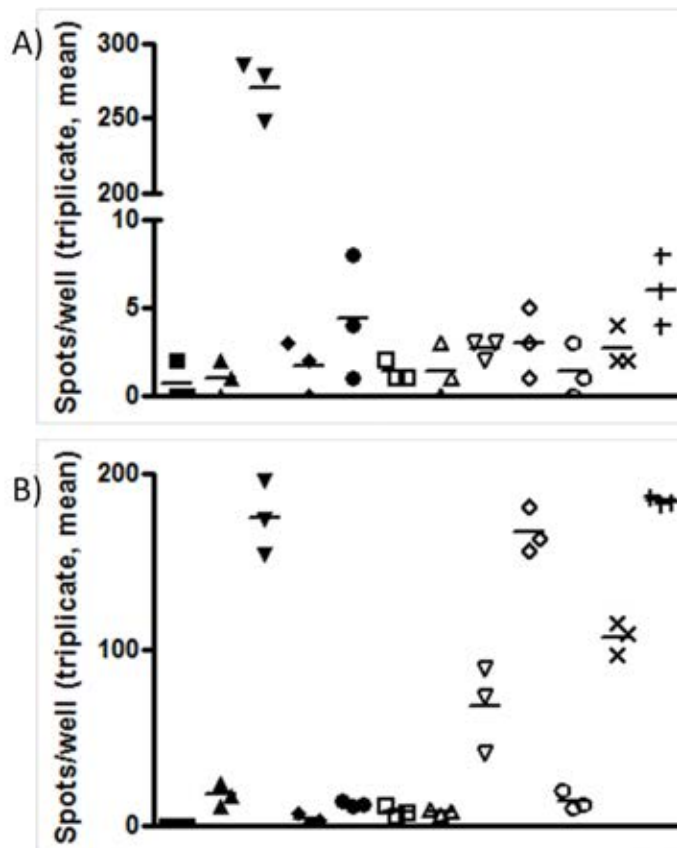
T cells		+	+	+		+	+		+	+	+		+	+		+	+
DCs		-	+	+		+	+		+	+	+		+	+		+	+
DMSO		-	+	-		-	-		-	-	-		-	-		-	-
Peptide		-	-	+		-	-		-	-	-		-	-		-	-
CL22-GFP		-	-	-		+	-		-	-	-		-	-		-	-
CL22-E1ΔGA		-	-	-		-	+		-	-	-		-	-		-	-
CL22-E1ΔGA-li		-	-	-		-	-		+	-	-		-	-		-	-
Nucleo-GFP		-	-	-		-	-		-	+	-		-	-		-	-
Nucleo-E1ΔGA		-	-	-		-	-		-	-	+		-	-		-	-
Nucleo-E1ΔGA-li		-	-	-		-	-		-	-	-		+	-		-	-
RNA-GFP		-	-	-		-	-		-	-	-		-	+		-	-
RNA-E1ΔGA		-	-	-		-	-		-	-	-		-	-		+	-
RNA-E1ΔGA-li		-	-	-		-	-		-	-	-		-	-		-	+

Figures 3.26 A and B. Recognition of EBNA1 expressing DCs by TSL (A) and HPV (B) specific T-cell clones in IFNγ ELISPOT assays. 24 hours after transfection, DCs were counted and used as targets (10^4 cells/well) with T-cell clones as effectors (10^3/well) in overnight IFNγ ELISPOT assays. Assays were set up in triplicate, and results are presented as triplicates and mean values. As a positive control, mature DCs were loaded with cognate peptide at 5μM or DMSO negative control. Abbreviations – Nucleo: DNA nucleofection, RNA: RNA electroporation, E1:EBNA1, GA:gly-ala repeat, li:invariant chain.

As shown in Figure 3.26A only DC transfected using RNA electroporation with EBNA1ΔGA-invariant chain RNA are recognised above background levels (i.e. GFP transfected DCs) by the TSL specific clone. This level of recognition is still very modest compared to maximal recognition with peptide-loaded DCs (5 spots v 170 spots).

In contrast, as shown in Figure 3.26B, there is definite evidence of EBNA1 407-417 HPV epitope presentation by cells transfected using DNA nucleofection and RNA electroporation. For both these transfection methods, both EBNA1 isoforms are clearly recognised by the HPV specific T cell clone at levels well above background (GFP expressing DCs). However, it is interesting to note that in both cases, addition of the invariant chain tag enhances Class I presentation. There is no major difference in recognition levels between DNA nucleofection and RNA electroporation for the invariant chain tagged EBNA1ΔGA. However, cells expressing unmodified EBNA1ΔGA after RNA electroporation are recognised at a higher level than those transfected by DNA nucleofection. CL22 transfected DC expressing EBNA1ΔGA are only recognised at a very low level by the HPV specific T cell clone (5 spot increase versus GFP expressing cells).

3.6.2.2. Immunogenicity of EBNA1 transfected DCs.

The ability of these transfected DCs expressing whole EBNA1 to expand the TSL 515-529 specific T-cell population was assessed using in-vitro stimulations of autologous non-adherent PBMCs. After two rounds of stimulation, cells were harvested and used as effector cells in overnight IFNγ ELISPOT assays with autologous B-cell blasts (loaded with 5µM TSL peptide or DMSO negative control) as target cells. In contrast to the results obtained in ELISPOT assays with the TSL specific T-cell clone, in terms of immunogenicity, all three transfection methodologies led to expansion of TSL specific T cells (Figure 3.27A). Once again, in the case of RNA electroporated or DNA nucleofected DCs, there was little difference between immunogenicity of cells expressing invariant chain tagged EBNA1ΔGA. However, DCs expressing unmodified EBNA1ΔGA were more immunogenic following RNA electroporation than DNA nucleofection. There is also a clear increase in TSL specific T cells in cell populations stimulated with DCs expressing EBNA1ΔGA versus GFP following CL22 transfection.

Finally, the ability of these DCs to present the HPV $_{407-417}$ epitope in an immunogenic fashion was determined using bulk

cytotoxicity ([51]Chromium release) assays with autologous B-cell blasts loaded with 5µM HPV peptide or DMSO (negative control) as targets. As shown in Figure 3.27B, there is only a minimal increase in HPV specific cytotoxic activity following stimulation with DCs expressing EBNA1 versus GFP after CL22 transfection. However, there is a definite increase in HPV specific lysis when cells are stimulated with DNA nucleofected or RNA electroporated DC expressing EBNA1 versus GFP. For both invariant chain tagged and unmodified EBNA1, RNA electroporated DC appear more immunogenic than DNA nucleofected ones. In addition, the superiority of invariant chain tagged EBNA1 is less marked with RNA electroporated as compared to DNA nucleofected DCs.
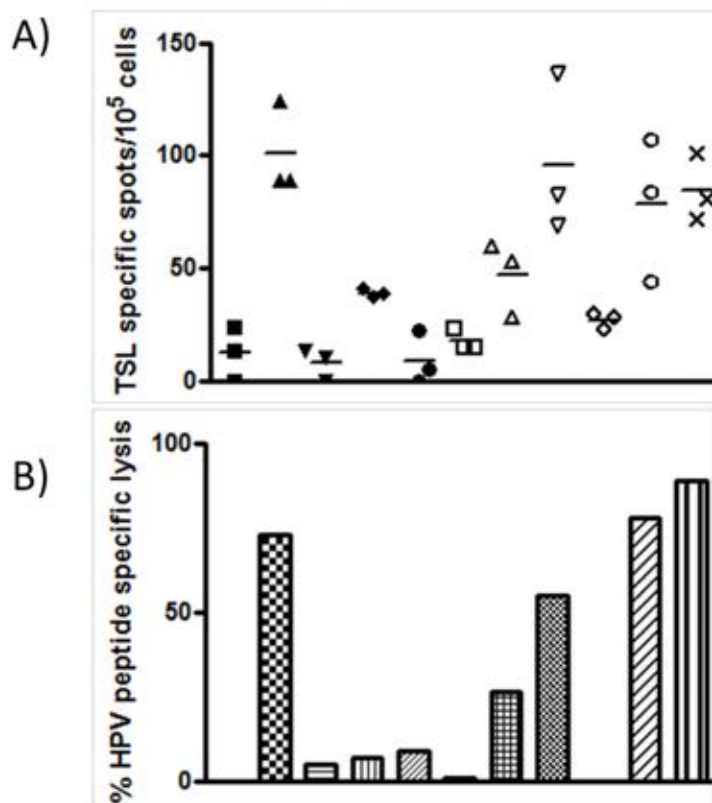
Stimulator DCs:											
DMSO	+	-	-	-	-	-	-	-	-	-	-
Peptide	-	+	-	-	-	-	-	-	-	-	-
CL22-GFP	-	-	+	-	-	-	-	-	-	-	-
CL22-E1ΔGA	-	-	-	+	-	-	-	-	-	-	-
CL22-E1ΔGA-li	-	-	-	-	+	-	-	-	-	-	-
Nucleo-GFP	-	-	-	-	-	+	-	-	-	-	-
Nucleo-E1ΔGA	-	-	-	-	-	-	+	-	-	-	-
Nucleo-E1ΔGA-li	-	-	-	-	-	-	-	+	-	-	-
RNA-GFP	-	-	-	-	-	-	-	-	+	-	-
RNA-E1ΔGA	-	-	-	-	-	-	-	-	-	+	-
RNA-E1ΔGA-li	-	-	-	-	-	-	-	-	-	-	+

Figures 3.27A and B . Immunogenicity of EBNA1 expressing DCs. Polyclonal cultures were set up using autologous non-adherent PBMCs as responder cells with EBNA1 transfected DCs as stimulator cells. A) For TSL specific responses (A), PBMC (10^5/well) were used as effectors with autologous B-blasts (3 x 10^4/well) (loaded with TSL peptide/DMSO) as stimulators in overnight IFNγ ELISPOT assays. TSL specific spots are calculated as spots in the presence of TSL peptide loaded B-blasts – spot count in the presence of DMSO loaded B-blasts. B) For analysis of HPV specific cytolytic activity, ^{51}Cr release assays were set up using autologous B-blasts as targets and PBMC as effectors in triplicate. % HPV specific lysis is calculated as %maximal lysis of HPV peptide loaded B-blasts - %maximal lysis of DMSO loaded targets.

Chapter 4: CL22 peptide based transfection of dendritic cells: discussion.

4.1. Humoral responses to vaccination with CL22 transfected DCs in clinical trial.

Humoral responses to tumour-associated-antigens are well described (Reuschenbach et al., 2008) and many TAAs were discovered by screening recombinant expression libraries derived from tumour cell lines with cancer patient sera (Sahin et al., 1995). Occasionally, levels of TAA specific antibodies provide prognostic information (Silk et al., 2009).

In tumour-antigen specific immunotherapy or vaccination, immune monitoring as a surrogate marker of therapeutic effect almost exclusively concentrates on cellular responses (Clay et al., 2001).

The focus was IgG responses as they are a surrogate marker of cognate CD4 T lymphocyte help and indeed very few IgM responses to tumour antigens have been demonstrated (Reuschenbach et al., 2008).

Experiments demonstrated that many laboratory donors had detectable levels of anti Melan-A IgG, consistent with recent reports that Melan-A specific CD8 T lymphocytes can be detected directly ex-vivo (using tetramers) from lab donor blood (Lee et al., 1999 and Petitt et al., 1999), and that highly cytotoxic CD8 T-cells can be induced from PBMCs of lab donors (van Elsas et al., 1996).

For patients, there were again detectable levels of anti Melan-A IgG in plasma. However, overall, there was no increase or decrease in absorbance after DC vaccination at any of the three dilutions tested.

The detection of these antibodies contrasts with the findings of Stockert et al (1998) who failed to detect them in 127 metastatic melanoma patients. More recently, anti Melan-A IgG was detected in melanoma patients who had a co-existent CD4 T cell response but not in lab donors (Bioley et al., 2006).

Although some patients with increases in anti Melan-A levels had prolonged clinical responses, it is unlikely that the increase in antibody level had a direct therapeutic effect

as the protein is intracellular and inaccessible to antibodies. It more likely represents the development of an augmented, coordinated immune response.

In these experiments, plasma was used rather than serum. Generally, antibody assays are carried out on serum and it is possible that the presence of fibrinogen and other coagulation factors could have had an influence on the results obtained.

The specificity of the assay for Melan-A was demonstrated by pre-incubating plasma with Melan-A and a control protein and showing that Melan-A preincubation only attenuated the observed responses. However, the control protein was bovine serum albumen which was not produced in the same way as Melan-A (produced in E.Coli from recombinant DNA). Thus, the possibility that some of the observed increases in absorbance in wells coated with Melan-A protein are due to antibodies reactive to contaminating (i.e. E.Coli) proteins cannot be totally excluded. In future, this experiment should be repeated using an irrelevant protein produced in an identical fashion from the same source. In other studies, control wells (i.e. antigen-negative) have been coated with histidine or GST tags without protein.

Melan-A specific antibody levels did not increase after vaccination, possibly because cellular and humoral responses may have different kinetics, and assays may have been performed too soon to detect any possible increase.

The assay may have lacked sensitivity to detect small changes in antibody levels. In future, it may be preferable to perform serial dilutions of each plasma sample and determine the dilution at which there is no increase in absorbance between Melan-A protein coated and control wells, rather than simply measuring absorbance at three predefined dilutions. This is how antibody titres are determined and reported in the clinical setting.

Finally, recruitment of CD4 help may have caused an increased in antibody affinity rather than antibody concentrations and future experiments should investigate the affinity of Melan-A specific antibodies before and after vaccination and also, perhaps, include later time points if possible.

4.2. Presentation of Melan A 26-35 and gp100 280-288 epitopes by CL22 peptide transfected DCs in melanoma clinical trial.

In the clinical trial, there was no correlation between vaccine characteristics including markers of maturation, whole antigen expression or surrogate immunologic markers (i.e. frequency of T-cell responses in PBMCs) and clinical response to vaccination (Steele et al., 2011).

Using a T-cell clone specific for the Melan-A $_{26-35}$ epitope, it was demonstrated that a proportion (5 of 18) vaccine preparations analysed showed a degree of recognition by the clone above background levels of Melan-A negative, A2 positive cells loaded with irrelevant peptide (GLC). This suggested that epitope presentation was occurring despite very low percentages of cells expressing whole antigen. The level of recognition was, however, rather low ranging from 0 to 9% of maximal levels. This likely reflects the insensitivity of the clone for native peptide; it was noted that even for the ELA (A27L) variant peptide, the 50% maximal peptide concentration is 10^{-6}M and the recognition of A2 targets cells loaded with EAA peptide was barely detectable above background. In future, it is possible that this lack of sensitivity could be improved by using a T-cell clone generated by antigenic stimulation with EAA (26-35) or even Melan A $_{27-35}$ rather than ELA peptide.

There was no relation between the percentage of Melan-A positive cells at 48 hours after transfection and epitope presentation, in fact after exclusion of an outlying sample (where Melan- A positivity was 98%); a modest inverse correlation was revealed. One explanation for this would be rapid degradation of the protein with subsequent appearance of the A2-peptide complex at the cell surface. This would predict that whole antigen levels would be higher and epitope display less robust at early time points. This prediction was tested in later experiments involving RNA transfection of DCs.

In the case of gp100, measurement of epitope display was less straightforward as no gp100 $_{280-288}$ specific T-cell clone was available. However, a novel reagent, a biotin-tagged A2-YLE specific recombinant T-cell receptor was used for this purpose. Preliminary experiments with the TCR showed that detection of TCR binding to MHC-peptide using the strepavidin-phycoerythrin secondary reagent followed by flow cytometry lacked sensitivity for detecting epitopes produced from endogenous antigen. Single cell fluorescence microscopy may have been sufficiently sensitive, but was impractical owing to the large number of samples to be assessed.

Thus, a TCR-anti CD3 fusion protein was used to detect epitope presentation in re-directed T-cell IFNγ ELISPOT assays. Epitope display was determined as the increase in spot count in the presence versus absence of TCR-fusion protein.

In terms of patient DC preparations, the majority showed detectable gp100 $_{280-288}$ specific spots (defined as spot count in the presence (10^{-9}M) of TCR-fusion protein – spot count in its absence). Of the 18 vaccine preparations tested, 13 showed spot counts at least twice that of those obtained with control cells (A2 positive, gp100 negative, GLC peptide). However the level of epitope presentation was relatively modest in comparison to peptide-loaded target cells (0-11% maximal). There was no relation between whole antigen expression and gp100 280-288 positivity.

The key limitation here relates to the negative control group. The best negative control to absolutely verify that observed increases in spot count in the presence of the TCR were only due to presence of the gp100 280-288 epitope would have been a TCR-fusion protein of irrelevant specificity or anti-CD3 alone rather than no TCR-fusion protein. However,

the other alternate TCR-fusion protein available was Melan-A 26-35 specific. Since patient DCs co-expressed Melan-A and gp100, this would not have been a suitable negative control. In future, this experiment could be repeated with a TCR-fusion protein of unrelated specificity as a negative control (e.g. NY-ESO).

To put the results obtained into context, the average epitope specific spot count for patient DC preparations was 6 spots per well. In experiments using the fusion protein at 10^{-9}M with the same number of effector cells (10^3/well), similar spot counts were obtained with target cells pulsed with 10^{-10}M YLE peptide.

The other concern with the results obtained using the gp100 $_{280-288}$ specific TCR-anti CD3 protein relates the actual number of epitope specific spots obtained. The manufacturer of the fusion protein reviewed these results and felt that, whilst suggestive of epitope presentation, were not especially robust in comparison to other cell types overexpressing gp100 (Jakobsen B, personal communication). It is possible that the number of DCs per well was not optimal, and in future further detailed optimisation experiments using

antigen-presenting-cells expressing whole antigen would be necessary.

In both of these experiments, there was no negative control for the transfection process – that is, all DC vaccine preparations had been transfected, using CL22 peptide, with gp100 and Melan-A encoding DNA. The absence of an untransfected control group is due to a need to maximise the yield of mature, transfected DCs for each patient and at the transfection stage it would not have been ethical to put aside DC as a control and potentially compromise the yield of cellular product available for re-administration.

This appears to be the first time epitope display has been measured in a cellular product used therapeutically in patients. In terms of melanoma antigens, adenovirally transduced moDC expressing full-length Melan-A have been used to treat metastatic melanoma patients in a Phase I/II clinical trial (Butterfield et al., 2008). However, there was no measurement of antigen expression or epitope presentation.

In the setting of ampullary, breast and pancreatic cancers expressing Mucin-1, an autologous DC vaccine expressing MUC1 after cationic lipid transfection of plasmid DNA has been investigated in the Phase I/II setting (Pecher et al., 2002). Here, whole antigen expression was measured and was variable, but epitope presentation was not evaluated.

These results are highly suggestive that Class I restricted epitopes are being presented, perhaps at a low level, by CL22 peptide transfected DCs of metastatic melanoma patients and this extends the initial observations made with this transfection system using viral antigens and laboratory donor DCs (Irvine et al., 2000).

In terms of clinical trials of DC vaccination, these data raised questions regarding the importance and relevance of whole antigen detection 48 hours after transfection to vaccine antigenicity – certainly for melanoma differentiation antigens. In future, the use of recombinant T-cell receptors specific for epitopes derived from these antigens should be seriously considered as a quality control for the cellular product.

In terms of physiological relevance, the main limitation of these experiments is that they are only measuring epitope display over a limited time-frame – 48-64 hours after transfection. In vivo the subcutaneously administered DCs would take at least a further 48 hours (Lappin et al., 1999 and de Vries et al., 2003) to reach T-cell zones of secondary lymphoid tissues and begin to interact with T-cells. There is also accumulating evidence that epitope persistence and the maturation status of DCs is equally, if not more, important than merely the number of peptide-MHC complexes per cell.

4.3. TLR9 expression in monocyte derived DCs and immune-stimulatory effects of CL22 transfection of plasmid DNA.

Initial experiments determined that immature DC did express TLR9 as assessed by intracellular antibody staining and flow cytometry. Mature DC showed a lower level of TLR9 expression. Contaminating lymphocytes and undifferentiated monocytes showed low-level TLR9 expression.

Although an isotype matched control antibody was used to confirm specificity of the observed staining, in future it would be helpful to perform the staining on a cell type

209

known or suspected to be TLR9 negative (e.g. epithelial cell lines) and also on cells ectopically over-expressing the protein, perhaps after DNA transfection to establish definitive positive and negative controls.

Cells had been fixed and permeabilised before staining in these experiments. Although TLR9 positivity was demonstrated, it was not possible to distinguish between cell surface and intracellular expression as analysis was performed by flow cytometry. Future experiments should determine localisation, either by staining with and without permeabilisation or using fluorescence microscopy.

Previously, there have been conflicting findings regarding TLR9 expression on monocyte-derived (i.e. myeloid) DCs. In the murine setting, the bone-marrow derived DCs of TLR9 double knockout mice did not secrete IL12 or Type 1 interferon in response to hypomethylated CpG oligonucleotides or plasmid DNA (Tudor et al., 2004). In human monocyte derived DCs, TLR9 expression was detectable by flow cytometry, but not by Western blotting, and levels of expression were significantly lower than those seen in plasmacytoid DCs or TLR9 transfected HEK293 cells (Hoene et

al., 2006). This study additionally demonstrated that moDCs were response to stimulation with CpG oligonucleotides.

In contrast however, Bauer et al (2001) showed that monocyte derived DCs were entirely unresponsive to stimulation with bacterial DNA and CpG oligonucleotides and did not contain detectable TLR9 mRNA transcripts by RT-PCR. CD123 positive plasmacytoid DCs and B-lymphocytes, however, were responsive to hypomethylated DNA and were TLR9 mRNA positive. The consensus view has been that myeloid DCs are TLR9 negative and plasmacytoid DCs are positive (Shortman and Liu, 2002).

Encouraged by the detection of TLR9 on immature moDCs, experiments moved forward to determine whether or not introduction of plasmid DNA into DCs, using the CL22 peptide transfection system, could have activating and immune stimulating effects on the DCs.

Plasmid DNA encoding GFP was used for these experiments for two reasons – firstly transfection efficiency can be easily monitored by flow cytometry, and secondly, GFP is likely to be a relatively non-immunogenic protein. This is important

to allow separation of the effects of protein production from those of introduction of DNA into the cell.

Exposure to DNA transfection, regardless of the presence or absence of proinflammatory cytokines, increased the proportion of DCs expressing CD25.

It has been generally accepted that CD25 expression is a marker of 'mature' DCs (Steinman, Pack and Inaba, 1997) and in the trial, exposure to proinflammatory cytokines increased the proportion of positive DCs. However, some work has suggested that mature, CD83 positive moDCs with robust T-cell stimulatory abilities only express CD25 very weakly (Zhou and Tedder, 1996). Certainly, the functional role of the α-chain of the IL2 receptor (CD25) on dendritic cells remains unclear. The β-chain is not co-expressed, which makes any biological effect of IL2 on the cell very unlikely. In fact, CD25 may distinguish tolerogenic DCs that coexpress the the enzyme IDO (von Bergwelt-Baildon et al., 2006). Surface CD25 on DCs can be cleaved to a soluble form which can act as an IL2 decoy receptor and lead to IL2 sequestration and decrease T-cell activation and proliferation.

In agreement with phenotyping results from the trial, CCR7 expression is noted to be very low in all three DC preparations regardless of exposure to DNA or cytokines. Although CCR7 expression seems to be closely linked to migratory ability of DCs (Ohl et al., 2004), there is some evidence that CCR7 independent pathways must exist as CCR7 -/- knockout mice still exhibit resident DCs in lymph node tissue (Hintzen et al., 2006).

In future, the scope of these experiments could be extended. Although CCR7 may be a marker of potential to migrate, the actual ability of DCs to migrate in response to a chemokine stimulus could be directly measured in transwell assays. Also, in view of the uncertain significance of CD25 expression, further experiments could include determination of cleaved, soluble CD25 in culture supernatants and assessment of IDO expression and activity.

The ability of DCs to stimulate the proliferation of allogeneic lymphocytes was assessed in ^{3}H thymidine proliferation assays. In two of three donors, there were increases in allogeneic proliferation when cells were tranfected with GFP DNA regardless of the presence of cytokines. This likely reflects increases in MHC Class II

expression on the surface of DCs. In future, these experiments could be extended to include assessment of other properties of the allogeneic responders such as cytokine release and Th1 (IFNγ, TNFα) versus Th2 (IL4, IL10) profiles.

Cytokine production by DCs is a vitally important property of these cells. Plasmid DNA transfection had unequivocal effects on the cytokines secreted by all three of these DC preparations.

IL12 is produced by dendritic cells, cells of monocyte/ macrophage lineage and neutrophils in response to foreign pathogens via TLR signalling. The main target cells are B cells where IgG production is enhanced and IgA and IgE production reduced, and T cells where Th1 cytokine production is increased (TNFα, IFNγ) (Trinchieri, 2003). IL12 is a heterodimeric protein consisting of heavy (p40) and light chain (p35) subunits. The expression of the p35 subunit is almost ubiquitous amongst cell types. IL12p40 expression is inducible. However, only the disulphide-bonded heterodimer has biological activity (i.e. IL12p70). The p35 subunit can only be secreted as part of the p70 heterodimer, whereas p40 may be secreted alone.

IL12p40 production was increased by DNA tranfection in the absence of cytokines in one donor, and only in the presence of cytokines in another donor. In the final donor, there was no effect of DNA transfection on p40 production. In terms of IL12p70 release, this was essentially undetectable in two of three donors, but in one donor there was evidence of low-level IL12p70 production only in the presence of DNA transfection and exogenous cytokines.

These barely detectable levels of bioactive IL12 release from dendritic cells are entirely consistent with the current two-signal model of DC activation. For secretion of large amounts of IL12p70, the first signal necessary is signalling through Toll-like receptors and the second is receipt of T-cell derived signals such as IFNγ and CD40 ligation (Mosca et al., 2000). In this case, there may have been TLR9 stimulation by plasmid DNA but an absence of T-cell signals prevents strong IL12p70 release. It should borne in mind, however, in terms of DC vaccine design, that in terms of timing, high-level IL12p70 release early after transfection may not be necessary and such 'hyper-stimulated' DCs may be functionally exhausted on reaching T-cell zones of secondary lymphoid tissue (Kaka et al., 2008).

It is also noted that the effects of transfection of plasmid DNA using the CL22 peptide seemed to vary according to the level of transgene expression. In two donors, there is barely detectable GFP expression (less than 1.5% positive cells) and these DCs do show signs of 'maturation' in terms of phenotype, allostimulation and cytokine release on DNA exposure. The other donor had more robust GFP expression (8%) but the only definite change upon DNA exposure was detectable IL12p70 release.

CL22 peptide forms complexes with DNA that are actively taken up, by endocytosis, in immature DCs (Haines et al., 2000). The complexes enter the endolysosomal compartment, where instead of being degraded by lysosomal proteases they persist due to concomitant administration of chloroquine that inhibits acidification. This allows access of DNA to the nucleus for transcription and later translation in the cytoplasm. Recent evidence suggests that TLR9 is located in the endoplasmic reticulum in resting cells and on activation it translocates to lysosomes to interact with incoming foreign DNA (Latz et al., 2004). It is therefore possible that when CL22-DNA complexes move rapidly through the endolysosomes to the nucleus, allowing good transgene expression, there is less time for interaction with TLR9 and consequently fewer 'maturation' effects.

In conclusion, these experiments show that TLR9 is expressed on monocyte derived DCs and that transfection of plasmid DNA using the CL22 peptide system can have immune enhancing effects on immature DCs.

The importance of this, in the setting of clinical use of DC vaccines, is that it represents a further advantage of using methods of nucleic acid transfection to express whole antigen in comparison to other techniques of antigen loading. Also, most known TLR ligands are difficult to adapt for clinical use, so delivery of TLR agonist signals via nucleic acids themselves would be useful way of circumventing this. There are toll-like receptors that interact with viral RNA such as RIG-I receptors (Habjan et al., 2008), raising the possibility that RNA transfection may also possess intrinsic immune-adjuvant effects.

Future experiments could usefully include knockdown of TLR9 in DCs, for example by using anti-sense oligodeoxynucleotides, to determine whether or not the observed effects are due to TLR9 signalling or not. It would also be pertinent to determine whether or not such immune-adjuvant effects are also observed when electrical

methods (i.e. electroporation) of DNA are employed, as there is some preliminary evidence that direct, electrically-mediated transfer of plasmids to lung tissue bypasses the endolysosomal compartment and does not activate TLR9 (Zhou et al., 2007).

4.4. CL22 peptide based transfection of EBNA1 DNA into DCs leads to presentation of MHC Class I and II restricted epitopes.

Transfection of human monocyte derived DCs with plasmid DNA encoding influenza nucleoprotein, using the CL22 peptide, led to presentation of the B8 restricted NP 380-388 epitope in the autologous system. Transfection using CL22 was almost as effective as adenoviral transduction in terms of generating EBNA3c 258-266 specific cytotoxic T-cells in a B27 positive autologous system. In the murine setting, vaccination with CL22 transfected DCs expressing influenza NP led to development of anti NP specific IgG responses, suggesting recruitment of CD4 T cells (Irvine et al., 2000).

Here, we extend these observations by formally demonstrating that CL22 transfected DCs expressing EBNA1 present the HLA DR1 restricted TSL epitope – assessed by T-cell clone recognition assays and immunogenicity (bulk) assays. In agreement with the work of Irvine et al., presentation of

the B35 restricted HPV epitope coexists with presentation of TSL by these transfected DCs.

The presentation of epitopes mentioned above occurred despite both a very low transfection efficiency – assessed by GFP positivity in the control (i.e. EBNA1 negative) DCs, and very low proportions of EBNA1 transfected DCs being whole antigen positive by antibody staining at 48 hours. This again raises questions as to whether whole antigen detection in transfected DC vaccines is a useful or important surrogate marker of immunogenicity. It was also noted that the proportion of GFP positive and EBNA1 positive cells at 48 hours was very similar, suggesting that EBNA1 is a relatively stable protein in DCs.

The ability of DC preparations with low transgene expression to be immunogenic was also seen in the work of Irvine et al., where even DC vaccines with low (1-5%) transfection efficiencies could be highly immunogenic in vitro and in vivo.

The results presented here also illustrate the importance of assessing both the antigenicity (short term T-cell

recognition) and immunogenicity (ability of DCs to expand epitope-specific cells in PBL) of a DC preparation. In T-cell recognition assays, for TSL and to a lesser extent HPV, peptide-pulsed target cells are recognised at levels several-fold higher than transfected cells. In contrast, in immunogenicity assays, transfected DCs approach equivalence with peptide-loaded ones. One explanation for this could relate to antigen persistence. In order to stimulate outgrowth of T-cell clones, prolonged duration of epitope presentation is important particularly for CD4 cells (Obst et al., 2005), but also for CD8 T cells (Jusforgues-Saklani et al., 2008). Pulsing with exogenous peptides leads to presentation of a high density of peptide-MHC complexes for a relatively short period (12-18 hours), whereas endogenous whole antigen expression likely leads to a lower peptide density that is maintained over several days. It also possible that the concentration of peptide used for pulsing was supra-physiological and led to expansion of only very low avidity T-cell clones. There is some experimental evidence of this using gp100 Class I restricted epitopes in the murine setting (Bullock et al., 2000). The superiority of full-length EBNA1 in immunogenicity assays examining TSL and HPV specific responses lends support to the possible importance of antigen persistence as its distinguishing features is a slower translation rate and slower degradation rate in cells (Tellam et al., 2007). In fact, antibody

staining for EBNA1 on these DCs shows a slightly higher frequency of positive cells when full-length EBNA1 is the transgene.

That whole antigen detection in transfected DCs appears to be largely irrelevant to presentation of epitopes, particularly as assessed by the ability to expand epitope-specific T-cell populations in PBMCs, might relate to antigen transfer between DCs. However, a closer re-evaluation of the antigen-recognition results shows that 10^4 DCs were co-incubated with 10^3 effector T-cells. Based on EBNA1 staining, approximately 1 in 100 cells were clearly antigen positive, this would equate to 100 antigen positive DC per well. These cells directly presenting epitopes could still give rise to the small increases in T-cell activation seen – approximately 10-20 spots. In order to determine whether or not antigen transfer had a role in presentation of these epitopes by CL22 transfected DCs, experiments could be conducted with reducing numbers of target DC per well to ascertain whether or not T-cell recognition is still seen even when less than 100 targets per well are present. If this were the case, it would be experimental evidence of antigen transfer as direct presentation would be impossible.

4.5. Dendritic cell transfection methodologies – a systematic comparison.

The CL22 peptide based transfection system is one of the very few DNA based whole antigen expression systems that has actually been used in the clinical setting. However, both in the preclinical and clinical setting, this transfection platform is characterised by marked variability between individual donors and between individual DC preparations. There is also the important limitation that optimal transgene expression is only achieved when cells are transfected in the immature state as active endocytosis of peptide-DNA complexes is required. The large majority of recent clinical trials of DC vaccination for malignancy have used RNA as the nucleic acid of choice, and typically it has been introduced into mature DCs using electroporation.

On this background, a systematic comparison between three non-viral whole antigen expression methods was carried out. The aim of this was to determine the most efficacious method with which to carry out further experiments on MHC Class I and II restricted epitope presentation by DCs and, in terms of future clinical use, to assess CL22 peptide transfection in comparison with electrical methods.

The strengths of this experiment were the fact that all three transfections were performed in parallel, using dendritic cells derived from the same blood donation, using well characterised antigens (EBNA1ΔGA and EBNA1ΔGA-Invariant chain) and that immunogenicity and antigenicity of the DCs were measured. There has been a paucity of reported formal comparisons between dendritic cell transfection techniques in the literature. The work of Van Tendeloo (2001) suggests that human monocyte-derived DCs were far more amenable to transfection with in-vitro transcribed RNA using electroporation rather than cationic lipid preparations (85% versus 7.5% GFP positive viable DCs). It was also noted that cell viability was higher following electroporation (78% versus 72%). In terms of MHC Class I epitope presentation, the recognition of DCs lipofected with Melan-A encoding RNA by a 27-35 specific CTL clone was approximately half that of electroporated DCs.

In stem cell (CD34 positive) derived DCs, a comparison between mRNA and cDNA was performed. Interestingly, there was no difference in levels of recognition by the 27-35 specific CTL clone of GFP and Melan-A cDNA transfected cells, whereas specific recognition was evident with mRNA.

Earlier work (Van Tendeloo et al., 1998) had suggested that the type of in-vitro derived dendritic cell was crucial - monocyte derived DCs were refractory to transfection with cDNA regardless of whether cationic lipids or electroporaton were employed.

A comparison of GFP expression in human monocyte derived DCs was carried out by Irvine et al (2000). In line with the prevailing consensus view, the majority of cationic lipid preparations were ineffective in generating GFP positive DCs. However, there was detectable, albeit minimal (<1% GFP positive) transgene expression using 4 cationic lipids including clonfectin and FUgene. In comparison, the average transfection efficiency of CL22 peptide much higher at approximately 15% (Irvine et al., 2000).

A more comprehensive analysis of amenability of DCs to transfection was carried out by Lundquist et al (2002). Stem cell and monocyte derived DCs from cancer patients and lab donors were subjected to viral transduction and non-viral transfection. 60% of monocyte derived DCs expressed the transgene (GFP) after RNA electroporation, whereas no GFP expression was seen using DNA with the same electrical parameters and cell viability was compromised by DNA

electroporation. Lipid mediated gene transfer led to low levels (1-10%) of GFP expression using RNA but not DNA. In contrast, however, DNA delivered to DCs using particle bombardment ('gene gun') did lead to transgene expression at 1-2% positive cells. The analysis was extended to include viral transduction. Although the percentage of GFP positive cells was comparable for adenovirally transduced and RNA electroporated moDCs, the intensity of GFP expression was higher with the adenovirus. There was no deleterious effects of adenoviral transduction or electroporation of RNA on the allostimulatory capacity of DCs.

In a similar vein, the percentage of transgene positive monocyte derived DCs was comparable after lentiviral infection or mRNA electroporation at 24 hours, but maximum fluorescence intensity was higher with the viral construct (Dullaers et al., 2004). It was also demonstrated, in keeping with the results obtained in this work, that neither viral infection nor mRNA electroporation prevented subsequent phenotypic maturation of DCs following cytokine cocktail exposure.

In this work, GFP expression was less than 5% with CL22 peptide, around 40-50% with nucleofection of DNA and 90%

using RNA electroporation. Nucleofection of RNA was not studied as part of the formal comparison, because previous experiments had shown a rapid reduction in the proportion of GFP positive cells with time and also on the theoretical basis that the electrical parameters of nucleofection are designed to deliver nucleic acid to the nucleus which would be unnecessary for RNA. The reasons for this hierarchy of transgene expression could include: requirement of active endocytosis of DNA-peptide complexes with CL22 versus passive induction of cell membrane and nuclear pores with electrical methods and the lesser requirements of RNA as opposed to DNA – translation only rather than transcription and translation.

The key limitations of this set of experiments relates to the low yield of dendritic cells. Although the largest possible volume of blood was drawn, the starting number of monocytes was insufficient for a comprehensive analysis of DC function. It was intended to perform a full phenotypic analysis of DCs to ascertain the effects of transfection on phenotypic maturation, but this was not possible as DCs had to be preserved for experiments on antigen expression and immunogenicity. In future, this problem could be addressed in two ways. The most straightforward would be to take blood from the same donor on several occasions a few weeks

apart and freeze whole PBMCs each time. When a sufficient number of PBMCs were available from frozen stocks, cells could be thawed and used for plastic adherence to obtain the monocyte-enriched fraction. It was noted however, throughout this work, that the final yield of immature DCs was always lower when frozen rather than fresh PBMCs were used. This perhaps related to formation of clumps of cells after thawing. An alternative would be to use leukapharesis or use buffy-coat PBMCs after HLA typing.

In future, this comparative analysis should be extended to include other important DC characteristics including phenotypic markers of maturation, migratory capabilities, cytokine secretion. In addition, if cell numbers were sufficient, the antigenicity and immunogenicity could be more completely assessed. It would be highly informative to determine the functional avidity and affinity of the induced HPV and TSL specific T-cell populations by using a range of concentrations of exogenous peptide in the bulk cytotoxicity assays and ELISPOT assays and by altering target:effector ratios. For CD8 responses, use of the HPV specific tetramer to stain DC-stimulated PBMC population would allow an assessment of functional avidity based on the intensity of staining. In addition, the extent to which the induced T-cell populations are able to lyse target cells

227

physiologically expressing EBNA1 such as B-LCL or lymphoma cell lines (rather than peptide-loaded target cells) would be a useful extension to the work. This is particularly important as target cells were loaded with high, probably supraphysiologic concentrations of peptide in these experiments.

In terms of clinical DC vaccine design, these results clearly favour RNA electroporation of dendritic cells. This technique was the only one to lead to presentation of MHC Class I and II epitopes simultaneously as assessed by in-vitro stimulation assays and T-cell clone recognition. Although DNA nucleofection was immunogenic in certain circumstances, the marked loss of cellular viability would make this technique difficult to apply in the clinical setting. This difficulty is particularly troublesome when one considers the additional 24-48 hours migration that must occur from the injection site to draining lymph nodes. However, DNA nucleofection should not be totally discounted as fully mature DC can be nucleofected and could be immediately injected – this would possibly circumvent the described lack of phenotypic maturation seen in nucleofected immature DCs.

In the context of this comparative experiment, CL22 transfection was effective in generating immunogenic DCs – however, presentation of the HPV epitope was only seen in T-cell recognition assays and of the TSL epitope only seen in in-vitro stimulation assays.

Although the superiority of RNA electroporation may simply reflect a higher level of transgene expression, it is also possible that effects of the nucleic acid on DC maturation could be responsible. In fact, in vitro transcribed RNA has been found to contain structures which can lead to formation of double-stranded RNA which increases Type 1 interferon release, MHC Class II and CD80 and CD86 expression on porcine monocyte derived DCs after RNA electroporation (Ceppi et al., 2009).

These data also allowed an assessment of the importance of transfection efficiency to be made. Despite an absence of EBNA1 positive cells by immunofluorescence, CL22 transfected DCs do present the HPV and TSL epitope albeit at low levels. Furthermore, cellular localisation of antigen seems to be more important than the efficiency of transfection – invariant chain tagged EBNA1 is presented equally well to TSL specific clone by DNA nucleofected and RNA

electroporated DCs despite a twofold difference in transgene expression.

5. Relationship between detection of whole antigen and presentation of Class I restricted epitopes in RNA transfected dendritic cells.

5.1 Rationale and purpose

As discussed in Chapter 4, electroporation of0 in-vitro transcribed RNA into DCs leads to high levels of transgene expression and such DCs were highly antigenic and immunogenic for Class I and II restricted epitopes. This is in agreement with the recent literature on RNA electroporation of DCs (summarised in Ponsaerts et al., 2003).

Experiments assessing the levels of gp100 YLE and Melan A EAA/ELA epitope presentation by excess transfected (CL22 peptide method) melanoma patient DCs suggested that there was no relationship between the ability to detect whole antigen at 48 hours after transfection and epitope presentation. In fact, there was a modest negative correlation between these two variables in the case of Melan-A.

On the basis of these results, a more detailed examination of the relation between whole antigen and epitope presentation was made using all three antigens (i.e. EBNA1,

gp100 and Melan A) using the most efficient transfection method – electroporation of RNA. It was surmised that the more robust transfection method may provide more consistent and informative results than CL22 peptide based transfection or nucleofection where cell viability is poor.

The primary aim was to determine whether or not detection of whole antigen in transfected DCs was a necessary prerequisite for presentation of MHC Class I restricted epitopes, and the secondary aim was to determine whether or not the relation between epitope presentation and whole antigen detection was dependent on the nature of the antigen.

The overall clinical relevance of this set of experiments is to provide experimental evidence which can allow an informed decision to be taken regarding the utility of whole antigen detection as a surrogate marker of immunogenicity of DCs, and if not, to possibly suggest alternative markers of epitope presentation.

5.2. EBNA1 transfected DCs are both whole antigen and epitope positive.

Immature DC were prepared from a B35 positive donor and were electroporated with RNA encoding EBNA1ΔGA or mock-transfected.

24 hours after transfection, epitope presentation and whole antigen detection were measured. EBNA1 staining using the R4 antibody was performed by immunofluorescence microscopy. Presentation of the HLA B35 restricted epitope HPV (EBNA1 407-417) was determined by using the DCs as stimulator cells in polyclonal cultures. Responder cells in this assay were autologous non-adherent PBMCs that were stimulated twice with transfected and HPV peptide loaded DCs at weekly intervals. On day 7, low dose IL-2 was added to cultures. On day 14, HPV specific T-cells were quantified using a PE conjugated B35-HPV specific tetramer. Preliminary experiments had shown that a small population of tetramer positive cells were detected in a HLA B35 positive donor, whereas no such population was seen in a HLA B35 negative donor. Both donors were EBV seropositive. No tetramer staining was observed in a B35 positive, EBV seronegative donor.

In terms of whole antigen detection, there is strong, specific EBNA1 staining in transfected DCs ($\approx$90%) as compared to minimal background staining in mock transfected cells. EBV positive B-LCLs are EBNA1 positive. These results are shown in Figure 5.1. Staining intensity is higher in DCs than LCLs.

In terms of epitope presentation, there is an expansion of the B35-HPV specific CD8 T-cell population in cultures stimulated with EBNA1ΔGA transfected ($\approx$10 fold) and HPV peptide loaded ($\approx$30 fold) DCs compared to antigen-negative) DC. This result is shown in Figure 5.2 and indicates that epitope presentation is occurring.

Antigenicity was then determined. Presentation of the HPV epitope was assessed using the HPV specific T-cell clone in IFNγ ELISPOT assays. EBNA1 antibody staining was performed on transfected DCs. Approximately 35% of EBNA1 transfected DCs were whole antigen positive, whereas no positive cells were seen in the mock transfected group (Figure 5.3).

In terms of epitope presentation, the EBNA1 expressing DCs are recognised in a specific fashion by the HPV specific
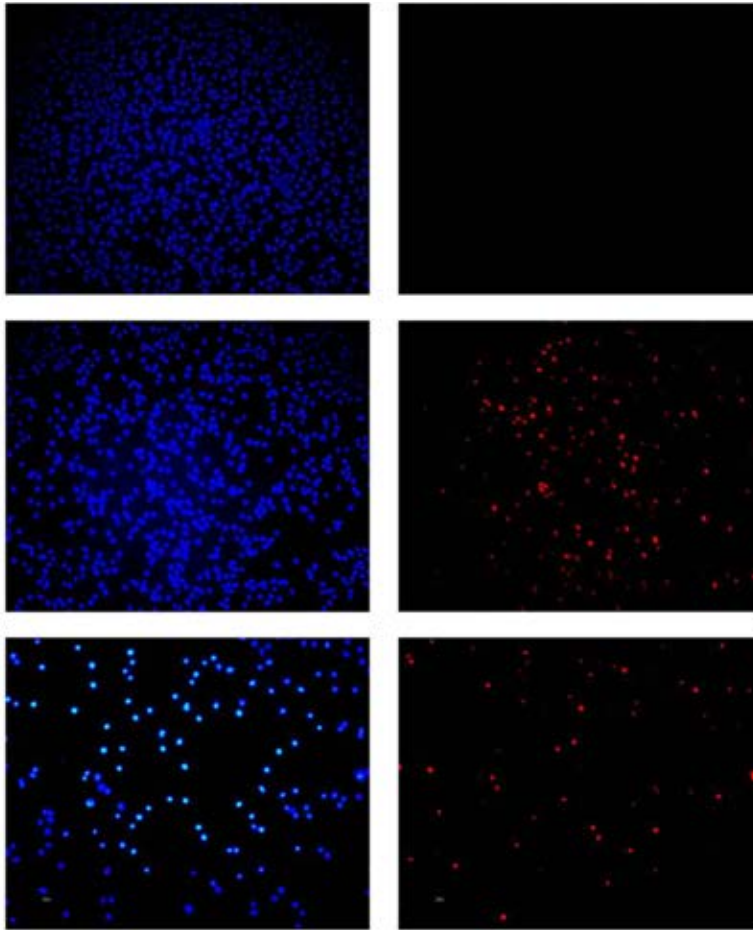
Figure 5.1. Detection of EBNA1 in DCs transfected with EBNA1ΔGA RNA. 10^4 DCs (mock transfected (no RNA) – top panels, EBNA1ΔGA – centre panels) were fixed, permeabilised and stained with polyclonal rabbit anti-EBNA1 antibody (R4) followed by anti rabbit Alexa 594 conjugated secondary antibody. After extensive washing, cells were analysed by fluorescence microscopy. As a positive control for EBNA1 staining, EBV positive B-lymphocytoid cells were also analysed (bottom panels). Left panels show nuclear staining with DAPI, right panels show red fluorescence indicative of EBNA1 staining. Representative images are shown. Magnification = x 10
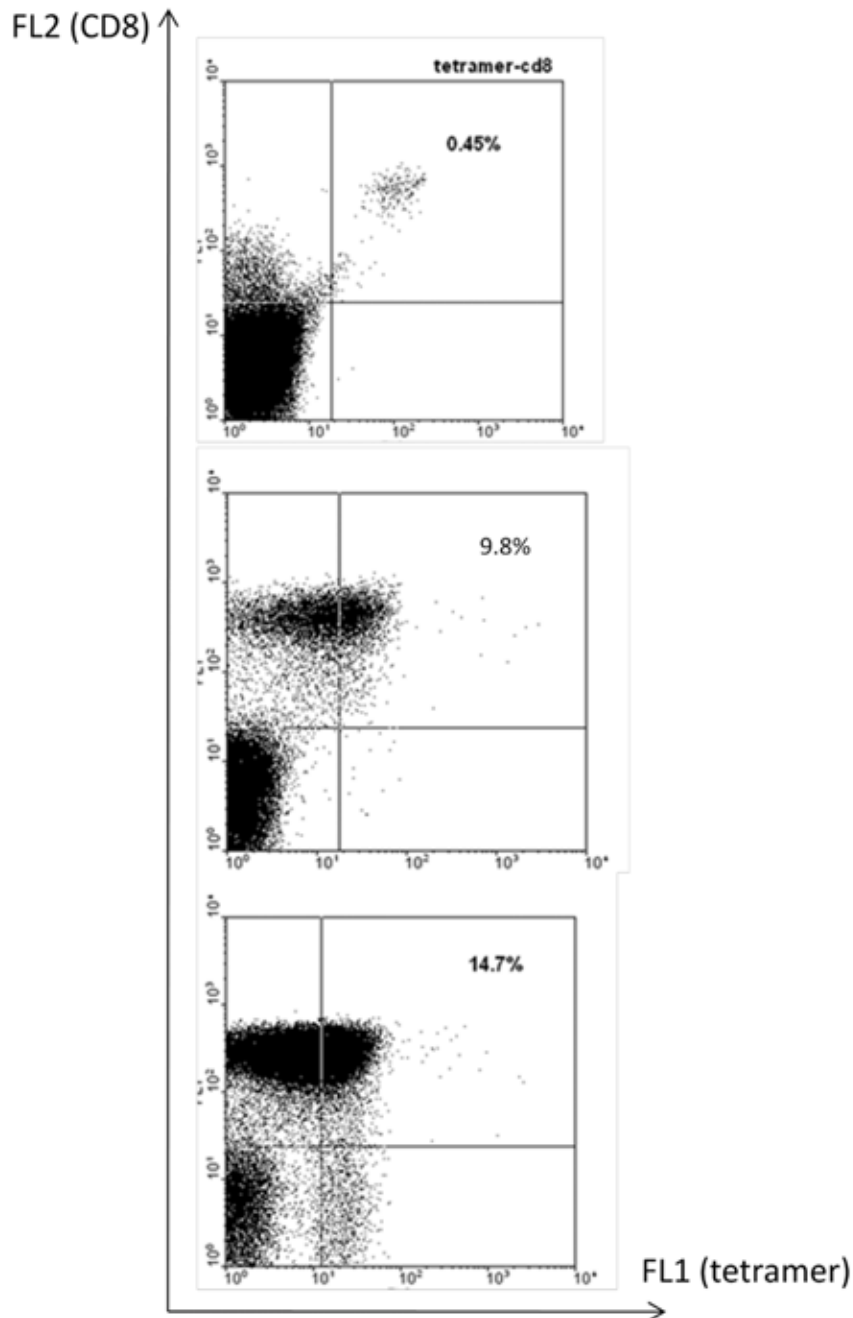
Figure 5.2. Quantification of HLA-B35-HPV specific T-cells in polyclonal cultures stimulated with EBNA1 transfected DCs. Non-adherent PBMC (10^6/well) from a B35 positive donor were coincubated with autologous DCs (1.5 x 10^5/well) transfected with EBNA1ΔGA (middle) or not (top). Mock transfected cells were loaded with HPV peptide as a positive control (bottom). After 2 weekly stimulations, cells were harvested and B35-HPV specific cells were quantified using a phycoerythrin conjugated tetramer. 10^6 PBMCs were stained with tetramer and CD8 antibody. Results are presented as dot plots showing the numbers of tetramer (X axis) and CD8 (Y-axis) positive cells. Percentages are % tetramer positive cells of all CD8 positive cells.
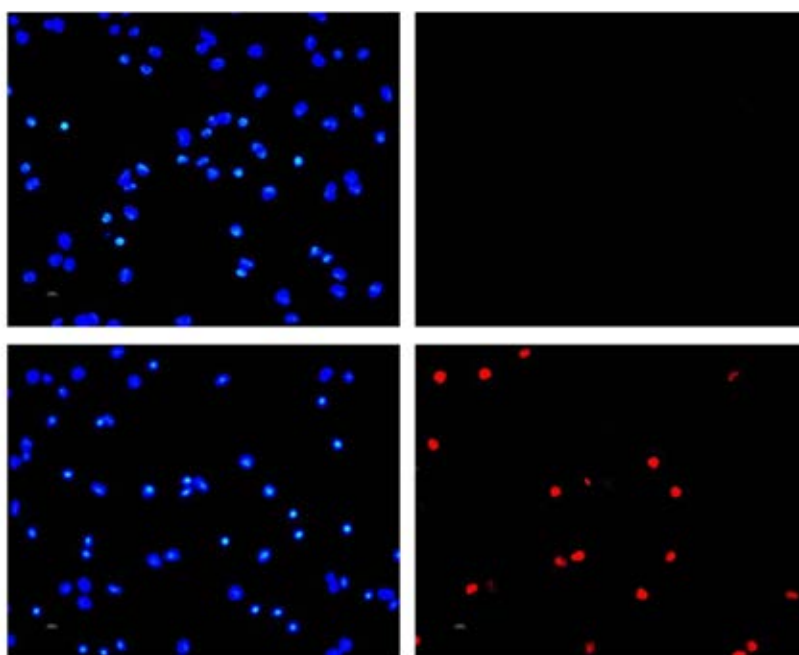
Figure 5.3. EBNA1 detection in EBNA1ΔGA RNA transfected DCs. 10^4 DCs (mock transfected (no RNA) – top panels, EBNA1ΔGA – lower panels) were fixed, permeabilised and stained with polyclonal rabbit anti-EBNA1 antibody (R4) followed by anti rabbit Alexa 594 conjugated secondary antibody. After extensive washing, cells were analysed by fluorescence microscopy. Left panels show nuclear staining with DAPI, right panels show red fluorescence indicative of EBNA1 staining. Representative images are shown. Magnification = x 20

clone. Levels of recognition are lower than those seen with exogenously added peptide alone, largely due to some background (non-specific) recognition of EBNA1 negative DCs by the T-cell clone. However, at both target:effector ratios (1:1 and 10:1) there is evidence of recognition (Figure 5.4).

It was confirmed that RNA electroporation had not impaired DC maturation. There is upregulation of CD25, CD83 and CD86, and to a lesser extent CCR7 after exposure to TNFα and IL1β (Figure 5.5).

These experiments demonstrate that there is no disconnection between whole antigen detection 24 hours after RNA transfection and presentation of a Class I restricted epitope from EBNA1.
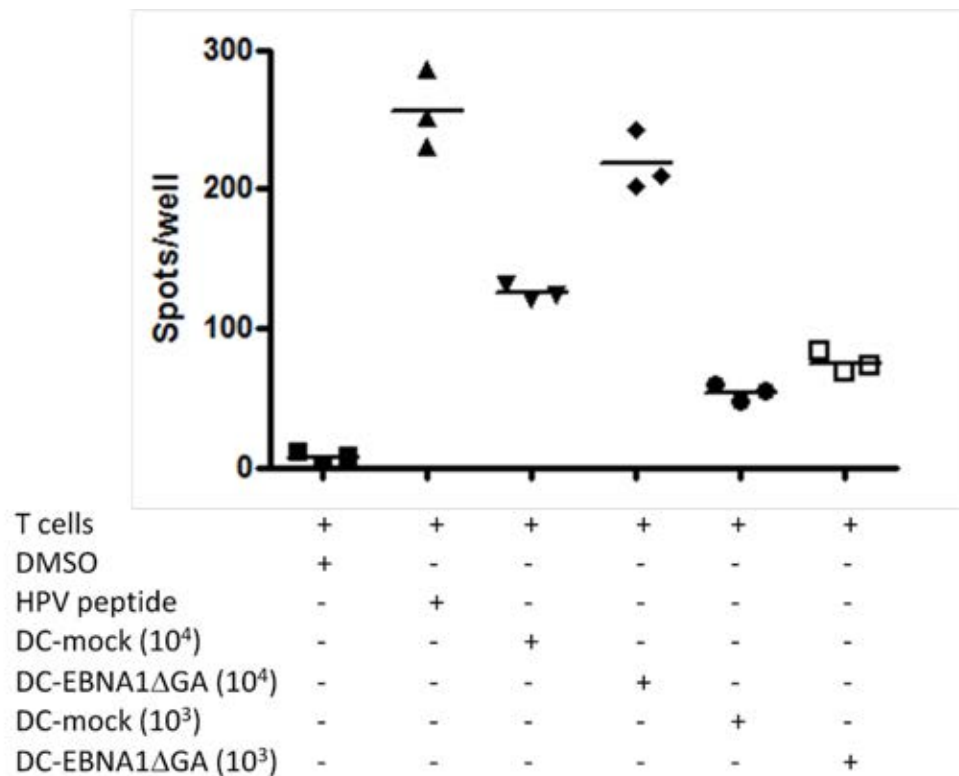
Figure 5.4. Recognition of EBNA1 expressing DCs by HPV specific T cell clone. DCs were prepared from a HLA 35 positive donor and were electroporated with EBNA1ΔGA RNA or in its absence (mock). After 24 hours , cells were harvested and used as targets (10^4 or 10^3/well) in overnight IFNγ ELISPOT assays with the HPV specific T cell clone (c41) as effector cells (10^3/well). Additionally, T cells were incubated in the absence of DCs but the presence of HPV peptide at 10μM or DMSO alone. Results are presented as invidual spot counts (triplicates) and mean values (horizontal bar).
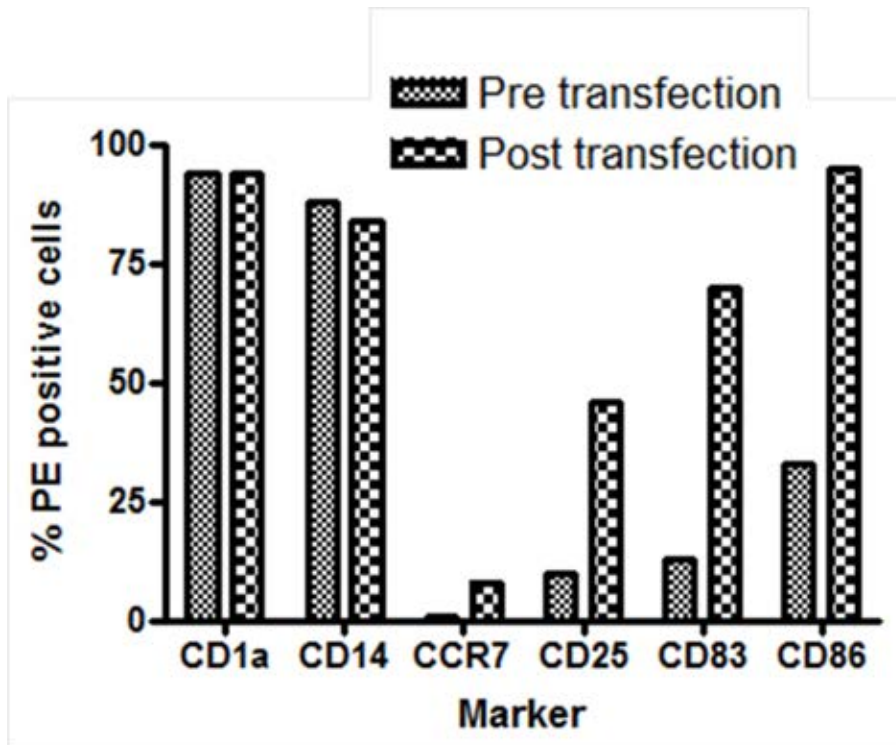
Figure 5.5. Immunophenotype of dendritic cells transfected with EBNA1ΔGA RNA before and after exposure to TNFα and IL1β. DCs, before transfection (pre) and 24 hours after transfection and cytokine exposure (post), were stained with a panel of phycoerythrin conjugated mouse monoclonal antibodies directed at CD1a, CD14, CCR7, CD25, CD83 and CD86. Fc receptors were blocked with polyclonal mouse IgG before staining. Cells were analysed by flow cytometry. 10^4 gated events were collected (DCs). %PE positive cells refers to the percentage of DCs that were PE positive with the specific antibody - % positive with isotype matched control antibody (background fluorescence was always set at <2%).

5.3. Melan-A transfected DCs are whole antigen negative yet are epitope positive.

5.3.1. Background and aims

The aim of these experiments was to determine whether there was a relationship between epitope presentation and whole Melan-A detection in DCs transfected with in-vitro transcribed RNA.

The immunodominant HLA-A2 restricted Melan A epitope is EAAGIGILTV (26-35). However, a heteroclitic variant exists with enhanced A2 binding stability and therefore immunogenicity. This is E**L**AGIGILTV. To maximise the likelihood of detecting epitope presentation from DCs endogenously expressing Melan-A, a DNA construct encoding the Melan-A 27A→L variant was generated. PCR-based site directed mutagenesis, utilising primers containing the desired base substitution, was used to create the new construct. Sanger dideoxy sequencing was used to check for the presence of the mutant sequence. Plasmids containing the mutant were taken forward and transfected into epithelial cells (HEK293). Cell lysates were prepared after 72 hours and were used in immunoblotting experiments to

detect the Melan A protein. As shown in Figure 5.6, the introduction of the amino-acid substitution has no deleterious effect on the protein as it is still detected by the A103 antibody, at the expected molecular weight of 20-22 kDa. One of the Melan-A A27L plasmids was used as a substrate for RNA synthesis.

5.3.2. DCs are negative for whole Melan-A after RNA transfection.

The initial aim was to determine whether or not Melan A RNA transfected DC are Melan A positive. HLA-A2 positive DC were electroporated with Melan-A RNA (wild-type and A27L variant), and gp100 and GFP encoding RNA as controls. GFP is an easily detected and its stability allows an accurate assessment of overall transfection efficiency regardless of intracellular processing. In parallel, Melan A RNA was also introduced into HEK293 cells by electroporation in order to verify that the RNAs were functional in vitro.

After 24 hours, cells stained for intracellular Melan-A protein using the A103 antibody in indirect immunofluorescence microscopy with fluorophore conjugated secondary antibodies. GFP was detected by fluorescence microscopy and flow cytometry.

kDa

1 2 3 4 5 6 7 8
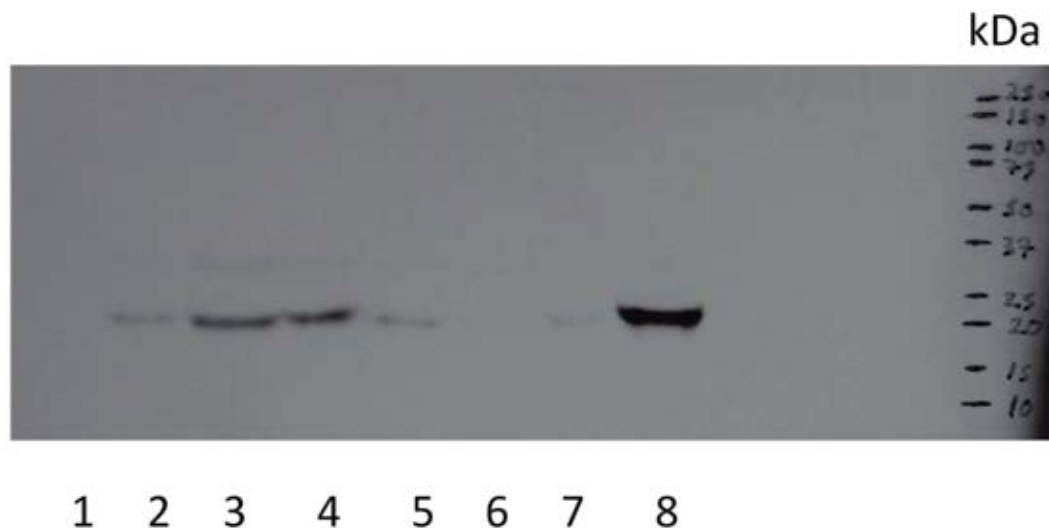
Figure 5.6. Verification of Melan-A protein production from plasmid DNA constructs encoding a 27A→L variant of Melan-A. To confirm the functionality of A27L variant plasmids, they were transfected into HEK293 cells using Lipofectamine 2000. 72 hours after transfection, cells were harvested and cell lysates were prepared. Proteins were separated by SDS-PAGE and then probed for the presence of Melan-A using the A103 mouse monoclonal antibody followed by anti mouse HRP conjugate. Chemiluminescent HRP substrate was added and X-ray films were exposed for 30 seconds. HEK293 transfectants - 1)pcDNA3.1 (empty plasmid) 2)pcDNA3.1-Melan-A 3-7)A27L variant plasmids. 8)SK23MEL cell line (positive control).

As shown in Figure 4.7A, there is strong GFP expression in the vast majority of cells assessed by microscopy. Approximately 98% of cells within the dendritic cell gate are positive for GFP compared to 0.5% of Melan-A transfected DCs, shown in Figure 5.7B. This result confirms that electrical settings had been optimised for DC.

Moving on to Melan A expression, there was successful Melan-A staining of HEK293 cells electroporated with Melan A RNA (wild-type and A27L variant). However, there was no evidence of Melan A positivity in the transfected dendritic cells, despite obvious Melan-A detection in the Melan-A positive melanoma line SK23MEL. These results are presented in Figure 5.8A-C. Of note, HEK293 cells and DCs were electroporated with RNA from the same aliquot on the same day, in parallel.

Thus results show that highly efficiency DC transfection has taken place, that RNA is functional in HEK293 cells and that successful Melan A staining has been performed. Despite this, 24 hours after transfection, dendritic cells appear to be Melan-A negative.
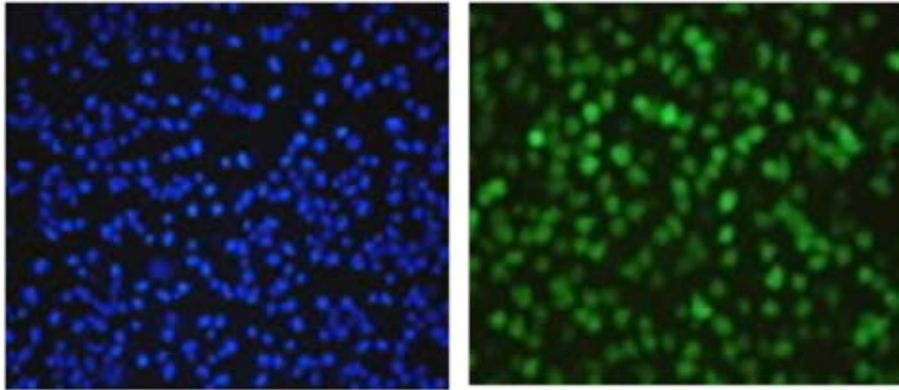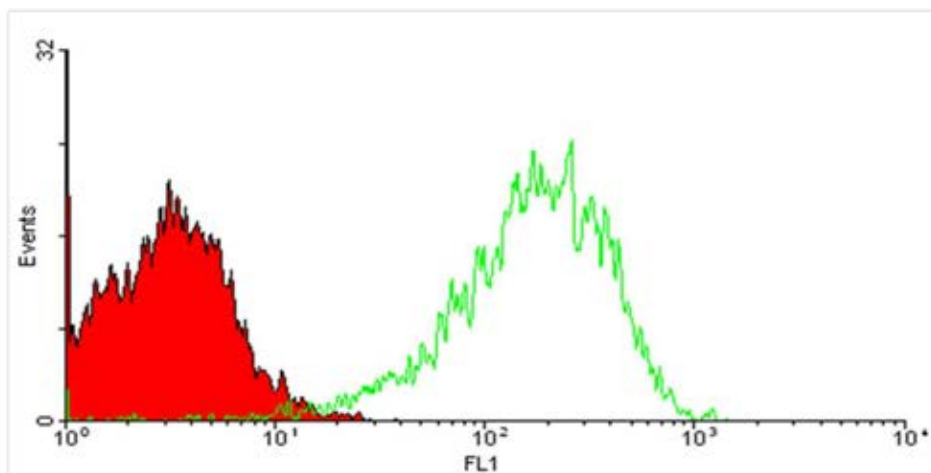
Figure 5.7. Expression of green fluorescent protein in RNA transfected dendritic cells. DCs were electroporated with in-vitro transcribed RNA encoding GFP, and after 24 hours further culture, they were harvested and analysed for the presence of GFP protein. A)Fluorescence microscopy of transfected DCs. GFP transfected DCs were fixed to microscopy slides, stained with DAPI and viewed on a fluorescence microscope. Left panel shows blue nuclear fluorescence with DAPI, and right panel shows green fluorescence indicative of GFP expression.
B)Melan A and GFP transfected DCs were analysed for green fluorescence protein by flow cytometry. Melan A expressing cells are not expected to show any green fluorescence and act as the negative control. Filled red histogram represents Melan A transfected cells, and hollow green histogram GFP transfected cells. 5000 gated events (DCs) were collected.
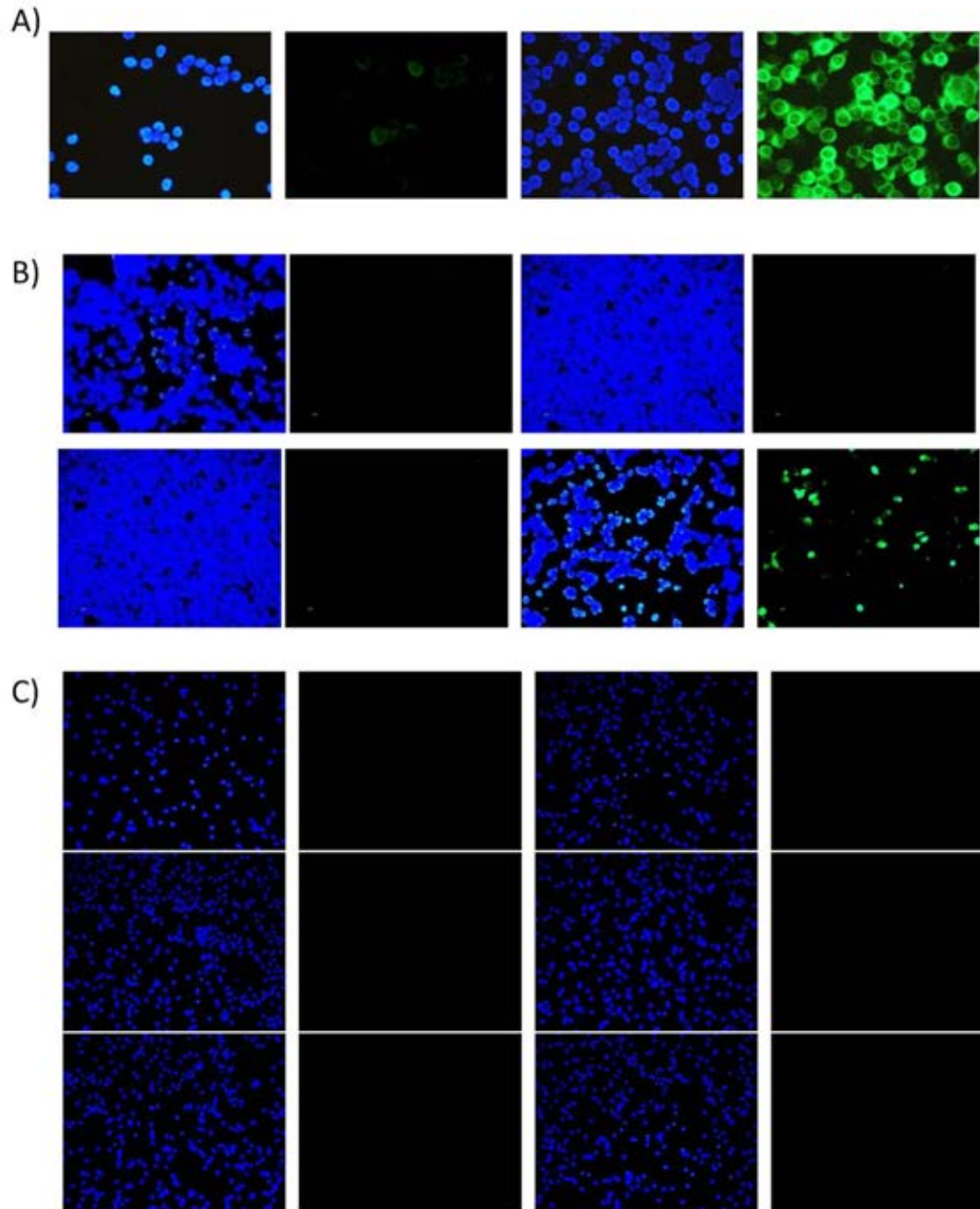
Figure 5.8. Intracellular Melan-A staining: A)SK23MEL cell line B)RNA transfected HEK293 cells C)RNA transfected dendritic cells. Cells were fixed, permeabilised and stained with a mouse monoclonal anti-Melan-A antibody, followed by goat anti mouse Alexa 594 conjugate. DAPI was used to stain nuclei. After washing, cells were viewed under a fluorescence microscope. Far left – DAPI, middle left – isotype control, middle right – DAPI, far right – Melan A antibody. B – upper panels – mock transfected, lower panels – Melan A transfected. C – transfected DCs – upper – gp100 RNA, centre – Melan A RNA, bottom – Melan A A27L RNA.

5.3.3. Melan A negative DCs are recognised by a Melan A 26-35 specific T-cell clone.

Melan-A transfected DCs were used as targets in overnight IFNγ ELISPOT assays with the Melan A $_{26-35}$ specific T-cell clone as effector cells. DC were loaded with ELA peptide (positive control) at 5µM in DMSO or with DMSO alone (negative control) and used as targets. The effector to target ratio was 1:10 and assays were performed in triplicate.

As shown in Figure 5.9, there is strong recognition of target DCs loaded with cognate peptide. However, there is also evidence of specific recognition of DCs transfected with Melan A wild-type and A27L variant RNA above background levels. The increase in average spot count with transfected DCs is approximately 8 fold less than that achieved with peptide-loaded cells. The wild type and A27L transfected DCs appear equivalent in terms of epitope presentation. These responses were also observed at T cell: DC ratios of 1:1 as shown in Figure 5.10.

T cells	+	-	+	+	+	+	+	+
DC-DMSO	-	+	+	-	-	-	-	-
DC-ELA peptide	-	-	-	+	-	-	-	-
DC-gp100 RNA	-	-	-	-	+	-	-	-
DC-GFP RNA	-	-	-	-	-	+	-	-
DC-Melan A RNA	-	-	-	-	-	-	+	-
DC-Melan A A27L RNA	-	-	-	-	-	-	-	+
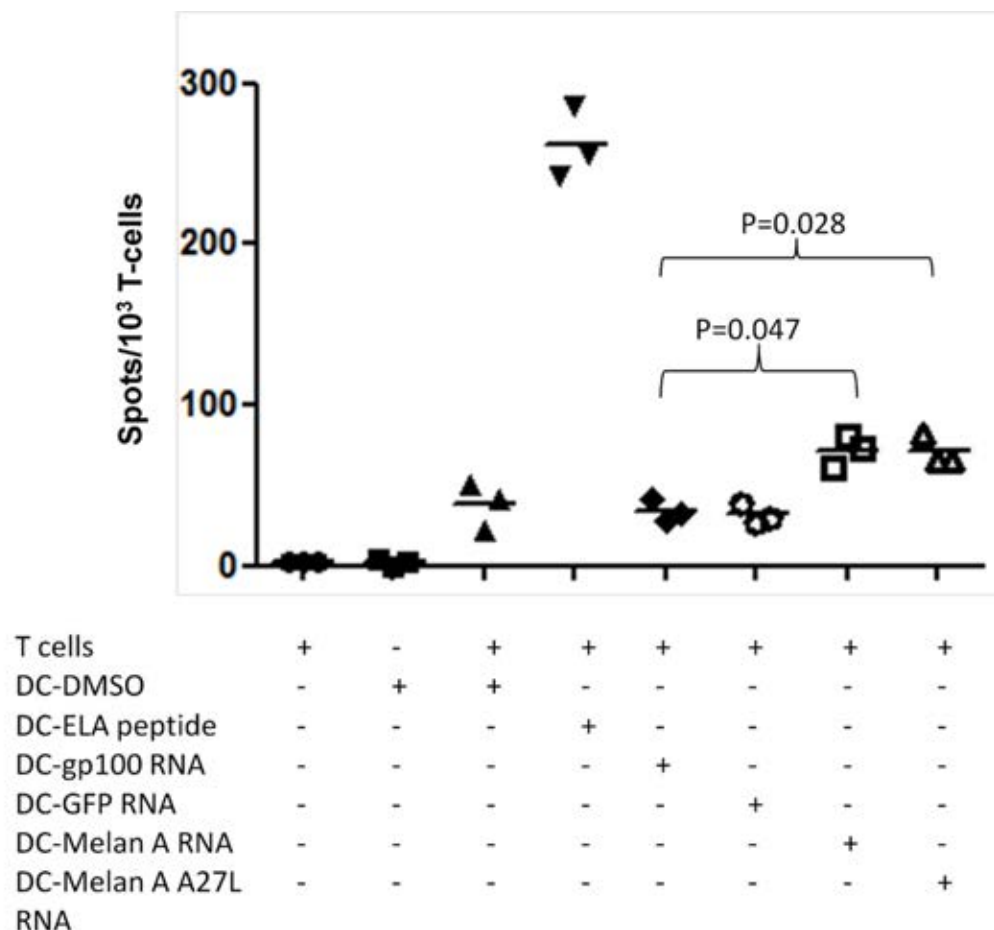
Figure 5.9. **Presentation of the Melan A $_{26-35}$ epitope by DCs endogenously expressing Melan-A after RNA transfection.** DCs (10^4/well) were used as target cells in overnight IFNγ ELISPOT assays with Mel c5 T-cell clone as responder cells (10^3/well). Assays were set up in triplicate. As a positive control, mature untransfected DCs were loaded with ELA peptide (5μM in DMSO) or DMSO alone (negative control). Results are presented as individual spot counts and mean values (horizontal bars). Significance of difference between means of experimental groups are calculated using Students' T-test.

T cells	+	-	+	+	+	+	+	+
DC-DMSO	-	+	+	-	-	-	-	-
DC-ELA peptide	-	-	-	+	-	-	-	-
DC-GFP RNA	-	-	-	-	+	-	-	-
DC-gp100 RNA	-	-	-	-	-	+	-	-
DC-Melan A RNA	-	-	-	-	-	-	+	-
DC-Melan A A27L RNA	-	-	-	-	-	-	-	+
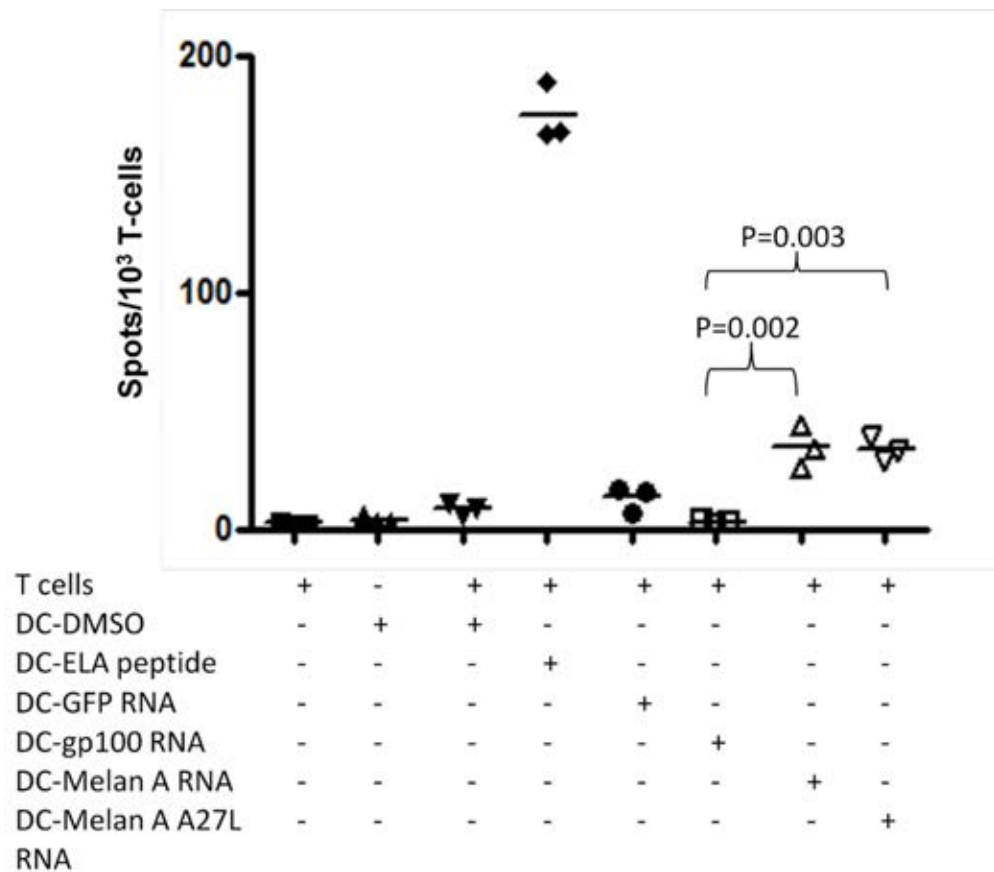
Figure 5.10. **Presentation of the Melan A 26-35 epitope by DCs endogenously expressing Melan-A after RNA transfection.** DCs (10^3/well) were used as target cells in overnight IFNγ ELISPOT assays with Mel c5 T-cell clone as responder cells (10^3/well). Assays were set up in triplicate. As a positive control, mature untransfected DCs were loaded with ELA peptide (5μM in DMSO) or DMSO alone (negative control). Results are presented as individual spot counts and mean values (horizontal bars). Significance of difference between means of experimental groups are calculated using Students' T-test.

5.3.4. Melan A negative DCs are Melan A 26-35 positive as assessed by recombinant T-cell receptor staining.

To extend these observations, that whole antigen negative DCs seem to be able to present a Class I restricted epitope, epitope presentation was assessed in a different way. A recombinant T-cell receptor specific for the A2 restricted ELA epitope was a kind gift from Immunocore Ltd, Abingdon, Oxon.

Initial experiments characterised the ability of this reagent to detect epitope presentation on cells loaded with cognate peptide, and expressing whole Melan-A. The aim was to determine the sensitivity of the reagent prior to its use on DC. The TCR is biotinylated, allowing detection by two-step staining followed by flow cytometry. The secondary reagent is streptavidin-phycoerythrin conjugate.

TCR staining was performed on HLA A2 positive B-cell blasts loaded with reducing concentrations of ELA and EAA peptide. These experiments indicated that the threshold of epitope detection was 10^{-7}M for ELA and 10^{-6}M for EAA peptide (Figure 5.11). These concentrations of exogenous peptide are relatively high, particularly compared to the expected
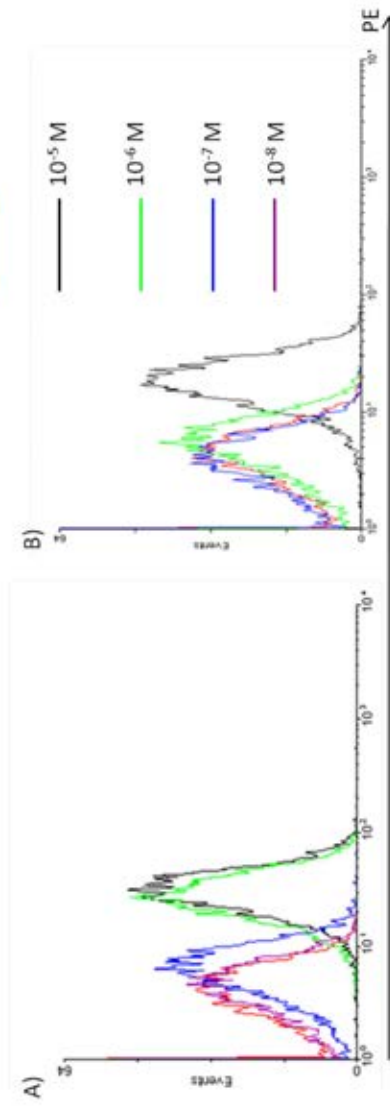
Figure 5.11. Detection of A2-ELA/EAA epitope by soluble T-cell receptor staining: peptide-loaded targets. B-cell blasts (5 x 10⁵) from an HLA-A2 positive laboratory donor were pulsed with the indicated concentration of ELA (A) or EAA (B) peptide in serum-free conditions for 90 minutes. Following washing to remove unbound peptide, cells (10⁵) were stained with soluble TCR followed by streptavidin-phycoerythrin secondary reagent. After extensive washing, cells were analysed for PE fluorescence by flow cytometry. At least 5000 gated events were collected in each case.

251

epitope densities on cells endogenously expressing and processing whole antigen.

Melan-A positive melanoma lines were stained with the TCR. SK23MEL is HLA A2 positive and 888MEL is negative and serves as a negative control. There was a small population of cells showing low-level TCR positivity with SK23MEL, whereas no such population was seen with the 888MEL cell line (Figure 5.12).

HEK293 cells are HLA-A2 positive and are readily transfectable. Therefore, they were transfected with Melan A A27L plasmid DNA or empty vector using Lipofectamine 2000. 72 hours after transfection, cells were stained for intracellular Melan-A protein. Approximately 15% of cells were Melan A positive. In terms of TCR staining, there was a small increase in TCR positive cells in the Melan-A expressing 293 cells. This was just above the limit of detection with flow cytometry (Figure 5.13).

These results show that whilst use of the Melan A 26-35 specific TCR in two-step staining and flow cytometry is able to detect cells pulsed with exogenous peptide at high
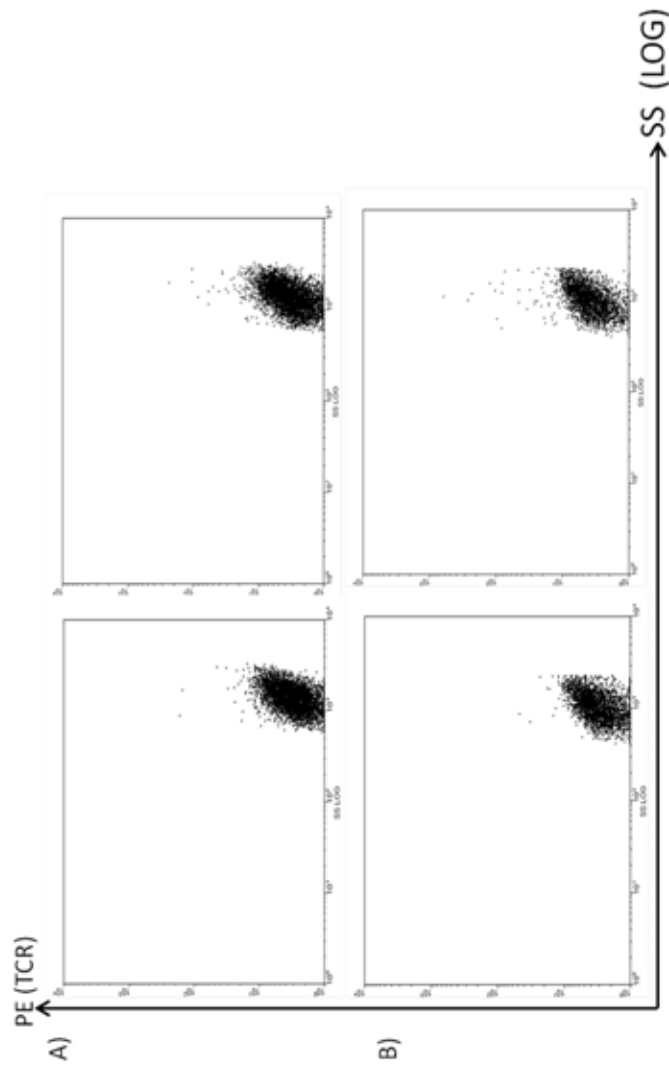
Figure 5.12. Detection of A2-ELA/EAA epitope by soluble T-cell receptor staining: endogenously expressing targets. Two step Melan A 26-35 TCR staining on melanoma cell lines was performed. Both cell lines are known to be Melan-A positive A)888MEL – HLA A2 negative. B)SK23MEL – HLA A2 positive. 10^5 cells were stained with the soluble TCR, followed by streptavidin-PE. After extensive washing, cells were analysed by flow cytometry. Left hand panels – no TCR. Right hand panels – TCR. At least 10^5 gated events were collected, and results for 2000 events are displayed.
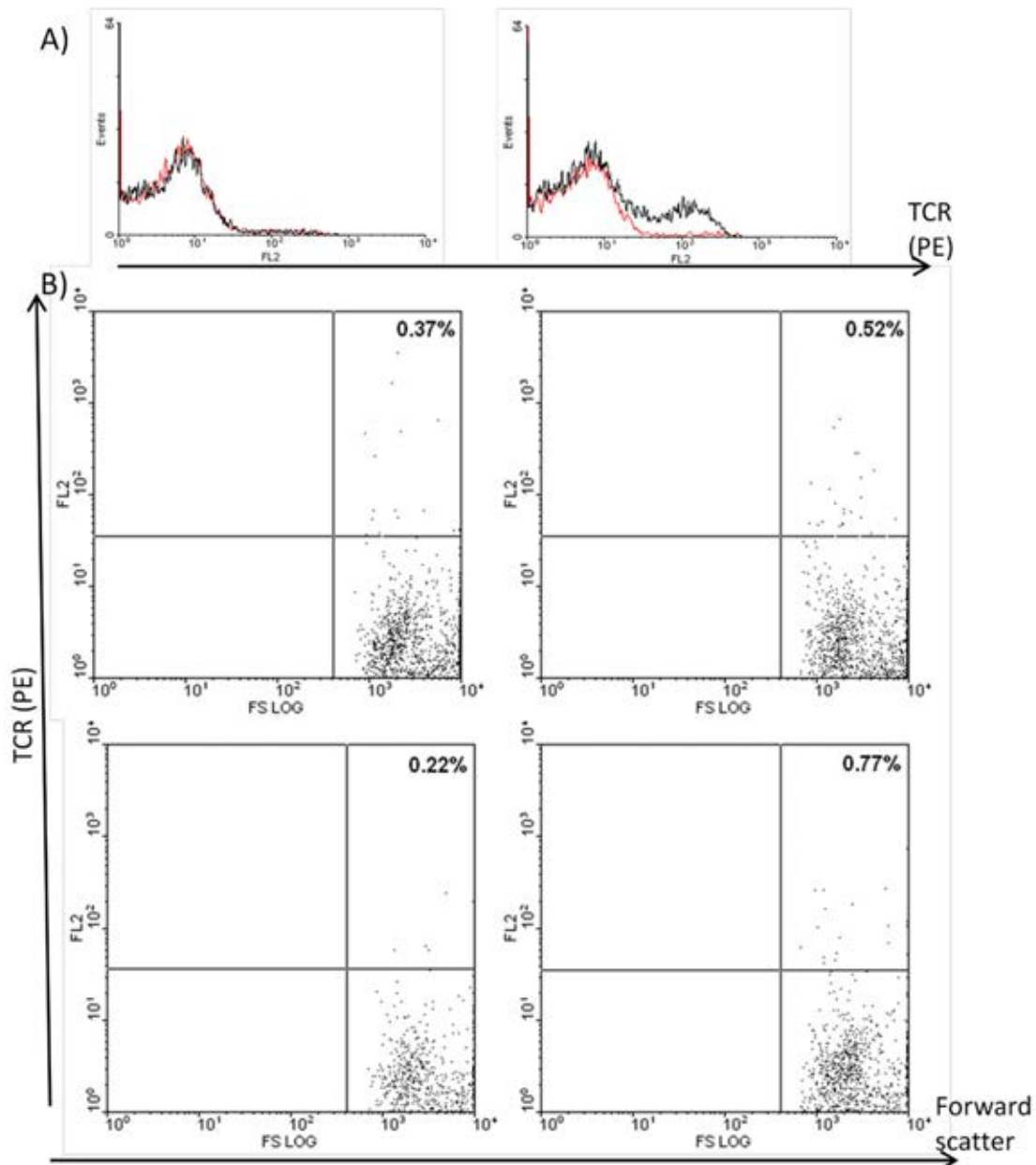
Figure 5.13. Detection of A2-ELA/EAA epitope by soluble T-cell receptor staining: endogenously expressing targets. HEK293s (A2 positive) were transfected using Lipofectamine 2000 with pcDNA3.1-Melan-A27L or empty vector . A)Cells were fixed, permeabilised and stained with Melan A antibody (black line) or matched isotype control antibody (red line), followed by anti-mouse-PE antibody. Left – pcDNA3.1, right – pcDNA3.1-Melan-A A27L. B)105 cells were stained with TCR, followed by streptavidin-PE. Cells were analysed by flow cytometry, where at least 105 events were collected and 2000 are shown. Upper panels – mock transfected 293 cells, Lower panels – Melan-A A27L transfected 293 cells. Left – no TCR . Right – TCR. Percentages show percentage of gated cells that are TCR positive.

concentrations, it may lack sensitivity to detect the likely low epitope densities on cells endogenously expressing antigen.

This lack of sensitivity may represent a technological limitation of flow cytometry, as it is estimated that 200-300 phycoerythrin signals per cell are necessary for reliable detection, and assuming a 1:1 epitope-TCR binding ratio this would be 200-300 epitopes/cell. Strategies to improve sensitivity have included use of additional amplification steps in the TCR staining procedure. However, in order to maximise the ability to detect epitopes, single live-cell fluorescence microscopy was used to enumerate epitopes based on a 1:1 relationship between epitopes and soluble TCR binding (Purbhoo et al., 2006).

Using this sensitive technique, presentation of the Melan-A 26-35 epitope by RNA transfected DCs was assessed. The negative control cells in this experiment were gp100 expressing DCs as it was suspected that green fluorescence from GFP positive cells might influence detection of phycoerythrin signals.

In order to ensure that any observed Melan-A 26-35 T-cell receptor staining was specific, a TCR of irrelevant specificity (HIV GAG epitope specific) was used as the negative control. This was particularly important in this assay as DCs had previously been cryoperserved and cellular viability was only 60-70%.

Results are presented as a histogram showing the epitope counts for each cell examined in each of the groups of DCs. A minimum of 30 cells were analysed in each group.

As shown in Figure 5.14, there is a non-specific background staining of approximately 25 epitopes per cell with the HIV GAG TCR regardless of which transfection DCs had undergone. However, in the Melan-A A27L expressing DCs only, there is a clear and distinct population of cells displaying epitope counts above this background that is not seen with the control TCR. This strongly suggests that these cells are presenting the epitope and is in concordance with the result obtained using the T-cell clone. Of note, there is no evidence of epitope presentation on DCs transfected with wild-type Melan-A RNA. There is a wide range of individual
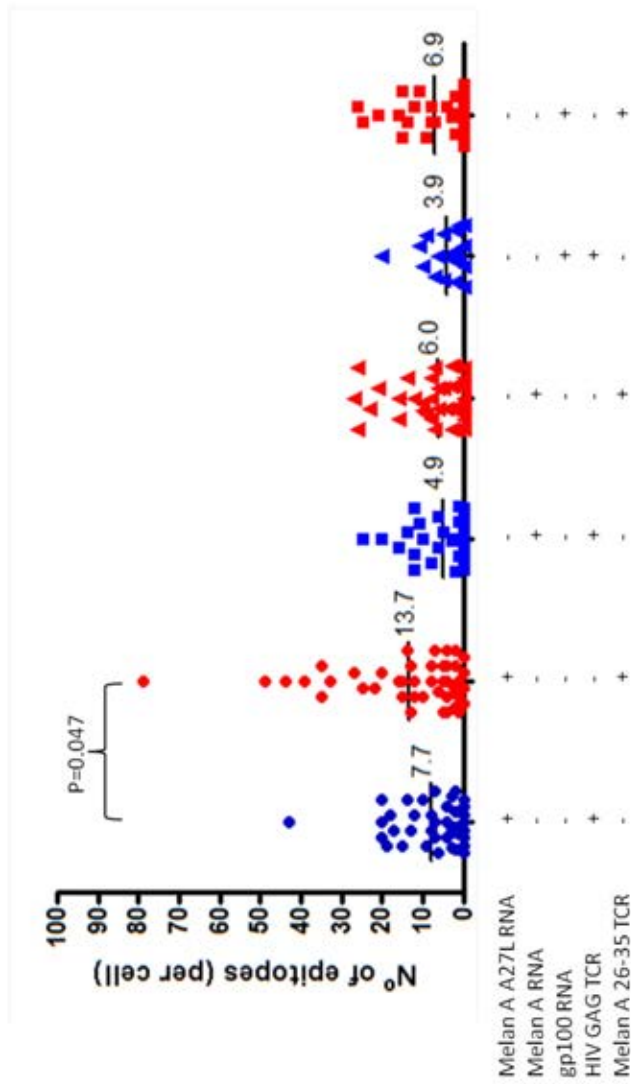
Figure 5.14. Presentation of Melan A 26-35 epitope by RNA transfected DCs assessed using recombinant T-cell receptor. 10^5 DCs (gp100, Melan A, and Melan A A27L RNA transfected) were stained with Melan A 26-35 specific TCR, followed by streptavidin-phycoerythrin secondary reagent. After extensive washes, cells were viewed under a fluorescence microscopy. Z-stack images throughout each cell were taken, and epitope counts were made manually. At least 30 cells were examined in each group. HIV GAG TCR is the negative control (non-specific). Results are presented as individual epitope counts per cell and mean values (horizontal bar). Students' T-test was used to calculate significance of difference of means as indicated.

epitope counts on positive cells ranging from 0 to 55 epitopes.

These experiments establish that, at 24 hours, Melan A transfected DCs are negative for whole Melan A yet they are able to present the immunodominant A2 restricted epitope from this antigen.

5.4. gp100 negative DCs are gp100 280-288 epitope positive as assessed by recombinant T-cell receptor.

In a series of experiments analogous to those described above, the relation between detection of whole gp100 protein in the DC and presentation of the gp100 $_{280-288}$ (YLE) epitope was determined. In the melanoma DC vaccine trial, gp100 was detectable in transfected cells 48 hours after transfection. However, levels were highly variable with percentages of positive cells ranging from 0 to 98%. The aim of this set of experiments was to show whether or not detection of whole gp100 was a necessary prerequisite for Class I epitope presentation.

HLA A2 positive DC were transfected with gp100 RNA or GFP RNA as a negative control. In parallel, HEK293 cells were also electroporated with gp100 encoding RNA. At 24 hours, cells were analysed for gp100 protein by indirect immunofluorescence microscopy. As shown in Figure 5.15A-C, there is abundant gp100 staining in transfected HEK293 cells, and also in SK23MEL gp100 positive melanoma cell line. However, there is an absence of gp100 staining in the transfected DCs, despite over 98% of cells expressing GFP.
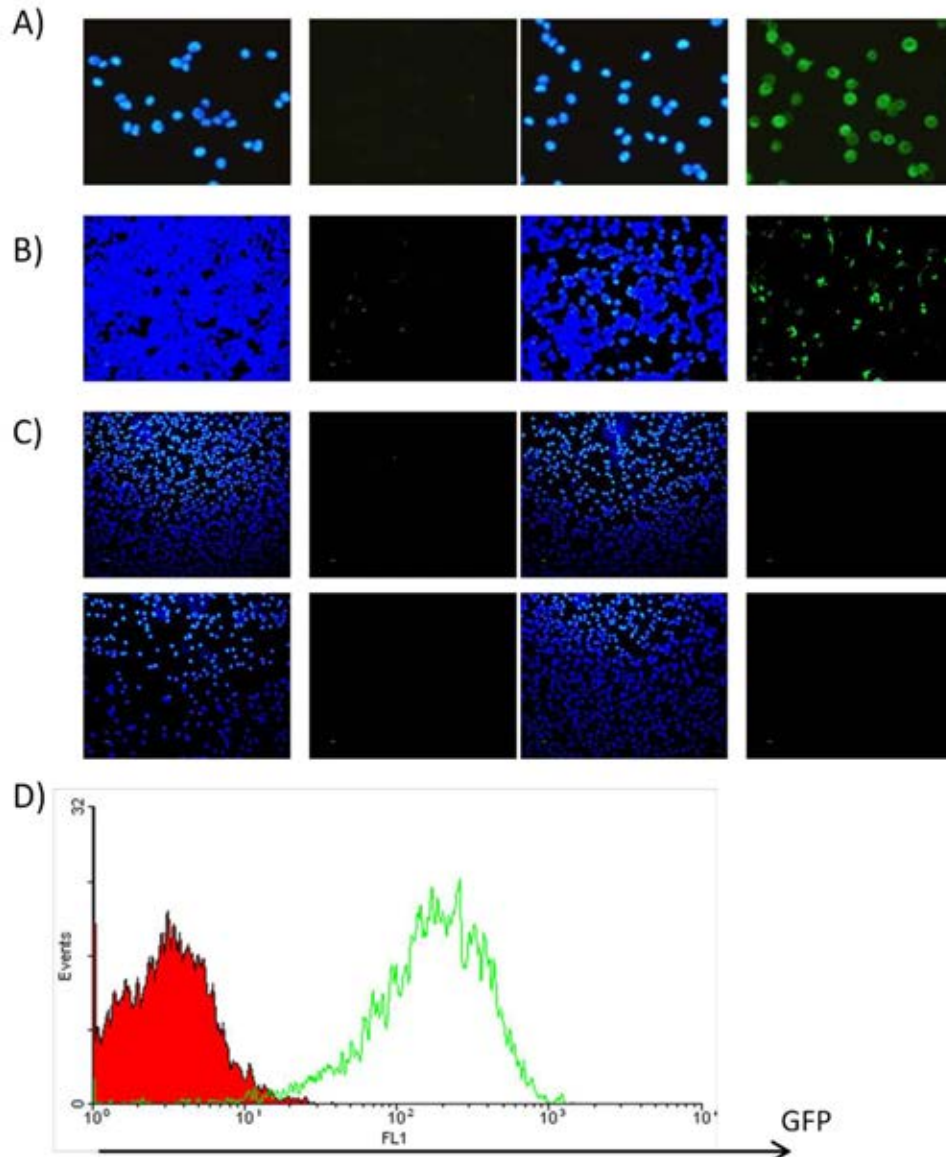
Figure 5.15. gp100 expression in gp100 RNA transfected DCs. A-C)Cells were fixed, permeabilised and stained with a mouse monoclonal anti gp100 antibody, followed by goat anti mouse Alexa 488 conjugate antibody. After extensive washing, cellular nucleic were stained with DAPI and cells were viewed under a fluorescence microscope. Far left– DAPI (isotype control), centre left – green (isotype control), centre right – DAPI (gp100 antibody), far right – green (gp100 antibody). A)SK23MEL gp100 positive cell line. B)HEK293 cells transfected with gp100 RNA. C)Upper panels – mock transfected DCs (no RNA), Lower panels – gp100 RNA transfected DCs. D)Analysis of GFP expression in GFP transfected DCs. Filled red histogram: gp100 transfected DCs, green hollow histogram – GFP transfected DCs.

The ability of these whole-antigen negative DCs to present the A2 restricted YLE epitope was assessed using a soluble recombinant T-cell receptor-anti CD3 fusion protein. Previous experiments with this reagent, using a T-cell clone of irrelevant specificity as a cellular readout, had suggested that it was sensitive enough to detect epitope presentation on cells endogenously expressing and physiologically processing whole antigen.

Figure 5.16 presents the number of gp100 YLE specific spots per well for peptide-loaded and RNA transfected DCs as a measure of epitope presentation. YLE specific spots are calculated as the spot count in the presence of the T-cell receptor-anti CD3 fusion protein at a concentration of 10^{-9}M – spot count in the absence of TCR-fusion protein. It can be seen that there is strong evidence of epitope presentation from DCs loaded with exogenous YLE peptide, but there is also an increase in spot count with gp100 transfected as opposed to mock transfected DCs. This suggests that these DC do indeed present the gp100 280-288 epitope, albeit at a far lower level than peptide-loaded DCs.
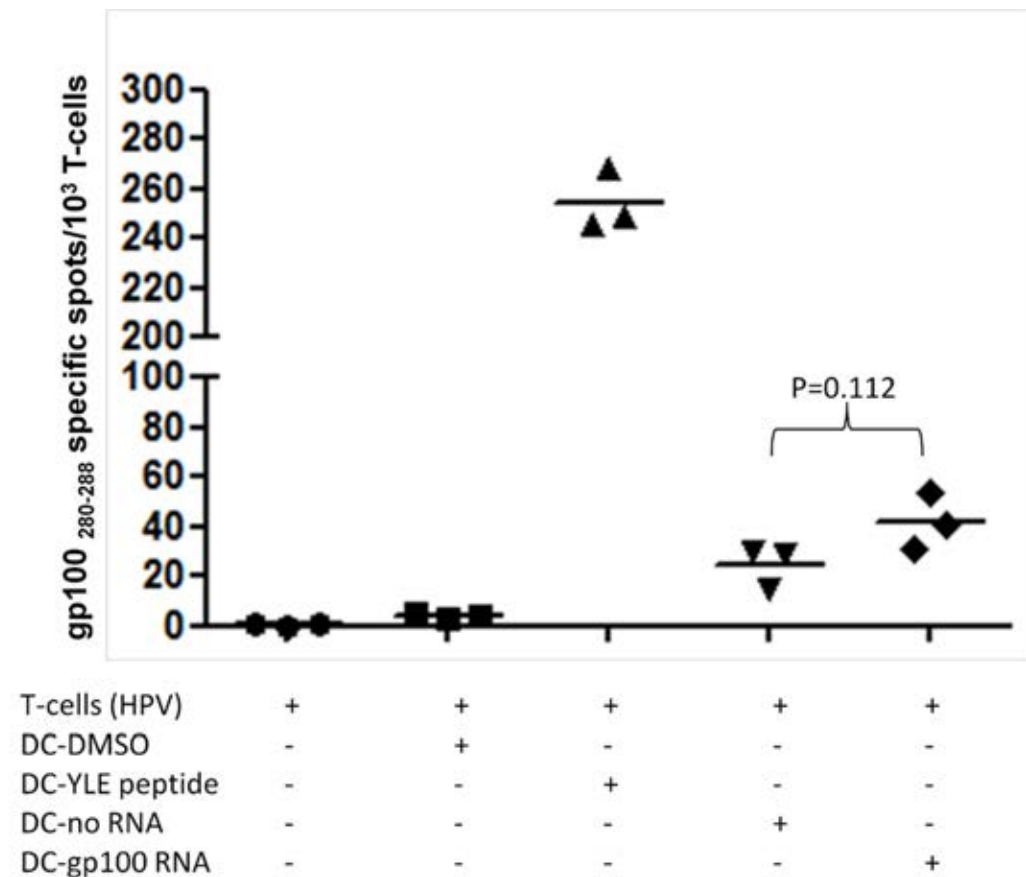
Figure 5.16. Presentation of gp100 280-288 (YLE) epitope by DCs transfected with gp100 RNA. Immature DCs were electroporated with gp100 encoding RNA or in its absence. After 24 hours, DCs (5×10^3/well) were coincubated with T-cells (10^3/well) of an irrelevant specificity (EBNA1, HPV epitope) in triplicate, in the presence of 10^{-9}M YLE specific TCR-anti CD3 fusion protein or its absence. Additionally, mature untransfected DCs were loaded with YLE peptide at 5μM or DMSO only (negative control). Results are presented as gp100 280-288 specific spots/well – spots counts and means (horizontal bars). This is calculated as spot count in the presence of TCR – spot count in the absence of TCR. Significance of difference between means of experimental groups are calculated using Students' T-test.

5.5. Melan-A and gp100 are detectable at earlier time points after transfection with RNA, albeit at different levels.

Studies have shown that antigens are expressed in RNA electroporated DC as soon as 30 minutes after electroporation (Ponsaerts et al., 2003), and the aim of these experiments was to determine the kinetics of antigen expression focussing on early time points.

Non HLA typed DC were transfected with GFP, gp100 and Melan-A encoding RNA. Cells were returned to TNFα and IL1β containing medium and at 2, 4, 8, 12 and 24 hours after transfection, cells were harvested and fixed onto microscopy slides. The next day, GFP transfected cells were immediately viewed under a fluorescence microscope, whereas the melanoma antigen expressing DCs were permeabilised and stained for gp100 and Melan A expression.

These results are presented visually in Figure 5.17 and graphically in Figure 5.18. For GFP expression, the vast majority of cells show strong green fluorescence at all times points after transfection. However, for Melan A there is a detectable population of Melan A positive cells at early time points after transfection – levels drop with time
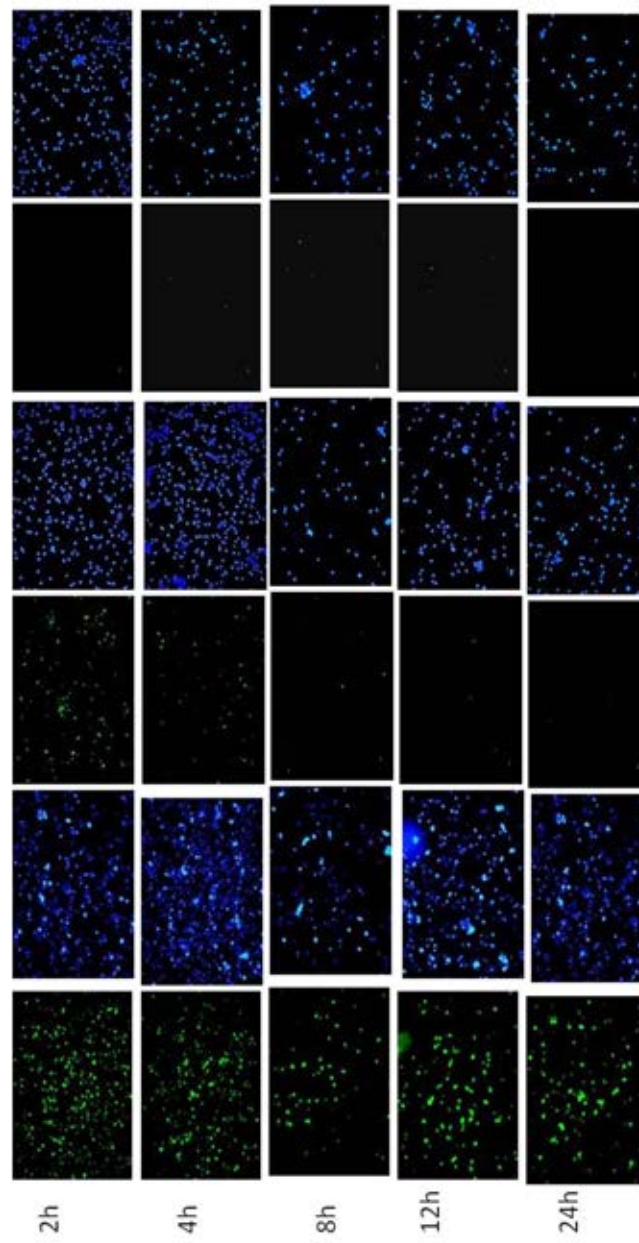
Figure 5.17. Kinetics of antigen expression in RNA transfected dendritic cells. Immature DCs were prepared from buffy-coat PBMCs. Cells were electroporated with RNA encoding GFP, Melan-A and gp100. At the indicated time-points after transfection, cells were harvested and fixed onto microscopy slides. At 24 hours, all cells were simulataneously permeabilised and stained with Melan-A or gp100 primary antibodies, followed by Alexa 488 conjugated secondary antibodies. After washing, cell nuclei were stained with DAPI and cells were viewed under a fluorescence microscope. Left panels shown green fluorescence, DAPI staining is shown on right panels.
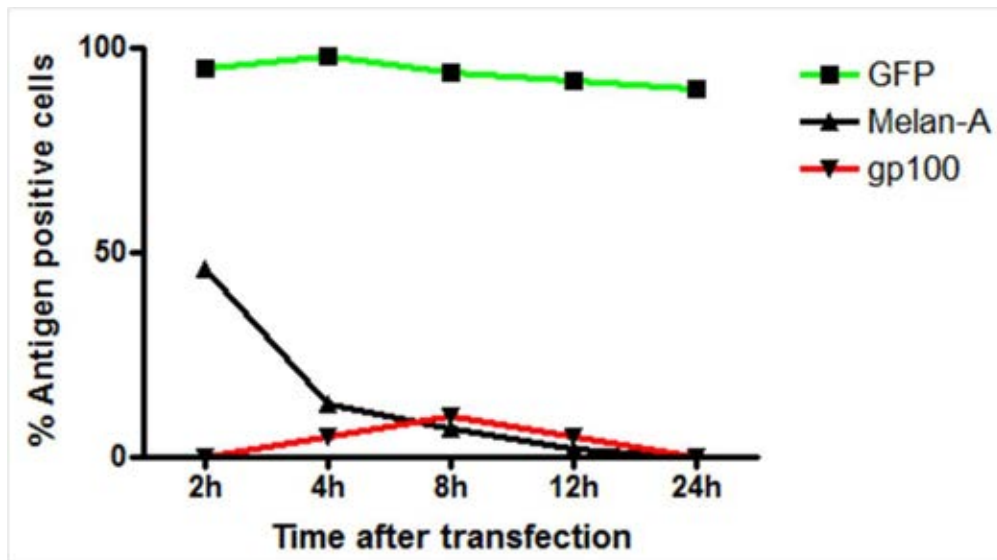
Figure 5.18. Kinetics of antigen expression following RNA transfection of DCs. Based on Figure 4.17, percentage of antigen positive cells at each time point after transfection is calculated as (total number of antigen positive cells/total number of cell nuclei) x 100.

and are undetectable by 24 hours. For gp100, there are a very few positive cells, again only seen at earlier time points.

5.6. Lysosomal acidification seems to be involved in the loss of Melan-A expression with time and with presentation of the Melan A 26-35 epitope in transfected DCs.

The observed reduction in proportion of Melan-A whole antigen positive cells with time, demonstrated in earlier sections, could be due to instability of the RNA and transient expression, or relate to active intracellular processing of the source protein.

In experiments on the kinetics of antigen expression, DCs were exposed to a proinflammatory stimulus (TNFα and IL1β) that is known to upregulate lysosomal acidification and enzymatic function (Amigorena and Savina, 2007).

Therefore, the primary aim of this set of experiments was to determine whether or not lysosomal or proteasomal processes might be involved in degradation of Melan-A in transfected DC, and the secondary objective was to determine whether such processes are involved in generation of the 26-35 epitope at the cell surface.

To achieve this, the effect of pharmacological inhibitors was studied. Bafilomycin A is a highly specific inhibitor

of lysosomal acidification through inhibition of the vacuolar H+/ATPase proton pump (Yoshimori et al., 1991). Epoxomycin is an inhibitor of proteasomal activity, specifically β5 subunit dependent chymotrysin-like peptidase function (Naujokat et al., 2007).

HLA A2 positive DC were prepared and transfected with RNA encoding Melan A or mock transfected (electroporated in the absence of RNA) and incubated for a further 24 hours in TNFα and IL1β supplemented medium. In addition, some immature DCs were left untransfected and transferred into maturation medium. RNA transfected cells were additionally exposed to epoxomycin, bafilomycin, or both for 24 hours after transfection. At this point, intracellular Melan-A staining was performed on the DCs, and they were used as targets in overnight IFNγ ELISPOT assays with the Mel c5 clone as effectors. DCs were washed extensively to remove excess bafilomycin or epoxomycin before cellular assays.

As shown in Figure 5.19, there is no Melan-A staining in cells left untreated, in line with Figure 4.8. Cells treated with epoxomycin are also antigen negative. However, DCs treated with bafilomycin alone do show Melan-A positivity, albeit in a very small proportion of cells

268

A)

No RNA	+	-	-	-	-	-	-	-	-
Melan A RNA	-	+	+	+	+	-	-	-	-
Melan A A27L RNA	-	-	-	-	-	+	+	+	+
Balifomycin A	-	-	+	-	+	-	-	+	+
Epoxomycin	-	+	-	+	-	+	-	-	+

B)

Figure 5.19. Effect of bafilomycin A and epoxomycin on whole antigen detection in DCs transfected with Melan-A RNA. A)HLA-A2 positive DCs were transfected with Melan-A RNA (wild-type or A27L variant) or in its absence. Cells were returned to medium supplemented with either bafilomycin A, epoxomycin, both or neither as shown. After 24 hours, cells were harvested, fixed, permeabilised and stained with a mouse monoclonal anti Melan-A antibody followed by goat anti-mouse Alexa 488 conjugate. After extensive washing, cells were viewed under a fluorescence microscope. Top panels show nuclear staining with DAPI, lower panels show green fluorescence indicative of Melan-A staining. B)Melan A staining of SK23 melanoma line. Left – DAPI. Right – green (Melan-A).

269

(approximately 1/100). There is successful staining of Melan-A in a melanoma cell line (SK23MEL). It is also noted that DCs treated with epoxomycin show decreased cellular viability (50-60%) as compared to other DC groups (90-100%), and exhibit abnormal (small, irregular, fragmented) nuclei on DAPI staining.

Moving forward to epitope presentation, there is again evidence that the Mel c5 T-cell clone recognises Melan A (wild-type and A27L variant) transfected DCs in a specific fashion in IFNγ ELISPOT assays. This is shown in Figure 5.20. The level of recognition is approximately 7 fold lower than maximal levels. The addition of epoxomycin and/or bafilomycin A markedly attenuates the observed responses. The reduction in recognition by the T-cell clone is greatest with epoxomycin (whether in combination with Bafilomycin or not), but there is clearly an inhibitory effect of bafilomycin alone. Melan A A27L variant DCs appear to be less affected by the pharmacological inhibitors, perhaps due to a greater sensitivity of the T-cell clone to the A27L variant.

These data suggest that the lysosome is involved in the degradation of Melan-A in transfected DCs, and that
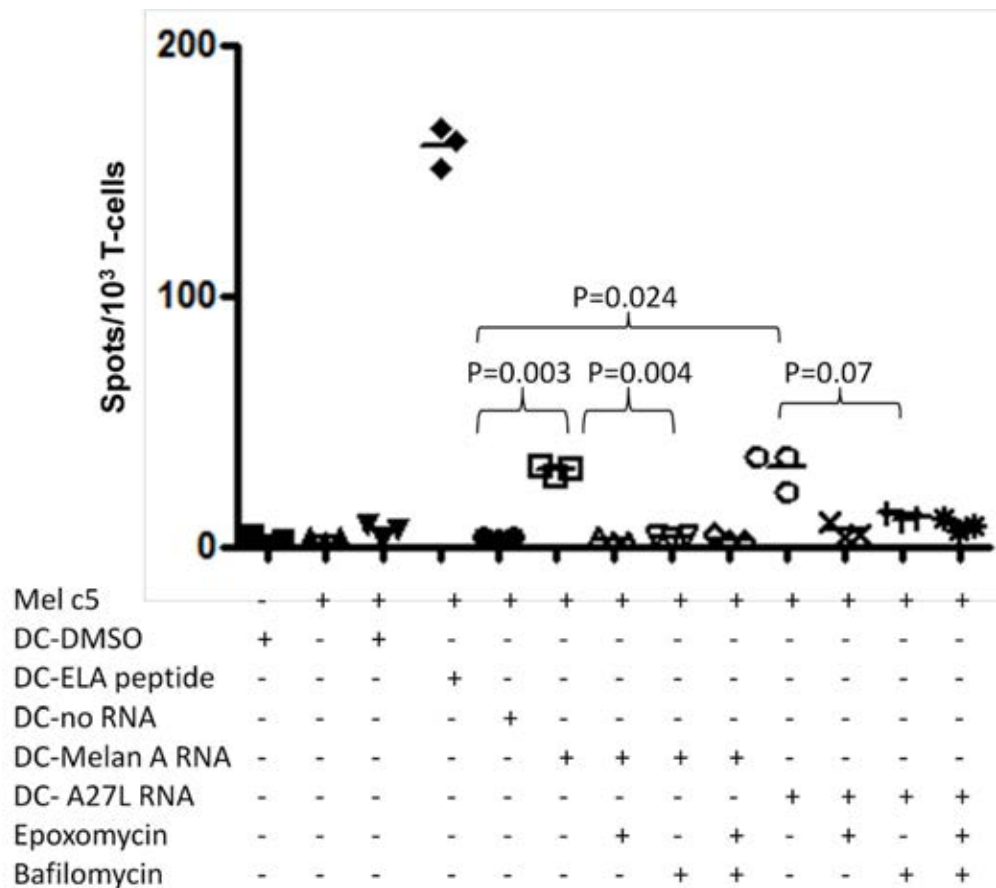
Figure 5.20. Presentation of Melan A 26-35 epitope by RNA transfected DCs – effect of bafilomycin A and epoxomycin. Immature DCs were prepared from an HLA-A2 positive donor. DCs were transfected with Melan A or Melan A A27L RNA or mock transfected (no RNA). Cells were transferred to medium containing bafilomycin A, epoxomycin, both inhibitors or neither for 24 hours. At this point, transfected and peptide-loaded (ELA peptide at 5μM or DMSO alone) DCs (10^4/well) were used as targets in overnight IFNγ ELISPOT assays with Mel c5 effector T-cells (10^3/well) in triplicate. Results are presented as individual values and means (horizontal bars). Students' T-test was used to calculate significance of difference of means as indicated.

generation of the A2 restricted 26-35 epitope may be dependent on both proteasomal and lysosomal processes. The possibility that the observed reduction T-cell recognition after treatment with inhibitors is partially due to non-specific negative effects on the DCs is not totally excluded however.

5.7. Lysosomal acidification does not appear to be involved in generation of a MHC Class I restricted epitope from EBNA1 in transfected DCs.

Melan-A RNA transfected DCs treated with bafilomycin A do show whole antigen positivity (at a very low level) and this treatment attenuates recognition by an A2 restricted T-cell clone. The aim of thse experiments was to determine whether this dependence of Class I epitope presentation on lysosomal processing was a general feature of dendritic cell function or whether it was antigen-specific.

To achieve this, the experiments detailed in Section 5.6 were repeated using a different antigen. EBNA1ΔGA was chosen for these experiments as it is a viral antigen that is efficiently processed via the proteasome and its localisation – nuclear – is likely to be different from Melan-A.

HLA-B35 positive DC were transfected with EBNA1ΔGA RNA or mock-transfected. After transfection, cells were again transferred to medium containing pharmacological inhibitors or not. At 24 hours, cells were harvested, washed and used as targets in overnight IFNγ ELISPOT assays using the B35 restricted HPV specific T-cell clone as effector cells. As a positive control, mature untransfected DCs were loaded with HPV peptide or DMSO (control). Whole antigen detection was performed on fixed and permeabilised cells using the R4 antibody.

As shown in Figure 5.21, in contrast to Melan-A transfected DCs, EBNA1 is easily detectable in all transfected cells except those transfected without RNA. The localisation appears nuclear. The percentages of positive cells are as follows: mock – 0%, EBNA1 no inhibitors – 51%, EBNA 1 epoxomycin – 33%, EBNA1 bafilomycin – 49%, EBNA1 both inhibitors – 44%. There appears to be a slight increase in staining intensity in bafilomycin treated DCs. Again, there are abnormal cell nuclei in epoxomycin treated cells, and cellular viability was reduced in this group (≈50%). There is no dramatic effect of inhibitors on whole EBNA1 detection.

No RNA	+	-	-	-	-
EBNA1ΔGA RNA	-	+	+	+	+
Epoxomycin	-	-	+	-	+
Bafilomycin A	-	-	-	+	+
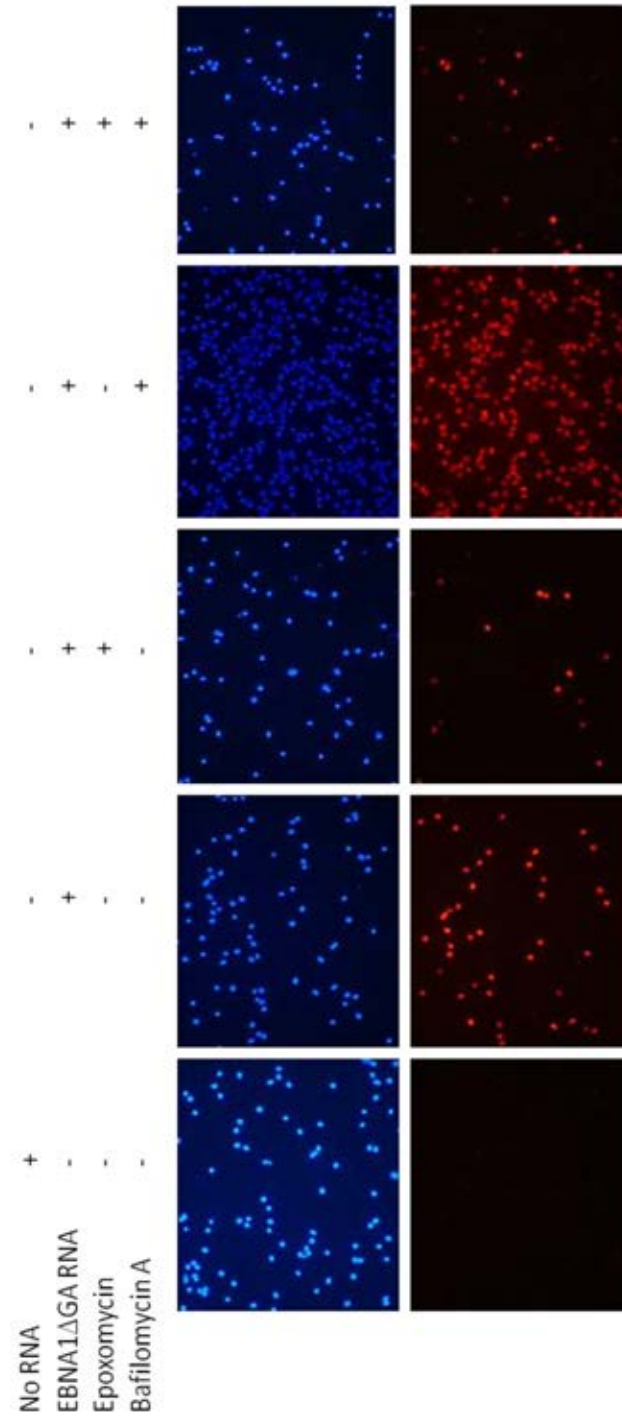
Figure 5.21. Detection of whole EBNA1 in EBNA1 transfected DCs – effect of bafilomycin and epoxomycin. DCs were prepared from a HLA B35 positive donor. Cells were transfected with EBNA1ΔGA RNA or in its absence (negative control) and were then exposed to epoxomycin, bafilomycin, both inhibitors or neither for 24 hours. At this point, cells were fixed, permeabilised and stained with rabbit polyclonal anti EBNA1 antibody (R4), followed by goat anti rabbit Alexa 594 secondary antibody. After nuclear staining with DAPI and extensive washing, cells were viewed under a fluorescence microscope. Top panels show nuclear staining with DAPI (blue), and lower panels show red fluorescence indicative of EBNA1 staining.

The ability of these DCs to present the B35 restricted HPV epitope to a specific T-cell clone is presented in Figure 5.22. There was obvious recognition of DCs loaded with exogenous HPV peptide, although background recognition of DCs loaded with DMSO only was slightly higher than usual. In terms of transfected DCs, there is recognition of EBNA1ΔGA expressing cells that is abrogated by exposure to the proteasome inhibitor epoxomycin. In contrast, exposure of DCs to bafilomycin seems to somewhat increase presentation of the epitope.

Taken together, these results (Sections 5.6 and 5.7) suggest that there is heterogeneity in antigen degradation pathways and Class I restricted epitope generation mechanisms between different antigens in transfected DCs. For Melan-A, lysosome inhibition increases detection of whole antigen and reduces epitope presentation. In the case of EBNA1, epitope presentation is actually increased in the presence of bafilomycin. This finding also reduces the likelihood that observed effects are due to off-target effects of bafilomycin, as these would be expected to be similar for both antigens.

T-cells (HPV)	+	-	+	+	+	+	+	+	+
DC-DMSO	-	+	+	-	-	-	-	-	-
DC-HPV peptide	-	-	-	+	-	-	-	-	-
DC-no RNA	-	-	-	-	+	-	-	-	-
DC-EBNA1ΔGA RNA	-	-	-	-	-	+	+	+	+
Epoxomycin	-	-	-	-	-	-	+	-	+
Bafilomycin A	-	-	-	-	-	-	-	+	+
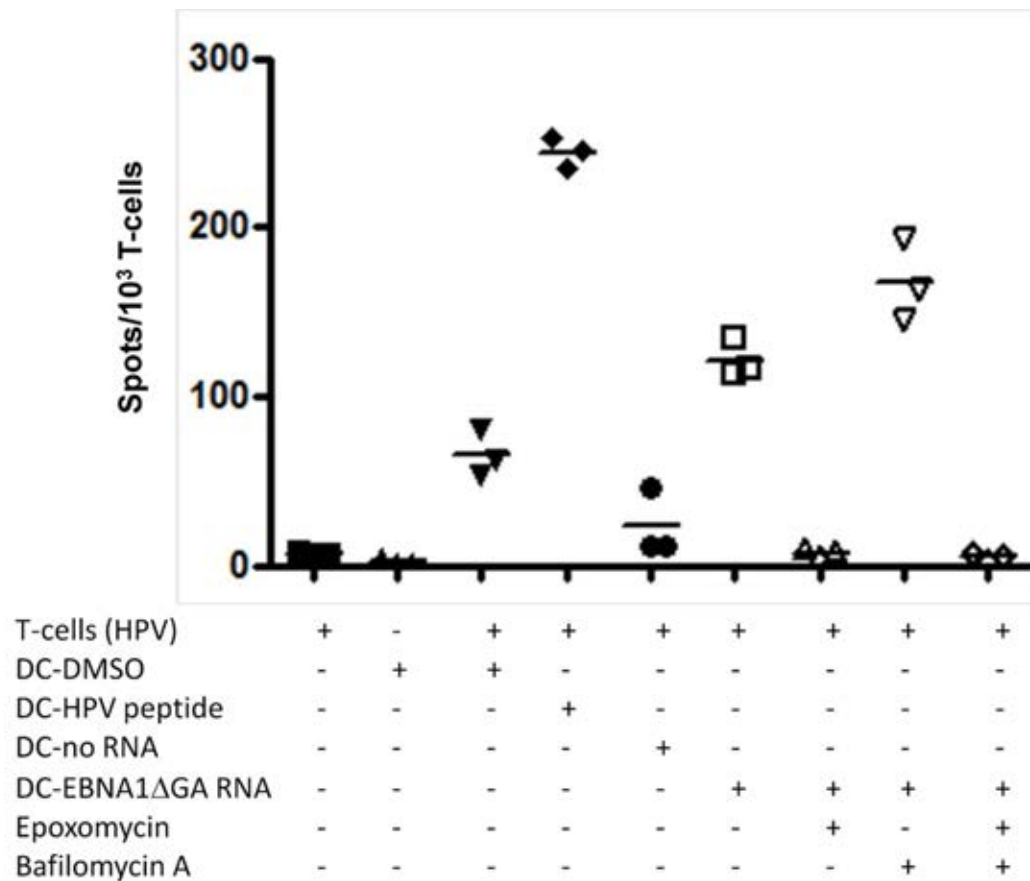
Figure 5.22. Presentation of EBNA1 $_{407-417}$ (HPV) epitope by RNA transfected DCs – effect of epoxomycin and bafilomycin A. Immature DCs were transfected with EBNA1ΔGA RNA or in its absence (no RNA). After 24 hours further culture and exposure to bafilomycin, epoxomycin, both or neither, DCs were harvested. DCs (10^4/well) were used as targets in overnight IFNγ ELISPOT assays with HPV specific T-cell clone c41 as effector cells (10^3/well). Assays were set up in triplicate, and results are presented as spot counts/well - individual triplicates and mean values (horizontal bars).

5.8. In transfected DCs, presentation of the Melan-A $_{26-35}$ epitope lags behind detection of whole Melan-A antigen.

After considering that Melan-A RNA transfected DC are whole antigen negative at 24 hours yet present the 26-35 epitope, and the result that at earlier time-points Melan-A is detected intracellularly, a simple question arises – 'Is epitope presentation also happening when cells are whole antigen positive shortly after transfection?'.

The aim of this set of experiments was to answer this question by comparing whole antigen detection and simultaneous epitope presentation at 4 and 24 hours after RNA transfection with wild type and A27L variant RNA. The maturation status of these DCs was assessed by antibody staining against a panel of DC.

HLA-A2 positive DC were prepared and transfected with Melan-A wild-type or Melan A A27L variant RNA or mock-transfected (control). After 3 and 24 hours after transfection, cells were stained for Melan-A and with a panel of cell surface antibodies, and were used as targets for recognition by the Melc5 T-cell clone in IFNγ ELISPOT assays. The same aliquot of T-cells was used for each assay. Additionally, at each

time-point untransfected DCs were loaded with exogenous peptide (ELA) or DMSO alone as a positive control for T-cell function.

For whole antigen detection, a small population of Melan-A positive DCs is seen at 3 hours post transfection. Approximately 1 in 8 cells are Melan-A positive. In contrast, at 24 hours no antigen positive cells are visible. Successful staining of Melan-A in a melanoma cell line (SK23MEL) is seen. Cells were fixed separately but all staining was performed in parallel. These results are presented in Figure 5.23.

Moving forward to presentation of the 26-35 epitope, there is definite evidence of specific recognition of transfected DCs by the T-cell clone at 24 hours, but this is not seen at 3 hours post transfection. Recognition appears more robust with DC expressing the A27L variant. There is strong recognition of DCs loaded with exogenous peptide at both time points, although spot counts were somewhat higher when the assay was performed at 24 hours. These results are presented in Figure 5.24.

A)

	Mock	Melan A	Melan A A27L	3 hours	24 hours
	+	-	-	+	-
	-	+	-	+	-
	-	-	+	+	-
	-	-	+	-	+
	-	+	-	-	+
	-	-	-	-	+

Figure 5.23. Detection of whole Melan-A in RNA transfected DCs: 3 and 24 hours after transfection. A)DCs were transfected with Melan A RNA (wild-type and A27L variant) or mock transfected (no RNA). At the indicated time points after transfection, cells were removed and fixed, permeabilised and stained with a mouse monoclonal anti-Melan A antibody followed by goat anti mouse Alexa 488 secondary antibody. After extensive washes, nuclei were stained with DAPI and cells were viewed under a fluorescence microscopy. Upper panels show nuclear staining with DAPI, lower panels show green fluorescence (Melan A) B)Melan A staining on SK23 melanoma cell line. Left panel – DAPI, right panel – green staining (Melan A)

280

Figure 5.24. Recognition of Melan-A RNA transfected DCs by Mel c5 (Melan A 26-35) specific T-cell clone: time course. HLA A2 positive immature DCs were transfected with Melan A RNA (wild-type and A27L variant) or in its absence (negative control). After 3 hours (A)and 24 hours (B) post-transfection, DCs were used as targets (10^4/well) in overnight IFNγ ELISPOT assays with Mel c5 as the effector clone (10^3/well). At each time point, mock transfected DCs were additionally loaded with 5µM exogenous ELA peptide as a positive control for T-cell functionality. Assays were set up in triplicate and results are presented as individual values and means (horizontal bars). Students' T-test was used to calculate significance of difference of means as indicated.

Finally, these same groups of DCs (3 and 24 hours post transfection) were analysed for a panel of cell surface markers of DC differentiation and maturation. The results of surface antibody staining are presented in Table 5.1.

Table 5.1. Phenotypic analysis of DC at 3 and 24 hours after transfection and maturation

	% DCs positive		
Cell surface marker	Pre transfection	3h post transfection	24h post transfection
CD1a	97.1	97.0	98.6
CCR7	9.8	9.2	9.8
CD14	73.9	73.6	53.8
CD25	4.3	4.3	9.0
CD83	6.3	11.9	36.5
CD86	25.8	95.3	84.5
MHC Class I	97.0	98.2	97.2

The result of staining for maturation markers CCR7, CD25, CD83 and CD86 and MHC Class I molecules is shown in Figure 4.25. There are increases in proportion of cells expressing CD83 and to a lesser extent CD25 at 24 hours compared to 3 hours. The staining intensity for MHC Class I may be lower at 3 hours. Phenotypic analysis suggests that at both time-points, DCs may be described as 'semi-mature'.
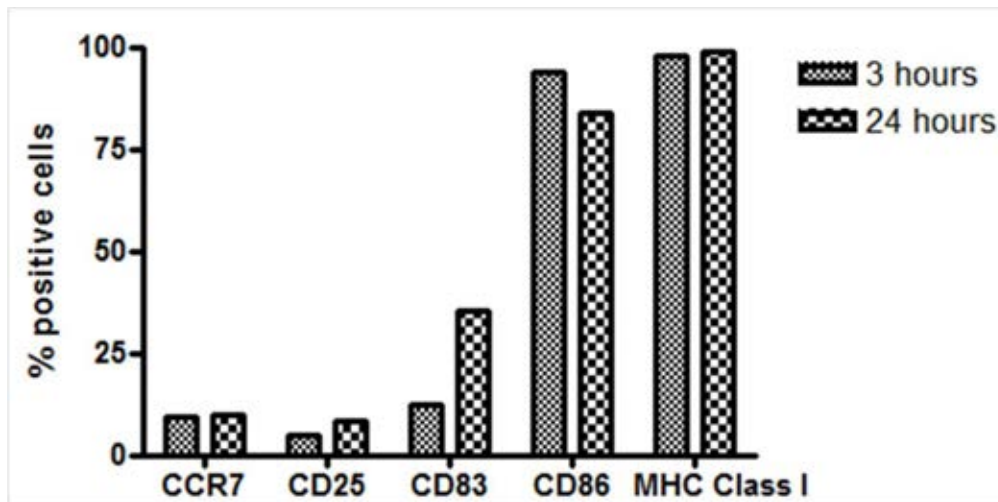
Figure 5.25. Immunophenotype of DCs 3 and 24 hours post transfection. DCs were transfected with Melan-A A27L RNA and 3 and 24 hours after, cells were stained with a panel of mouse monoclonal antibodies against human CCR7 (A), CD25 (B), CD83 (C), CD86 (D) and MHC Class I (E) or isotype controls. Primary antibodies were phycoerythrin conjugated and cells were analysed by flow cytometry. At least 10^4 gated events were collected. Percentages of cells positive are presented and were calculated as %positive cells with antibody of interest - %positive cells with isotype matched control antibody.

As a whole, this set of results suggests that in RNA transfected DCs, presentation of the Melan A 26-35 epitope from endogenous source protein lags behind detection of whole antigen. Exogenously supplied peptide can be presented at both time-points at comparable levels.

In conclusion, experiments suggest that early after transfection when whole antigen is detected epitope presentation is not occurring, whereas once more time has elapsed, DCs are epitope positive but whole antigen negative.

5.9. In transfected DCs, the relationship between detection of whole antigen and presentation of MHC Class I restricted epitopes is antigen dependent.

In the case of Melan-A transfected dendritic cells, there is a delay between detection of whole antigen that peaks at 2-4 hours post transfection and presentation of the 26-35 epitope to a specific T-cell clone that is only seen at 24 hours.

The aim of this set of experiments was to determine what the relationship between whole antigen detection and epitope presentation is for EBNA1 and Melan A in parallel, in the same experiment.

The glycine-alanine repeat deleted isoform of EBNA1 (EBNA1ΔGA) was chosen for these experiments as it has the same (nuclear) localisation as unmanipulated protein but it is less stable and more likely to produce DRIPs (Tellam et al., 2007) than full length antigen.

In this set of experiments, dendritic cells were prepared from a laboratory donor whose haplotype included both the

B35 and A2 alleles. This allowed detection of both the B35-HPV epitope of EBNA1, and the A2-EAA/ELA epitope of Melan-A.

HLA A2 and B35 positive immature DCs were transfected with EBNA1ΔGA RNA, Melan A (wild-type) or Melan A A27L variant RNA. Transfected DCs were returned to medium supplemented with TNFα and IL1β. At 4 hours and 24 hours after transfection, DCs were harvested and used for assays. At each time-point, cells were used for intracellular antigen staining and also as targets for T-cell recognition in IFNγ ELISPOT assays. In both antigen staining and T-cell recognition assays, the two antigens acted as internal negative controls for each other.

In terms of whole antigen detection, EBNA1 is detected is the majority (over 80%) of EBNA1ΔGA transfected DCs. This is seen at the 4 and 24 hour time point. The staining intensity and frequency of positive cells is similar at each time point. There is no non-specific EBNA1 fluorescence in Melan A transfected DCs. This is shown in Figure 5.26A.
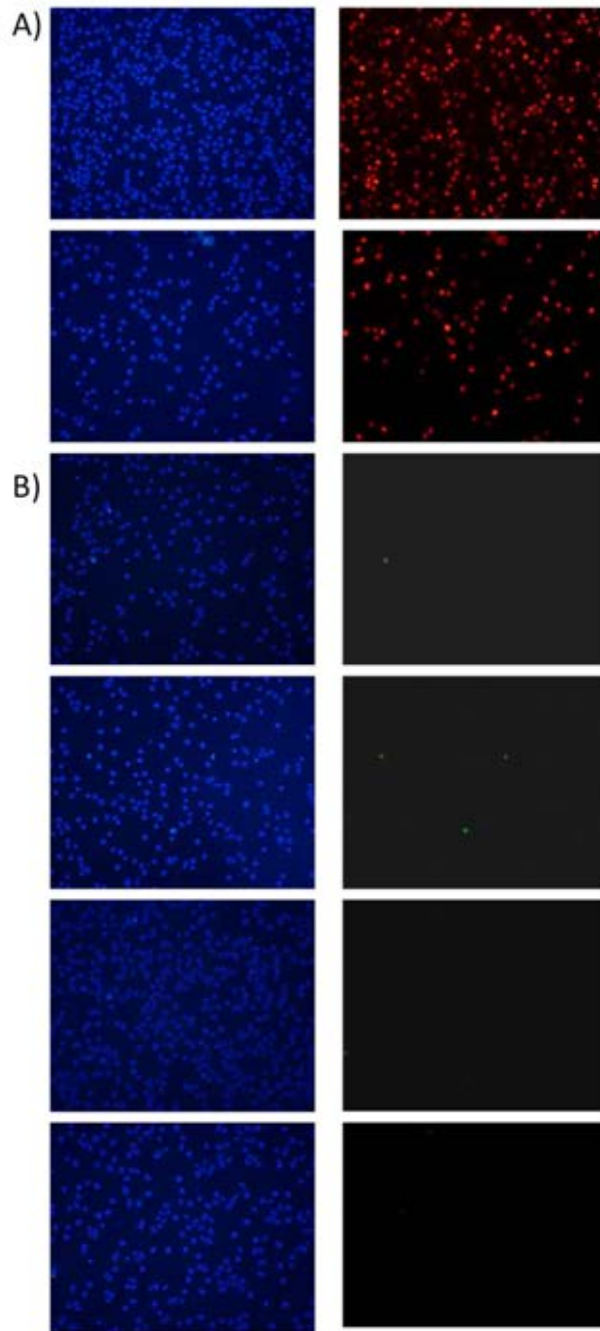
Figure 5.26. Whole antigen detection in RNA transfected DCs – EBNA1 and Melan-A. 105 transfected DCs were fixed, permeabilised and stained with primary antibodies against EBNA1 (R4) or Melan-A. After washes, secondary antibodies (goat anti rabbit Alexa 594 conjugate and goat anti mouse Alexa 488 conjugate respectively) were added. After nuclear staining with DAPI, and further washes, cells were viewed under a fluorescence microscopy. Left panels show nuclear staining with DAPI, and right panels show red fluorescence (EBNA) or green fluorescence (Melan-A). A)EBNA1ΔGA transfected DC with EBNA1 antibody. Upper panel – 4 hours, lower panel – 24 hours. B) Melan-A transfected DC with Melan-A antibody.

Moving on to Melan-A, there are occasional Melan-A positive cells seen at 4 hours post transfection, but no positive cells after 24 hours. There is no non-specific Melan-A staining of EBNA1ΔGA transfected DCs. There appears to be a higher frequency of positive cells with the wild-type as compared to A27L variant Melan-A. This is shown in Figure 5.26B.

In terms of epitope presentation, for EBNA1, there is definite recognition of EBNA1ΔGA expressing DCs above background levels with Melan-A transfected DCs. This approaches 70% of peptide-stimulated responses. The level of epitope presentation from endogenous EBNA1 is slightly higher at 4 compared to 24 hours (172 v 104 spot increase). These results are presented in Figure 5.27.

As shown in Figure 5.28, presentation of the Melan A 26-35 epitope to the Mel c5 clone is only clearly evident at 24 hours after transfection. After 4 hours, there is a slight suggestion of higher spot counts in Melan A and A27L transfected DCs versus EBNA1ΔGA expressing DCs, but the triplicates overlap. In contrast, at 24 hours, triplicates do not overlap, suggesting more robustly that epitope

c47 (HPV)	+	+	+	+
DC-Melan A RNA	-	+	-	+
DC-EBNA1 RNA	-	-	+	-
HPV peptide (5μM)	-	-	-	+
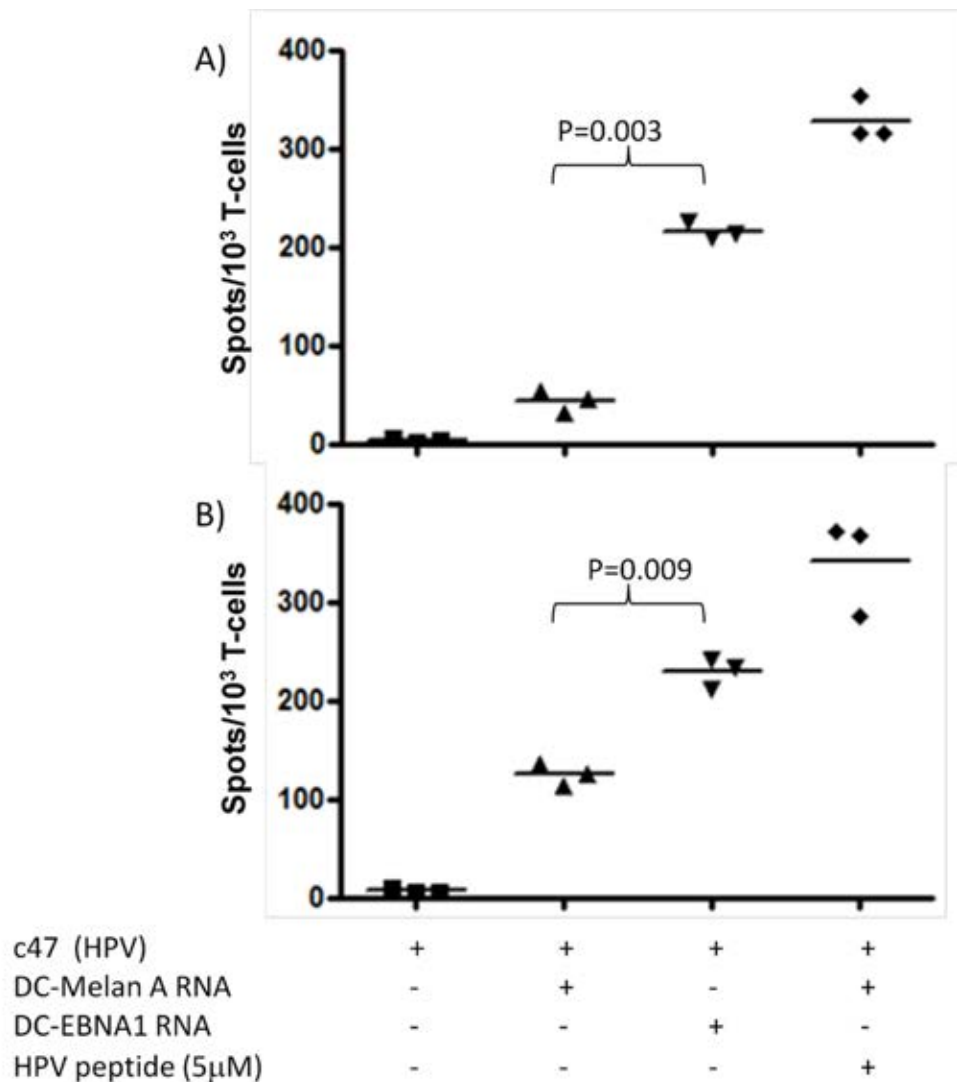
Figure 5.27. Presentation of EBNA1 407-417 (HPV) epitope by RNA transfected DCs: time course. HLA B35 (and A2) positive immature DCs were transfected with Melan A, Melan A A27L and EBNA1ΔGA RNA. At 4 (A) and 24 (B) hours after transfection, cells were harvested and used for assays. Melan-A transfected DCs were loaded with 5μM exogenous HPV peptide as a positive control for T cell functionality . Transfected and peptide-loaded DCs (10⁴/well)were used as targets in overnight IFNγ ELISPOT assays with a T-cell clone (c47, HPV specific) as effector cells (10³/well). Assays were set up in triplicate. Results are presented as individual and mean (horizontal bar) values. Students' T-test was used to calculate significance of difference of means as indicated.

Figure 5.28. Presentation of Melan A 26-35 epitope by transfected DCs: time course. HLA A2 (and B35) positive immature DCs were transfected with Melan A, Melan A A27L and EBNA1ΔGA RNA. At 4 (A) and 24 (B) hours after transfection, cells were harvested and used for assays. Melan-A transfected DCs were loaded with 5μM exogenous ELA peptide as a positive control for T cell functionality . Transfected and peptide-loaded DCs (10⁴/well) were used as targets in overnight IFNγ ELISPOT assays with a T-cell clone (c47, HPV specific) as effector cells (10³/well). Assays were set up in triplicate. Results are presented as individual and mean (horizontal bar) values. Students' T-test was used to calculate significance of difference of means as indicated.

b

presentation is occurring at this time. The peptide-stimulated responses are comparable at either time point.

A comparison of the kinetics of epitope presentation for the Melan A 26-35 epitope and EBNA1 407-417 epitope is made in Figure 5.29. It is clear that the fold-increase in recognition with Melan-A expressing DCs above background is greater at 24 compared to 4 hours, for the wild-type and variant A27L. In contrast, the fold-increase in recognition is twice as high at 4 hours compared to 24 hours for EBNA1ΔGA.

In summary, this set of experiments shows that the delay between detection of whole antigen and presentation of MHC Class I restricted epitopes is seen only with Melan-A and not with EBNA1. In the case of EBNA1, a high proportion of cells are EBNA1 positive by antibody staining early and late after transfection, and epitope presentation is occurring at both times.
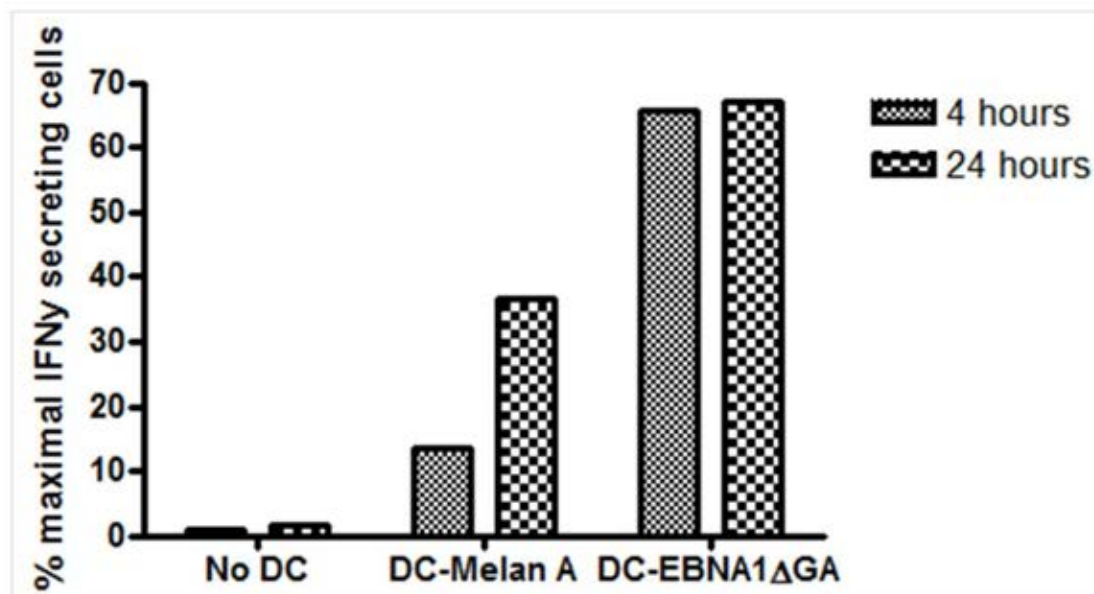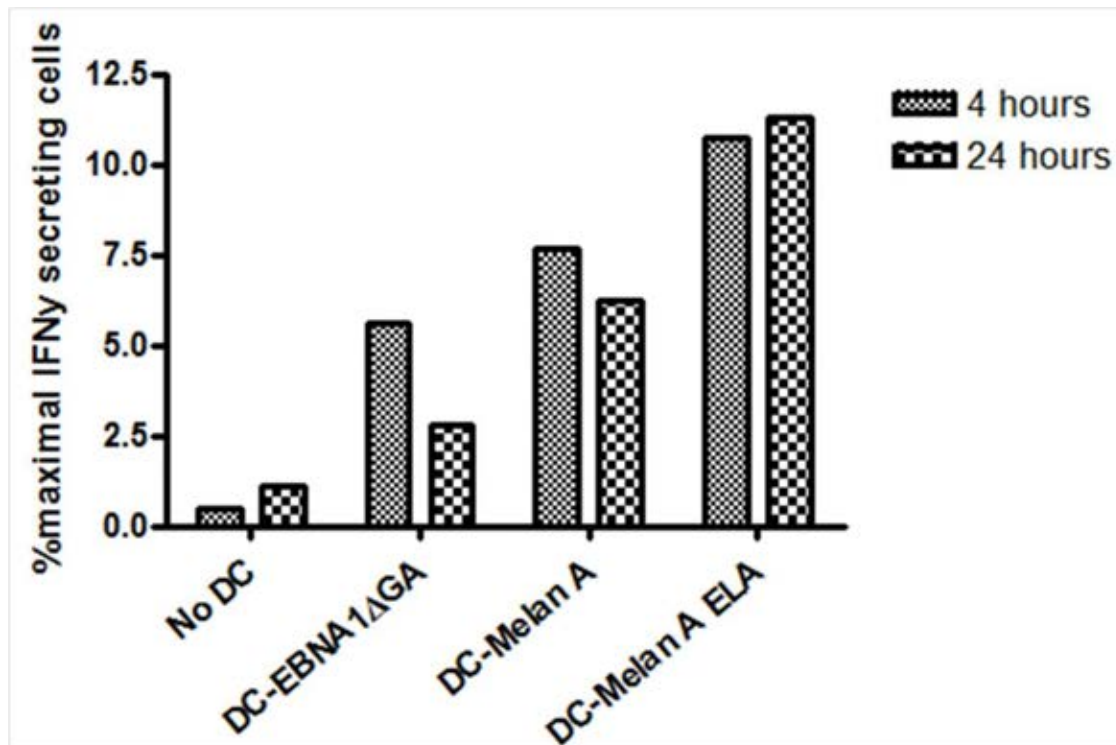
Figure 5.29. Recognition of transfected DCs by Melan A $_{26-35}$ specific (A) and EBNA1 $_{407-417}$ specific (B) T cell clones in IFNγ ELISPOT assays. Results are presented as the percentage of maximal IFNγ secreting cells (i.e. DCs loaded with 5μM cognate peptide).

Chapter 6: Presentation of MHC Class I restricted epitopes by transfected dendritic cells: discussion

6.1. The Melan-A 26-35 epitope is presented by Melan-A transfected DCs

The generation of MHC Class I restricted peptides is proteasome dependent and therefore understanding proteasomal physiology is vital in understanding Class I presentation. The concept of differential epitope generation by standard and immunoproteasomes has existed for over a decade. It is thought that substitution of the IFNγ inducible subunits (LMP2, LMP7 and Mecl-1, for β1, 2 and 5) leads to preferential polypeptide cleavage after hydrophobic or basic amino acid residues rather than after acidic residues (Cerundolo et al., 1995). Thus, the repertoire of final antigenic peptides produced may be different (Rock and Goldberg, 1999).

In terms of tumour antigens, Morel et al (2000) demonstrated that immunoproteasomes were unable to process an extended Melan-A 16-40 peptide into the 26-35 epitope, whereas standard proteasomes were able to do so - suggesting that the epitope is generated extremely inefficiently by the immunoproteasome.

However, experiments using purified proteasomes in vitro are not totally analogous to the situation in vivo, as i post-proteasomal processes contribute to the generation of final antigenic peptides for MHC loading (Rock, York and Goldberg, 2004).

Chapatte et al (2006) showed that human moDCs nucleofected with Melan-A plasmid DNA failed to be recognised by a Melan-A 26-35 specific T-cell clone despite 30% transfection efficiency and good recognition of peptide-loaded targets. However, no maturation stimulus was used. DC from LMP2 knockout mice (lacking immunoproteasomes) were able to present the epitope.

Held et al (2007) showed using MHC-peptide specific antibodies, that LCLs expressing Melan-A A27L as an ubiquitin fusion protein after viral transduction are epitope negative in comparison to cells expressing a 26-35 minigene construct. LCLs constitutively express immunoproteasomes.

However, the work presented here suggests that monocyte derived DC are able to present this epitope in an immunogenic fashion. Across several experiments with DC from different donors, there is recognition of Melan-A A27L and wild-type transfected DCs by a Melan-A 26-35 specific clone. Levels of recognition range from 8-20% maximal. Unlike Chapatte et al (2006), these experiments used cytokine-matured DC as targets. In addition, the transfection efficiency in these experiments approached 90% in contrast to 30-40% and nucleofection of DNA is associated with higher cellular mortality than RNA transfection. Chapatte et al. used immunomagnetic selection of CD14 positive monocytes, whereas this work used plastic adherence. The possibility that a greater proportion of contaminating cells could be contributing towards epitope presentation is not totally excluded. Also, T-cell recognition was measured by ELISPOT here, which allows quantification of individual IFNγ secreting cells and which may be more sensitive than ELISA.

In agreement with these results, several studies have shown that DC can present the epitope after Melan-A transfection. Using electroporation of in-vitro transcribed RNA, Melan-A transfected DC were able to induce Melan A 26-35 tetramer positive cells in autologous PBMCs (Abdel-Wahab et al., 2003

and Abdel-Wahab et al., 2005). Human moDC transfected with plasmid DNA encoding Melan-A using particle bombardment were also recognised by a 27-35 specific T-cell clone and were immunogenic in vitro (Tuting et al., 1998).

The 26-35 epitope has also been shown to be generated on DC expressing whole Melan-A after viral transduction – in terms of antigenicity (Butterfield et al., 1998) and immunogenicity (Kim et al., 1997). Viral transduction is, however, much more efficient than non-viral methods.

Residual expression of standard proteasomes could be responsible for the ability of these DCs to present the epitope. DCs generated from healthy donors in this institution, were found to express all 3 immunoproteasome subunits (Mecl-1, LMP2 and LMP7) prior to and after exposure to inflammatory cytokines. The presence of IFNγ in the culture medium did not influence the intensity of staining. The results are presented in Figure 6.1. Future experiments could attempt to quantify the relative proportion of proteasomes containing standard or inducible subunits.
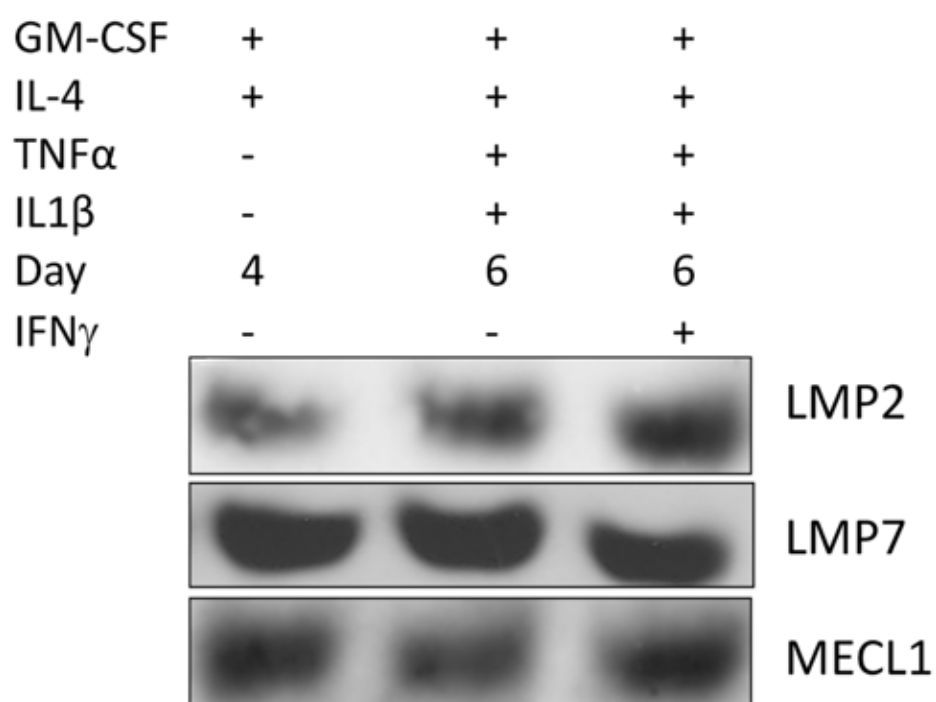
Figure 6.1. Expression of immuno-proteasome subunits in dendritic cells.
DC were generated from PBMC of a healthy laboratory donor as described in
'Methods'. Cells were cultured with IL4 and GM-CSF throughout, with the
addition of IL1β and TNFα from day 4 to day 6. On day 4, half of the DC were
exposed to IFNγ in addition to IL1β and TNFα. DC were harvested at day 4
and 6. Cell lysates were prepared and SDS-PAGE was carried out , followed
by Western blotting with anti LMP2, LMP7 and Mecl1 specific antibodies.
This experiment was carried out in collaboration with Miss S Berhane,
Institute for Cancer Studies, Birmingham University.

These results support the conclusion that DC expressing whole Melan-A antigen after RNA transfection do present the immunodominant A2 restricted epitope and this approach should remain under consideration for trials of DC vaccination in melanoma. These experiments could be extended to determine whether or not transfected DCs are able to expand a Melan A 26-35 specific T-cell population within PBMCs, as even normal laboratory donors are known to have responses to this epitope.

There is an obvious discrepancy between the ability of the 26-35 specific T-cell clone to recognise peptide-loaded and endogenously expressing target cells. As shown in Figure 3.16, this clone barely recognises A2 positive target cells loaded with native (EAA) peptide above background levels. However, in three separate experiments, DC expressing wild-type Melan-A were recognised above background. This could reflect the fundamental difference between loading of exogenous peptide onto the cell surface by occupation of empty HLA molecules or displacement of lower-affinity peptides compared to peptide editing and loading in MHC loading compartments intracellularly. The efficiency of binding of ELA peptide to A2 molecules is much higher than that of EAA (Rimoldi et al., 2001), thus, for EAA it may be the case that the 90 minutes for peptide-binding in vitro is

insufficient for formation of a significant number of peptide-MHC complexes whereas after endogenous production the longer time period for MHC loading (≈18-24 hours) compensates for this.

A Melan A 26-35 recombinant T-cell receptor was also used to guage epitope presentation. This approach has been successfully used to detect tumour antigens and HIV epitopes in cells physiologically expressing antigen and those overexpressing it after transfection (Varela-Rohena et al., 2008, Purbhoo et al., 2006, Purbhoo et al., 2007, Irvine et al., 2002).

Melan-A A27L RNA transfected DC were epitope positive by TCR analysis. There is a range of epitope positivity: the highest epitope density was 50 peptide-MHC complexes per cell and the average was 18 epitopes per cell (Figure 4.14).

Neethling et al (2008) showed that after endocytosis of mannose-receptor-tagged βHCG protein by moDCs, an A2 restricted epitope was presented between 24 and 72 hours

later. Epitope density was 60-300 epitopes per cell using TCR mimetic antibodies.

Using soluble T-cell receptors, it was demonstrated that an HLA-A2 positive bladder carcinoma cell line, transfected with a minigene construct encoding the epitope fused with ubiquitin, displayed approximately 13,000 epitopes per cell (Purbhoo et al., 2006). This is unsurprising as antigen is pre-processed and delivered peptide directly into the Class I pathway.

The level of epitope presentation on melanoma cell lines was far lower -25-45 epitopes per cell. In common with the results presented here, there was a great degree of variability from cell to cell in terms of epitope counts. Similar epitope densities were demonstrated on CD138 positive myeloma cells freshly isolated from bone marrow samples.

Although technological advances such as recombinant soluble T-cell receptors allow increasingly precise quantification of epitope numbers, it remains difficult to be certain about

the physiological relevance or importance of these densities.

T-cells are exquisitely sensitive to the presence of extremely low numbers of peptide-MHC complexes on the target cell surface (Irvine et al, 2002). Earlier studies in this area had suggested thresholds for recognition by CD4 cells of 50-200 peptides and 10-50 peptides for CD8 cells. These studies were, however, limited in that it is uncertain what proportion of the antigen-presenting-cell surface is available for interaction with T-cells and also loading of bulk populations of APCs probably leads to variability in the amount of peptide loaded onto each cell. In TCR transgenic mice, the presence of even a single cognate peptide-MHC complex on the APC surface was sufficient to generate a transient calcium influx suggestive of T-cell activation. More than 10 peptide MHC complexes per cell were able to produce sustained calcium influx, T-cell and APC stabilisation and formation of an 'immunological synapse' with mobilisation of ICAM-1. In fact, there was a plateau in calcium influx after the peptide-MHC density exceeded 10-20 per APC. Using CD8 T cell responders, almost identical peptide density sensitivity was demonstrated (Purbhoo et al., 2004). This work also showed that signalling via the CD8 co-receptor is vital for maximal

sensitivity of antigen recognition and that in terms of cytolytic activity, as few as 3 p-MHC complexes are sufficient to sensitise the target cell to killing.

In the work discussed above, effector memory T cells are being studied, and the relationship between epitope density and T-cell activation in naive cells interacting with antigen-presenting cells is not explored. Additional, this work is in a transgenic murine system with ectopically expressed recombinant TCR molecules.

Several other factors, aside from peptide-MHC density, need to be considered in terms of the ability of APCs to form stable and immune-stimulatory interactions with cognate T-cells. Although peptide-density is important, the affinity of the p-MHC:T-cell receptor interaction is highly relevant. In the presence of an optimal off-rate for the p-MHC-TCR interaction, low-peptide density is not disadvantageous (Vallitutti and Lanzavecchia, 1997). Other important factors are the ability of the T-cell to move and survey the APC surface and the stability of the immunological synapse. The presence of costimulatory molecules and bystander cells are also important.

The relationship between p-MHC density and T-cell responses is not linear. In a murine model using the gp100 antigen and mice transgenic for AAD, a chimeric MHC Class I molecule, it was demonstrated that bone-marrow derived dendritic cells loaded with 0.1-1µg/ml tyrosinase 369-377 peptide were significantly better inducers of try369 specific CD8 T-cells than DCs pulsed with higher concentrations of peptide (Bullock et al., 2000). A similar effect was observed for the gp100 280-288 epitope.

Again using transgenic mice, the magnitude of the primary immune response to tyrosinase 369 immunisation was related in a linear fashion to the quantity of peptide pulsed onto immunising DC. However, the functional and structural avidity of Tyrosinase 369 specific T-cells in recall responses was lower when higher concentrations of immunising peptide had been used. This inverse correlation between immunising peptide density and avidity of recall responses may relate to preferential selection of cells bearing higher avidity/affinity T-cell receptors (Bullock et al., 2003).

6.2. Melan-A transfected DCs are whole antigen negative but epitope positive 24 hours after RNA transfection

Melan-A transfected DCs are able to present the A2-EAA/ELA epitope. However, at 24 hours after transfection when T-cell assays were performed there is no Melan-A specific staining with the A103 antibody. This is not due to failure of antibody staining, degradation of RNA or low transfectability.

In the recently completed clinical trial of DC vaccination in metastatic melanoma (Steele et al., 2011), Melan-A was detectable, albeit at low levels, in CL22 peptide tansfected DC – in contrast to the findings presented in this thesis.

In terms of DC preparation, clinical trial DC were transfected on day 4 of culture as were experimental DC, but patient DC were exposed to inflammatory cytokines for 48 rather than 24 hours. The transfection method was different – RNA electroporation versus CL22 peptide-based DNA transfection and, of course, experimental DC were derived from healthy lab donors rather than metastatic cancer

patients. Also, in the trial, plasmid DNA encoded both Melan-A and gp100 rather than either antigen individually.

There could be several reasons behind the difference in Melan-A detection. In vitro transcribed RNA has a far shorter half-life than plasmid DNA and plasmid DNA is transcribed in-vivo and physiologically polyadenylated whereas in-vitro transcribed RNA was artificially polyadenylated using a yeast enzyme. RNA stability is partially governed by the length of Poly (A) tails. Although the integrity of RNA was assessed by gel electrophoresis and staining with ethidium bromide, there was no discernable difference in electrophoretic mobility between RNA pre and post polyadenylation. It would be informative in future to determine precisely the length of Poly-A tails and compare this to these achievable in vivo. The co-expression of gp100 with Melan-A could be relevant as it is thought that the two proteins interact and form a complex with each other, at least in melanocyte lineage cells (Hoashi et al., 2005).

There have been several studies of DC expressing whole Melan-A after either nucleic acid transfection (Abdel-Wahab et al., 2003, Abdel-Wahab et al., 2005 and Tuting et al.,

1998), or viral (Kim et al., 1997, Butterfield et al., 1998 and Perez-Diez et al., 1998) transduction. Only one investigated the presence of whole antigen after transfection (Butterfield et al., 1998). 48 hours after adenoviral transduction, Melan-A RNA was detectable by RT-PCR and continued to be so for 196 hours. At the protein level, immunocytochemistry showed that 90% of transduced cells expressed Melan-A protein at 24 hours. No specific maturation stimulus was applied to these DC, in contrast to the work presented here. There is evidence that the nature of the maturation stimulus used can have a profound influence on the ability to detect expression of tumour-associated-antigens in transfected DCs (Schuurhuis et al., 2009). Dendritic cell maturation is associated with a decrease in lysosomal pH which leads to activation of proteases and hydrolases.

It was demonstrated that epithelial cells show positive Melan-A fluorescence after RNA transfection and EBV transformed B-cells also exhibited Melan-A positivity, albeit at low levels. This could possibly be explained by higher levels of lysosomal activity in maturing DCs compared to B-cells (intermediate) and epithelial cells (low). This hypothesis could be further investigated by determining whether or not the presence of TNFα and IL1β in DC culture

medium affected the presence of whole Melan-A antigen in transfected cells. It is also possible that Melan-A RNA might have a different half-life in different cell types, although this appears less likely as the cell type had less of an effect on the detection of GFP.

That whole Melan-A negative DCs presented the 26-35 epitope is entirely consistent with earlier results that demonstrated a likely modest inverse correlation with percentage of whole Melan-A positive DCs and recognition by the Melan-A 26-35 specific T-cell clone.

The relationship between antigen detection and epitope presentation is, however, antigen-dependent and not merely a DC specific function. EBNA1 transfected DC are both epitope and whole antigen positive at 24 hours after RNA transfection. EBNA1 is easily detectable even though the RNA used encodes GA repeat deleted EBNA1 that is relatively unstable.

These results raise two, not mutually exclusive possibilities. The first is that, as suggested by the DRiP hypothesis, the predominant substrates for proteasomal

processing and MHC Class I loading are misfolded or prematurely truncated translation products rather than mature, full length proteins. Thus, the ability to detect whole protein would be irrelevant to the ability to present immunogenic epitopes. The second possibility is that further destructive processing of full-length antigen is required in order to generate peptide-epitopes.

The relationship between whole antigen expression and presentation of MHC Class I restricted epitopes has been examined in melanoma cell lines (Michaeli et al., 2009). Cell lines with high levels of tyrosinase mRNA and protein had low surface A2 restricted epitope densities and vice versa. In general, epitope presentation was inversely related to the antigen's half-life in the cell.

Although this study examined melanoma cell lines as opposed to professional APCs and the cells naturally expressed the antigens, it is in agreement with the results presented here that whole Melan-A negative cells do present the epitope.

6.3. Melan-A transfected DCs are whole antigen positive at early time points and lysosomal function is involved in Melan-A degradation and Class I epitope generation after RNA transfection.

The diminuition of whole Melan-A positivity in RNA transfected DC with time could be explained by instability of the in vitro transcribed RNA or further intracellular processing of the antigen. The constant GFP levels with time and the effect of cell type suggest that further destructive processing of Melan-A may be responsible. Although the kinetics of Melan-A expression were not formally studied by protein synthesis inhibition and pulse-chase experiments, the rapid drop in antigen positivity between 4 and 8 hours would be compatible with the previously determined half life of Melan-A of approximately 4-5 hours in epithelial cells (Michaeli et al., 2009). It has been estimated as 3-4 hours in pigmented melanoma cell lines (SK23MEL) (De Maziere et al., 2002).

To determine whether intracellular protein degradation plays a role, DC were transfected with Melan-A RNA and immediately exposed to inhibitors of lysosomal acidification and proteasomal function in addition to the proinflammatory maturation stimulus. The effect of these inhibitors on

epitope presentation was also determined. In order to assess whether or not any observed effects were antigen specific or a feature of dendritic cell physiology, experiments were performed in parallel with EBNA1ΔGA where Class I processing and presentation are classically proteasome dependent.

In the presence of balifomycin, occasional cells were Melan-A positive and EBNA1 transfected DCs showed a slightly more intense staining, although only a single concentration of bafilomycin was used in this experiment and it had been chosen on the basis of experiments on lysosomal inhibition in LCLs (G.Taylor, personal communication). The reason for a very modest increase in antigen expression could have been an inadequate concentration of bafilomycin. In future, the optimal concentration for lysosome inhibition in DCs should be determined. This could be achieved by staining for LAMP1 in the presence of a range of bafilomycin concentrations. These data suggest that Melan A, and perhaps to a lesser extent EBNA1 are subject to lysosomal degradation within maturing DCs.

In contrast, the presence of epoxomycin had little effect on antigen detection. That proteasomal inhibition did not lead

to an increase in whole antigen detection is unsurprising as the substrates for proteasomes are generally thought to be DRiPs rather than full length antigen, and the antibodies used to detect whole antigen only bind to a specific epitope which may not be present in prematurely truncated or misfolded proteins. It was also noted that cells treated with epoxomycin exhibited abnormally shaped nuclei and the cell viability was lower in this group. This has been found to be the case in other published work (Naujokat et al., 2007) – where inhibition of $\beta5$ chymotrypsin-like proteasomal activity led to reductions in cell surface HLA and co-stimulatory molecules, increased apoptosis and decreased secretion of IL12p70 and IL12p40 cytokines.

In terms of epitope presentation, inhibition of proteasomal function led to abrogation of T-cell recognition by clones specific for the EBNA1409-419 and Melan A 26-35 epitopes, as expected. However, the results obtained do not totally exclude the possibility of non-specific effects particularly in view of the lower cell viability and the known effects of proteasome inhibition on HLA molecule expression. It remains possible that the lack of T-cell recognition of epoxomycin treated DCs could be due to poor viability and low MHC Class I surface expression rather than decreased peptide generation intracellularly. In future, this could

be addressed by loading epoxomycin-treated DCs with exogenous peptide to confirm that the cells were viable and surface HLA molecules were present.

However, treatment of transfected DCs with bafilomycin clearly attenuated the level of T-cell recognition of Melan-A transfected DCs by the 26-35 specific clone. In contrast, lysosomal inhibition of EBNA1ΔGA expressing DCs in fact slightly enhanced the level of EBNA1 409-419 presentation. This result suggests that lysosomal processing may be involved in the generation of an MHC Class I restricted epitope in the case of Melan-A but not EBNA1. The fact that lower levels of T-cell recognition are only seen with Melan-A and not EBNA1 strongly suggests that there is a degree of specificity and the effects are not due to off-target actions of bafilomycin. However, in future it would be prudent to attempt to load bafilomycin treated DCs with exogenous peptide as a positive control.

Presentation of the Melan A 26-35 epitope seems to depend upon lysosomal acidification as well as proteasomal function. This is a departure from the conventional doctrine that there is a segregation between lysosome

dependent Class II and proteasome dependent Class I presentation (Peters et al., 1991).

Melan-A is a melanosome associated protein in common with other melanoma antigens including gp100/PMEL17, tyrosinase and TRP1 and 2 (Kawakami, 1998). In pigmented melanoma cells, there was significant overlap between punctate structures that were positive for Melan-A and melanosomal markers although the majority of Melan-A staining was seen in a peri-nuclear location (De Maziere et al., 2002). Melan-A is enriched in early melanosomes but is also present in lysosomes.

There are two potential mechanisms by which Melan-A could come to be present in endolysosomes – it could naturally localise there due to melanosomal targeting sequences or the protein could be secreted and then re-internalised. Once in the MHC Class II loading compartments, cross presentation could occur.

This would not be without precedent, as it is known that some melanosomal proteins naturally localise to

endolysosomes in non-melanocyte lineage cells. In the case of gp100/PMEL17 (Lepage and Lapointe, 2006), there was evidence of LAMP-1 and gp100 co-localisation in transfected human epithelial cells and melanoma cells. It was also demonstrated that deletion of the last 70 amino acids or the internal transmembrane domain of the protein led to loss of MHC Class II presentation in the face of maintained Class I presentation. These mutants showed no vesicular localisation and no LAMP-1 co-localisation. Finally, it was demonstrated that addition of these sequences to GFP led to an endolysosomal localisation of GFP.

In terms of EBV viral antigens, there is accumulating evidence that redirection of the EBNA1 antigen into endolysosomal compartments by fusion with LAMP1 (Taylor et al., 2006) or the invariant chain has no deleterious effect on the presentation of MHC Class I restricted epitopes, indeed this is often seen to be enhanced. This supports the concept that MHC Class I binding peptides can be sourced that the endolysosomal compartment.

For gp100, however, Class I presentation in melanoma cells, epithelial cells or B-cells was not inhibited by chloroquine (Lepage and Lapointe, 2006). Chloroquine inhibits lysosomal

acidification in similar way to bafilomycin but dendritic cells were not studied.

It has also been demonstrated that the melanosomal protein gp100 localises to conventional endosomes in non-pigmented melanoma cell lines (Robila et al., 2008).

6.4. Presentation of the Melan A 26-35 epitope is delayed in transfected DC compared to the EBNA1 409-419 epitope.

The rationale for this set of experiments was the fact that Melan-A is detectable from 2 to 8 hours post transfection and that experiments using patient DCs suggest an inverse correlation between antigenicity and whole antigen detection. The aim was to determine whether or not Melan-A positive cells did, in fact, present the 26-35 epitope.

It was demonstrated that the level of recognition of Melan-A A27L transfected DCs by the Melan-A 26-35 specific clone was much lower at 3-4 hours as compared to 24 hours. As expected, Melan-A positive DCs were only seen at the earlier time point. This conclusion remained unchanged even after variations in maximal responsiveness of the T-cell clone were taken into account and T-cell recognition was calculated as percentages of maximal responses. Thus there is a delay between whole antigen detection and generation of surface epitopes. The minor differences in HLA expression at 4 and 24 hours are probably insufficient to explain the differences in T-cell recognition.

In understanding this result, one must consider dendritic cell aggresome related structures (DALIS) (Lelouard et al., 2002). These structures form approximately 4 hours after a maturation stimulus (such as lipopolysaccharide (Watts et al., 2007)) is applied to DCs, and typically have disaggregated by 24-36 hours. They contain newly synthesised proteins and polyubiquitination occurs in the DALIS; which likely function as a depot for antigenic substrates (Lelouard et al., 2004). These structures delay Class I mediated antigen presentation in DCs, so that epitope density is maximal at the time with interactions with T-cells are likely to be occurring. Delayed epitope presentation to cytotoxic T-cells, by approximately 10 hours has been observed in dendritic cells infected with influenza virus – in contrast no such delay was noted in lymphoma or epithelial cell lines (Herter et al., 2005).

However, EBNA1 transfected DC were whole-antigen positive at both 3 and 24 hours after transfection and there was no difference in epitope presentation at the two time points. Thus, delayed epitope presentation and dissociation of antigen detection and epitope generation are only seen in the case of Melan-A and not EBNA1ΔGA. However, EBNA1ΔGA is translated rapidly and is rapidly degraded by the proteasome (Tellam et al., 2007) and could be described as having a

317

natural affinity for the proteasome. It is therefore possible that the production of high levels of defective ribosomal products exceeds the storage capacity of DALIS and leads to early epitope presentation being detectable. Future experiments should extend these observations by including a range of other tumour antigens that do not have a natural affinity for endolysosomes or proteasomes – full length EBNA1 for example.

In view of the modest inverse correlation between Melan-A 26-35 epitope presentation and whole antigen detection in clinical DC preparations, the slight increase in whole antigen detection on exposure of transfected DCs to bafilomycin, and the dependence of 26-35 epitope generation on lysosomal acifidication, it is reasonable to propose that initially Melan-A localises in endolysosomal compartments and antigen processing occurs here prior to transport to the cytosol and subsequent proteasomal processing and MHC Class I loading. This 'two compartment sequential' processing takes longer than direct proteasomal processing (i.e. in the case of EBNA1ΔGA). There is an obvious precedent for this as DC are known to be able to cross present exogenously acquired antigen via the Class I pathway.

This model would predict that endogenous Melan-A should be presented via the Class II pathway, and in the next section evidence suggestive of this is presented.

There is a close relationship between endolysosomes and melanosomes. Melanosomes are considered to be specialised endolysosomes and both organelles have a common biogenetic origin (Orlow, 1995). These melanin-rich organelles are, in the murine setting, found to be enriched in lysosomal hydrolases including cathepsin B and L (Diment et al., 1995). LAMP-1 is also expressed in melanosomes (Zhou et al., 1993) Acid phosphatise is expressed in lysosomes and also in melanosomes (Seiji and Kukuchi, 1969).

There is also clinico-pathological evidence for a shared origin of the two organelles. These are the 'melano-lysosomal' syndromes. In Chediak-Higashi syndrome (Barton et al., 2004), there are also a host of other associated features, many of which can be attributed to abnormal lysosomal function in cells such as platelets, neutrophils and lymphocytes – such as hepatosplenomegaly, lymphadenopathy, bleeding tendency and immunodeficiency.

This condition is inherited in an autosomal recessive fashion, and the fact that a single genetic mutation gives rise to functional deficits in melanosomal and lysosomal function provides further support for the concept that the two organelles are intimately related (Novak and Swank, 1979).

Furthermore, there is a shared acidic pH in the two organelle compartments. Estimated melanosomal pH is 3-5 (Bhatnagar et al., 1993).

6.5. gp100/PMEL17 is not seen 24 hours after transfection of DCs with gp100 RNA although such DCs are positive for the gp100 $_{280-288}$ epitope.

As for Melan-A, at 24 hours after RNA transfection, there is evidence of the gp100 $_{280-288}$ epitope being displayed despite the cells being negative for whole gp100. SK23 melanoma cells, known to be gp100 positive, were strongly stained by the HMB45 antibody in parallel experiments, GFP positivity of control DCs was over 90% and HEK293 cells transfected with the same batch of gp100 RNA were also strongly gp100 positive. It should be noted that the control group in the YLE epitope display assay was DC transfected in the absence of RNA; the ideal control would have been DC transfected with RNA encoding an irrelevant antigen such as GFP or Melan-A.

In contrast to these results, other clinical and preclinical studies have demonstrated that gp100 is detectable after whole antigen transfection.

Prabakaran et al (2007) showed 20% gp100 positivity using the HMB50 antibody in virally transduced DC, although the proportion of gp100 positive cells was far smaller than the stable marker protein B-galatosidase. This is in keeping

with the results presented here. However, the antibody used recognised a different epitope within gp100 (HMB50 versus HMB45), gp100 expression was achieved by viral transduction rather than RNA electroporation and the DCs used were generated with IL12 and IL2 rather than IL4 in conjunction with GM-CSF.

Schuurhuis et al (2009) found gp100 positive DC by immunocytochemistry using HMB45 in dissected lymph nodes following intralymphatic injection in melanoma, approximately 24 hours after RNA transfection. It is unclear what proportion of total DCs was gp100 positive however. This group also demonstrated that human moDC electroporated with gp100 encoding RNA were gp100 positive as soon as 30 minutes after electroporation. These cells were electroporated with gp100 RNA in the mature state and maximal gp100 expression occurred 2-4 hours after transfection, but gp100 positive cells remained detectable 72 hours after transfection. However, cells were fully matured before transfection and this could, conceivably, lead to differences in antigen handling.

Even at earlier time points after transfection, only a very small proportion of DCs show detectable gp100 fluorescence

after antibody staining. Positive cells are seen from 4 to 8 hours after transfection. There is minimal background (non-specific staining) with an isotype control antibody and very little staining of gp100 negative cells with the gp100 antibody, alongside strong gp100 staining in the SK23 melanoma cell line. Approximately 1/50 to 1/100 cells are gp100 positive by immunocytochemistry.

These results are quite different to previously published results and those seen in the clinical trial (Steele et al., 2011).

The intracellular processing and maturation of gp100/PMEL17 is complex, and it has only been studied in the context of melanocyte-lineage. There are 5 potential N-glycosylation sites and active intracellular processing of the protein by enzymes including endoglycosidases, proprotein convertases, metalloproteinases and γ-secretases produces a variety of smaller protein fragments. This is summarised in Figure 7.2.

Additionally PMEL17 is extensively alternatively spliced and four different splice variants can be produced depending on which exons are included in the transcript (Adema et al., 1994).
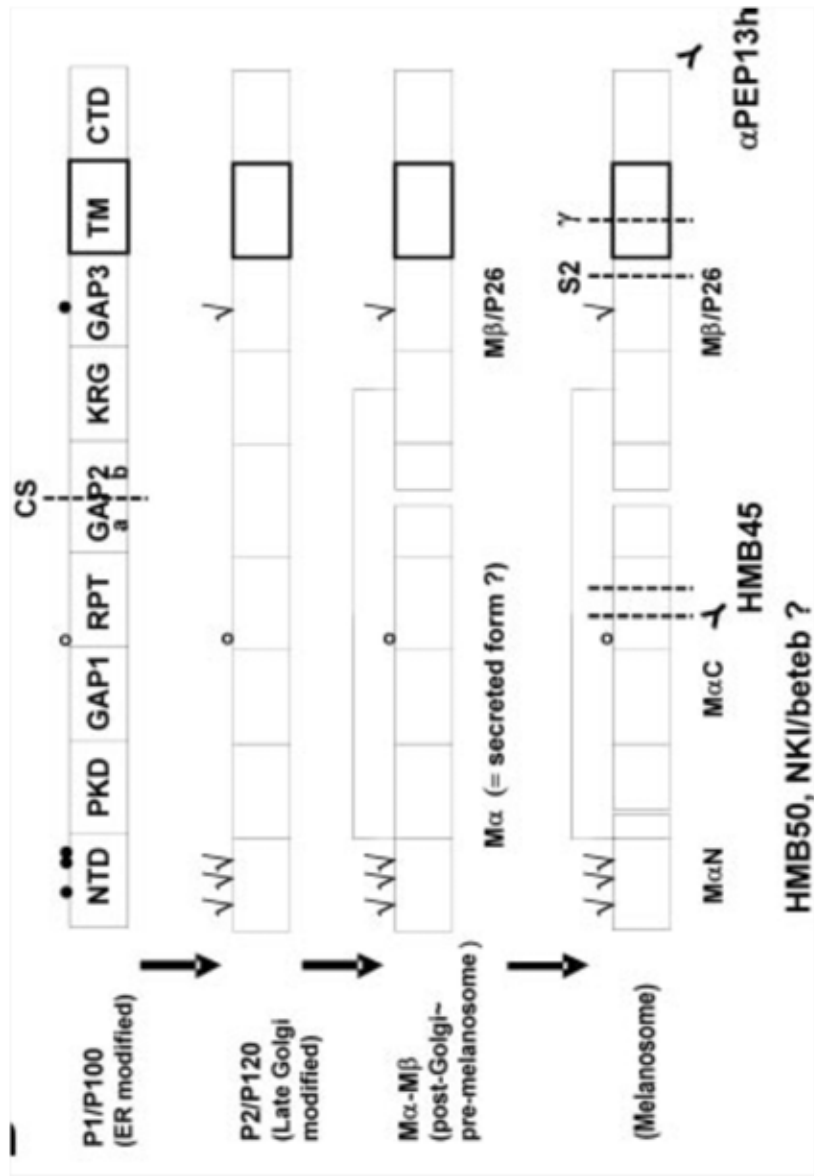
Figure 6.2. Intracellular processing of gp100. This schematic represents the intracellular processing and handling of gp100 protein and shows the four isoform variants known to exist in vivo. The putative locations of the isoforms are shown as are the epitopes to which several monoclonal antibodies bind. Reproduced from Hoashi et al. (2005).

The gp100 protein appears to play an essential structural role in more mature melanosomes and it forms a scaffold upon which melanin deposit can begin (Berson et al., 2001). Formation of fibrillar structures within early Stage 2 melanosomes is dependent on normal gp100 function (Hoashi et al., 2005).

There are several different monoclonal antibodies that recognise gp100 – illustrated in Figure 7.2. However, each one has unique epitope specificity. Thus, not all breakdown products of gp100 will react with all of the antibodies (de Vries et al., 2001). HMB45, the antibody used for gp100 detection in this work and in the DC vaccine clinical trial, reacts with a sialyated epitope in the RPT domain of the protein (Hoashi et al. 2006). It reacts with the form of gp100 found in Stage 2 melanosomes. In this vein, WM266-4 melanoma cells were found, by immunoblotting, to be gp100 non-reactive using the HMB45 antibody but positive using αPEP13h (Hoashi et al., 2005).

There is also evidence that gp100 can be secreted from cells, and indeed a small proportion of total gp100 is found at the cell surface (Berson et al., 2001 and Maresh et al., 1994). It is possible that increased activity of the

secretory pathway could lead to active secretion of gp100 from DCs, and this could explain why very few cells stain positive for the protein. This could be further investigated in future experiments by collecting DC supernatants and performing immunoblotting.

It is possible that in RNA transfected dendritic cells, active intracellular processing leads to the production of breakdown products of gp100 that are not recognised by HMB45 – either because the epitope is cleaved or because sialyation does not occur normally (Kapur et al., 1992). The fact that DCs expressing gp100 from plasmid DNA after CL22 transfection does require explanation, however.

There are two possible reasons. First, there are fundamental differences between the two transfection processes – use of electrical impulses, exposure of cells to chloroquine, and crucially differences in the nucleic acid used. It is not inconceivable that the activation/maturation programme in DCs exposed to plasmid DNA could be very different to that occurring in those electroporated with RNA. There is some evidence of this in published work. For example, NOD2 stimulation by bacterial muramyldipeptides induces autophagy in maturing DCs (Cooney

et al., 2009). This could lead to alterations in gp100 processing. The second key difference is that in the work presented here, single-species gp100 encoding RNA was transfected into the DCs rather than the plasmid encoding both Melan-A and gp100 in the clinical trial. An interaction between gp100 and Melan-A has been suggested (Hoashi et al., 2005). In the absence of Melan-A, the stability of PMEL17 is reduced. There was, in melanocytic cells, complex formation between the two proteins. Complexes also formed in non-melanocytic cells transiently transfected with gp100 and Melan-A DNA. Critically, in normal melanocytes and a melanoma line (SK28MEL), Melan-A knockdown with small interfering RNA leads to a reduction in gp100 reactivity using HMB45. In fact, attenuation of HMB45 reactive gp100 is sensitive to even slight downregulation of Melan-A function. In the clinical trial, co-expression of both antigens could have led to stabilisation, and subsequent detection, of gp100. In pre-trial experiments, transfection of plasmid DNA encoding only gp100 into HEK293 cells led to detectable gp100 levels at 48 hours, however this was not formally demonstrated in dendritic cells (Jane Steele, personal communication). Future experiments should co-transfect Melan-A and gp100 RNA into DCs and determine whether this increases the proportion of gp100 positive DCs.

In future, it would be important to utilise the full range of gp100 specific antibodies in view of the complexity of intracellular processing of the protein in order to ascertain whether or not the vast majority of transfected DCs are genuinely gp100 negative or merely express forms of the protein that are not recognised by the HMB45 antibody.

Further experimental work is required in order to elucidate the significance of the vast majority (≈98-99%) of gp100 whole antigen negative cells within RNA transfected DC populations. In the re-directed T-cell ELISPOT assay, using the gp100 280-288 specific T-cell receptor fusion protein, there is a ten-fold excess of target DCs over effector T-cells. Thus, in each well of the ELISPOT assay, there should be approximately 100 whole antigen positive cells. Although there is evidence of epitope presentation, these data do not discriminate between direct presentation by the ≈100 antigen positive cells or indirect presentation by the majority antigen negative DCs. In future, this should be investigated by using a range of input DC numbers/well in the ELISPOT assay. If epitope presentation remained detectable when fewer than 100 DCs were used per well, then the whole antigen negative cells must be epitope positive.

Finally, the fact that gp100 can, under certain circumstances, be a cell-surface or secreted protein means that it would be important, in future, to determine whether or not antigen transfer plays a role.

7. Presentation of MHC Class II restricted epitopes by RNA transfected clinical-grade dendritic cells.

7.1. Aims.

The aim of this set of experiments were to determine whether presentation of MHC Class II restricted peptide epitopes from endogenous antigen, in RNA transfected DCs, depends upon the nature and cellular localisation of the antigens. The antigens studied were EBNA1 and Melan-A.

7.2: Presentation of MHC Class II restricted epitopes from endogenous Melan-A in RNA transfected DCs.

7.2.1. Generation of Melan A specific CD4 T-cell clones.

Attempts to generate these T-cell clones focussed on a laboratory donor who had a detectable Melan-A IgG response in plasma, on the basis that this IgG response would have required a CD4 helper T-cell response.

The initial aim was to determine whether or not there were Melan-A specific T-cells, in particular CD4 cells, within the PBMCs of this donor. In order to maximise the likelihood of detection of CD4 helper T cell responses, the antigenic stimulus used was exogenously delivered whole

(recombinant) Melan-A protein. As shown in Figure 7.1, there is evidence of cells secreting IFNγ in response to Melan-A protein at a frequency of approximately 0.025% in overnight ELISPOT assays. There was no dose-response relationship. In order to assess the relative contribution of CD4 and CD8 T-cells to the observed response, whole PBMCs were depleted of CD8 positive cells using magnetic beads before analysis. The number of cells secreting IFNγ in response to Melan-A protein was greater in the CD8 depleted group (Figure 7.2). This suggests that CD4 T cells may make a large contribution towards the observed responses.

Similar assays were performed, using a range of Melan-A protein concentrations, assessing cellular proliferation rather than cytokine release. In 7 day cellular proliferation assays, it was shown that there was an impressive increase in proliferation with exogenous Melan-A protein as compared to in its absence. The proliferative response approached that of the non-specific mitogen PHA, although it is noted that the peak effect of PHA probably occurs before the time of the proliferation assay. There was, again, no dose-response relationship within the protein concentrations tested. These data are shown in Figure 7.3.
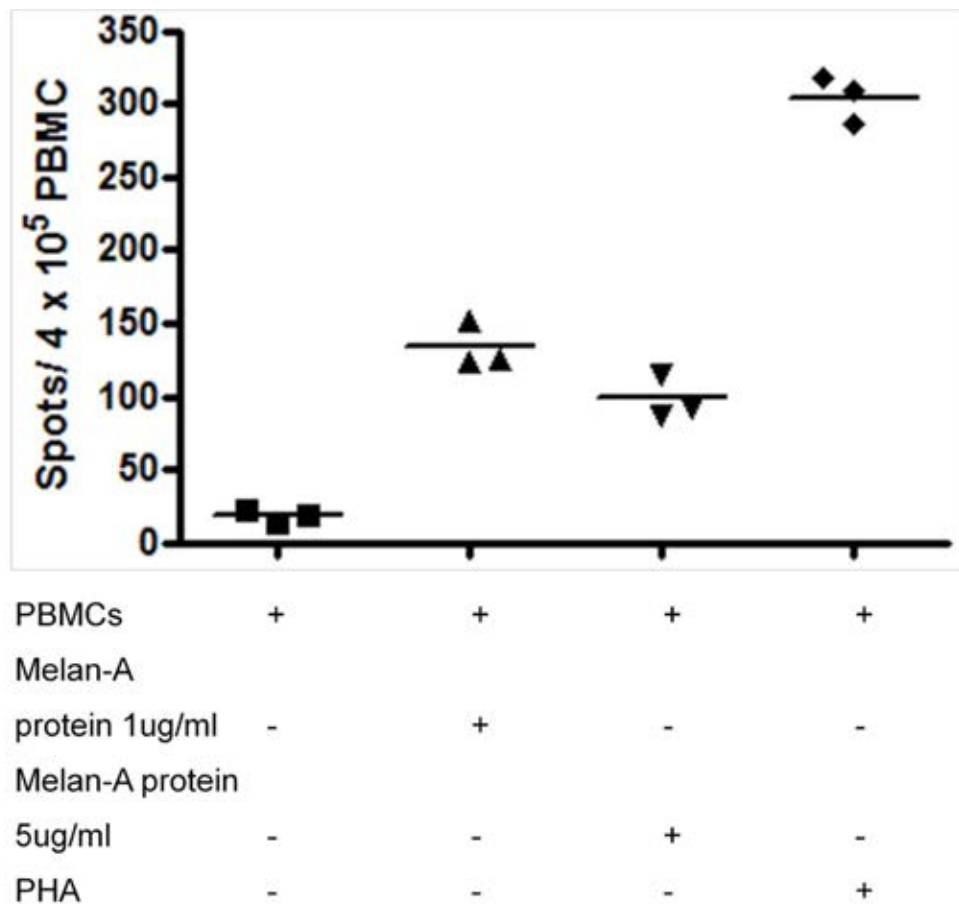
Figure 7.1. **Demonstration of IFNγ response to exogenous Melan-A protein in lab donor PBMCs**. PBMCs were freshly prepared from venous blood. 4×10^5 PBMC were incubated per well in triplicate overnight (I6h) IFNγ ELISPOT assays. Melan A was added at final concentrations of 1 and 5 μg/ml or not at all. As a positive control for functionality of PBMCs, phytohaemagglutinin (PHA) was also added at a final concentration of 1ug/ml. Results are presented as individual spot counts and mean values (horizontal bars).
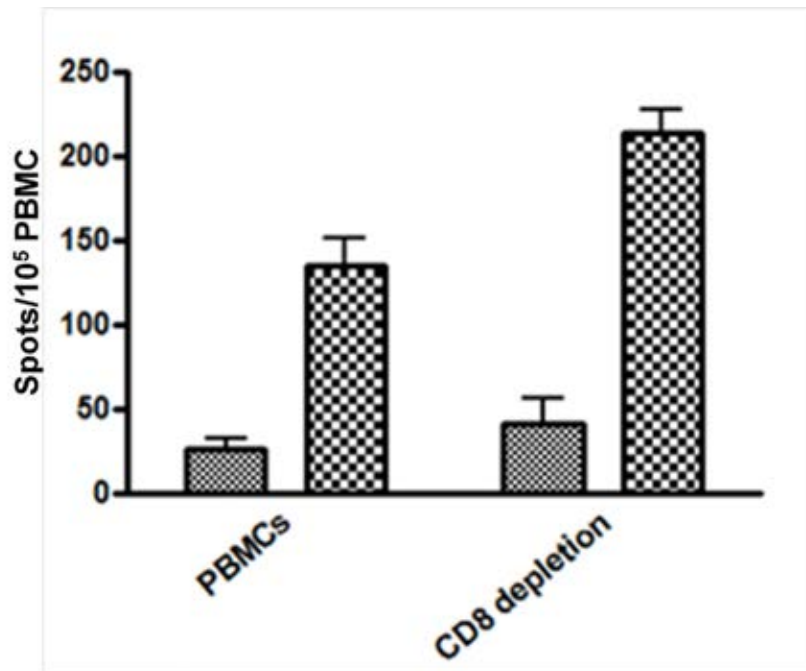
Figure 7.2. **Effect of depletion of CD8 T cells on IFN gamma responses to exogenous Melan-A protein.** PBMCs were isolated from whole blood of a laboratory donor previously demonstrated to have an IFNγ response to Melan-A protein. Cells were then co-incubated with anti CD8 conjugated magnetic beads in serum free conditions at 4°C for 30 minutes. Bead-labelled cells were separated using a magnet and discarded. The resulting cell population was used in overnight IFNγ ELISPOT assays in the presence and absence of exogenous Melan-A protein at 1μg/ml final concentration. Results are presented as mean and range of spot counts/well. ▨ Melan-A protein, ▨ no Melan-A protein.

PBMCs	+	+	+	+	+
Melan A					
Protein					
0.5μg/ml	-	+	-	-	-
1μg/ml	-	-	+	-	-
2.5μg/ml	-	-	-	+	-
PHA	-	-	-	-	+
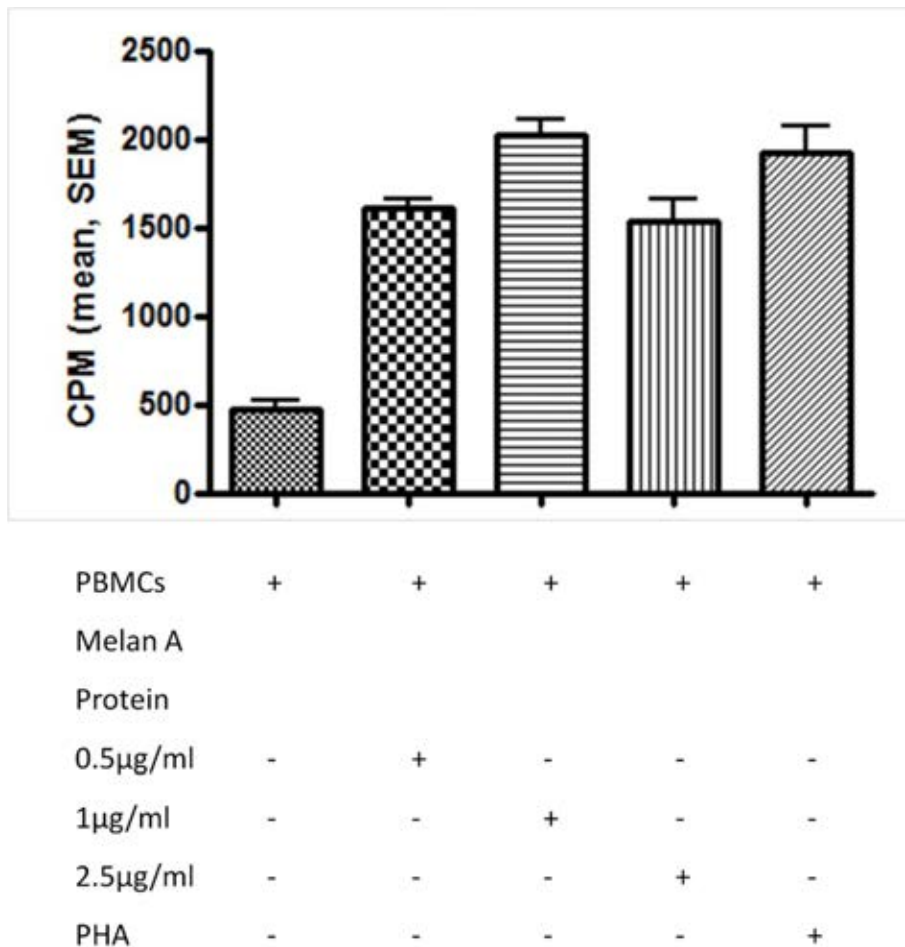
Figure 7.3. **Demonstration of proliferative response to exogenous Melan-A protein in lab donor PBMCs.** 1.5×10^5 freshly isolated PBMCs from a healthy laboratory donor were incubated in quadruplicate proliferation assays. Exogenous Melan-A protein was added to cells at the indicated final concentrations (0.5, 1, 2.5 μg/ml). Phytohaemagglutinin was added at a final concentration of 1ug/ml as a positive control for proliferative capacity of PBMCs. Assays were assembled and on day 7, 1μCi of 3H methyl-thymidine was added to each well. After a further 16 hours cell culture, cells were harvested. Incorporated radioactivity was measured on a liquid scintillation counter. Results are presented as counts per minute (mean +- standard error of mean).

On the basis of these results, an attempt to generate Melan-A specific T-cells of a CD4 phenotype was made. Initially, polyclonal cultures were generated from PBMC. At first, the antigenic stimulus was exogenous Melan-A protein alone, and after one week, a further stimulation with autologous dendritic cells loaded with exogenous Melan-A protein was performed. T-cell cloning was performed as described in Methods. Five micro cultures were obtained that proliferated in the presence of Melan-A. Of these, 2 had been cloned at 0.3 cells/well and 3 at 3 cells per well.

7.2.2. Characterisation of Melan A specific T-cell clones.

The ability of these 'clones' to proliferate in response to antigenic stimulation with whole Melan-A protein was determined in 4 day ^{3}H thymidine proliferation assays. T-cells were cultured with autologous irradiated PBMCs in the presence or absence of Melan-A protein, and ^{3}H thymidine incorporation was measured between 72 and 88 hours. As shown in Figure 7.4, there were strong proliferative responses to Melan-A protein with proliferation indices ranging from 4-8. The ability of one of these clones, the one exhibiting maximal growth, to secrete IFNγ in response to exogenously added Melan-A protein is shown in Figure 7.5. The possible MHC restriction of the clone was also examined
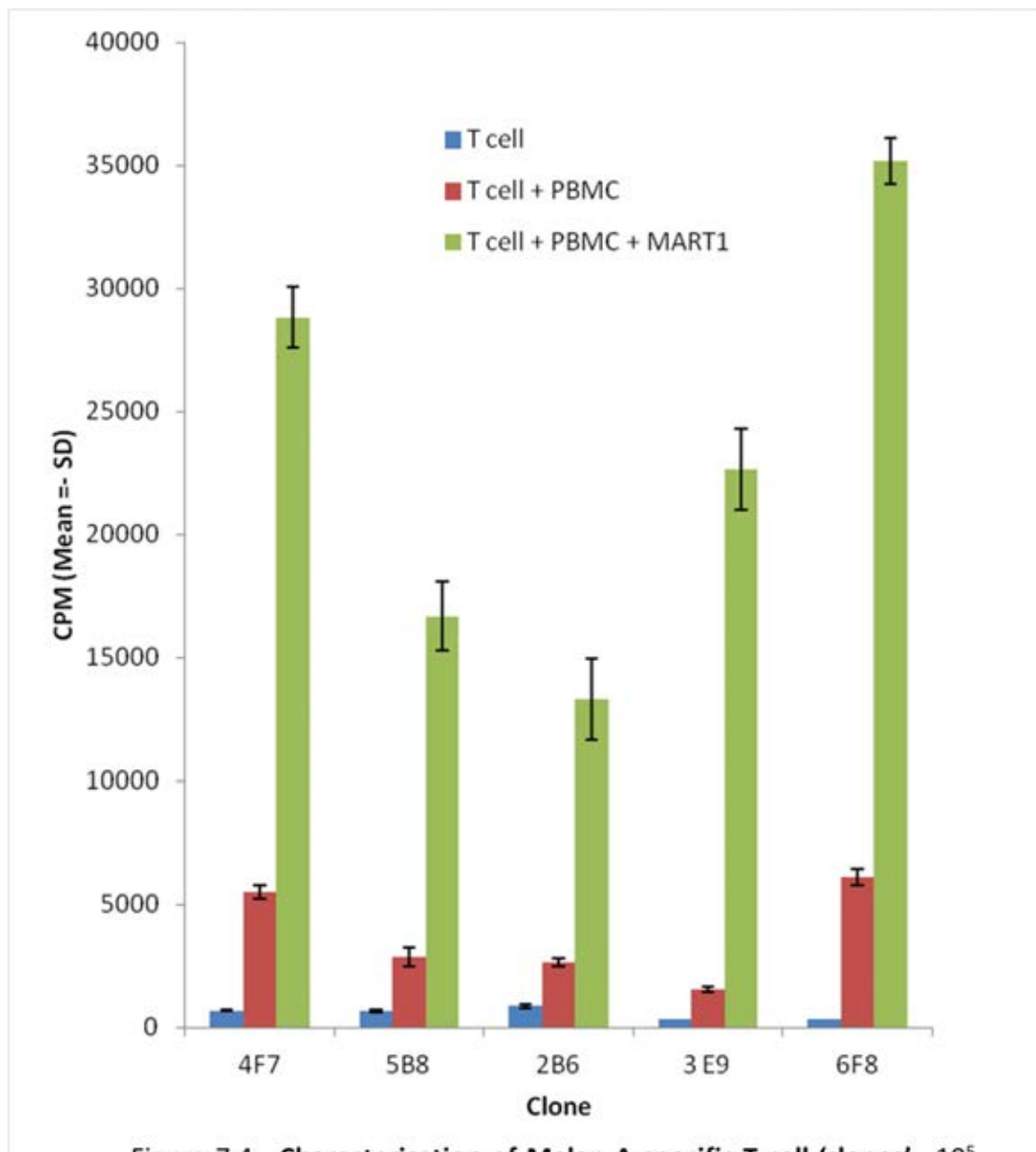
Figure 7.4. **Characterisation of Melan A specific T-cell 'clones'.** 10^5 T-cells were coincubated with autologous irradiated (6000R) PBMC in the presence or absence of exogenous Melan-A protein at a final concentration of 5µg/ml. Assays were set up in quadruplicate and after 48 hours , 1µCi ^{3}H methyl-thymidine was added to each well. After 16 hours, incorporated radioactivity was measured after cell harvesting and liquid scintillation counting. Results are presented as counts per minute (mean +- standard error of mean). Blue bars – T-cells alone, right bars, T-cells and irradiated PBMCs, green bars – T cells, irradiated PBMCs and Melan-A (MART1) protein at 5ug/ml.

T cells	+	+	+	+	+	+
PBMCs	-	+	+	+	+	+
Melan A Protein	-	-	+	+	+	+
Anti MHC-I	-	-	-	+	-	-
Anti DQ	-	-	-	-	+	-
Anti DR	-	-	-	-	-	+
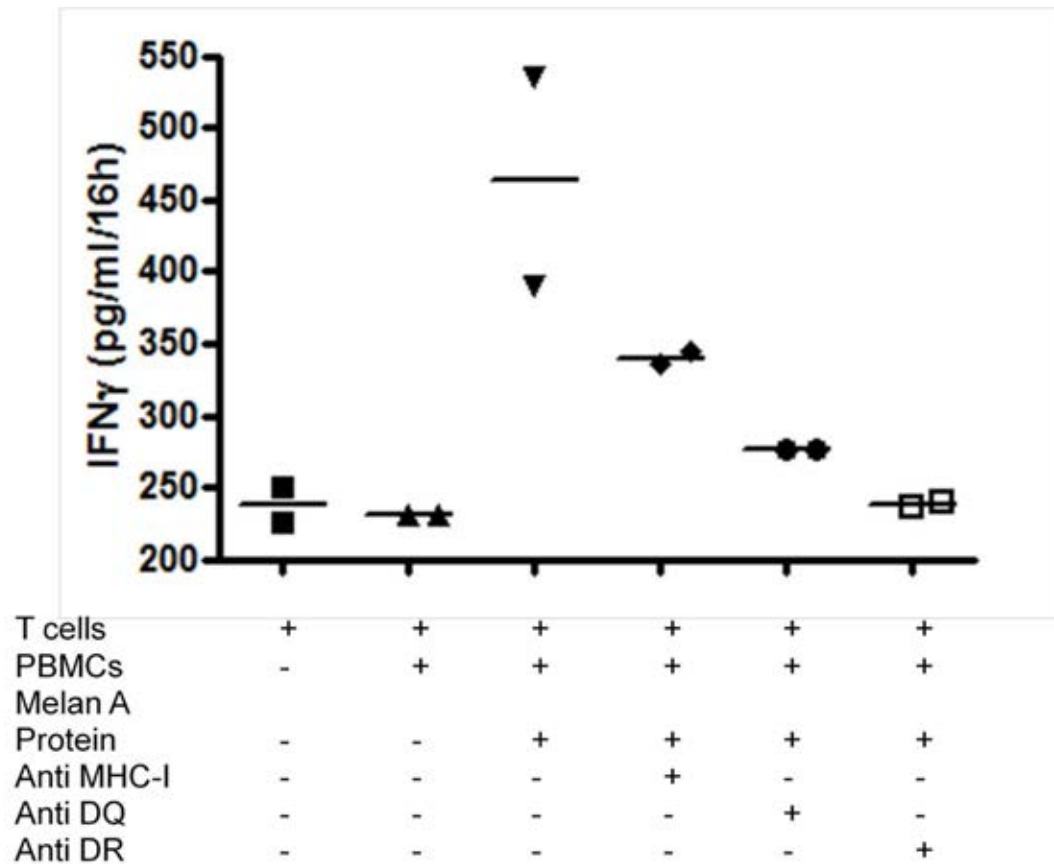
Figure 7.5. **MHC Restriction of Melan A specific clone 5B8.** T-cells (10^4/well) were coincubated with autologous irradiated PBMCs (2×10^3) in the presence or absence of recombinant Melan-A protein in duplicate overnight. After 16 hours, 50ul of supernantant was removed and assayed for IFNγ concentration in ELISA assays. A standard curve was generated in parallel using recombinant human IFNγ. In addition, MHC blocking antibodies were added to target cells 30 minutes before addition of T cell effectors: anti MHC Class I, anti DQ and anti DR. Results are presented as duplicates and mean values (horizontal bars).

using blocking antibodies raised against MHC Class I, HLA DR and HLA DQ. There was evidence of low-level IFNγ secretion in response to Melan-A, and the anti MHC-I antibody has less of an inhibitory effect than the HLA DQ and HLA DR antibodies. This suggests MHC Class II restriction.

The phenotype of these T-cell populations was also determined by surface antibody staining and as expected, all clones showed a CD8 negative and CD4 positive phenotype. Antibody staining on one T-cell clone (5B8) is shown in Figure 7.6.

7.2.3. Recognition by Melan A specific CD4 T-cell clone of transfected and protein-loaded DCs.

The aim of these experiments was to determine whether or not DC endogenously expressing Melan-A after RNA transfection are able to present MHC Class II restricted epitopes from the antigen. In order to achieve this, the ability of Melan-A specific CD4 T-cell clones to recognise DCs transfected with Melan-A RNA in IFNγ ELISPOT and proliferation assays was determined. The positive control was DCs loaded with exogenous Melan-A protein.
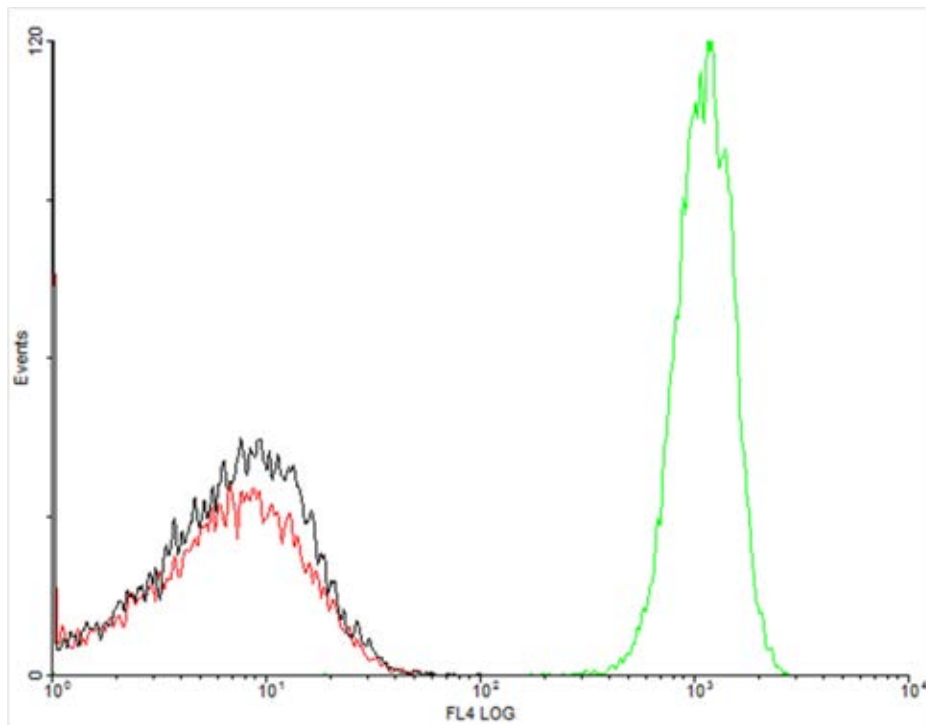
Figure 7.6. **Immunophenotype of Melan A specific clone 5B8**. Clone 5B8 was stained with a mouse monoclonal anti CD4 (green line), anti CD8 (red line) and matched isotype control antibody (black line). All antibodies were tricolour conjugated. After extensive washing, TC fluorescence was analysed by flow cytometry on the FL4 channel. At least 10,000 gated events (lymphocytes) were collected each time.

As shown in Figure 7.7, both in terms of IFNγ secretion and cellular proliferation, there was recognition of DC loaded with exogenous Melan-A protein above background (DC not loaded with protein). In terms of cytokine release, there was a relatively low level of cytokine production ($\approx$100 pg/ml/24 hours), whereas there was an eight-fold increase in thymidine incorporation when DCs loaded with Melan-A protein were used as targets compared to cells not loaded with protein. This would be expected, as delivery of the antigen as exogenously protein requiring internalisation by DCs should lead to endolysosomal processing and Class II restricted epitope presentation.

Experiments moved forward to determine whether a similar recognition by this CD4 T-cell clone occurred when the dendritic cells had been transfected with Melan-A RNA and expressed the antigen endogenously. Unfortunately, at the time this experiment was performed recombinant Melan-A protein was no longer commercially available to act as a positive control. However, dendritic cells were derived from the same donor as all experiments were performed within the autologous system. In addition, the same T-cell clone was used (5B8).

T-cells (5B8)	+	-	+	+
Autologous DCs	-	+	+	+
Melan-A protein	-	-	-	+
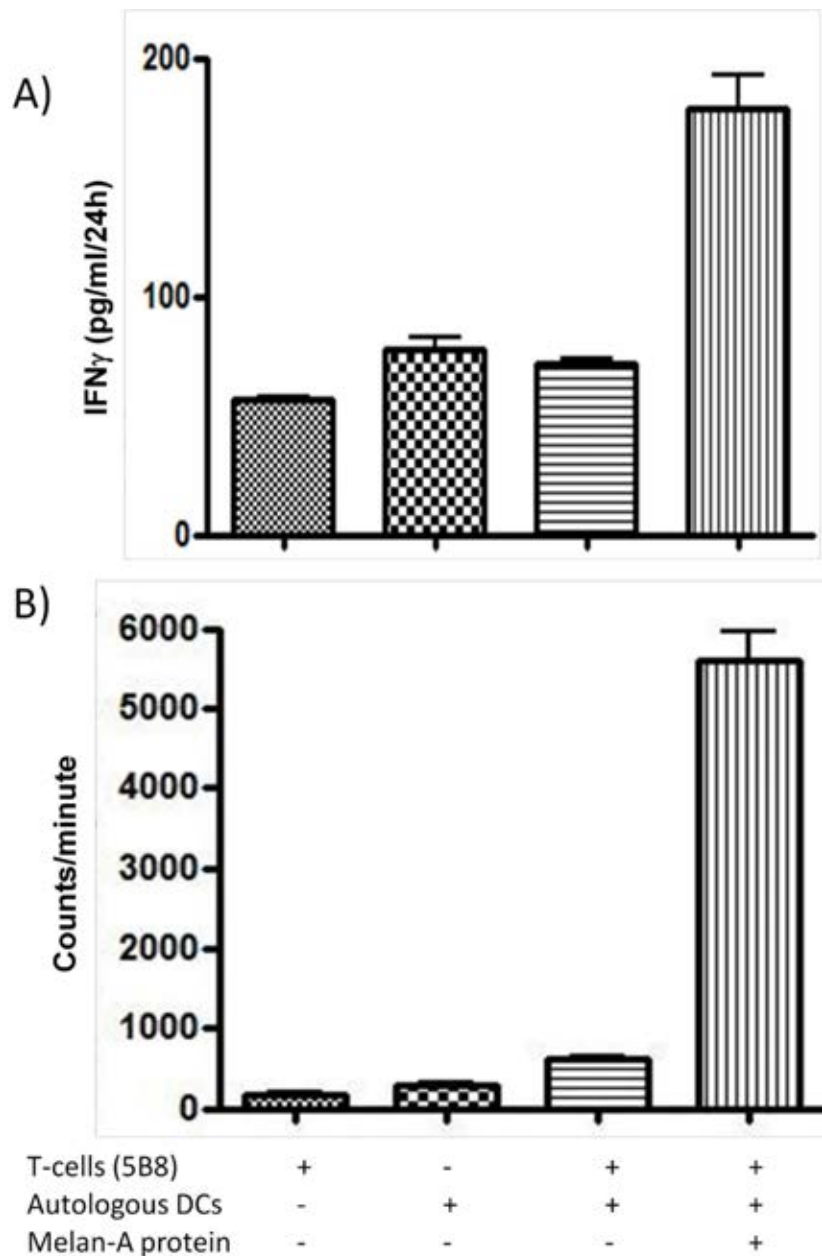
Figure 7.7. **Recognition of Melan-A protein loaded DCs by Melan-A specific CD4 clone 5B8.** Immature DCs were prepared from the same donor as T-cell clone 5B8 was derived from. Immature DCs were incubated with Melan-A protein or not in serum-free medium at 37°C for 16 hours. iDCs were then exposed to TNFα and IL1β for 24 hours. At this point, DCs were used as targets in IFNγ ELISA assays and proliferation (3^H thymidine) assays at 10^4 cells/well. Effectors were T-cell clone 5B8 at 10^4 cells/well. For proliferation, 1μCi 3H methyl-thymidine was added to cells at 48 hours, and 16 hours later incorporated radioactivity was measured by liquid scintillation. Assays were set up in quadruplicate and results are presented as mean values and standard error of the mean (error bars). A)IFNγ ELISA B)Proliferation assay.

341

In order to control for the efficiency of RNA transfection, the ability of transfected DCs to present the Melan A 26-35 epitope to a specific CD8 T-cell clone (Mel c5) was also measured in IFNγ ELISPOT assays in parallel. This takes advantage of the fact that this laboratory donor possessed the HLA-A2 allele.

As shown in Figure 7.8, there was definite evidence of recognition of the transfected DCs by the Mel c5 clone in overnight IFNγ ELISPOT assays. In line with previous experiments, the level of recognition of transfected DC was approximately 7 times lower than that of peptide-loaded cells. This result showed that these DCs expressed Melan-A and processed it normally via the Class I pathway.

Finally, the ability of these DCs to present epitopes to the Melan-A specific CD4 clone 5B8 was determined in parallel cellular proliferation and IFNγ ELISPOT assays. In terms of cytokine release, there was no evidence of recognition by the 5B8 clone – spot counts were very similar whether gp100 or Melan-A expressing DCs were used as targets.
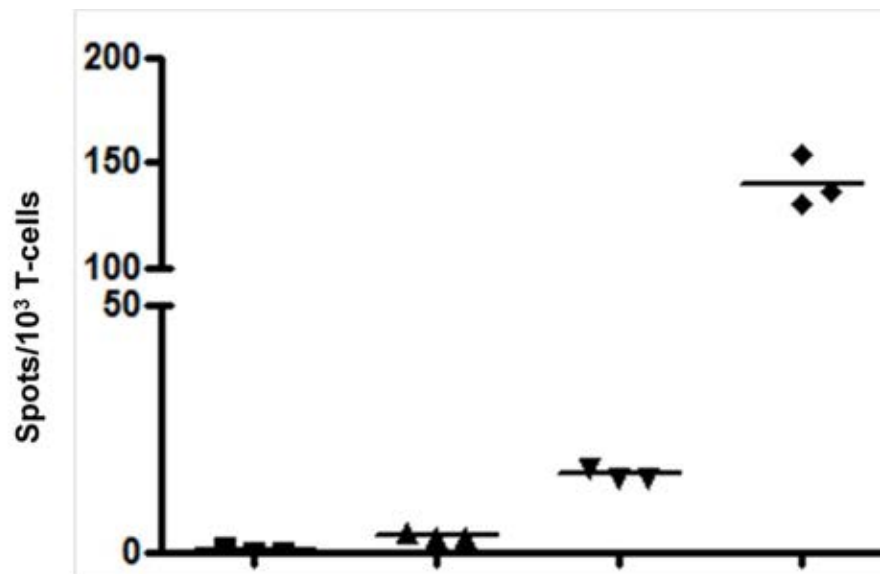
T-cells (Mel c5)	+	+	+	+
DC-gp100 RNA	-	+	-	+
DC-Melan A RNA	-	-	+	-
ELA peptide	-	-	-	+

Figure 7.8. **Presentation of Melan-A $_{26-35}$ epitope by Melan-A RNA transfected dendritic cells.** Immature DCs were prepared from an HLA-A2 positive lab donor. Cells were transfected with gp100 or Melan-A (wild-type) RNA and then transferred to TNFα and IL1β supplemented medium for 24 hours. At this point, a proportion of gp100 expressing DCs were additionally loaded with exogenous ELA peptide at 5μM. DCs were used as targets (10^4/well) in overnight IFNγ ELISPOT assays with Mel c5 T-cells (10^3/well) as effectors. Assays were set up in triplicate. Results are presented as individual spot counts per well and mean values (horizontal bars).

However, in the 3^H thymidine proliferation assays, there was evidence of recognition of Melan-A expressing DCs above gp100 expressing ones. Proliferation was 1.5 times greater when Melan-A expressing DCs were used as targets. This was not accounted for by increased proliferation in the dendritic cells alone (Figure 7.9).

The lack of recognition in IFNγ release assays of these transfected DCs may relate to the kinetics of antigen presentation and the timing of the assays. The proliferation assay is carried out 48 hours after transfection, whereas the IFNγ ELISPOT assay takes place after 24 hours. It is possible that presentation of antigen via the MHC Class II pathway takes longer when the antigen is produced intracellularly rather than being delivered directly to the endolysosomal compartment after endocytosis. This could explain the IFNγ response seen when Melan-A protein loaded DCs are used as targets and its absence in transfected cells.

In conclusion, this set of experiments suggested that Melan-A specific CD4 T-cells recognise DCs endogenously expressing Melan-A after RNA transfection. However, this was only seen when proliferation rather than IFNγ release was the read-out.
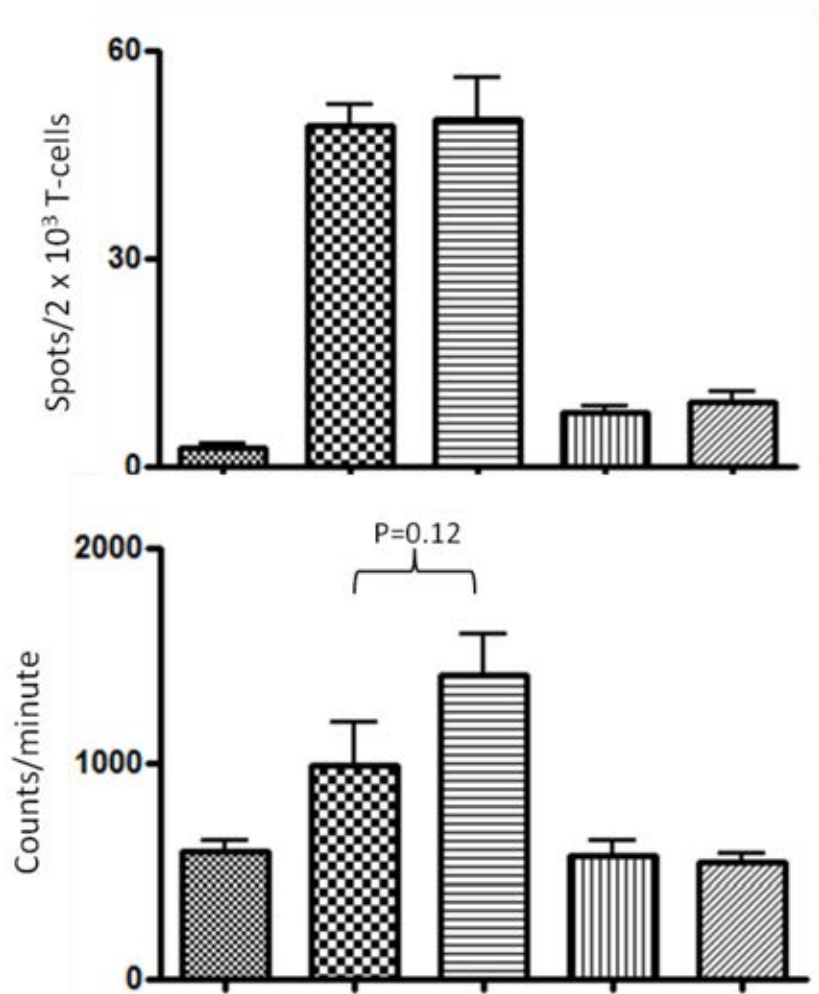
T cells (5B8)	+	+	+	-	-
DC-gp100 RNA	-	+	-	+	-
DC-Melan-A RNA	-	-	+	-	+

Figure 7.9. **Recognition of Melan-A RNA transfected DCs by Melan-A specific CD4 T-cell clone 5B8.** Autologous immature dendritic cells were prepared and transfected with Melan-A (wild-type) or gp100 (negative control) RNA. After a further 24 hours cell culture in the presence of TNFα and IL1β, cellular assays were performed. DCs (2 x 10^3/well) were used as targets in overnight IFNγ ELISPOT assays (in triplicate) with clone 5B8 as effectors (2 x 10^3/well) – A. In the proliferation assay (B), 10^4 DCs were coincubated with 10^4 T cells in quadruplicate. At 48 hours, 1μCi 3^H methylthymidine was added to each well. After 16 hours, cells were harvested and incorporated radioactivity measured by liquid scintillation counting. Results are presented as mean values and range (error bars). Students' T-test was used to compare the mean values of experimental groups as indicated.

Proliferative responses to DCs loaded with exogenous protein are larger in magnitude than responses to Melan-A transfected DCs – approximately 10 fold versus 1.5 fold.

7.3. Cellular localisation of Melan-A after RNA transfection of dendritic cells.

Experiments presented in Sections 5.6 and 5.7 show that presentation of a Class I restricted epitope from Melan-A may be dependent upon lysosomal acidification, that inhibition of lysosomal function increases detection of whole Melan-A antigen, and that Melan-A transfected DCs are recognised by Melan-A specific T-cells of a CD4 positive phenotype.

One explanation for these results may be that Melan-A localises to endolysomal compartments after synthesis in ribosomes after RNA transfection. The aim of this set of experiments was to determine whether there was any degree of co-localisation of Melan-A with the lysosomal marker protein LAMP1 in dendritic cells after RNA transfection.

Immature DCs were transfected with Melan-A (wild-type) RNA and after 3 hours they were fixed, permeabilised and co-stained with anti LAMP1 and anti Melan-A antibody. Appropriate secondary antibodies were added and after extensive washing and nuclear staining with DAPI, cells were viewed under a fluorescence microscope.

A representative high-power field (x 90) is shown in Figure 7.10. In the upper right quadrant of the images is a cell that showed intense green fluorescence indicating the presence of Melan-A protein, and also intense red fluorescence indicative of LAMP1. When the images were merged, there was a clear circular area appearing white as a result of combined blue (nuclear), red and green fluorescence. This could suggest that Melan-A can co-localise with the lysosomal marker LAMP-1. However, it was noted that whilst suggestive these results do not absolutely confirm co-localisation of the two proteins as they are two-dimensional images. It would be necessary to perform confocal microscopy to verify the result.

The aim of the next experiment was to determine whether or not similar co-localisation of the two antigens was present in another Melan-A positive cell. For this, the SK23 melanoma cell line was studied, as it is not a professional antigen-presenting-cell and it contains melanosomes. Once again, intracellular staining for Melan-A and LAMP1 was performed and cells were analysed by fluorescence microscopy. In Figure 7.11, two typical cells are shown at a magnification of x90. There was definite punctate staining throughout the cells of both Melan-A and LAMP1. However, the intensity of staining of both proteins was

Nuclei – blue (DAPI)   Melan-A – green   LAMP1 – red   Overlay (red, blue, green)
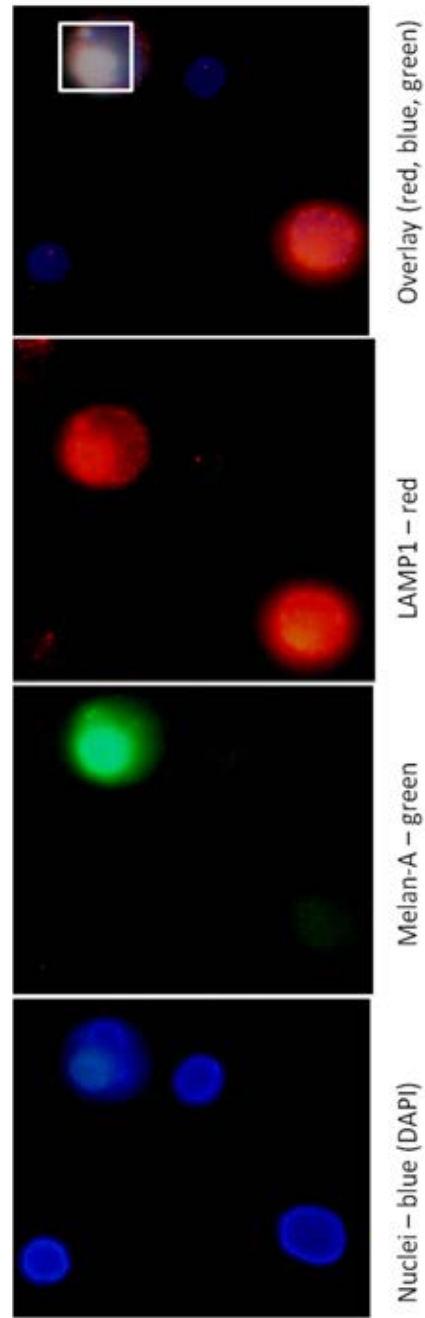
Figure 7.10. **Possible co-localisation of LAMP1 and Melan-A in RNA transfected dendritic cells.** Immature DCs were prepared from PBMC of an anonymous blood donor. Cells were transfected with RNA encoding wild-type Melan-A. After 3 hours further culture in TNFα and IL1β supplemented medium, DCs were harvested. Cells were fixed and permeabilised before being stained, in parallel with polyclonal rabbit anti LAMP1 antibody and monoclonal mouse anti Melan-A antibody, followed by appropriate secondary antibodies: goat anti rabbit-Alexa 594 and goat anti mouse Alexa 488 respectively. After extensive washes, and nuclear staining with DAPI, cells were viewed under a fluorescence microscope at x90 magnificate. A representative high-power field is shown. White box indicates region of LAMP1 and Melan-A co-localisation.

349
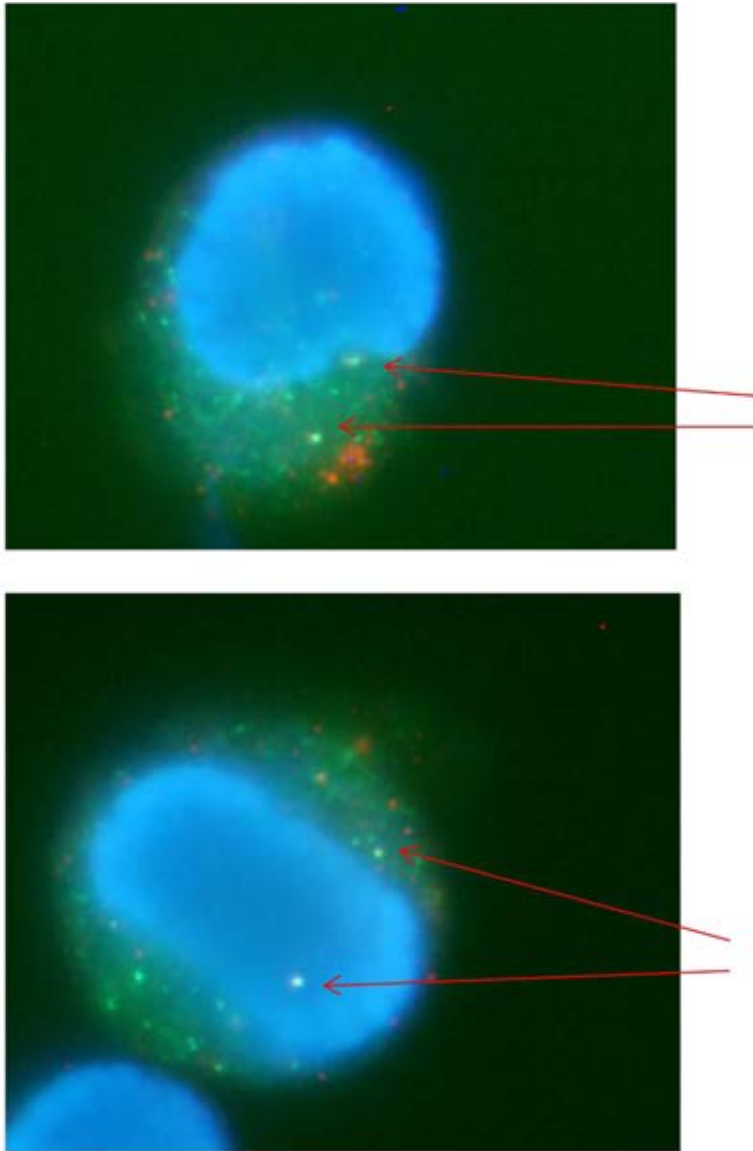
Figure 7.11. **Co-localisation of LAMP1 and Melan-A in SK23 melanoma cells.** SK23MEL melanoma cell line was fixed, permeabilised and co-stained with polyclonal rabbit anti LAMP1 antibody and monoclonal mouse anti Melan-A antibody. After washing, secondary antibodies were applied – goat anti rabbit Alexa 594 and goat anti mouse Alexa 488. After further washes and nuclear staining with DAPI, cells were viewed under a fluorescence microscope at a magnification of x90. Red fluorescence indicates LAMP1, and green fluorescence Melan-A. Long red arrows indicate areas of co-localisation.

lower than that seen in transfected DC. In terms of co-localisation, there was a low degree of partial co-localisation. This is shown by very occasional yellow punctate staining – highlighted by red arrows.

In conclusion, these experiments suggested that there was a greater degree of co-localisation of Melan-A and LAMP1 in transfected dendritic cells as compared with a melanoma cell line.

7.4: Cellular localisation of EBNA1 influences presentation of MHC Class II restricted epitopes in transfected DCs.

The experiments described above suggest that after RNA transfection and endogenous production of Melan-A protein in clinical-grade dendritic cells, presentation of MHC Class II restricted epitopes to CD4 T-cells occurs. Additionally, in transfected DCs, there is some evidence of co-localisation of Melan-A and a lysosomal marker – LAMP1 – at early time points after transfection.

Experiments using CL22 peptide-based transfection indicate that when full-length, native EBNA1 was produced in dendritic cells, the HLA-DR restricted TSL epitope was presented, as assessed by T-cell clone recognition and in-vitro stimulation assays. However, the transfection efficiency in these experiments, whilst detectable by immunocytochemistry, was very low and this makes drawing definitive conclusions from this experiment more difficult.

The aim of this set of experiments was, therefore, to determine whether or not cellular localisation of EBNA1 had any effect on the ability of transfected DCs expressing whole antigen to present MHC Class II restricted epitopes in an immunogenic fashion.   In order to achieve this, the

transfection methodology chosen was electroporation of in-vitro transcribed RNA, as this has been shown to lead to high levels of transgene expression and excellent cellular viability.

Plasmid DNA encoding full length EBNA1 (EBNA1), glycine-alanine repeat deleted EBNA1 (EBNA1ΔGA), glycine-alanine repeat deleted EBNA1 with nuclear localisation signal mutation (EBNA1ΔGA-NLS) and glycine-alanine repeat deleted EBNA1-invariant chain fusion protein (EBNA1ΔGA-Ii) have been described in Chapter 3. The functionality of these plasmids was confirmed using HEK293 cells transfected using Lipofectamine 2000. It was demonstrated that proteins had the expected molecular weights by western blotting, and that the mutation of the nuclear localisation sequence did indeed lead to a cytoplasmic distribution of protein by immunocytochemistry. These plasmids were used as templates for in vitro transcription to produce RNA encoding these proteins.

Presentation of the TSL epitope was assessed using specific CD4 T-cell clones. These have been described in Chapter 3 – they are DR1 restricted, specific and able to recognise target cells loaded with as little as 1nM exogenous peptide.

Immature DCs were prepared from an HLA B35 and DR1 positive laboratory donor. The coexistence of these two HLA alleles on the same DCs allowed simultaneous measurement of Class I (HPV) and II (TSL) restricted epitope presentation. It was important to assess Class I presentation as a marker of normal DC function and maturation as Class I presentation would be predicted to occur from an endogenous antigen. These cells were electroporated with in-vitro transcribed RNA encoding all four EBNA1 species in parallel and were cultured in the presence of TNFα and IL1β for a further 24 hours. DCs were also transfected with GFP encoding RNA – as an internal positive control for transfection efficiency and as an antigen-negative control in immunogenicity and antigenicity assays.

At this point, cells were harvested and presentation of the HPV and TSL epitopes was measured; as was whole antigen expression. Epitope presentation was assessed in two ways: recognition of DCs in overnight IFNγ ELISPOT assays with specific T-cell clones (TSL and HPV) as responders, and use of DCs as stimulator cells in polyclonal cultures with autogous lymphocytes as responder cells. DCs were fixed,

permeabilised and stained with an EBNA1 specific antibody; EBNA1 expression was visualised by fluorescence microscopy.

Whole antigen expression is shown in Figure 7.12. There was strong EBNA1 expression in DCs transfected with EBNA1ΔGA and EBNA1ΔGA-NLS RNA, intermediate level expression in cells expressing native full-length EBNA1 and weak expression in those cells expressing the invariant-chain fusion protein (Figure 7.12A). However, the proportion of DCs displaying detectable EBNA1 expression was 70-80% regardless of the EBNA1 isoform used. The stronger EBNA1 expression in cells expressing glycine-alanine repeat deleted antigen (as opposed to full length protein) may relate to the known inhibitory effect of the GAr on the rate of mRNA translation and protein production (Tellam et al., 2007), particularly as antigen expression is measured only 24 hours after transfection. The weak expression in cells expressing the invariant chain fusion protein reflects ectopic expression in endolysosomes (Chaux et al., 1999) and rapid degradation. There is no EBNA1 staining in GFP expressing cells, confirming the specificity of the staining. In Figure 7.12B, a higher magnification view of the cells demonstrates that the NLS mutation does indeed redistribute the protein from exclusively nuclear to nuclear and cytoplasmic compartments. Figure 7.12C shows higher power views of
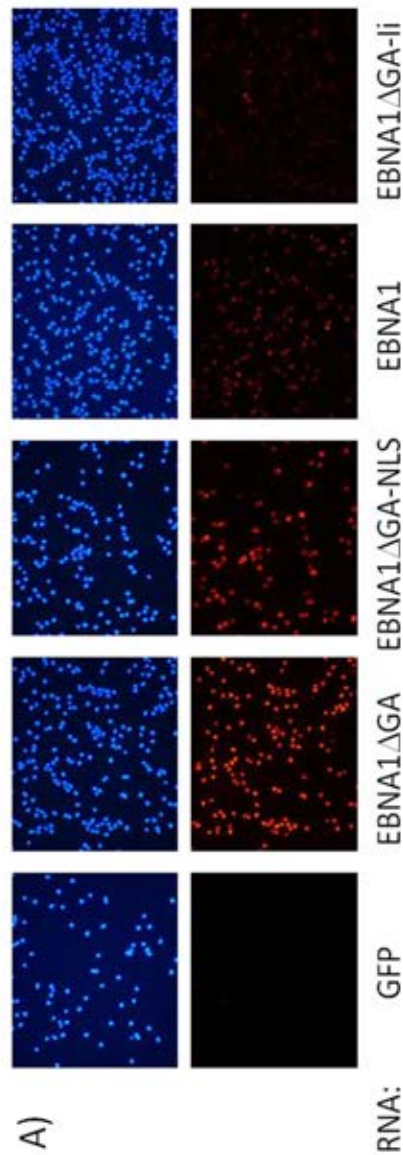
Figure 7.12. **EBNA1 expression in RNA transfected DCs.** DCs transfected with GFP or EBNA1 RNA. After 24 hours, cells were fixed, permeabilised and stained with rabbit anti EBNA1 antibody (R4), followed by goat anti-rabbit Alexa 594 conjugate and DAPI. Cells were viewed under a fluorescence microscope. A)EBNA1 staining – upper panels show nuclear fluorescence (blue) and lower panels show red fluorescence (EBNA1). B)Upper panel – EBNA1ΔGA-NLS transfected DCs, lower panel – EBNA1ΔGA. C)EBNA1ΔGA-Ii transfected DCs – upper DAPI (blue), lower EBNA1 (red). D)GFP transfected DCs – upper DAPI (blue), lower – green (GFP)
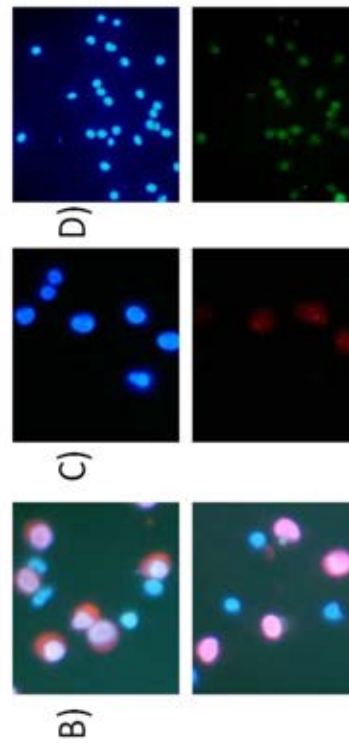
cells expressing the invariant chain fusion protein, and diffuse punctate staining in seen throughout the cytoplasm. Finally, as shown in Figure 7.12D, almost all GFP transfected cells show obvious green fluorescence as expected.

The next experiments assessed the antigenicity of these EBNA1 positive DCs. The cells' antigenicity was measured in overnight IFNγ ELISPOT assays using DCs as target cells for recognition by HPV (Class I) and TSL (Class II) specific T-cell effectors. The positive control in these assays was GFP transfected (i.e EBNA1 negative) DCs loaded with exogenous peptide. As shown in Figure 7.13A, there was clear-cut recognition of DCs expressing all glycine-alanine repeat deleted forms of EBNA1 above background levels by the HPV specific clone. Epitope presentation by EBNA1ΔGA was slightly more efficient than both cytoplasmic and invariant chain tagged EBNA1ΔGA. There was no recognition of full-length EBNA1; this was not unexpected given the inhibitory effect of the GAr on proteasomal degradation (Tellam et al., 2001) and DriP generation (Tellam et al., 2007). Recognition of transfected DCs by the HPV specific clone was approximately 75% of maximal levels.

T-cells	+	-	+	+	+	+	+	+
DC-GFP	-	+	+	+	-	-	-	-
DC-EBNA1ΔGA	-	-	-	-	+	-	-	-
DC-EBNA1ΔGA -NLS	-	-	-	-	-	+	-	-
DC-EBNA1	-	-	-	-	-	-	-	+
DC-EBNA1ΔGA-li	-	-	-	-	-	-	-	+
Peptide (TSL/HPV)	-	-	-	+	-	-	-	-
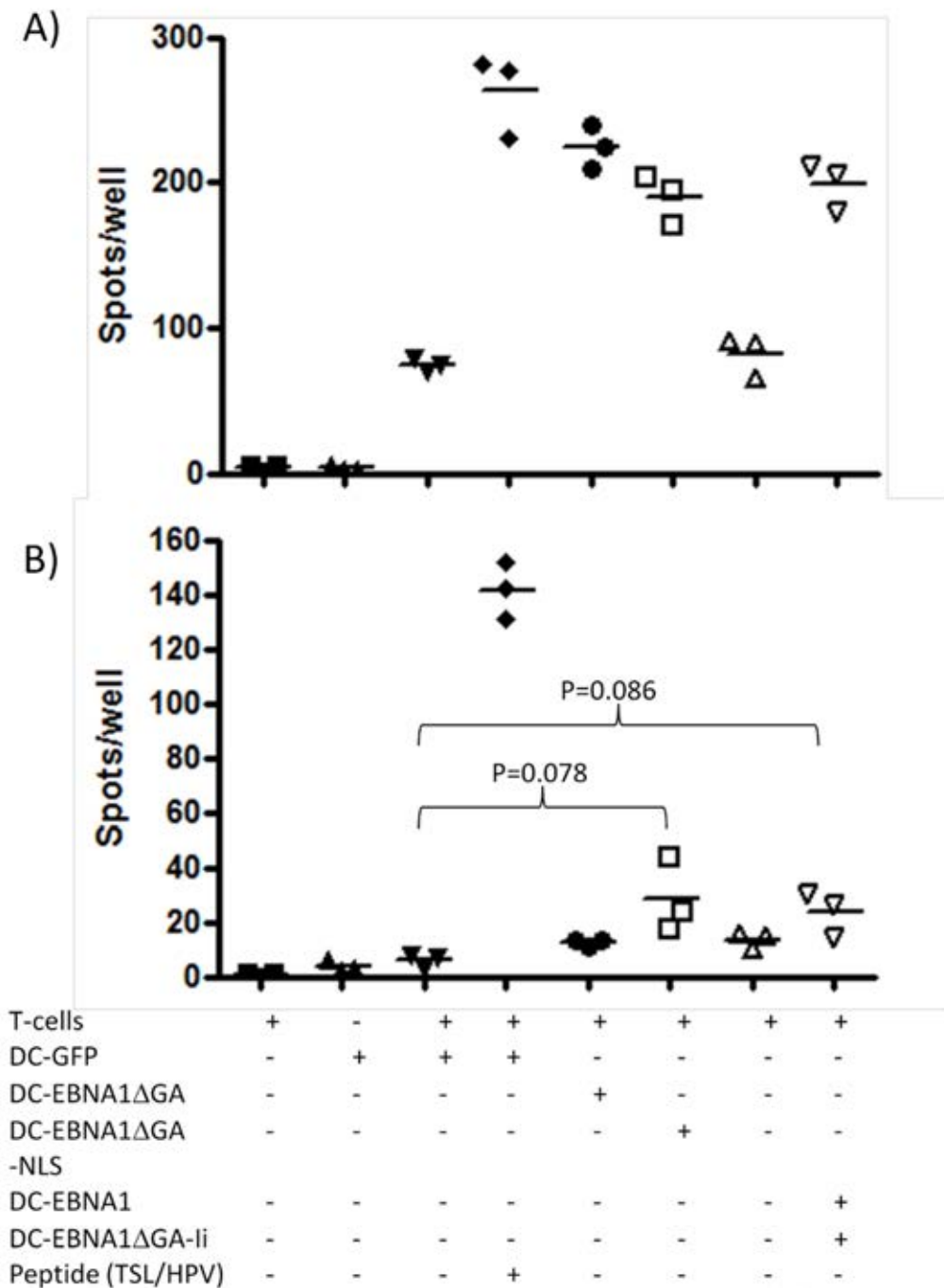
Figure 7.13. **Recognition of EBNA1 expressing DCs by HPV (A) and TSL (B) specific T-cells.** B35 and DR1 positive immature DCs were transfected with GFP (control) or EBNA1 RNA. After 24 hours, presentation of the HPV/TSL epitope was assessed in triplicate overnight IFNγ ELISPOT assays with DCs as targets (10^4/well) and T-cells as effectors (10^3/well). Results are presented as individual spot counts/well and mean values (horizontal bars). Antigen negative DCs (GFP transfected) were loaded with cognate peptide at 5μM as a positive control. Comparison of mean values of experimental groups was made by Students' T-test as indicated.

In terms of presentation of a Class II restricted epitope (TSL), there was evidence of recognition by the TSL-specific clone of DCs expressing only invariant chain tagged or cytoplasmic EBNA1ΔGA. These results are presented in Figure 7.13B. There was no evidence of recognition of nuclear EBNA1 (whether full length or GA repeat deleted). Compared with MHC Class I restricted epitope presentation, presentation of the TSL epitope from endogenous EBNA1 appeared to be less efficient – levels of recognition were approximately 20% of maximal. This is of the same order of magnitude as recognition of LCL overexpressing EBNA1ΔGA-invariant chain from MVA virus vectors.

Taken together, these results suggest that cellular localisation of antigen in DCs after RNA transfection may influence the presentation of Class II restricted epitopes, with cytoplasmic and endolysosomal protein able to access the MHC Class II loading machinery in contrast to nuclear protein. For Class I presentation, the presence or absence of the glycine-alanine repeat is the critical factor. However, these conclusions are based on the detection of epitope presentation at a single, predetermined time point 24-40 hours after transfection. In terms of dendritic cell physiology in vivo, this may not be the most relevant time-point. After intradermal administration of DCs, migration

359

to T-cell zones of lymph nodes takes about 48 hours (Adema et al., 2005) and so persistence of antigen presentation is an important consideration.

For this reason, and in view of the delayed presentation of MHC Class II (as compared to I) restricted EBNA1 epitopes in transfected B-cells (Mackay et al., 2009) and the reliance of Class II presentation on stable, long-lived proteins rather than DRiPs, experiments were extended to assess immunogenicity rather than antigenicity.

The influence of time after transfection on epitope display is also suggested by a comparison of presentation of the TSL epitope by DCs following CL22 peptide-based transfection and RNA electroporation. In the former experiment, there was recognition of full-length EBNA1 expressing DCs by the TSL clone, whereas when RNA transfected DCs were used as targets 24 hours earlier, no recognition was evident.

The aim of the immunogenicity experiments was to measure epitope display by transfected DCs over a longer time period than T-cell recognition assays. To achieve this, DCs were coincubated with autologous lymphocytes (i.e. non-adherent

PBMCs) in polyclonal cultures. After 7 days culture in the absence of exogenous cytokines, a further stimulation with transfected DCs was performed and low-dose IL2 was added. At 14 days, polyclonal lines were analysed for the presence of HPV and TSL peptide specific T-cells. Positive control was again GFP transfected DCs loaded with exogenous peptide.
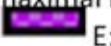
For HPV-specific T-cell responses, quantification was by bulk cytotoxicity assay. As shown in Figure 7.14, polyclonal lines stimulated with HPV peptide loaded DCs show strong specific lysis of HPV peptide-loaded targets. However, DCs transfected with all isoforms of EBNA1, including the full-length protein, generate polyclonal lines with HPV specific cytolytic activity. The cytotoxic activity of cultures driven by EBNA1 full length transfected DCs is lower, but still detectable. However, there is an obvious reduction in cytotoxicity at the E:T ratio of 5:1 in these cultures. It is also noted that at the lower effector: target ratio, cells transfected with EBNA1 are more immunogenic than those loaded with exogenous peptide. This could reflect greater persistence of antigen presentation with endogenous whole protein expression. This result suggests that full-length EBNA1 can be presented via the Class I pathway if sufficient time is available.
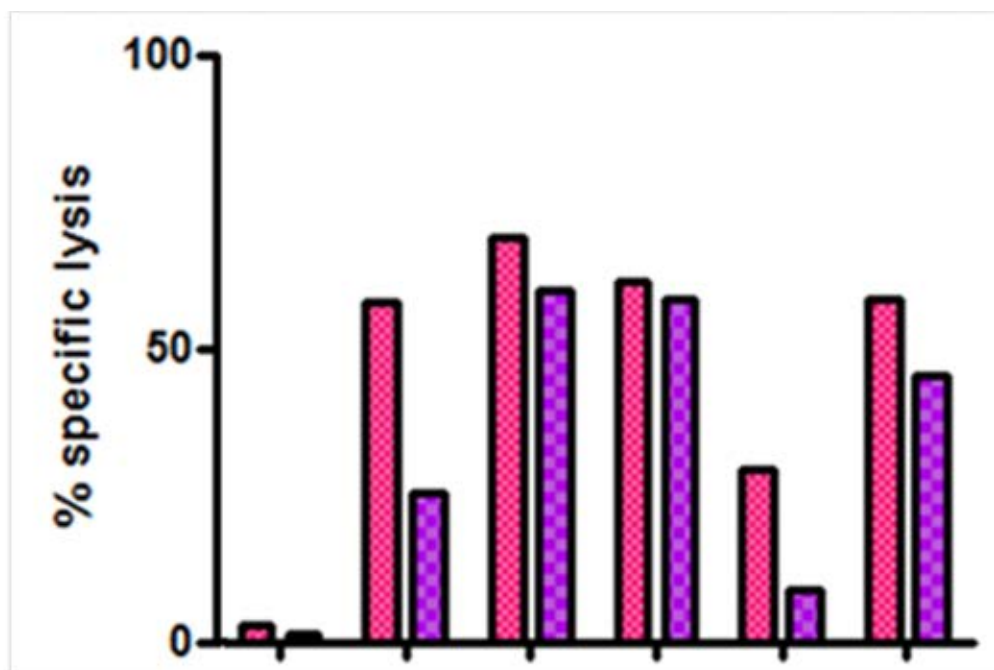
Stimulating DCs:

DC-GFP	+	+	-	-	-	-
DC-EBNA1ΔGA	-	-	+	-	-	-
DC-EBNA1ΔGA-NLS	-	-	-	+	-	-
DC-EBNA1	-	-	-	-	+	-
DC-EBNAΔGA-li	-	-	-	-	-	+
HPV peptide (5μM)	-	+	-	-	-	-

Figure 7.14. **Presentation of HPV epitope by EBNA1 transfected DCs – immunogenicity.** Transfected DCs (1.5×10^5/well) were coincubated with autologous lymphocytes (10^6/well) for 7 days. A further stimulation with transfected DCs was performed at this point, and IL-2 was added. As a positive control, GFP expressing DCs were loaded with exogenous HPV peptide. On day 14, polyclonal lines were harvested. To quantify HPV specific responses, 51Cr chromium release assays were performed. Target cells were autologous B-cell blasts (5×10^3 cells/well)loaded with 5μM HPV peptide or DMSO only (control). Effectors were polyclonal lines at either 2.5×10^4/well (E:T=5:1 (purple bars)) or 10^5/well (E:T=20:1 (pink bars)). Targets (5×105) were loaded with 100μM 51Cr simultaneously with peptide. Targets were treated with 10% SDS (maximal lysis) or medium alone (background). After 6 hours, supernatants were analysed for radioactivity. Results are presented as % HPV specific lysis (%maximal lysis of HPV loaded targets - %maximal lysis of DMSO loaded targets). 🟥 E:T = 20:1 🟪 E:T = 5:1

Figure 7.15. **Presentation of TSL epitopeby EBNA1 RNA transfected DCs: immunogenicity**. Transfected DCs (1.5 x 10^5/well) were coincubated with autologous lymphocytes (10^6/well) for 7 days. A further stimulation with transfected DCs was performed at this point, and IL-2 was added. As a positive control, GFP expressing DCs were loaded with exogenous HPV peptide. On day 14, polyclonal lines were harvested. To determine the frequency of TSL specific T-cells, overnight IFNγ ELISPOT assays were set up with autologous B-cell blasts loaded with TSL peptide at 5μM or DMSO alone as target cells (3 x 10^4/well) and polyclonal lines (1.5 x 10^5/well) as responders. Assays were assembled in triplicate. TSL specific spots are calculated as spot counts in the presence of TSL loaded B-blasts − spot counts in the presence of DMSO only B-blasts. Results are presented as individual and mean (horizontal bar) values. Students' T-test was used to compare mean values of experimental groups, as indicated.

For presentation of the TSL epitope, TSL specific T-cell responses were quantified in polyclonal cultures using autologous B-cell blasts loaded with TSL peptide or DMSO alone as stimulator cells in overnight IFNγ ELISPOT assays. There is evidence of an increase in frequency of TSL specific T-cells in polyclonal cultures stimulated with EBNA1 compared to GFP transfected DCs, as shown in Figure 7.15. The size of the TSL-specific population is similar regardless of which isoform of EBNA1 stimulating DCs were transfected with. The frequency of TSL specific cells is approximately 50-60% of peptide-driven levels. This result is quite different to that obtained using the TSL specific clone in recognition assays. Firstly, the dependence on cytoplasmic or lysosomal localisation of EBNA1 is not seen – nuclear protein is equally well presented via the Class II pathway. This could suggest that even nuclear EBNA1 can gain access to the MHC Class II pathway but by a slower mechanism than cytoplasmic protein. Secondly, there is a much less dramatic difference between peptide driven responses and those seen with transfected DCs. Once again, this could reflect persistence of epitope display.

7.5: Presentation of TSL epitope by DCs nucleofected with EBNA1 encoding DNA.

The aim of this experiment was to determine whether nucleofection of DNA into mature DCs led to presentation of Class II restricted epitopes (i.e. the TSL epitope). The ability of nucleofected DC to present immunogenic epitopes has not been reported by other investigators. Mature DCs, rather than immature ones, were selected for use in this experiment as previous experiments had suggested that nucleofection impairs the ability of DCs to respond to the maturation stimulus (IL1β and TNFα).

In the previously described three way comparison of transfection methods, nucleofection of invariant-chain tagged EBNA1ΔGA into immature DC followed by maturation led to a very low level of recognition by the TSL clone. Presentation of the HPV epitope was, however, easily detected.

Mature DCs were prepared from an HLA DR1 and B35 positive laboratory donor. On day 4 cells were exposed to TNFα and IL1β for a further 48 hours. Cells were stained with a panel of antibodies against phenotypic markers. As shown in

Figure 7.16, these cells displayed a typical phenotype of mature DCs with high CD83, CD86 and CD25 expression. CD14 expression was retained however, and CCR7 expression was unimpressive; as would be expected in the absence of PGE_2 in the maturation cocktail.

DCs were nucleofected with EBNA1 encoding plasmid DNA or antigen negative controls - empty vector (pcDNA3.1) and GFP DNA. After 8 hours further culture to allow time for transcription and translation to occur, antigen expression and antigenicity were determined. This time point was chosen as previous experiments had shown that after 12 hours viability of nucleofected cells rapidly decreased. The presence of large numbers of non-viable cells would be suspected to lead to high levels of background (non-specific) recognition by T-cell clones.

Whole antigen expression was determined by antibody staining and fluorescence microscopy. As shown in Figure 7.17, the majority of GFP transfected cells were GFP positive (≈80%) as were the majority of EBNA1 transfected DCs (≈60%). There was no EBNA1 staining on cells transfected with empty vector; indicating the specificity of antibody staining.
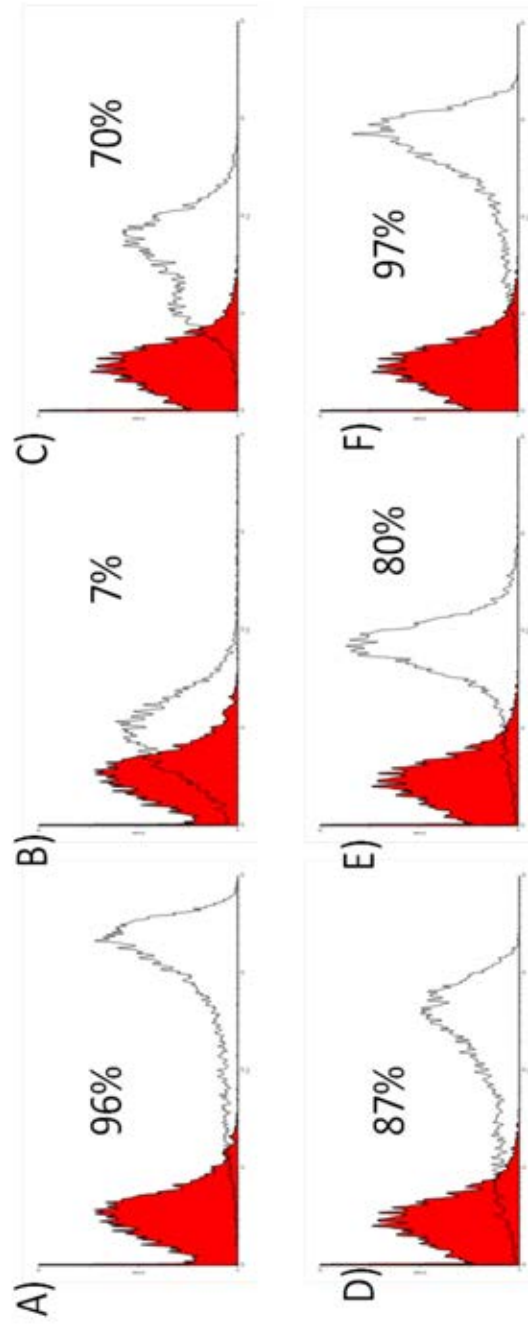
Figure 7.16. **Phenotypic analysis of dendritic cells immediately prior to nucleofection with EBNA1 DNA.** Cells had been exposed to TNFα and IL1β for 48 hours. Cells were stained with phycoerythrin (PE) conjugated antibodies against CD1a (A), CCR7 (B), CD14 (C), CD25 (D), CD83 (E) and CD86 (F). Filled red histograms show staining with isotype matched control antibodies, and hollow black is specific antibody staining. At least 10,000 gated events were collected. Percentages indicate the percentage of cells showing specific staining (% PE positive with specific antibody - % positive with isotype matched control antibody).

Plasmid DNA:

A) GFP

B) Empty vector

EBNA1ΔGA

EBNA1ΔGA-NLS

EBNA1

EBNA1ΔGA-Ii
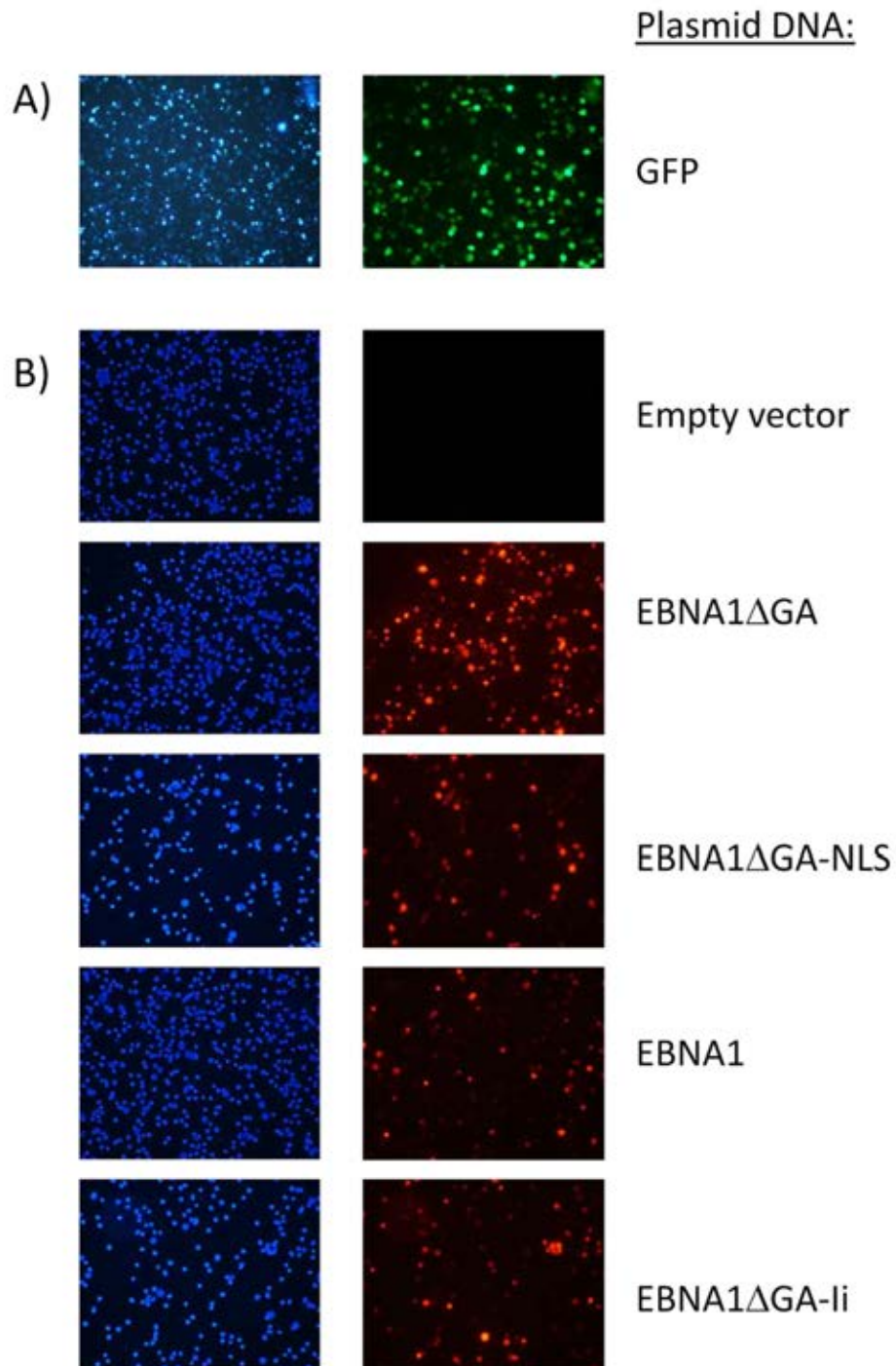
Figure 7.17. **EBNA1 expression in nucleofected mature DCs.** Mature DCs were nucleofected with plasmid DNA encoding EBNA or GFP (control). After 6 hours culture in non cytokine supplemented medium, cells were harvested. Cells were fixed, permeabilised and stained with rabbit anti EBNA1 antibody followed by goat anti rabbit Alexa 594 antibody. Nuclei were stained with DAPI and cells were viewed under a fluorescence microscope. Green fluorescence represents GFP, and red fluorescence EBNA1. Left panels – nuclei (DAPI, blue), right panels – GFP (green), EBNA1 (red).

Presentation of the HPV and TSL epitopes by these nucleofected DCs is shown in Figure 7.18. As shown in Figure 7.18A, there was evidence of recognition of nucleofected DC by the HPV specific T-cell clone. DCs expressing all isoforms of EBNA1 were recognised, although recognition of EBNA1 full-length expressing DCs was slightly lower. Recognition levels are approximately 75% of maximal (peptide-driven) responses.

Moving on to presentation of the TSL epitope, there was recognition of DCs loaded with exogenous TSL peptide, although this appeared to be suboptimal(Figure 7.18B). In previous experiments with this clone, maximal responses were typically 150-200 IFNγ secreting cells/1000 T-cells, whereas in this case only approximately 75 spots/well were seen.

Despite this, there was evidence that the TSL epitope is presented by DCs expressing EBNA1. Again, full-length EBNA1 expressing DCs were only recognised slightly above background levels. However, a critical difference in epitope presentation was seen compared to the experiment where DCs were transfected by RNA electroporation. In this experiment, there was no difference in epitope presentation between cells expressing nuclear or cytoplasmic EBNA1ΔGA.
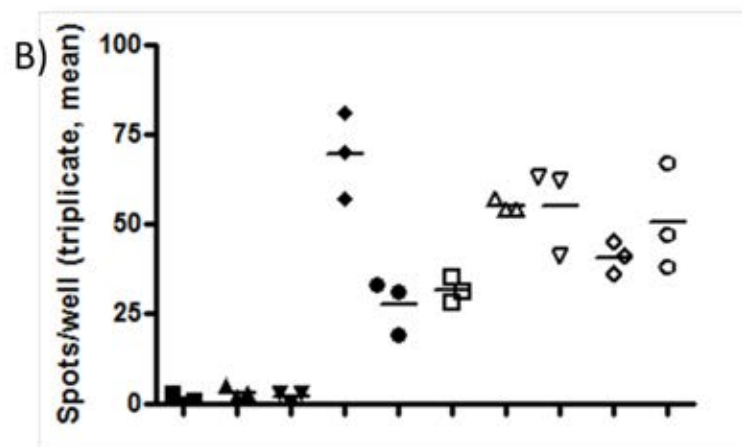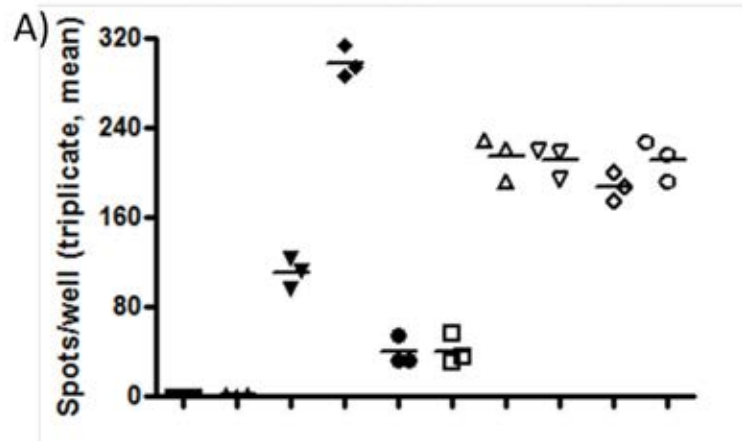
T-cells	+	-	+	+	+	+	+	+	+	+
DC-DMSO	-	+	+	-	-	-	-	-	-	-
DC-Peptide 5μM	-	-	-	+	-	-	-	-	-	-
DC-GFP	-	-	-	-	+	-	-	-	-	-
DC-empty vector	-	-	-	-	-	+	-	-	-	-
DC-EBNA1ΔGA	-	-	-	-	-	-	+	-	-	-
DC-EBNA1ΔGA-NLS	-	-	-	-	-	-	-	+	-	-
DC-EBNA1	-	-	-	-	-	-	-	-	+	-
DC-EBNA1ΔGA-li	-	-	-	-	-	-	-	-	-	+

Figure 7.18. **Recognition of DCs nucleofected with EBNA1 DNA by HPV specific clone c41 (A) and TSL specific clone B5 (B).** Mature DCs were prepared from an HLA-DR1 positive lab donor. Cells (7.5×10^5) were nucleofected with 5μg of plasmid DNA encoding EBNA1, GFP or empty vector alone. After 6 hours further culture in non cytokine supplemented medium, cells were harvested. DCs were used as targets (10^4/well) in triplicate overnight IFNγ ELISPOT assays with T cell clones as effectors (10^3/well). Additional targets included mature DC loaded with HPV or TSL peptide at 5μM or DMSO alone (control). Results are presented as individual spots counts per well and mean values (horizontal bars).

These two experiments, whilst similar are not identical: the nucleic acid used is different, as is the maturation state of the DCs and the time after transfection when T-cells assays were performed.

A further examination of antigen expression in these DCs is presented in Figure 7.19, where higher-power views of EBNA1 staining are presented. At a magnification of x60, it is clear that there was no difference in cellular localisation between cells expressing the various forms of EBNA1. Essentially, in all cases the protein was cytoplasmic in distribution. This would be expected for the invariant chain fusion protein and also EBNA1ΔGA with a NLS mutation. However, it was unexpected for nuclear EBNA1. This antibody staining was performed as early as 8 hours after nucleofection, and it is possible that this was insufficient time for the effect of the nuclear localisation sequence to be felt.

Taken as a whole, these experiments lend further support to the conclusion that cellular localisation of EBNA1 in transfected DCs influences presentation of Class II restricted epitopes. In nucleofected DCs, early after antigen expression, the protein is cytoplasmic regardless of

371
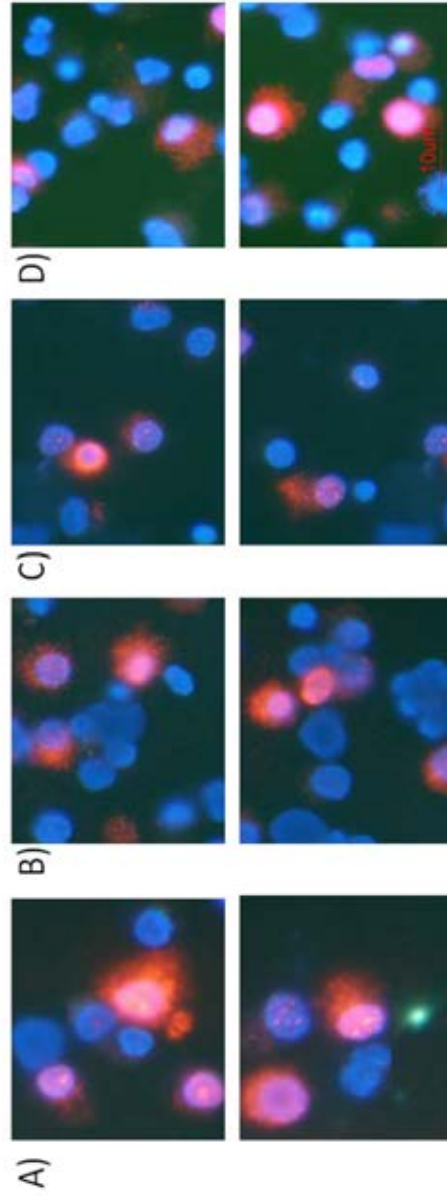
Figure 7.19. **Higher power views of EBNA1 staining on EBNA1 transfected DCs.** DCs were nucleofected with DNA encoding EBNA1ΔGA (A), EBNA1ΔGA-NLS (B), EBNA1 full-length (C) and EBNA1ΔGA-Ii. After 8 hours further culture, cells were fixed, permeabilised and stained with rabbit anti EBNA1 antibody followed by goat anti rabbit Alexa 594 secondary antibody. After extensive washes and nuclear staining with DAPI, cells were viewed under a fluorescence microscope. Two representative high-power fields are shown. Blue fluorescence represents nuclei (DAPI) and red fluorescence EBNA1. Magnification = x60.

whether EBNA1ΔGA or EBNA1ΔGA-NLS DNA and there is a similar level of recognition by the TSL specific T-cell clone.

7.6. Investigation of the mechanism of presentation of the TSL epitope by DCs expressing cytoplasmic EBNA1ΔGA.

As suggested in sections 7.4 and 7.5 above, cytoplasmic (and invariant chain tagged) EBNA1 can be presented via the MHC Class II pathway to T-cells specific for the DR1 restricted TSL epitope. With time, however, the influence of cellular location wanes.

The aim of this set of experiments was to ascertain the relative importance of two putative mechanisms of MHC Class II restricted epitope (i.e. TSL) presentation from endogenous antigen.

One mechanism is antigen transfer between DCs (Mendoza-Naranjo et al., 2007). This could take the form of release of whole antigen by DCs followed by re-uptake by endocytosis and endolysosomal processing, or transfer of pre-processed peptides between DCs. To explore the possible involvement of this process, experiments using HLA-matched (DR1 positive) and mismatched (DR1 negative) DCs were conducted. There were three experimental groups of DCs – positive control (DR1 positive - EBNA1ΔGA-NLS RNA, DR1 negative – no RNA), negative control (DR1 positive – no RNA, DR1 negative

– no RNA) and experimental group – (DR1 positive – no RNA, DR1 negative – EBNA1ΔGA-NLS RNA). Negative control cells were loaded with exogenous peptide as a control for T-cell function. Mixed DC populations were used as targets for T-cell recognition in overnight IFNγ ELISPOT assays with TSL specific T-cells as effectors. Antigen expression was also assessed by antibody staining.

As shown in Figure 7.20, the level of antigen expression was relatively low compared to what was typically seen with electroporation of RNA. For DR1 positive DCs electroporated with RNA (and mixed with mock transfected DR1 negative DCs) approximately 25% of cells showed EBNA1 fluorescence, this was about 50% for DR1 negative EBNA1 transfected cells.

As shown in Figure 7.21, there was evidence of recognition of EBNA1 negative target DCs when loaded with exogenous TSL peptide, but no recognition of DR1 positive EBNA1 transfected DCs mixed with DR1 negative mock transfected DCs. This was unexpected and may relate to the low level of whole antigen or to the effects of contaminating lymphocytes in DC populations.
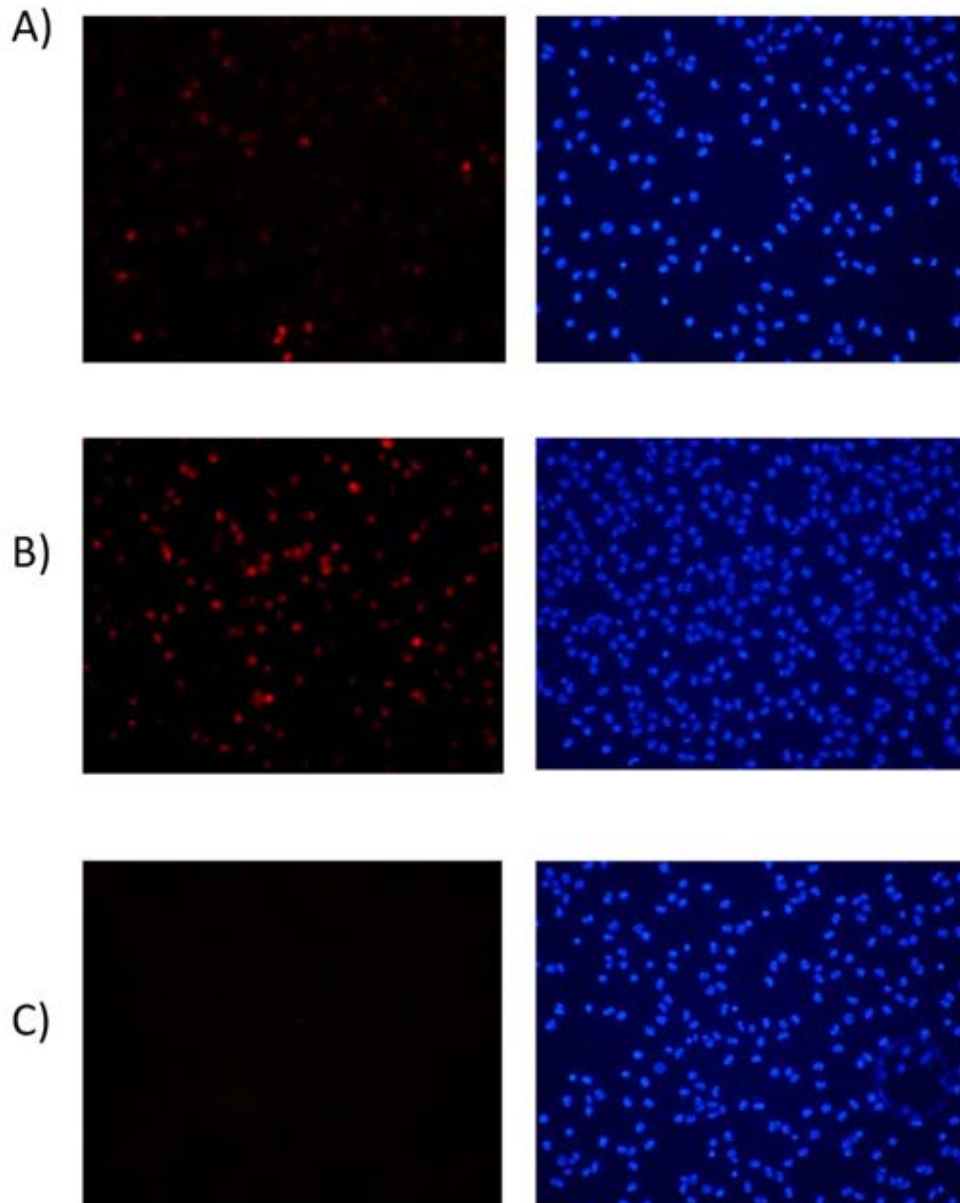
Figure 7.20. **Expression of EBNA1 in RNA transfected DCs.** Immature DCs were prepared from HLA DR1 positive and negative donors. Cells were electroporated with RNA and mixed – A)DR1 positive + EBNA1GA-NLS RNA, DR1 negative + no RNA B)DR1 negative + EBNA1ΔGA-NLS, DR1 positive + no RNA C)DR1 positive + no RNA, DR1 negative – no RNA. After 48 hours in culture, mixed DC populations were fixed, permeabilised and stained with rabbit anti EBNA1 antibody, followed by goat anti rabbit Alexa 594 secondary antibody. After extensive washes and staining of nuclei with DAPI, cells were viewed under a fluorescence microscope. Left panels show red fluorescence (EBNA1) and right panels show nuclear staining (DAPI). Magnification = x20.
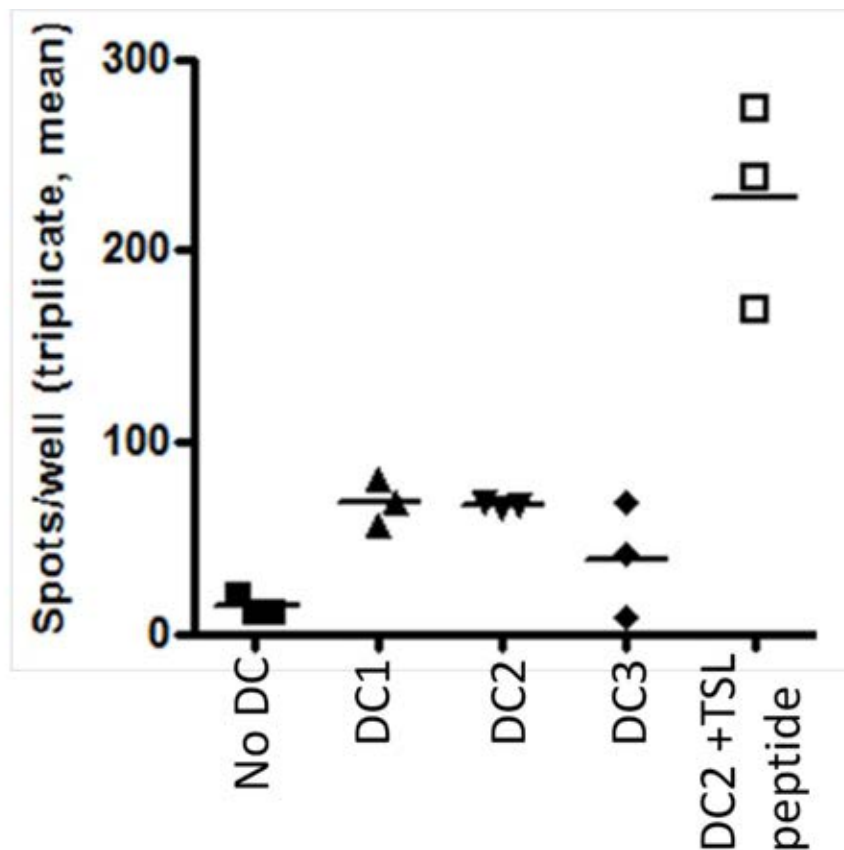
Figure 7.21. **Recognition of mixed DC populations, transfected with EBNA1GA-NLS RNA, by TSL specific T-cell clone B5.** Immature DCs were prepared from HLA DR1 positive and negative lab donors. Cells were electroporated with EBNA1ΔGA-NLS RNA or no RNA (mock) and then mixed. DC1 – DR1 negative + RNA, DR1 positive + no RNA. DC2 – DR1 positive + no RNA, DR1 negative + no RNA. DC3 – DR1 positive +RNA, DR1 negative + no RNA. Exogenous peptide was added to DC2 at a final concentration of 5μM. Epitope presentation was measured in overnight IFNγ ELISPOT assays with TSL clone B5 as effectors (10^3/well) and DCs (10^4/well) as targets. Assays were set up in triplicate. Results are presented as individual spot counts and mean values (horizontal bars).

Finally, experiments moved forward to assess the possible role of macroautophagy (Blum et al., 2008) in presentation of an MHC Class II restricted epitope from endogenous EBNA1 in transfected DC. In the B-cell system, autophagy has been demonstrated to have a role in this process (Paludan et al., 2005).

The aim of this set of experiments was to determine whether or not inhibition of autophagy with 5-methyladenine led to attenuation of presentation of the TSL epitope by DCs endogenously expressing EBNA1.

In order to assess presentation of Class I and II restricted epitopes simultaneously, immature DCs were prepared from an HLA B35 and DR1 positive laboratory donor. Cells were electroporated with RNA encoding cytoplasmic EBNA1ΔGA or in the absence of RNA (mock). DCs were returned to culture medium either supplemented with 3-MA or not. After 48 hours culture in the presence of TNFα and IL1β, cells were harvested. EBNA1 expression was measured by intracellular antibody staining and fluorescence microscopy. As shown in Figure 7.22, there was again sub-optimal expression EBNA1 in transfected DCs. Approximately 20% of DCs show detectable EBNA1 expression in the absence of 3-MA and this rises to
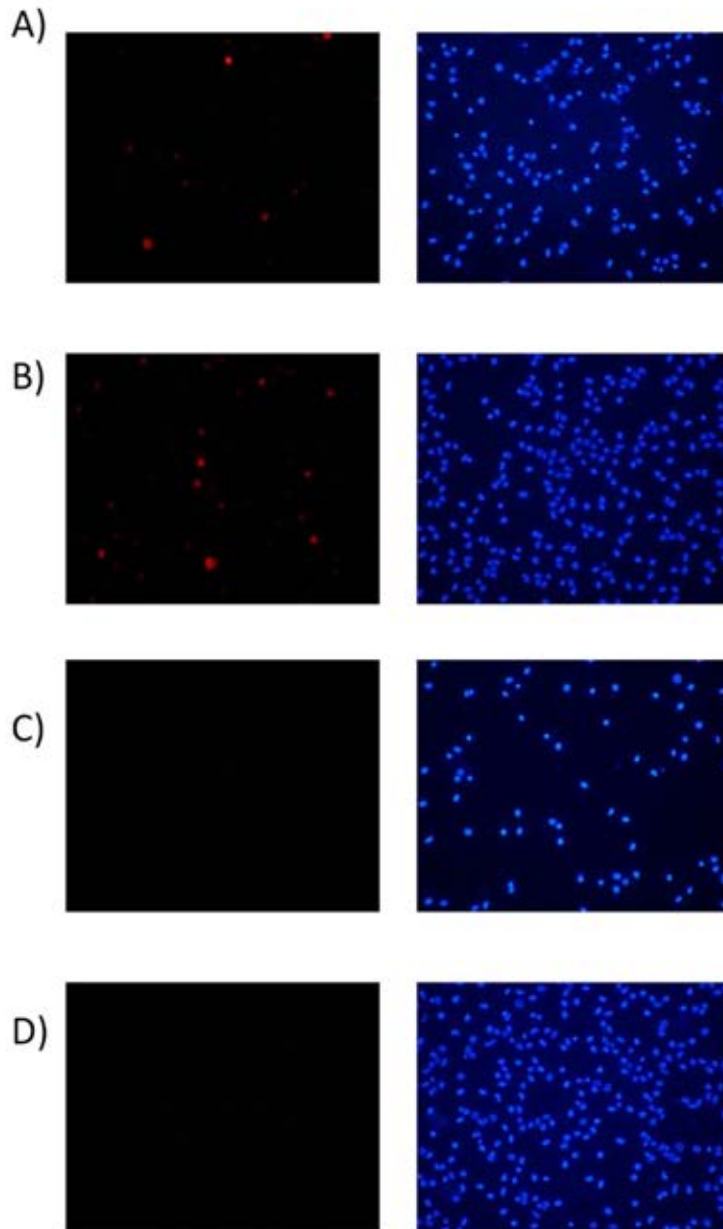
Figure 7.22. **EBNA1 antibody staining on transfected DCs – effect of 3-methyladenine.** Immature DCs, from a HLA DR1 and B35 positive donor, were prepared. Cells were transfected with EBNA1ΔGA-NLS RNA or not (mock). After transfection, cells were exposed to TNF1α and IL1β for 48 hours in the presence of absence of 3-methyladenine. At this point, cells were fixed, permeabilised and stained with rabbit anti EBNA1 antibody, washes and then stained with goat anti rabbit Alexa 594 secondary antibody. After further washes and nuclear staining with DAPI, cells were viewed under a fluorescence microscope (x20). A)EBNA1ΔGA-NLS RNA, no 3-MA. B) A)EBNA1ΔGA-NLS RNA, 3-MA. C)No RNA, no 3-MA. D)No RNA, 3-MA. Left panels show red fluorescence (EBNA1), right panels show blue fluorescence (nuclei)

around 40% in 3-MA treated cells. There was no EBNA1 staining on mock transfected cells.

The ability of these DCs to present the HPV and TSL epitopes was assessed in overnight IFNγ ELISPOT assays using specific T-cell clones as effectors. As shown in Figure 7.23A, there was evidence of recognition of EBNA1 expressing DCs by the HPV specific clone above background levels. However, levels of recognition were only 25% of maximal (peptide-driven) levels. This is in contrast to previous experiments with this clone, where typically 60-70% maximal recognition was seen. This could reflect suboptimal transfection efficiency. It was also noted that exposure of target DCs to 3-MA actually abrogates this recognition by the HPV specific clone. This was unexpected as 3-MA, at the concentrations used, is thought to be a highly specific inhibitor of autophagy.

Unfortunately, as shown in Figure 7.23B, although there was recognition of peptide-loaded DCs, there was no recognition of EBNA1 expressing DC above background. Once again, this could reflect weak EBNA1 expression. In the presence of 3-methyladenine, however, spot counts were slightly higher with EBNA1ΔGA-NLS expressing as compared to mock transfected

T-cells	+	-	+	+	+	+	+	+
DC-DMSO	-	+	+	-	-	-	-	-
DC-peptide	-	-	-	+	-	-	-	-
DC-mock	-	-	-	-	+	+	-	-
DC-EBNA1ΔGA-NLS	-	-	-	-	-	-	+	+
3-methyladenine	-	-	-	-	-	+	-	+
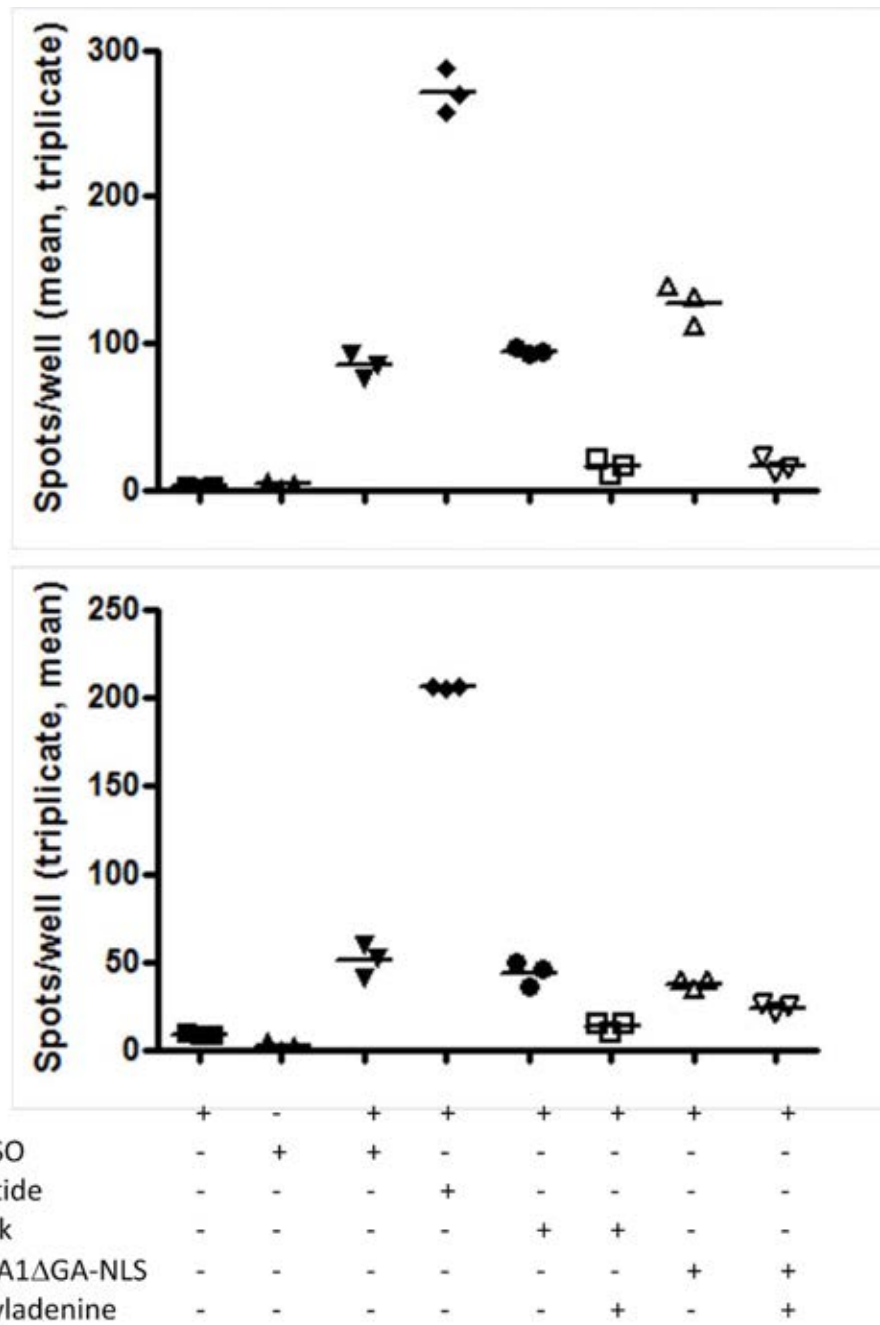
Figure 7.23. **Presentation of HPV and TSL epitopes by EBNA1ΔGA-NLS transfected DCs – effect of 3-methyladenine.** HLA B35 and DR1 positive immature DCs were transfected with EBNA1ΔGA-NLS RNA or not (mock). Cells were exposed to 3-MA or not for 48 hours. Untransfected DCs were loaded with cognate peptide or DMSO alone (control). Overnight IFNγ ELISPOT assays were set up, in triplicate, with DCs as targets (104/well) and T-cell clones as effectors (103/well). Results are presented as individual spot counts and mean values (horizontal bars).

381

DCs. This could suggest that involvement of an autophagy independent process that is unmasked when autophagy is inhibited by 3-MA.

In conclusion, these experiments do not provide further insight into the mechanism by which cytoplasmic EBNA1ΔGA is presented via the MHC Class II pathway. However, an incidental finding that autophagy may be involved in presentation of a Class I restricted epitope in transfected DCs, is noted. These experiments also lend support to the theory that, for endogenously produced antigens, MHC Class I processing and presentation in more efficient than MHC Class II; which may be more dependent on high levels of whole antigen within the cell.

Chapter 8: MHC Class II processing and presentation in clinical grade dendritic cells.

As discussed in the introduction in more detail, the CD4 T-cell response to tumour associated antigens is of central importance in a coordinated and effective immune response against malignancy. One of the putative advantages of whole antigen transfection methods for vaccine dendritic cells is the presentation of a range of both Class I and II restricted epitopes. Of course, this goes against the conventional immunological dogma that MHC Class II substrates are exogenously acquired by endocytosis into endo-lysosomal compartments. The aim of this set of experiments was to determine the extent to which the nature and localisation of antigen influences access to the Class II loading machinery in DCs.

8.1. Presentation of a MHC Class II restricted Melan-A epitope by RNA transfected dendritic cells.

Results presented so far suggest that Melan-A may have a natural affinity for the lysosomal compartment in transfected DC: the rapid loss of protein expression from 4 to 24 hours, the slight increase in proportion of Melan-A positive cells at 24 hours on exposure to bafilomycin-A, the dependence of Class I presentation (26-35 epitope) on lysosomal acidification, delayed epitope presentation compared to EBNA1 and preliminary experiments showing a degree of co-localisation of LAMP1 and Melan-A.

If the hypothesis that Melan-A enters endolysosomal compartments in DCs is correct, it would be predicted that MHC Class II restricted epitopes should be presented to CD4 T-cells without additional modifications to the antigen.

The generation of a Melan-A specific CD4 positive T-cell clone allowed this hypothesis to be tested within an autologous system. RNA electroporated DC were used as targets for this experiment in order to maximise transgene expression. It was shown that the proliferative response of the CD4 clone to DCs transfected with Melan-A RNA was somewhat higher than that seen with gp100 (control) transfected DCs. However, the response was relatively modest compared to that obtained with DCs loaded with

exogenous recombinant Melan-A protein. It was shown that these same target DCs were also recognised by the Melan-A 26-35 specific CD8 T-cell clone in parallel IFNγ ELISPOT assays.

This result is in keeping with published work that Melan-A (Bioley et al., 2006 and Godefroy et al., 2006) and other melanoma antigens (Lepage and Lepointe, 2006) are presented via the Class II pathway when endogenously expressed in DCs or other cell types.

However, there are several limitations with this set of experiments (presentation of endogenous Melan-A to CD4 clones).

First, due to the sudden and unexpected unavailability of commercially sourced recombinant Melan-A protein it was not possible to perform a positive control assay (using recombinant protein) simultaneously with the transfected DC assay. This makes it difficult to make an accurate assessment of the efficiency of Class II presentation from an endogenous compared to an exogenous Melan-A source, although a historical comparison has been presented.

Second, there is the issue of the true specificity of these T-cell clones. Unfortunately, at no point along the development pathway for these cells were they tested against a control (irrelevant) recombinant protein. The ideal negative control would have been a protein produced in an identical fashion to Melan-A. In future, this would be a crucial experiment as the possibility remains that contaminants in the protein preparation (particularly residual E.Coli proteins) could have driven the proliferation of these cells in cultures.

Despite this limitation, it is possible that the clones are truly Melan-A specific, as the manufacturer states that protein preparations are 99.8% pure and protein electrophoresis shows a single discrete band. However, the second limitation is that the specific epitope recognised by these T-cells is, at present, undetermined. There are several described MHC Class II epitopes from Melan-A in the literature and in future it would be important to try to determine the precise epitope recognised. This could achieved by the use of a pool of overlapping peptides spanning the entire coding sequences of Melan-A – this approach would be relatively straightforward in view of the small size of Melan-A. Alternatively, computer algorithms

on peptide-MHC binding could be used to predict likely epitopes based on the donor's haplotype and these could be tested individually.

Third, although the cells have a CD8 negative and CD4 positive phenotype, it was not possible to convincingly demonstrate that the observed recognition of Melan-A protein loaded target cells was MHC Class II restricted. Although the greatest reduction in IFNγ secretion was seen with anti HLA-DR and DQ antibodies there was also a degree of inhibition with a pan MHC Class I specific antibody.

Perhaps most interesting is the observation that the proliferative responses of these T-cells to antigen (whether exogenous or endogenous Melan-a) are far more impressive than the IFNγ responses. As mentioned previously, one explanation might relate to the kinetics of antigen presentation - IFNγ assays were performed early after transfection, whereas proliferation was assessed over a 72 hour period. However, even when exogenous Melan-A protein was used, IFN gamma responses were modest.

It is important to consider the origin of these T-cells. They were isolated from the PBMCs of a healthy laboratory donor with no evidence of dermatological malignancy or vitiligo. In this context, it might perhaps not be unusual for the cells to release little IFNγ as persistent CD4 T-cell help would lead to the development of powerful cytolytic responses against skin antigens. In addition, the CD4 helper subset of T-cells are known to produce a wide range of effector cytokines not merely IFNγ. The fact that detectable levels of anti Melan-A IgG antibodies were seen in the plasma of this donor, and that directly ex-vivo there were IFNγ responses detected by ELISPOT argues that they are probably Th1 cells. It is possible that cells became functionally exhausted after repeated rounds of in-vitro stimulation with Melan-A protein loaded dendritic cells and levels of IFN gamma production declined.

In terms of Melan-A specific CD8 responses that have been found in healthy individuals, there are some functional differences between responses seen in lab donors and melanoma patients. For example, in healthy donors Melan A [27-35] tetramer positive cells, whilst detectable, do not seem to be able to respond to antigen with cytokine secretion in contrast to cells from a subset of melanoma patients (Dunbar et al., 2000). In fact, in a lab donor with a particularly

large [27-35] tetramer positive CD8 population, the cells were ultimately found to be cross-reactive with a mycobacterium tuberculosis antigen (Voelter et al., 2008). A survey of CD8 responses to this epitope in lab donors also raised the possibility that they may partly be due to cross-reactive subsets of naive CD8 T cells (DuToit et al., 2002).

It should be borne in mind that, in comparison to other published work on generation of Melan-A specific CD4 T-cells that used IFNγ capture based assays for selection of T-cell clones (Bioley et al., 2006, Godefroy et al., 2006 and Zarour et al., 2000), this work relied upon selection based on cell proliferation. The microcultures that showed good viability and dense cellular proliferation by light microscopy were selected for amplification. It is entirely possible that T-cells with a lower turnover rate could have been producing more IFNγ and would have been discarded.

Future work should include a more comprehensive analysis of these T-cell clones. This would encompass phenotypic analysis using antibodies specific for markers of Th17 cells, regulatory T-cells (FOXP3, CD25) and naive, effector and memory CD4 subsets. In addition the ability of the cells to secrete additional cytokines in response to Melan-A

stimulation needs to be determined – these would include other Th1 cytokines such as GM-CSF and TNFα, IL2 and Th2 cytokines such as IL10 and IL4. The formal demonstration that the cells are MHC Class II restricted remains problematic in the absence of a defined epitope particularly if cell proliferative is the only cellular readout. The proliferation assay is a longer term assay and so the short duration of action of MHC blocking antibodies make this a difficult approach to apply.

8.2. Presentation of a MHC Class II restricted epitope from EBNA1 RNA transfected dendritic cells.

Several human malignancies are associated with EBV infection. These include epithelial (nasopharngeal carcinoma) and lymphoid cancers (Hodgkin's lymphoma, Burkitt lymphoma and post-transplant lymphoproliferative disease). Predisposing factors include possession of certain HLA haplotypes particularly in NPC and the presence of T-cell immunosuppression.

Immunotherapeutic approaches, particularly in classical PTLD, have had some success in the clinical setting. Adoptive transfer of donor derived EBV specific cytotoxic T-cell clones driven by LCLs after allogeneic stem cell transplantation has been highly effective in the therapeutic and prophylactic setting for PTLD (Heslop et al., 2010). After solid organ transplantation and refractory PTLD, 50% duration remission rates were achieved using third-party HLA matched T-cell clones stimulated with LCLs (Haque et al., 2010). In contrast to PTLD, other EBV associated malignancies express a more limited set of EBV antigens, making the use of LCL driven T-cells more difficult. Attempts to overcome these difficulties have included the

use of LCLs loaded with specific epitope peptides or overexpressing the particular antigen (Bollard et al., 2007) expressed in the tumour type of interest.

Vaccination approaches have also been studied. In particular, for NPC, intradermal vaccination with a MVA virus vector expressing a LMP2-EBNA1 fusion protein has been shown to reactivate memory CD4 and CD8 T-cell responses with minimal toxicity (Taylor GS, personal communication).

It is interesting that all EBV driven malignancies express EBNA1 and that whilst MVA vaccination is being attempted, no clinical trials have used EBNA1 expressing dendritic cells as a therapeutic vaccine for EBV positive cancers.

On this basis, the rationale for this set of experiments was to determine whether or not EBNA1 expressing dendritic cells could present Class I and II epitopes from EBNA1 and whether or not cellular localisation had an effect on epitope presentation. It is pertinent to note that this work has potential therapeutic relevance as both in Hodgkin's disease (Heller et al., 2008) and Burkitt lymphoma suboptimal CD4 T-cell responses to EBNA1 have been observed. The extent to

which this reflects a cause or consequence of the disease is as yet undetermined. On a more fundamental note, the fact that in-vivo CD4 T cell responses to EBNA1 do exist and yet in-vitro derived B-LCLs are barely recognised by most of these CD4 clones requires explanation. One possibility is that dendritic cells are involved in-vivo (Subklewe, 2002).

Electroporation of in-vitro transcribed RNA was used to transfect dendritic cells, as prior experiments had shown this to be the most immunogenic transfection method with good cellular viability. The TSL specific T-cell clone has a functional avidity of 10^{-7}M (approximately 100nM) which is similar to previously published work (Long et al., 2005) and is able to recognise target cells endogenously expressing invariant chain tagged EBNA1.

The results showed that DCs were efficiently transfected and expressed high levels of EBNA1 and that alterations in the nuclear localisation sequences and invariant chain tag did demonstrably affect the pattern of EBNA1 staining seen on indirect immunofluorescence. As a whole, presentation of the EBNA1 HPV (B35) epitope was easily detectable at levels that approached maximal (peptide-driven) levels in T-cell recognition and in-vitro stimulation assays. As predicted

from the known inhibitory effect of the GA repeat on proteasomal processing (Levitskaya et al., 1995), the full length construct is less immunogenic for the HPV epitope.

For the HLA-DR1 restricted TSL epitope, a quite different pattern emerges. In terms of T-cell recognition assay, in which surface epitope display is measured between 24 and 40 hours post transfection, there is no increase in IFNγ secreting responder T-cell counts with nuclear EBNA1. This is in line with the work of Mautner et al (2004) who found that EBNA1 specific CD4 T-cell clones only recognised LCLs when nuclear (full length or ΔGA) when the protein was overexpressed 60 times above physiologic levels. There is low-level recognition of invariant chain tagged and cytoplasmic EBNA1. However, the recognition of invariant chain EBNA expressing DCs remains low in comparison to TSL peptide loaded targets. It is difficult to explain this, as several studies in the B-cell system suggest that expression of EBNA1 as a fusion protein with the cytoplasmic domain of the invariant chain (aa 1-80) leads to near maximal recognition by CD4 clones. There is, however, some evidence that in murine DCs the invariant chain may play less of a role in control of MHC Class II presentation than in other cell types (Rovere et al., 1998). It is also interesting to note that in clinical trials of DC vaccination, the LAMP1

sequence has been used to redirect antigen to endolysosomes rather than the invariant chain. It would be interesting in future to generate a LAMP1-EBNA1 fusion RNA to determine whether this was more effective in generating EBNA1 CD4 epitopes.

In in-vitro stimulation assays, the derived T-cell populations show much less variation in the proportion of TSL specific T-cells regardless of which isoform of EBNA1 the stimulating DCs were transfected with.

Having demonstrated that certainly in short term T-cell recognition assays, the cellular localisation of EBNA1 does influence presentation of the EBNA1 515-529 epitope, attempts were made to determine the route by which cytoplasmic EBNA1 comes to interact with the MHC Class II loading pathway. Unfortunately, experiments using 3 methyladenine to determine the role of macro-autophagy and antigen transfer experiments with HLA matched and mismatched DCs were not successful due to low levels of EBNA1 expression and lack of immunogenicity, as indicated by whole antigen staining and a suboptimal recognition by the HPV specific clone. However, a close evaluation of the results

shows that in fact, in the presence of 3-methyladenine, there is a slight increase in TSL clone response with cells expressing cytoplasmic EBNA1 compared to GFP control. This raises the possibility that under conditions of limited antigen availability autophagy inhibition unmasks an unrelated pathway for Class II presentation of endogenous antigens.

However, there was an incidental finding of note. In experiments with 3-MA, the presentation of the B35 restricted HPV epitope from EBNA1 was markedly attenuated by exposure of cells to 3-methyladenine after transfection. Since the positive control in this experiment was untransfected DCs loaded with cognate peptide rather than peptide-loaded 3-MA exposed DCs, the possibility remains that the observed effect is due to an off target effect of 3-MA. However, the dose of 3-MA used typically does not have off-target actions and the cell viability by light microscopy remained excellent.

Macroautophagy has been found in many recent studies to inhibit the presentation of MHC Class II restricted epitopes from viral and tumour antigen in various cell types

(Croetzer and Blum, 2008). However, there is a precedent for its involvement in MHC Class I epitope generation in macrophages – antigen-presenting-cells that share some characteristics of DCs such as an ability to cross-present antigens. English et al (2009) examined in detail the presentation of an MHC Class I restricted epitope from HSV-1 in infected murine macrophages. Presentation of the epitope was determined by the response of a specific T-cell hybridoma of the CD8 positive phenotype. Epitope display was determined in the first 12 hours after infection as cytopathic effects of HSV-1 began after this time. T-cell recognition occurred from 6 hours after infection and was markedly reduced by pre-exposure of cells to brefeldin A and a proteasome inhibitor (MG-132). However, between 8 and 12 hours post infection bafilomycin-A strongly inhibited recognition. Interestingly, although resting macrophages were negative for LC3, a marker of macroautophagy, this protein was induced on HSV infection and 3-MA also reduced the size of T-cell responses. This finding is also relevant to the result presented earlier that the presentation of Melan A 26-35 from endogenous Melan-A protein is dependent on lysosomal acidification. It is also important to note that in a previous experiment comparing antigen processing of Melan-A and EBNA1, there was no inhibitory effect of Balifomycin-A treatment on presentation of the HPV epitope

from nuclear EBNA1ΔGA, in contrast to the finding with cytoplasmic antigen.

The finding that surface display of the TSL epitope depends upon cellular localisation in the short, but not the longer term extends some very recently published observations on CD4 T-cell responses to EBNA1 (Leung et al., 2010 and Mackay et al., 2010). The key differences between these studies and this work are the cell type – DC versus B-cells, different nucleic acid for transfection (RNA versus DNA) and a different CD4 epitope was studied (TSL). Of note, TSL is in fact an overlapping epitope with VYG.

In the work of Leung, levels of recognition of HLA matched LCLs by three different EBNA1 specific CD4 T-cell clones varies – there is a very low level of recognition (less than 2% maximal) by VYG (509-528, DR11) and SNP (474-493, DR52) specific clones and no recognition by PQC (529-548, DR11) specific ones. This does raise the question of how the responses are generated in vitro. When target LCLs were loaded with cognate peptide, powerful T-cell recognition was restored. An exogenous-reinternalisation route to the MHC Class II pathway was excluded by experiments with concentrated cell supernatants. Overexpression of EBNA1,

EBNA1ΔGA and EBNA1ΔGA-invariant chain from a doxycycline-inducible episomal vector achieved 100 fold increases in antigen expression over 72 hours, yet recognition by VGY and SNP clones was minimal (2-3 times background). There was no recognition of the PQC epitope. However, invariant chain EBNA1 transfected LCL were recognised by all three clones and nuclear EBNA1 overexpression upregulated recognition by the CD8 HPV clone. On unmanipulated LCLs, autophagy inhibition with 3-MA abrogated presentation of the SNP epitope but actually enhances presentation of VYG. Transfection with cytoplasmic EBNA1ΔGA however led to easily detectable presentation of all 3 Class II epitopes early after transfection at levels of 25-50% of invariant chain tagged EBNA1. The production of all epitopes from cytoplasmic EBNA1 was autophagy dependent as assessed by 3-MA and ATG7 knockdown.

The kinetics of Class I and II epitope presentation from endogenous EBNA1 was examined in some detail by Mackay et al (2009). In this work, B-cells were transformed with a Chinese strain of the virus – CKL. This viral isolate has sequence variations compared to the B95.8 isolate and these markedly attenuate certain CD8 and CD4 T-cell responses. Into these CKL-LCLs, a doxycyline inducible DNA construct encoding EBNA1 was introduced by electroporation. Stable

transfectants were immuno-magnetically selected and used as targets in T-cell recognition assays. Expression of EBNA1 and EBNA1ΔGA increased after doxycycline induction and reached steady state (equivalent to long-term induced cells) by 72 hours, although the peak expression was earlier and stronger with EBNA1ΔGA. As expected, presentation of two Class I restricted epitopes (HPV, B35 and IPQ, B7) was detected as early as 12 hour post induction and was maximal within 48 hours. However, for the CD4 epitopes there was no recognition within the first 72 hours and after this there was a slow increase in recognition with levels not reaching those of long-term induced cells by 168 hours. This profound delay in Class II epitope presentation was not due to a requirement for inter-cellular antigen transfer and was not due to general characteristics of LCLs as re-routing antigen into the Class II pathway with an invariant chain tag allowed early Class II presentation to occur. It was finally demonstrated that presentation of Class II epitopes was much less affected by termination of protein synthesis than Class I presentation, suggested that CD4 T-cell recognition of EBNA depended more on mature, stable protein than DRiPs. These data, that nuclear EBNA1 can be presented via the Class II pathway albeit very slowly, are entirely consistent with the findings presented here that cytoplasmic

or endolysosomal localisation of EBNA1 only affects presentation of the TSL epitope in the short term.

Future work should seek to extend the range of epitopes studied in DCs, although clearly there would be limitations on the number of different epitopes that could be examined simultaneously in the same target cells due to HLA haplotype limitations. In terms of in-vitro stimulation assays, it would be important to dissect further functional characteristics of the induced TSL specific T-cell populations in terms of functional avidity by varying the concentrations of stimulating peptide used and effector – target ratios. The route by which cytoplasmic or nuclear EBNA1 gains access to the Class II pathway in DCs remains undetermined. Further attempts to elucidate this should include a formal determination of the optimal concentration of 3-MA to inhibit macroautophagy in DCs using an indicator protein such as the neomycin resistance gene, and then T-cell recognition assays in the presence or absence of 3-MA. Although EBNA1 has never been shown to reach the Class II pathway by an extracellular route in B-cells, DCs have a higher phagocytic and endocytic capacity and the levels of cell death in DC cultures may be higher than LCLs, and so experiments to determine whether or not transfected (mismatched) DC culture supernatants can sensitise HLA

matched DCs to T-cell recognition would be important. It would be especially useful to elucidate how nuclear EBNA1 is presented via the Class II pathway over a longer time period. This could be achieved by culturing transfected DCs for a prolonged period (7 days) and performing T-cell recognition assays daily in the presence of autophagy inhibitors.

In conclusion, these results show that the localisation and stability of antigen, as well as the time-frame over which epitope display is assessed, can influence MHC Class II presentation of an endogenous viral antigen in clinical grade DCs. This would have clinical implications for vaccine design. It would be important to study the localisation of antigen within the cell after transfection and to assess whether there was any overlap with endolysosomes or autophagosomes and to judge whether or not manipulation of cell localisation might be necessary to optimise Class II presentation. They also emphasise the fluidity and non-exclusivity of the MHC Class I and II loading compartments.

CHAPTER 9: CONCLUSIONS AND CLINICAL IMPLICATIONS

Despite the undeniable promise of ex-vivo derived DC vaccines for cancer (Gilboa, 2007) and isolated reports of durable clinical responses, the labour-intensive and individualised nature of these therapies means that constant re-evaluation and re-appraisal are necessary, especially in light of emerging evidence that in-vivo targeting of DC in situ may be feasible and efficacious (Tacken et al., 2007).

The recently completed clinical trial of DC vaccination in metastatic melanoma (Steele et al., 2011) is only the second clinical application of plasmid DNA transfected DC expressing whole antigen after non-viral transfection. It is distinguished from the previous study (Pecher et al., 2002) by a more homogenous and precisely defined patient group, more objective assessment of clinical response and a more thorough characterisation of the vaccine and immune responses. There was an increase in frequency of gp100 and Melan-A specific T-cell responses with vaccination that was not seen for control viral epitopes. However, it remained crucial – as a proof-of-principle - to formally demonstrate that patient DC presented epitopes as there was no control (unvaccinated or vaccinated with irrelevant antigen) group

and experiments with CL22 transfection had studied viral rather than self-antigens and had used healthy donor DC. In this work low-level presentation of Class I restricted epitopes from gp100 and Melan-A is seen. In the case of Melan-A, this is seen despite low whole antigen expression. The result is in contrast to many studies that suggest that human DC are extremely poorly immunogenic after transfection of DNA, rather than RNA.

The lack of correlation between epitope presentation and whole antigen detection in transfected vaccine DC has important clinical implications. Quality control of the DC vaccine cellular product remains in its infancy and there is uncertainty over desirable and necessary vaccine characteristics. This work suggests that quantification of the proportion of cells expressing whole antigen by antibody staining at a fixed time point after RNA transfection does not define a group of more immunogenic DC. However, it was possible to use a soluble, recombinant T-cell receptor to detect immunogenic Class I epitopes on the DC surface and further consideration should be given to this technique in DC quality control. This would be more reproducible, standardised and less labour-intensive than using T-cell clones for such purposes. However, it would not be straightforward to determine the significance of very low-

level epitope presentation and in this work epitope detection using recombinant TCR required either single cell fluorescence microscopy or use of a re-directed T-cell assay. In either case, this is less than ideal and in future efforts will be needed to adapt the technique to flow cytometric methods if possible.

In DNA based DC transfection, quantification of tumour-associated-antigen transcripts by RT-PCR would allow detection of an intermediate that would be expected to lead to translation and subsequently Class I epitope generation. The relation between mRNA and epitope presentation would then need to be determined. Of course, if RNA transfection is used, then measurement of RNA levels would not be very informative as it would not discriminate between presence of RNA and translation of RNA.

If direct detection of defective ribosomal products were possible, this would appear to be the ideal surrogate marker for immunogenicity, certainly via the MHC Class I pathway, as the consensus view is that the majority of proteasomal substrates are DRiPs (Pierre, 2005).

In general terms, DRiP generation can be monitored by protein synthesis inhibition followed by delivery of radiolabelled precursor amino acids and pulse-chase experiments. However, measurement of a specific DRiP is more problematic.

Long lasting and highly-avid CTL responses, the ultimate goal of DC vaccination, require support from CD4 T-cells. It was established that a viral tumour antigen (EBNA1) was able to gain access to the MHC Class II processing and presentation pathway after endogenous expression following CL22 peptide-based transfection. This occurred even in the absence of an endolysosomal targeting sequence and after transient DC exposure to chloroquine that inhibits endolysosomal acidification. This had not been determined previously (Irvine, 2000). This is a significant result particularly because in the clinical trial, there were few known Class II epitopes to determine frequency of induced CD4 responses and because T-cell responses to nucleofected B-cell blasts were not analysed as separate CD4 and CD8 subsets.

It was also possible to put CL22 peptide based transfection into context, in terms of other transfection methodologies.

It was distinguished by the highest cellular viability, of paramount importance, particularly as vaccine DC must survive a further 48 hours after administration to reach lymph nodes and initiate T-cell responses. Despite very low transfection efficiencies, there was epitope presentation particularly for Class II restricted epitopes. Importantly, in terms of ability to amplify specific T-cell responses within a bulk T-cell population, CL22 transfection was not especially inferior to nucleofection of DNA or RNA electroporation. Insertion of plasmid DNA into DC using CL22 peptide also appeared to have immune-stimulatory effects on the vaccine cells, although this was not investigated in nucleofected or RNA transfected DC. This would be another potential benefit of CL22 transfection.

Building on the observation of lack of correlation between whole antigen expression and immunogenicity in trial patient DC, it was demonstrated using a highly efficient transfection method (RNA electroporation) that at 24 hours after transfection, DC were whole antigen negative but Class I restricted epitope positive. At early time points after transfection, Melan-A and to a lesser extent gp100 whole antigen was detectable. In contrast, the viral antigen EBNA1 was easily detected at all time points. This result illustrates the vital importance of understanding the

407

kinetics of antigen expression in the cell type of interest for the particular antigen being vaccinated against, if whole antigen detection is to be used. The finding that, for the Melan-A antigen, presentation of Class I restricted epitopes is time-dependent suggests that it will be important to determine when optimal epitope presentation is occurring and try to align this with when the DCs arrive in lymphoid tissues.

In terms of MHC Class II restricted presentation, this was detected for two classes of tumour antigen – differentiation (Melan-A) and viral (EBNA1), even though the antigen was produced endogenously within the cell. Unmanipulated Melan-A antigen was presented in a specific fashion by RNA electroporated DC to CD4 T-cell clones, and this may well have been due to localisation of Melan-A to lysosomes by virtue of their similarity to melanosomes. There was some preliminary evidence of co-localisation of a lysosomal marker and Melan-A in transfected DC. In contrast, for EBNA1, Class II presentation was dependent on cellular localisation and was only observed when the protein was routed into cytoplasmic or endolysosomal compartments. However, the influence of cellular localisation was reduced when experiments measured epitope presentation over a longer time-frame rather than as a short-term 'snap-shot' using T-

cell clones. When epitope presentation was measured in this way, even DC preparations with few whole antigen positive cells were able to reactivate specific T-cell responses within PBMC. In terms of vaccine design, these results raise the possibility of optimising immunogenicity by manipulation of cellular localisation and this has already been attempted in some clinical trials (Su et al., 2005). It is possible that ectopically expressing antigens in the cytoplasm rather than lysosomes might be advantageous by allowing more prolonged epitope presentation rather than a short-lived pulse.

Ex-vivo dendritic cell vaccination remains a promising option for treatment of immunologically visible malignancies such as malignant melanoma and renal cell carcinoma. In future, an improved understanding of transfection methodologies, determinants of immunogenicity and intracellular handling of antigen will all lead to more effective vaccines. As DC vaccination is used in patients with less advanced disease and lesser degrees of immune-paresis such as those with minimal residual disease, and in combination with more established therapies such as chemotherapy and immune modulation, its true potential is likely to be realised.

REFERENCES

1.   Abdel-Wahab Z, Cisco R, Dannull J, Ueno T, Abdel-Wahab O, Kalady MF, et al. Cotransfection of DC with TLR4 and MART-1 RNA induces MART-1-specific responses. The Journal of surgical research. 2005;124(2):264-73. Epub 2005/04/12.

2.   Abdel-Wahab Z, Kalady MF, Emani S, Onaitis MW, Abdel-Wahab OI, Cisco R, et al. Induction of anti-melanoma CTL response using DC transfected with mutated mRNA encoding full-length Melan-A/MART-1 antigen with an A27L amino acid substitution. Cellular immunology. 2003;224(2):86-97. Epub 2003/11/12.

3.   Adams DH, Yannelli JR, Newman W, Lawley T, Ades E, Rosenberg SA, et al. Adhesion of tumour-infiltrating lymphocytes to endothelium: a phenotypic and functional analysis. British journal of cancer. 1997;75(10):1421-31. Epub 1997/01/01.

4.   Adema GJ, de Boer AJ, Vogel AM, Loenen WA, Figdor CG. Molecular characterization of the melanocyte lineage-specific antigen gp100. The Journal of biological chemistry. 1994;269(31):20126-33. Epub 1994/08/05.

5.   Adema GJ, de Vries IJ, Punt CJ, Figdor CG. Migration of dendritic cell based cancer vaccines: in vivo veritas? Current opinion in immunology. 2005;17(2):170-4. Epub 2005/03/16.

6.   Albert ML, Sauter B, Bhardwaj N. Dendritic cells acquire antigen from apoptotic cells and induce class I-restricted CTLs. Nature. 1998;392(6671):86-9. Epub 1998/03/24.

7.   Alexandroff AB, Jackson AM, O'Donnell MA, James K. BCG immunotherapy of bladder cancer: 20 years on. Lancet. 1999;353(9165):1689-94. Epub 1999/05/21.

8.   Alijagic S, Moller P, Artuc M, Jurgovsky K, Czarnetzki BM, Schadendorf D. Dendritic cells generated from peripheral blood transfected with human tyrosinase induce specific T cell activation. European journal of immunology. 1995;25(11):3100-7. Epub 1995/11/01.

9.   Allan RS, Smith CM, Belz GT, van Lint AL, Wakim LM, Heath WR, et al. Epidermal viral immunity induced by CD8alpha+ dendritic cells but not by Langerhans cells. Science. 2003;301(5641):1925-8. Epub 2003/09/27.

10.   Allavena P, Sica A, Garlanda C, Mantovani A. The Yin-Yang of tumor-associated macrophages in neoplastic progression and immune surveillance. Immunological reviews. 2008;222:155-61. Epub 2008/03/28.

11.   Amoscato AA, Prenovitz DA, Lotze MT. Rapid extracellular degradation of synthetic class I peptides by human dendritic cells. Journal of immunology. 1998;161(8):4023-32. Epub 1998/10/21.

12.   Anderson MW, Gorski J. Cutting edge: TCR contacts as anchors: effects on affinity and HLA-DM stability. Journal of immunology. 2003;171(11):5683-7. Epub 2003/11/25.

13.   Andersson T, Patwardhan A, Emilson A, Carlsson K, Scheynius A. HLA-DM is expressed on the cell surface and colocalizes with HLA-DR and invariant chain in human Langerhans cells. Archives of dermatological research. 1998;290(12):674-80. Epub 1999/01/08.

14.   Anichini A, Maccalli C, Mortarini R, Salvi S, Mazzocchi A, Squarcina P, et al. Melanoma cells and normal melanocytes share antigens recognized by HLA-A2-restricted cytotoxic T cell clones from melanoma patients. The Journal of experimental medicine. 1993;177(4):989-98. Epub 1993/04/01.

15. Appay V, Jandus C, Voelter V, Reynard S, Coupland SE, Rimoldi D, et al. New generation vaccine induces effective melanoma-specific CD8+ T cells in the circulation but not in the tumor site. Journal of immunology. 2006;177(3):1670-8. Epub 2006/07/20.

16. Arunachalam B, Phan UT, Geuze HJ, Cresswell P. Enzymatic reduction of disulfide bonds in lysosomes: characterization of a gamma-interferon-inducible lysosomal thiol reductase (GILT). Proceedings of the National Academy of Sciences of the United States of America. 2000;97(2):745-50. Epub 2000/01/19.

17. Ashley DJ. On the incidence of carcinoma of the prostate. The Journal of pathology and bacteriology. 1965;90(1):217-24. Epub 1965/07/01.

18. Atkins MB. Interleukin-2: clinical applications. Seminars in oncology. 2002;29(3 Suppl 7):12-7. Epub 2002/06/18.

19. Bacik I, Cox JH, Anderson R, Yewdell JW, Bennink JR. TAP (transporter associated with antigen processing)-independent presentation of endogenously synthesized peptides is enhanced by endoplasmic reticulum insertion sequences located at the amino- but not carboxyl-terminus of the peptide. Journal of immunology. 1994;152(2):381-7. Epub 1994/01/15.

20. Badoual C, Hans S, Rodriguez J, Peyrard S, Klein C, Agueznay Nel H, et al. Prognostic value of tumor-infiltrating CD4+ T-cell subpopulations in head and neck cancers. Clinical cancer research : an official journal of the American Association for Cancer Research. 2006;12(2):465-72. Epub 2006/01/24.

21. Bakker AB, Schreurs MW, de Boer AJ, Kawakami Y, Rosenberg SA, Adema GJ, et al. Melanocyte lineage-specific antigen gp100 is recognized by melanoma-derived tumor-infiltrating

lymphocytes. The Journal of experimental medicine. 1994;179(3):1005-9. Epub 1994/03/01.

22. Bakker AB, Schreurs MW, Tafazzul G, de Boer AJ, Kawakami Y, Adema GJ, et al. Identification of a novel peptide derived from the melanocyte-specific gp100 antigen as the dominant epitope recognized by an HLA-A2.1-restricted anti-melanoma CTL line. International journal of cancer Journal international du cancer. 1995;62(1):97-102. Epub 1995/07/04.

23. Banchereau J, Palucka AK, Dhodapkar M, Burkeholder S, Taquet N, Rolland A, et al. Immune and clinical responses in patients with metastatic melanoma to CD34(+) progenitor-derived dendritic cell vaccine. Cancer research. 2001;61(17):6451-8. Epub 2001/08/28.

24. Barton LM, Roberts P, Trantou V, Haworth C, Kelsey H, Blamires T. Chediak-Higashi syndrome. British journal of haematology. 2004;125(1):2. Epub 2004/03/16.

25. Basombrio MA. Search for common antigenicities among twenty-five sarcomas induced by methylcholanthrene. Cancer research. 1970;30(10):2458-62. Epub 1970/10/01.

26. Bauer S, Kirschning CJ, Hacker H, Redecke V, Hausmann S, Akira S, et al. Human TLR9 confers responsiveness to bacterial DNA via species-specific CpG motif recognition. Proceedings of the National Academy of Sciences of the United States of America. 2001;98(16):9237-42. Epub 2001/07/27.

27. Baumeister W, Walz J, Zuhl F, Seemuller E. The proteasome: paradigm of a self-compartmentalizing protease. Cell. 1998;92(3):367-80. Epub 1998/02/26.

28. Becker Y. Milestones in the research on skin epidermal Langerhans/dendritic cells (LCs/DCs) from the discovery of Paul Langerhans 1868-1989. Virus genes. 2003;26(2):131-4. Epub 2003/06/14.

29.	Belardelli F, Ferrantini M, Proietti E, Kirkwood JM. Interferon-alpha in tumor immunity and immunotherapy. Cytokine & growth factor reviews. 2002;13(2):119-34. Epub 2002/03/20.

30.	Benacerraf B, Gell PG. Studies on hypersensitivity. III. The relation between delayed reactivity to the picryl group of conjugates and contact sensitivity. Immunology. 1959;2:219-29. Epub 1959/07/01.

31.	Beninga J, Rock KL, Goldberg AL. Interferon-gamma can stimulate post-proteasomal trimming of the N terminus of an antigenic peptide by inducing leucine aminopeptidase. The Journal of biological chemistry. 1998;273(30):18734-42. Epub 1998/07/21.

32.	Bennett SR, Carbone FR, Karamalis F, Miller JF, Heath WR. Induction of a CD8+ cytotoxic T lymphocyte response by cross-priming requires cognate CD4+ T cell help. The Journal of experimental medicine. 1997;186(1):65-70. Epub 1997/07/07.

33.	Benvenuti F, Lagaudriere-Gesbert C, Grandjean I, Jancic C, Hivroz C, Trautmann A, et al. Dendritic cell maturation controls adhesion, synapse formation, and the duration of the interactions with naive T lymphocytes. Journal of immunology. 2004;172(1):292-301. Epub 2003/12/23.

34.	Berson JF, Harper DC, Tenza D, Raposo G, Marks MS. Pmel17 initiates premelanosome morphogenesis within multivesicular bodies. Molecular biology of the cell. 2001;12(11):3451-64. Epub 2001/11/06.

35.	Bevan MJ. Minor H antigens introduced on H-2 different stimulating cells cross-react at the cytotoxic T cell level during in vivo priming. Journal of immunology. 1976;117(6):2233-8. Epub 1976/12/01.

36.	Bevan MJ. Helping the CD8(+) T-cell response. Nature reviews Immunology. 2004;4(8):595-602. Epub 2004/08/03.

37. Bhardwaj N. Processing and presentation of antigens by dendritic cells: implications for vaccines. Trends in molecular medicine. 2001;7(9):388-94. Epub 2001/09/01.

38. Bhatnagar V, Anjaiah S, Puri N, Darshanam BN, Ramaiah A. pH of melanosomes of B 16 murine melanoma is acidic: its physiological importance in the regulation of melanin biosynthesis. Archives of biochemistry and biophysics. 1993;307(1):183-92. Epub 1993/11/15.

39. Billingham RE. Dendritic cells. Journal of anatomy. 1948;82(Pts 1-2):93-109. Epub 1948/04/01.

40. Bioley G, Jandus C, Tuyaerts S, Rimoldi D, Kwok WW, Speiser DE, et al. Melan-A/MART-1-specific CD4 T cells in melanoma patients: identification of new epitopes and ex vivo visualization of specific T cells by MHC class II tetramers. Journal of immunology. 2006;177(10):6769-79. Epub 2006/11/04.

41. Birkeland SA, Storm HH, Lamm LU, Barlow L, Blohme I, Forsberg B, et al. Cancer risk after renal transplantation in the Nordic countries, 1964-1986. International journal of cancer Journal international du cancer. 1995;60(2):183-9. Epub 1995/01/17.

42. Blander JM, Medzhitov R. On regulation of phagosome maturation and antigen presentation. Nature immunology. 2006;7(10):1029-35. Epub 2006/09/21.

43. Bloch. The problem of pigment formation. American Journal of Medical Sciences. 1929;107:609-18.

44. Bollard CM, Cooper LJ, Heslop HE. Immunotherapy targeting EBV-expressing lymphoproliferative diseases. Best practice & research Clinical haematology. 2008;21(3):405-20. Epub 2008/09/16.

45. Bollard CM, Gottschalk S, Leen AM, Weiss H, Straathof KC, Carrum G, et al. Complete responses of relapsed lymphoma following genetic modification of tumor-antigen presenting cells and T-lymphocyte transfer. Blood. 2007;110(8):2838-45. Epub 2007/07/05.

46. Bonehill A, Heirman C, Tuyaerts S, Michiels A, Breckpot K, Brasseur F, et al. Messenger RNA-electroporated dendritic cells presenting MAGE-A3 simultaneously in HLA class I and class II molecules. Journal of immunology. 2004;172(11):6649-57. Epub 2004/05/22.

47. Bosch GJ, Joosten AM, Kessler JH, Melief CJ, Leeksma OC. Recognition of BCR-ABL positive leukemic blasts by human CD4+ T cells elicited by primary in vitro immunization with a BCR-ABL breakpoint peptide. Blood. 1996;88(9):3522-7. Epub 1996/11/01.

48. Bozzacco L, Trumpfheller C, Siegal FP, Mehandru S, Markowitz M, Carrington M, et al. DEC-205 receptor on dendritic cells mediates presentation of HIV gag protein to CD8+ T cells in a spectrum of human MHC I haplotypes. Proceedings of the National Academy of Sciences of the United States of America. 2007;104(4):1289-94. Epub 2007/01/19.

49. Brandacher G, Perathoner A, Ladurner R, Schneeberger S, Obrist P, Winkler C, et al. Prognostic value of indoleamine 2,3-dioxygenase expression in colorectal cancer: effect on tumor-infiltrating T cells. Clinical cancer research : an official journal of the American Association for Cancer Research. 2006;12(4):1144-51. Epub 2006/02/21.

50. Brossart P, Heinrich KS, Stuhler G, Behnke L, Reichardt VL, Stevanovic S, et al. Identification of HLA-A2-restricted T-cell epitopes derived from the MUC1 tumor antigen for broadly applicable vaccine therapies. Blood. 1999;93(12):4309-17. Epub 1999/06/11.

51. Brossart P, Stuhler G, Flad T, Stevanovic S, Rammensee HG, Kanz L, et al. Her-2/neu-derived peptides are tumor-associated antigens expressed by human renal cell and colon carcinoma lines and are recognized by in vitro induced specific cytotoxic T lymphocytes. Cancer research. 1998;58(4):732-6. Epub 1998/03/04.

52. Bullock TN, Colella TA, Engelhard VH. The density of peptides displayed by dendritic cells affects immune responses to human tyrosinase and gp100 in HLA-A2 transgenic mice. Journal of immunology. 2000;164(5):2354-61. Epub 2000/02/29.

53. Bullock TN, Mullins DW, Engelhard VH. Antigen density presented by dendritic cells in vivo differentially affects the number and avidity of primary, memory, and recall CD8+ T cells. Journal of immunology. 2003;170(4):1822-9. Epub 2003/02/08.

54. Burnet FM. Immunological aspects of malignant disease. Lancet. 1967;1(7501):1171-4. Epub 1967/06/03.

55. Butterfield LH, Jilani SM, Chakraborty NG, Bui LA, Ribas A, Dissette VB, et al. Generation of melanoma-specific cytotoxic T lymphocytes by dendritic cells transduced with a MART-1 adenovirus. Journal of immunology. 1998;161(10):5607-13. Epub 1998/11/20.

56. Carbone FR, Belz GT, Heath WR. Transfer of antigen between migrating and lymph node-resident DCs in peripheral T-cell tolerance and immunity. Trends in immunology. 2004;25(12):655-8. Epub 2004/11/09.

57. Carven GJ, Stern LJ. Probing the ligand-induced conformational change in HLA-DR1 by selective chemical modification and mass spectrometric mapping. Biochemistry. 2005;44(42):13625-37. Epub 2005/10/19.

58. Cassell D, Forman J. Linked recognition of helper and cytotoxic antigenic determinants for the generation of cytotoxic T lymphocytes. Annals of the New York Academy of Sciences. 1988;532:51-60. Epub 1988/01/01.

59. Castellino F, Zappacosta F, Coligan JE, Germain RN. Large protein fragments as substrates for endocytic antigen capture by MHC class II molecules. Journal of immunology. 1998;161(8):4048-57. Epub 1998/10/21.

60. Cecka JM, Gjertson DW, Terasaki PI. Pediatric renal transplantation: a review of the UNOS data. United Network for Organ Sharing. Pediatric transplantation. 1997;1(1):55-64. Epub 1997/08/01.

61. Cella M, Engering A, Pinet V, Pieters J, Lanzavecchia A. Inflammatory stimuli induce accumulation of MHC class II complexes on dendritic cells. Nature. 1997;388(6644):782-7. Epub 1997/08/21.

62. Ceppi M, Clavarino G, Gatti E, Schmidt EK, de Gassart A, Blankenship D, et al. Ribosomal protein mRNAs are translationally-regulated during human dendritic cells activation by LPS. Immunome research. 2009;5:5. Epub 2009/12/01.

63. Cernadas M, Lu J, Watts G, Brenner MB. CD1a expression defines an interleukin-12 producing population of human dendritic cells. Clinical and experimental immunology. 2009;155(3):523-33. Epub 2009/02/18.

64. Cerundolo V, Kelly A, Elliott T, Trowsdale J, Townsend A. Genes encoded in the major histocompatibility complex affecting the generation of peptides for TAP transport. European journal of immunology. 1995;25(2):554-62. Epub 1995/02/01.

65. Chapatte L, Ayyoub M, Morel S, Peitrequin AL, Levy N, Servis C, et al. Processing of tumor-associated antigen by the proteasomes of dendritic cells controls in vivo T-cell responses. Cancer research. 2006;66(10):5461-8. Epub 2006/05/19.

66. Chaux P, Vantomme V, Stroobant V, Thielemans K, Corthals J, Luiten R, et al. Identification of MAGE-3 epitopes presented by HLA-DR molecules to CD4(+) T lymphocytes. The Journal of experimental medicine. 1999;189(5):767-78. Epub 1999/03/02.

67. Chen YT. Cancer vaccine: identification of human tumor antigens by SEREX. Cancer journal. 2000;6 Suppl 3:S208-17. Epub 2000/06/30.

68. Cheng F, Wang HW, Cuenca A, Huang M, Ghansah T, Brayer J, et al. A critical role for Stat3 signaling in immune tolerance. Immunity. 2003;19(3):425-36. Epub 2003/09/23.

69. Cho YW, Terasaki PI, Cecka JM, Gjertson DW, Takemoto S. Should excessive height and weight differences between the kidney donor and recipient be avoided? Transplantation proceedings. 1997;29(1-2):104-5. Epub 1997/02/01.

70. Clay TM, Hobeika AC, Mosca PJ, Lyerly HK, Morse MA. Assays for monitoring cellular immune responses to active immunotherapy of cancer. Clinical cancer research : an official journal of the American Association for Cancer Research. 2001;7(5):1127-35. Epub 2001/05/15.

71. Cohen NR, Garg S, Brenner MB. Antigen Presentation by CD1 Lipids, T Cells, and NKT Cells in Microbial Immunity. Advances in immunology. 2009;102:1-94. Epub 2009/05/30.

72. Coley WB. II. Contribution to the Knowledge of Sarcoma. Annals of surgery. 1891;14(3):199-220. Epub 1891/09/01.

73. Colgan DF, Manley JL. Mechanism and regulation of mRNA polyadenylation. Genes & development. 1997;11(21):2755-66. Epub 1997/11/14.

74. Collins DS, Unanue ER, Harding CV. Reduction of disulfide bonds within lysosomes is a key step in antigen processing. Journal of immunology. 1991;147(12):4054-9. Epub 1991/12/15.

75. Cooney R, Baker J, Brain O, Danis B, Pichulik T, Allan P, et al. NOD2 stimulation induces autophagy in dendritic cells influencing bacterial handling and antigen presentation. Nature medicine. 2010;16(1):90-7. Epub 2009/12/08.

76. Correale P, Walmsley K, Nieroda C, Zaremba S, Zhu M, Schlom J, et al. In vitro generation of human cytotoxic T lymphocytes specific for peptides derived from prostate-specific antigen. Journal of the National Cancer Institute. 1997;89(4):293-300. Epub 1997/02/19.

77. Coussens LM, Werb Z. Inflammation and cancer. Nature. 2002;420(6917):860-7. Epub 2002/12/20.

78. Cox AL, Skipper J, Chen Y, Henderson RA, Darrow TL, Shabanowitz J, et al. Identification of a peptide recognized by five melanoma-specific human cytotoxic T cell lines. Science. 1994;264(5159):716-9. Epub 1994/04/29.

79. Cresswell P. Invariant chain structure and MHC class II function. Cell. 1996;84(4):505-7. Epub 1996/02/23.

80. Cresswell P, Bangia N, Dick T, Diedrich G. The nature of the MHC class I peptide loading complex. Immunological reviews. 1999;172:21-8. Epub 2000/01/13.

81. Crotzer VL, Blum JS. Cytosol to lysosome transport of intracellular antigens during immune surveillance. Traffic. 2008;9(1):10-6. Epub 2007/10/06.

82. Crotzer VL, Blum JS. Autophagy and its role in MHC-mediated antigen presentation. Journal of immunology. 2009;182(6):3335-41. Epub 2009/03/07.

83. Cruz M, Nandi D, Hendil KB, Monaco JJ. Cloning and characterization of mouse Lmp3 cDNA, encoding a proteasome beta subunit. Gene. 1997;190(2):251-6. Epub 1997/05/06.

84. Cunha D, Pacheco FA, Cardoso J. Vitiligo: a good prognostic factor in melanoma? Dermatology online journal. 2009;15(2):15. Epub 2009/04/02.

85. Cyster JG. Chemokines and the homing of dendritic cells to the T cell areas of lymphoid organs. The Journal of experimental medicine. 1999;189(3):447-50. Epub 1999/02/02.

86. Czerniecki BJ, Roses RE, Koski GK. Development of vaccines for high-risk ductal carcinoma in situ of the breast. Cancer research. 2007;67(14):6531-4. Epub 2007/07/20.

87. Dadaglio G, Nelson CA, Deck MB, Petzold SJ, Unanue ER. Characterization and quantitation of peptide-MHC complexes produced from hen egg lysozyme using a monoclonal antibody. Immunity. 1997;6(6):727-38. Epub 1997/06/01.

88. D'Arena G, Laurenti L, Minervini MM, Deaglio S, Bonello L, De Martino L, et al. Regulatory T-cell number is increased in chronic lymphocytic leukemia patients and correlates with progressive disease. Leukemia research. 2011;35(3):363-8. Epub 2010/10/01.

89. Dauer M, Lam V, Arnold H, Junkmann J, Kiefl R, Bauer C, et al. Combined use of toll-like receptor agonists and prostaglandin E(2) in the FastDC model: rapid generation of human monocyte-derived dendritic cells capable of migration and IL-12p70 production. Journal of immunological methods. 2008;337(2):97-105. Epub 2008/07/29.

90. Dauer M, Schad K, Herten J, Junkmann J, Bauer C, Kiefl R, et al. FastDC derived from human monocytes within 48 h effectively prime tumor antigen-specific cytotoxic T cells. Journal of immunological methods. 2005;302(1-2):145-55. Epub 2005/07/05.

91. De Maziere AM, Muehlethaler K, van Donselaar E, Salvi S, Davoust J, Cerottini JC, et al. The melanocytic protein Melan-A/MART-1 has a subcellular localization distinct from typical melanosomal proteins. Traffic. 2002;3(9):678-93. Epub 2002/08/23.

92. de Vries IJ, Lesterhuis WJ, Scharenborg NM, Engelen LP, Ruiter DJ, Gerritsen MJ, et al. Maturation of dendritic cells is a prerequisite for inducing immune responses in advanced melanoma patients. Clinical cancer research : an official journal of the American Association for Cancer Research. 2003;9(14):5091-100. Epub 2003/11/14.

93. de Vries TJ, Smeets M, de Graaf R, Hou-Jensen K, Brocker EB, Renard N, et al. Expression of gp100, MART-1, tyrosinase, and S100 in paraffin-embedded primary melanomas and locoregional, lymph node, and visceral metastases: implications for diagnosis and immunotherapy. A study conducted by the EORTC Melanoma Cooperative Group. The Journal of pathology. 2001;193(1):13-20. Epub 2001/02/13.

94. Delamarre L, Pack M, Chang H, Mellman I, Trombetta ES. Differential lysosomal proteolysis in antigen-presenting cells determines antigen fate. Science. 2005;307(5715):1630-4. Epub 2005/03/12.

95. den Haan JM, Bevan MJ. Constitutive versus activation-dependent cross-presentation of immune complexes by CD8(+) and CD8(-) dendritic cells in vivo. The Journal of experimental medicine. 2002;196(6):817-27. Epub 2002/09/18.

96. Dhodapkar KM, Krasovsky J, Williamson B, Dhodapkar MV. Antitumor monoclonal antibodies enhance cross-presentation ofcCellular antigens and the generation of myeloma-specific killer T cells by dendritic cells. The Journal of experimental medicine. 2002;195(1):125-33. Epub 2002/01/10.

97. Dhodapkar MV, Bhardwaj N. Active immunization of humans with dendritic cells. Journal of clinical immunology. 2000;20(3):167-74. Epub 2000/08/15.

98. Dhodapkar MV, Steinman RM. Antigen-bearing immature dendritic cells induce peptide-specific CD8(+) regulatory T cells in vivo in humans. Blood. 2002;100(1):174-7. Epub 2002/06/19.

99. Dieckmann D, Schultz ES, Ring B, Chames P, Held G, Hoogenboom HR, et al. Optimizing the exogenous antigen loading of monocyte-derived dendritic cells. International immunology. 2005;17(5):621-35. Epub 2005/04/13.

100. Diment S, Eidelman M, Rodriguez GM, Orlow SJ. Lysosomal hydrolases are present in melanosomes and are elevated in melanizing cells. The Journal of biological chemistry. 1995;270(9):4213-5. Epub 1995/03/03.

101. Disis ML. Enhancing cancer vaccine efficacy via modulation of the tumor microenvironment. Clinical cancer research : an official journal of the American Association for Cancer Research. 2009;15(21):6476-8. Epub 2009/10/29.

102. Disis ML, Cheever MA. Oncogenic proteins as tumor antigens. Current opinion in immunology. 1996;8(5):637-42. Epub 1996/10/01.

103. Do Y, Nagarkatti PS, Nagarkatti M. Role of CD44 and hyaluronic acid (HA) in activation of alloreactive and antigen-specific T cells by bone marrow-derived dendritic

cells. Journal of immunotherapy. 2004;27(1):1-12. Epub 2003/12/17.

104. Dong H, Strome SE, Salomao DR, Tamura H, Hirano F, Flies DB, et al. Tumor-associated B7-H1 promotes T-cell apoptosis: a potential mechanism of immune evasion. Nature medicine. 2002;8(8):793-800. Epub 2002/07/02.

105. Dorfel D, Appel S, Grunebach F, Weck MM, Muller MR, Heine A, et al. Processing and presentation of HLA class I and II epitopes by dendritic cells after transfection with in vitro-transcribed MUC1 RNA. Blood. 2005;105(8):3199-205. Epub 2004/12/25.

106. Dubsky P, Saito H, Leogier M, Dantin C, Connolly JE, Banchereau J, et al. IL-15-induced human DC efficiently prime melanoma-specific naive CD8+ T cells to differentiate into CTL. European journal of immunology. 2007;37(6):1678-90. Epub 2007/05/12.

107. Dullaers M, Breckpot K, Van Meirvenne S, Bonehill A, Tuyaerts S, Michiels A, et al. Side-by-side comparison of lentivirally transduced and mRNA-electroporated dendritic cells: implications for cancer immunotherapy protocols. Molecular therapy : the journal of the American Society of Gene Therapy. 2004;10(4):768-79. Epub 2004/09/29.

108. Dunbar PR, Smith CL, Chao D, Salio M, Shepherd D, Mirza F, et al. A shift in the phenotype of melan-A-specific CTL identifies melanoma patients with an active tumor-specific immune response. Journal of immunology. 2000;165(11):6644-52. Epub 2000/11/22.

109. Dutoit V, Taub RN, Papadopoulos KP, Talbot S, Keohan ML, Brehm M, et al. Multiepitope CD8(+) T cell response to a NY-ESO-1 peptide vaccine results in imprecise tumor targeting.

The Journal of clinical investigation. 2002;110(12):1813-22. Epub 2002/12/19.

110. Elliott T, Neefjes J. The complex route to MHC class I-peptide complexes. Cell. 2006;127(2):249-51. Epub 2006/10/24.

111. English L, Chemali M, Duron J, Rondeau C, Laplante A, Gingras D, et al. Autophagy enhances the presentation of endogenous viral antigens on MHC class I molecules during HSV-1 infection. Nature immunology. 2009;10(5):480-7. Epub 2009/03/24.

112. Evel-Kabler K, Song XT, Aldrich M, Huang XF, Chen SY. SOCS1 restricts dendritic cells' ability to break self tolerance and induce antitumor immunity by regulating IL-12 production and signaling. The Journal of clinical investigation. 2006;116(1):90-100. Epub 2005/12/17.

113. Falconieri G, Luna MA, Pizzolitto S, DeMaglio G, Angione V, Rocco M. Eosinophil-rich squamous carcinoma of the oral cavity: a study of 13 cases and delineation of a possible new microscopic entity. Annals of diagnostic pathology. 2008;12(5):322-7. Epub 2008/09/09.

114. Fallas JL, Tobin HM, Lou O, Guo D, Sant'Angelo DB, Denzin LK. Ectopic expression of HLA-DO in mouse dendritic cells diminishes MHC class II antigen presentation. Journal of immunology. 2004;173(3):1549-60. Epub 2004/07/22.

115. Fehling HJ, Swat W, Laplace C, Kuhn R, Rajewsky K, Muller U, et al. MHC class I expression in mice lacking the proteasome subunit LMP-7. Science. 1994;265(5176):1234-7. Epub 1994/08/26.

116. Figdor CG, de Vries IJ, Lesterhuis WJ, Melief CJ. Dendritic cell immunotherapy: mapping the way. Nature medicine. 2004;10(5):475-80. Epub 2004/05/04.

117. Frumento G, Rotondo R, Tonetti M, Damonte G, Benatti U, Ferrara GB. Tryptophan-derived catabolites are responsible for inhibition of T and natural killer cell proliferation induced by indoleamine 2,3-dioxygenase. The Journal of experimental medicine. 2002;196(4):459-68. Epub 2002/08/21.

118. Gaczynska M, Rock KL, Goldberg AL. Gamma-interferon and expression of MHC genes regulate peptide hydrolysis by proteasomes. Nature. 1993;365(6443):264-7. Epub 1993/09/16.

119. Gajewski J, Gjertson D, Cecka M, Tonai R, Przepiorka D, Hunt L, et al. The impact of T-cell depletion on the effects of HLA DR beta 1 and DQ beta allele matching in HLA serologically identical unrelated donor bone marrow transplantation. Biology of blood and marrow transplantation : journal of the American Society for Blood and Marrow Transplantation. 1997;3(2):76-82. Epub 1997/06/01.

120. Gajewski TF, Meng Y, Harlin H. Immune suppression in the tumor microenvironment. Journal of immunotherapy. 2006;29(3):233-40. Epub 2006/05/16.

121. Galon J, Costes A, Sanchez-Cabo F, Kirilovsky A, Mlecnik B, Lagorce-Pages C, et al. Type, density, and location of immune cells within human colorectal tumors predict clinical outcome. Science. 2006;313(5795):1960-4. Epub 2006/09/30.

122. Gaspari AA. Mechanism of action and other potential roles of an immune response modifier. Cutis; cutaneous medicine for the practitioner. 2007;79(4 Suppl):36-45. Epub 2007/05/19.

123. Giermasz AS, Urban JA, Nakamura Y, Watchmaker P, Cumberland RL, Gooding W, et al. Type-1 polarized dendritic cells primed for high IL-12 production show enhanced activity as cancer vaccines. Cancer immunology, immunotherapy : CII. 2009;58(8):1329-36. Epub 2009/01/22.

124. Gilboa E. How tumors escape immune destruction and what we can do about it. Cancer immunology, immunotherapy : CII. 1999;48(7):382-5. Epub 1999/09/29.

125. Gilboa E. DC-based cancer vaccines. The Journal of clinical investigation. 2007;117(5):1195-203. Epub 2007/05/04.

126. Giordano F, Bonetti C, Surace EM, Marigo V, Raposo G. The ocular albinism type 1 (OA1) G-protein-coupled receptor functions with MART-1 at early stages of melanogenesis to control melanosome identity and composition. Human molecular genetics. 2009;18(23):4530-45. Epub 2009/09/01.

127. Gjertsen MK, Saeterdal I, Thorsby E, Gaudernack G. Characterisation of immune responses in pancreatic carcinoma patients after mutant p21 ras peptide vaccination. British journal of cancer. 1996;74(11):1828-33. Epub 1996/12/01.

128. Gjertson DW. Look-up survival tables for renal transplantation. Clinical transplants. 1997:337-83. Epub 1997/01/01.

129. Gjertson DW, Terasaki PI, Cecka JM, Takemoto S, Cho YW. Senior citizens pool for aged kidneys. Transplantation proceedings. 1997;29(1-2):129. Epub 1997/02/01.

130. Glickman MH, Ciechanover A. The ubiquitin-proteasome proteolytic pathway: destruction for the sake of construction. Physiological reviews. 2002;82(2):373-428. Epub 2002/03/28.

131. Godefroy E, Scotto L, Souleimanian NE, Ritter G, Old LJ, Jotereau F, et al. Identification of two Melan-A CD4+ T cell epitopes presented by frequently expressed MHC class II alleles. Clinical immunology. 2006;121(1):54-62. Epub 2006/07/04.

132. Goldberg AL, Rock KL. Proteolysis, proteasomes and antigen presentation. Nature. 1992;357(6377):375-9. Epub 1992/06/04.

133. Goth S, Nguyen V, Shastri N. Generation of naturally processed peptide/MHC class I complexes is independent of the stability of endogenously synthesized precursors. Journal of immunology. 1996;157(5):1894-904. Epub 1996/09/01.

134. Grasser FA, Murray PG, Kremmer E, Klein K, Remberger K, Feiden W, et al. Monoclonal antibodies directed against the Epstein-Barr virus-encoded nuclear antigen 1 (EBNA1): immunohistologic detection of EBNA1 in the malignant cells of Hodgkin's disease. Blood. 1994;84(11):3792-8. Epub 1994/12/01.

135. Groothuis T, Neefjes J. The ins and outs of intracellular peptides and antigen presentation by MHC class I molecules. Current topics in microbiology and immunology. 2005;300:127-48. Epub 2006/04/01.

136. Grunebach F, Muller MR, Nencioni A, Brossart P. Delivery of tumor-derived RNA for the induction of cytotoxic T-lymphocytes. Gene therapy. 2003;10(5):367-74. Epub 2003/02/26.

137. Habjan M, Andersson I, Klingstrom J, Schumann M, Martin A, Zimmermann P, et al. Processing of genome 5' termini as a strategy of negative-strand RNA viruses to avoid RIG-I-dependent interferon induction. PloS one. 2008;3(4):e2032. Epub 2008/05/01.

138. Haigh TA, Lin X, Jia H, Hui EP, Chan AT, Rickinson AB, et al. EBV latent membrane proteins (LMPs) 1 and 2 as immunotherapeutic targets: LMP-specific CD4+ cytotoxic T cell recognition of EBV-transformed B cell lines. Journal of immunology. 2008;180(3):1643-54. Epub 2008/01/23.

139. Haines AM, Irvine AS, Mountain A, Charlesworth J, Farrow NA, Husain RD, et al. CL22 - a novel cationic peptide for

efficient transfection of mammalian cells. Gene therapy. 2001;8(2):99-110. Epub 2001/04/21.

140. Haque T, McAulay KA, Kelly D, Crawford DH. Allogeneic T-cell therapy for Epstein-Barr virus-positive posttransplant lymphoproliferative disease: long-term follow-up. Transplantation. 2010;90(1):93-4. Epub 2010/07/08.

141. Heiser A, Coleman D, Dannull J, Yancey D, Maurice MA, Lallas CD, et al. Autologous dendritic cells transfected with prostate-specific antigen RNA stimulate CTL responses against metastatic prostate tumors. The Journal of clinical investigation. 2002;109(3):409-17. Epub 2002/02/06.

142. Held G, Wadle A, Dauth N, Stewart-Jones G, Sturm C, Thiel M, et al. MHC-peptide-specific antibodies reveal inefficient presentation of an HLA-A*0201-restricted, Melan-A-derived peptide after active intracellular processing. European journal of immunology. 2007;37(7):2008-17. Epub 2007/06/15.

143. Heller KN, Arrey F, Steinherz P, Portlock C, Chadburn A, Kelly K, et al. Patients with Epstein Barr virus-positive lymphomas have decreased CD4(+) T-cell responses to the viral nuclear antigen 1. International journal of cancer Journal international du cancer. 2008;123(12):2824-31. Epub 2008/09/11.

144. Henry RM, Hoppe AD, Joshi N, Swanson JA. The uniformity of phagosome maturation in macrophages. The Journal of cell biology. 2004;164(2):185-94. Epub 2004/01/14.

145. Hernando JJ, Park TW, Fischer HP, Zivanovic O, Braun M, Polcher M, et al. Vaccination with dendritic cells transfected with mRNA-encoded folate-receptor-alpha for relapsed metastatic ovarian cancer. The lancet oncology. 2007;8(5):451-4. Epub 2007/05/01.

146. Herter S, Osterloh P, Hilf N, Rechtsteiner G, Hohfeld J, Rammensee HG, et al. Dendritic cell aggresome-like-induced structure formation and delayed antigen presentation coincide in influenza virus-infected dendritic cells. Journal of immunology. 2005;175(2):891-8. Epub 2005/07/09.

147. Heslop HE, Slobod KS, Pule MA, Hale GA, Rousseau A, Smith CA, et al. Long-term outcome of EBV-specific T-cell infusions to prevent or treat EBV-related lymphoproliferative disease in transplant recipients. Blood. 2010;115(5):925-35. Epub 2009/11/03.

148. Heufler C, Koch F, Stanzl U, Topar G, Wysocka M, Trinchieri G, et al. Interleukin-12 is produced by dendritic cells and mediates T helper 1 development as well as interferon-gamma production by T helper 1 cells. European journal of immunology. 1996;26(3):659-68. Epub 1996/03/01.

149. Higano CS, Schellhammer PF, Small EJ, Burch PA, Nemunaitis J, Yuh L, et al. Integrated data from 2 randomized, double-blind, placebo-controlled, phase 3 trials of active cellular immunotherapy with sipuleucel-T in advanced prostate cancer. Cancer. 2009;115(16):3670-9. Epub 2009/06/19.

150. Hiltbold EM, Roche PA. Trafficking of MHC class II molecules in the late secretory pathway. Current opinion in immunology. 2002;14(1):30-5. Epub 2002/01/16.

151. Hintzen G, Ohl L, del Rio ML, Rodriguez-Barbosa JI, Pabst O, Kocks JR, et al. Induction of tolerance to innocuous inhaled antigen relies on a CCR7-dependent dendritic cell-mediated antigen transport to the bronchial lymph node. Journal of immunology. 2006;177(10):7346-54. Epub 2006/11/04.

152. Hoashi T, Muller J, Vieira WD, Rouzaud F, Kikuchi K, Tamaki K, et al. The repeat domain of the melanosomal matrix protein PMEL17/GP100 is required for the formation of

organellar fibers. The Journal of biological chemistry. 2006;281(30):21198-208. Epub 2006/05/10.

153. Hoashi T, Watabe H, Muller J, Yamaguchi Y, Vieira WD, Hearing VJ. MART-1 is required for the function of the melanosomal matrix protein PMEL17/GP100 and the maturation of melanosomes. The Journal of biological chemistry. 2005;280(14):14006-16. Epub 2005/02/08.

154. Hodi FS, O'Day SJ, McDermott DF, Weber RW, Sosman JA, Haanen JB, et al. Improved survival with ipilimumab in patients with metastatic melanoma. The New England journal of medicine. 2010;363(8):711-23. Epub 2010/06/08.

155. Hoene V, Peiser M, Wanner R. Human monocyte-derived dendritic cells express TLR9 and react directly to the CpG-A oligonucleotide D19. Journal of leukocyte biology. 2006;80(6):1328-36. Epub 2006/09/27.

156. Hom SS, Topalian SL, Simonis T, Mancini M, Rosenberg SA. Common expression of melanoma tumor-associated antigens recognized by human tumor infiltrating lymphocytes: analysis by human lymphocyte antigen restriction. Journal of immunotherapy : official journal of the Society for Biological Therapy. 1991;10(3):153-64. Epub 1991/06/01.

157. Hopwood P, Crawford DH. The role of EBV in post-transplant malignancies: a review. Journal of clinical pathology. 2000;53(4):248-54. Epub 2000/05/24.

158. Hung K, Hayashi R, Lafond-Walker A, Lowenstein C, Pardoll D, Levitsky H. The central role of CD4(+) T cells in the antitumor immune response. The Journal of experimental medicine. 1998;188(12):2357-68. Epub 1998/12/22.

159. Ikehara S, Pahwa RN, Fernandes G, Hansen CT, Good RA. Functional T cells in athymic nude mice. Proceedings of the

National Academy of Sciences of the United States of America. 1984;81(3):886-8. Epub 1984/02/01.

160. Irvine AS, Trinder PK, Laughton DL, Ketteringham H, McDermott RH, Reid SC, et al. Efficient nonviral transfection of dendritic cells and their use for in vivo immunization. Nature biotechnology. 2000;18(12):1273-8. Epub 2000/12/02.

161. Irvine DJ, Purbhoo MA, Krogsgaard M, Davis MM. Direct observation of ligand recognition by T cells. Nature. 2002;419(6909):845-9. Epub 2002/10/25.

162. Itano AA, McSorley SJ, Reinhardt RL, Ehst BD, Ingulli E, Rudensky AY, et al. Distinct dendritic cell populations sequentially present antigen to CD4 T cells and stimulate different aspects of cell-mediated immunity. Immunity. 2003;19(1):47-57. Epub 2003/07/23.

163. Ito D, Visus C, Hoffmann TK, Balz V, Bier H, Appella E, et al. Immunological characterization of missense mutations occurring within cytotoxic T cell-defined p53 epitopes in HLA-A*0201+ squamous cell carcinomas of the head and neck. International journal of cancer Journal international du cancer. 2007;120(12):2618-24. Epub 2007/02/13.

164. Jancic C, Chuluyan HE, Morelli A, Larregina A, Kolkowski E, Saracco M, et al. Interactions of dendritic cells with fibronectin and endothelial cells. Immunology. 1998;95(2):283-90. Epub 1998/11/21.

165. Janeway T, Walport, Schlomik. Immunobiology: the immune system in health and disease. 2005.

166. Janssen EM, Droin NM, Lemmens EE, Pinkoski MJ, Bensinger SJ, Ehst BD, et al. CD4+ T-cell help controls CD8+ T-cell memory via TRAIL-mediated activation-induced cell death. Nature. 2005;434(7029):88-93. Epub 2005/03/04.

167. Janssen EM, Lemmens EE, Wolfe T, Christen U, von Herrath MG, Schoenberger SP. CD4+ T cells are required for secondary expansion and memory in CD8+ T lymphocytes. Nature. 2003;421(6925):852-6. Epub 2003/02/21.

168. Jensen PE. Recent advances in antigen processing and presentation. Nature immunology. 2007;8(10):1041-8. Epub 2007/09/20.

169. Jongmans W, Tiemessen DM, van Vlodrop IJ, Mulders PF, Oosterwijk E. Th1-polarizing capacity of clinical-grade dendritic cells is triggered by Ribomunyl but is compromised by PGE2: the importance of maturation cocktails. Journal of immunotherapy. 2005;28(5):480-7. Epub 2005/08/23.

170. Jonuleit H, Kuhn U, Muller G, Steinbrink K, Paragnik L, Schmitt E, et al. Pro-inflammatory cytokines and prostaglandins induce maturation of potent immunostimulatory dendritic cells under fetal calf serum-free conditions. European journal of immunology. 1997;27(12):3135-42. Epub 1998/02/17.

171. Jusforgues-Saklani H, Uhl M, Blachere N, Lemaitre F, Lantz O, Bousso P, et al. Antigen persistence is required for dendritic cell licensing and CD8+ T cell cross-priming. Journal of immunology. 2008;181(5):3067-76. Epub 2008/08/21.

172. Kaka AS, Foster AE, Weiss HL, Rooney CM, Leen AM. Using dendritic cell maturation and IL-12 producing capacity as markers of function: a cautionary tale. Journal of immunotherapy. 2008;31(4):359-69. Epub 2008/04/09.

173. Kalinski P, Vieira PL, Schuitemaker JH, de Jong EC, Kapsenberg ML. Prostaglandin E(2) is a selective inducer of interleukin-12 p40 (IL-12p40) production and an inhibitor of bioactive IL-12p70 heterodimer. Blood. 2001;97(11):3466-9. Epub 2001/05/23.

174. Kapur RP, Bigler SA, Skelly M, Gown AM. Anti-melanoma monoclonal antibody HMB45 identifies an oncofetal glycoconjugate associated with immature melanosomes. The journal of histochemistry and cytochemistry : official journal of the Histochemistry Society. 1992;40(2):207-12. Epub 1992/02/01.

175. Katz SC, Pillarisetty V, Bamboat ZM, Shia J, Hedvat C, Gonen M, et al. T cell infiltrate predicts long-term survival following resection of colorectal cancer liver metastases. Annals of surgical oncology. 2009;16(9):2524-30. Epub 2009/07/02.

176. Kawakami Y, Eliyahu S, Delgado CH, Robbins PF, Rivoltini L, Topalian SL, et al. Cloning of the gene coding for a shared human melanoma antigen recognized by autologous T cells infiltrating into tumor. Proceedings of the National Academy of Sciences of the United States of America. 1994;91(9):3515-9. Epub 1994/04/26.

177. Kawakami Y, Eliyahu S, Sakaguchi K, Robbins PF, Rivoltini L, Yannelli JR, et al. Identification of the immunodominant peptides of the MART-1 human melanoma antigen recognized by the majority of HLA-A2-restricted tumor infiltrating lymphocytes. The Journal of experimental medicine. 1994;180(1):347-52. Epub 1994/07/01.

178. Kawakami Y, Robbins PF, Wang RF, Parkhurst M, Kang X, Rosenberg SA. The use of melanosomal proteins in the immunotherapy of melanoma. Journal of immunotherapy. 1998;21(4):237-46. Epub 1998/07/22.

179. Kennedy MK, Glaccum M, Brown SN, Butz EA, Viney JL, Embers M, et al. Reversible defects in natural killer and memory CD8 T cell lineages in interleukin 15-deficient mice. The Journal of experimental medicine. 2000;191(5):771-80. Epub 2000/03/08.

180. Kern DH, Sondak VK, Morgan CR, Hildebrand-Zanki SU. Clinical application of the thymidine incorporation assay. Annals of clinical and laboratory science. 1987;17(6):383-8. Epub 1987/11/01.

181. Khan N, Hislop A, Gudgeon N, Cobbold M, Khanna R, Nayak L, et al. Herpesvirus-specific CD8 T cell immunity in old age: cytomegalovirus impairs the response to a coresident EBV infection. Journal of immunology. 2004;173(12):7481-9. Epub 2004/12/09.

182. Khan S, de Giuli R, Schmidtke G, Bruns M, Buchmeier M, van den Broek M, et al. Cutting edge: neosynthesis is required for the presentation of a T cell epitope from a long-lived viral protein. Journal of immunology. 2001;167(9):4801-4. Epub 2001/10/24.

183. Kim CJ, Prevette T, Cormier J, Overwijk W, Roden M, Restifo NP, et al. Dendritic cells infected with poxviruses encoding MART-1/Melan A sensitize T lymphocytes in vitro. Journal of immunotherapy. 1997;20(4):276-86. Epub 1997/07/01.

184. Kitamura R, Sekimoto T, Ito S, Harada S, Yamagata H, Masai H, et al. Nuclear import of Epstein-Barr virus nuclear antigen 1 mediated by NPI-1 (Importin alpha5) is up- and down-regulated by phosphorylation of the nuclear localization signal for which Lys379 and Arg380 are essential. Journal of virology. 2006;80(4):1979-91. Epub 2006/01/28.

185. Klionsky DJ. Autophagy. Current biology : CB. 2005;15(8):R282-3. Epub 2005/04/28.

186. Klionsky DJ, Emr SD. Autophagy as a regulated pathway of cellular degradation. Science. 2000;290(5497):1717-21. Epub 2000/12/02.

187. Kobayashi H, Kokubo T, Sato K, Kimura S, Asano K, Takahashi H, et al. CD4+ T cells from peripheral blood of a

melanoma patient recognize peptides derived from nonmutated tyrosinase. Cancer research. 1998;58(2):296-301. Epub 1998/01/27.

188. Kobayashi H, Lu J, Celis E. Identification of helper T-cell epitopes that encompass or lie proximal to cytotoxic T-cell epitopes in the gp100 melanoma tumor antigen. Cancer research. 2001;61(20):7577-84. Epub 2001/10/19.

189. Kyte JA, Mu L, Aamdal S, Kvalheim G, Dueland S, Hauser M, et al. Phase I/II trial of melanoma therapy with dendritic cells transfected with autologous tumor-mRNA. Cancer gene therapy. 2006;13(10):905-18. Epub 2006/05/20.

190. Landi A, Babiuk LA, van Drunen Littel-van den Hurk S. High transfection efficiency, gene expression, and viability of monocyte-derived human dendritic cells after nonviral gene transfer. Journal of leukocyte biology. 2007;82(4):849-60. Epub 2007/07/14.

191. Langenkamp A, Messi M, Lanzavecchia A, Sallusto F. Kinetics of dendritic cell activation: impact on priming of TH1, TH2 and nonpolarized T cells. Nature immunology. 2000;1(4):311-6. Epub 2001/03/23.

192. Lankat-Buttgereit B, Tampe R. The transporter associated with antigen processing: function and implications in human diseases. Physiological reviews. 2002;82(1):187-204. Epub 2002/01/05.

193. Lapenta C, Santini SM, Spada M, Donati S, Urbani F, Accapezzato D, et al. IFN-alpha-conditioned dendritic cells are highly efficient in inducing cross-priming CD8(+) T cells against exogenous viral antigens. European journal of immunology. 2006;36(8):2046-60. Epub 2006/07/21.

194. Lappin MB, Weiss JM, Delattre V, Mai B, Dittmar H, Maier C, et al. Analysis of mouse dendritic cell migration in vivo

upon subcutaneous and intravenous injection. Immunology. 1999;98(2):181-8. Epub 1999/12/14.

195. Larsson M, Fonteneau JF, Somersan S, Sanders C, Bickham K, Thomas EK, et al. Efficiency of cross presentation of vaccinia virus-derived antigens by human dendritic cells. European journal of immunology. 2001;31(12):3432-42. Epub 2001/12/18.

196. Latchman Y, Wood CR, Chernova T, Chaudhary D, Borde M, Chernova I, et al. PD-L2 is a second ligand for PD-1 and inhibits T cell activation. Nature immunology. 2001;2(3):261-8. Epub 2001/02/27.

197. Latz E, Visintin A, Espevik T, Golenbock DT. Mechanisms of TLR9 activation. Journal of endotoxin research. 2004;10(6):406-12. Epub 2004/12/14.

198. Lee PP, Yee C, Savage PA, Fong L, Brockstedt D, Weber JS, et al. Characterization of circulating T cells specific for tumor-associated antigens in melanoma patients. Nature medicine. 1999;5(6):677-85. Epub 1999/06/17.

199. Leen A, Meij P, Redchenko I, Middeldorp J, Bloemena E, Rickinson A, et al. Differential immunogenicity of Epstein-Barr virus latent-cycle proteins for human CD4(+) T-helper 1 responses. Journal of virology. 2001;75(18):8649-59. Epub 2001/08/17.

200. Leight ER, Sugden B. EBNA-1: a protein pivotal to latent infection by Epstein-Barr virus. Reviews in medical virology. 2000;10(2):83-100. Epub 2000/03/14.

201. Lelouard H, Ferrand V, Marguet D, Bania J, Camosseto V, David A, et al. Dendritic cell aggresome-like induced structures are dedicated areas for ubiquitination and storage of newly synthesized defective proteins. The Journal of cell biology. 2004;164(5):667-75. Epub 2004/02/26.

202. Lelouard H, Gatti E, Cappello F, Gresser O, Camosseto V, Pierre P. Transient aggregation of ubiquitinated proteins during dendritic cell maturation. Nature. 2002;417(6885):177-82. Epub 2002/05/10.

203. Lenz P, Bacot SM, Frazier-Jessen MR, Feldman GM. Nucleoporation of dendritic cells: efficient gene transfer by electroporation into human monocyte-derived dendritic cells. FEBS letters. 2003;538(1-3):149-54. Epub 2003/03/14.

204. Lepage S, Lapointe R. Melanosomal targeting sequences from gp100 are essential for MHC class II-restricted endogenous epitope presentation and mobilization to endosomal compartments. Cancer research. 2006;66(4):2423-32. Epub 2006/02/21.

205. Lesterhuis WJ, De Vries IJ, Schreibelt G, Schuurhuis DH, Aarntzen EH, De Boer A, et al. Immunogenicity of dendritic cells pulsed with CEA peptide or transfected with CEA mRNA for vaccination of colorectal cancer patients. Anticancer research. 2010;30(12):5091-7. Epub 2010/12/29.

206. Leung CS, Haigh TA, Mackay LK, Rickinson AB, Taylor GS. Nuclear location of an endogenously expressed antigen, EBNA1, restricts access to macroautophagy and the range of CD4 epitope display. Proceedings of the National Academy of Sciences of the United States of America. 2010;107(5):2165-70. Epub 2010/02/06.

207. Levitskaya J, Coram M, Levitsky V, Imreh S, Steigerwald-Mullen PM, Klein G, et al. Inhibition of antigen processing by the internal repeat region of the Epstein-Barr virus nuclear antigen-1. Nature. 1995;375(6533):685-8. Epub 1995/06/22.

208. Li MO, Flavell RA. Contextual regulation of inflammation: a duet by transforming growth factor-beta and interleukin-10. Immunity. 2008;28(4):468-76. Epub 2008/04/11.

209. Liljedahl M, Kuwana T, Fung-Leung WP, Jackson MR, Peterson PA, Karlsson L. HLA-DO is a lysosomal resident which requires association with HLA-DM for efficient intracellular transport. The EMBO journal. 1996;15(18):4817-24. Epub 1996/09/16.

210. Lindquist RL, Shakhar G, Dudziak D, Wardemann H, Eisenreich T, Dustin ML, et al. Visualizing dendritic cell networks in vivo. Nature immunology. 2004;5(12):1243-50. Epub 2004/11/16.

211. Long HM, Haigh TA, Gudgeon NH, Leen AM, Tsang CW, Brooks J, et al. CD4+ T-cell responses to Epstein-Barr virus (EBV) latent-cycle antigens and the recognition of EBV-transformed lymphoblastoid cell lines. Journal of virology. 2005;79(8):4896-907. Epub 2005/03/30.

212. Lundquist CA, Tobiume M, Zhou J, Unutmaz D, Aiken C. Nef-mediated downregulation of CD4 enhances human immunodeficiency virus type 1 replication in primary T lymphocytes. Journal of virology. 2002;76(9):4625-33. Epub 2002/04/05.

213. Macagno A, Gilliet M, Sallusto F, Lanzavecchia A, Nestle FO, Groettrup M. Dendritic cells up-regulate immunoproteasomes and the proteasome regulator PA28 during maturation. European journal of immunology. 1999;29(12):4037-42. Epub 1999/12/22.

214. Mackay LK, Long HM, Brooks JM, Taylor GS, Leung CS, Chen A, et al. T cell detection of a B-cell tropic virus infection: newly-synthesised versus mature viral proteins as antigen sources for CD4 and CD8 epitope display. PLoS pathogens. 2009;5(12):e1000699. Epub 2009/12/19.

215. Maresh GA, Wang WC, Beam KS, Malacko AR, Hellstrom I, Hellstrom KE, et al. Differential processing and secretion of the melanoma-associated ME20 antigen. Archives of biochemistry and biophysics. 1994;311(1):95-102. Epub 1994/05/15.

216. Marincola FM, Jaffee EM, Hicklin DJ, Ferrone S. Escape of human solid tumors from T-cell recognition: molecular mechanisms and functional significance. Advances in immunology. 2000;74:181-273. Epub 1999/12/22.

217. Marsden MJ, Cox D, Secombes CJ. Antigen-induced release of macrophage activating factor from rainbow trout Oncorhynchus mykiss leucocytes. Veterinary immunology and immunopathology. 1994;42(2):199-208. Epub 1994/08/01.

218. Mathew RM, Cohen AB, Galetta SL, Alavi A, Dalmau J. Paraneoplastic cerebellar degeneration: Yo-expressing tumor revealed after a 5-year follow-up with FDG-PET. Journal of the neurological sciences. 2006;250(1-2):153-5. Epub 2006/10/03.

219. Mautner J, Pich D, Nimmerjahn F, Milosevic S, Adhikary D, Christoph H, et al. Epstein-Barr virus nuclear antigen 1 evades direct immune recognition by CD4+ T helper cells. European journal of immunology. 2004;34(9):2500-9. Epub 2004/08/13.

220. McKenna HJ, Stocking KL, Miller RE, Brasel K, De Smedt T, Maraskovsky E, et al. Mice lacking flt3 ligand have deficient hematopoiesis affecting hematopoietic progenitor cells, dendritic cells, and natural killer cells. Blood. 2000;95(11):3489-97. Epub 2000/05/29.

221. Meisel R, Zibert A, Laryea M, Gobel U, Daubener W, Dilloo D. Human bone marrow stromal cells inhibit allogeneic T-cell responses by indoleamine 2,3-dioxygenase-mediated tryptophan degradation. Blood. 2004;103(12):4619-21. Epub 2004/03/06.

222. Mellman I. Antigen processing and presentation by dendritic cells: cell biological mechanisms. Advances in experimental medicine and biology. 2005;560:63-7. Epub 2005/06/04.

223. Mellman I. Antigen processing and presentation by dendritic cells: cell biological mechanisms. Advances in experimental medicine and biology. 2005;560:63-7. Epub 2005/06/04.

224. Mellor AL, Munn DH. Tryptophan catabolism prevents maternal T cells from activating lethal anti-fetal immune responses. Journal of reproductive immunology. 2001;52(1-2):5-13. Epub 2001/10/16.

225. Mendoza-Naranjo A, Saez PJ, Johansson CC, Ramirez M, Mandakovic D, Pereda C, et al. Functional gap junctions facilitate melanoma antigen transfer and cross-presentation between human dendritic cells. Journal of immunology. 2007;178(11):6949-57. Epub 2007/05/22.

226. Michaeli Y, Denkberg G, Sinik K, Lantzy L, Chih-Sheng C, Beauverd C, et al. Expression hierarchy of T cell epitopes from melanoma differentiation antigens: unexpected high level presentation of tyrosinase-HLA-A2 Complexes revealed by peptide-specific, MHC-restricted, TCR-like antibodies. Journal of immunology. 2009;182(10):6328-41. Epub 2009/05/06.

227. Mohamadzadeh M, Berard F, Essert G, Chalouni C, Pulendran B, Davoust J, et al. Interleukin 15 skews monocyte differentiation into dendritic cells with features of Langerhans cells. The Journal of experimental medicine. 2001;194(7):1013-20. Epub 2001/10/03.

228. Momburg F, Neefjes JJ, Hammerling GJ. Peptide selection by MHC-encoded TAP transporters. Current opinion in immunology. 1994;6(1):32-7. Epub 1994/02/01.

229. Monaco JJ, McDevitt HO. The LMP antigens: a stable MHC-controlled multisubunit protein complex. Human immunology. 1986;15(4):416-26. Epub 1986/04/01.

230. Mora JR, Bono MR, Manjunath N, Weninger W, Cavanagh LL, Rosemblatt M, et al. Selective imprinting of gut-homing T cells by Peyer's patch dendritic cells. Nature. 2003;424(6944):88-93. Epub 2003/07/04.

231. Morel S, Levy F, Burlet-Schiltz O, Brasseur F, Probst-Kepper M, Peitrequin AL, et al. Processing of some antigens by the standard proteasome but not by the immunoproteasome results in poor presentation by dendritic cells. Immunity. 2000;12(1):107-17. Epub 2000/02/08.

232. Morse MA, Coleman RE, Akabani G, Niehaus N, Coleman D, Lyerly HK. Migration of human dendritic cells after injection in patients with metastatic malignancies. Cancer research. 1999;59(1):56-8. Epub 1999/01/19.

233. Morse MA, Nair SK, Boczkowski D, Tyler D, Hurwitz HI, Proia A, et al. The feasibility and safety of immunotherapy with dendritic cells loaded with CEA mRNA following neoadjuvant chemoradiotherapy and resection of pancreatic cancer. International journal of gastrointestinal cancer. 2002;32(1):1-6. Epub 2003/03/13.

234. Morse MA, Nair SK, Mosca PJ, Hobeika AC, Clay TM, Deng Y, et al. Immunotherapy with autologous, human dendritic cells transfected with carcinoembryonic antigen mRNA. Cancer investigation. 2003;21(3):341-9. Epub 2003/08/07.

235. Mosca PJ, Hobeika AC, Clay TM, Nair SK, Thomas EK, Morse MA, et al. A subset of human monocyte-derived dendritic cells expresses high levels of interleukin-12 in response to combined CD40 ligand and interferon-gamma treatment. Blood. 2000;96(10):3499-504. Epub 2000/11/09.

236. Mu LJ, Kyte JA, Kvalheim G, Aamdal S, Dueland S, Hauser M, et al. Immunotherapy with allotumour mRNA-transfected dendritic cells in androgen-resistant prostate cancer

patients. British journal of cancer. 2005;93(7):749-56. Epub 2005/09/02.

237. Munn DH, Sharma MD, Lee JR, Jhaver KG, Johnson TS, Keskin DB, et al. Potential regulatory function of human dendritic cells expressing indoleamine 2,3-dioxygenase. Science. 2002;297(5588):1867-70. Epub 2002/09/14.

238. Munn DH, Zhou M, Attwood JT, Bondarev I, Conway SJ, Marshall B, et al. Prevention of allogeneic fetal rejection by tryptophan catabolism. Science. 1998;281(5380):1191-3. Epub 1998/08/26.

239. Nair S, McLaughlin C, Weizer A, Su Z, Boczkowski D, Dannull J, et al. Injection of immature dendritic cells into adjuvant-treated skin obviates the need for ex vivo maturation. Journal of immunology. 2003;171(11):6275-82. Epub 2003/11/25.

240. Naito Y, Saito K, Shiiba K, Ohuchi A, Saigenji K, Nagura H, et al. CD8+ T cells infiltrated within cancer cell nests as a prognostic factor in human colorectal cancer. Cancer research. 1998;58(16):3491-4. Epub 1998/08/29.

241. Nakai N, Hartmann G, Kishimoto S, Katoh N. Dendritic cell vaccination in human melanoma: relationships between clinical effects and vaccine parameters. Pigment cell & melanoma research. 2010;23(5):607-19. Epub 2010/06/29.

242. Naujokat C, Berges C, Hoh A, Wieczorek H, Fuchs D, Ovens J, et al. Proteasomal chymotrypsin-like peptidase activity is required for essential functions of human monocyte-derived dendritic cells. Immunology. 2007;120(1):120-32. Epub 2006/11/07.

243. Nedergaard BS, Ladekarl M, Nyengaard JR, Nielsen K. A comparative study of the cellular immune response in patients with stage IB cervical squamous cell carcinoma. Low numbers of

several immune cell subtypes are strongly associated with relapse of disease within 5 years. Gynecologic oncology. 2008;108(1):106-11. Epub 2007/10/20.

244. Neethling FA, Ramakrishna V, Keler T, Buchli R, Woodburn T, Weidanz JA. Assessing vaccine potency using TCRmimic antibodies. Vaccine. 2008;26(25):3092-102. Epub 2008/03/21.

245. Nestle FO, Farkas A, Conrad C. Dendritic-cell-based therapeutic vaccination against cancer. Current opinion in immunology. 2005;17(2):163-9. Epub 2005/03/16.

246. Nie Y, Yang G, Song Y, Zhao X, So C, Liao J, et al. DNA hypermethylation is a mechanism for loss of expression of the HLA class I genes in human esophageal squamous cell carcinomas. Carcinogenesis. 2001;22(10):1615-23. Epub 2001/09/29.

247. Nimmerjahn F, Milosevic S, Behrends U, Jaffee EM, Pardoll DM, Bornkamm GW, et al. Major histocompatibility complex class II-restricted presentation of a cytosolic antigen by autophagy. European journal of immunology. 2003;33(5):1250-9. Epub 2003/05/06.

248. Novak EK, Swank RT. Lysosomal dysfunctions associated with mutations at mouse pigment genes. Genetics. 1979;92(1):189-204. Epub 1979/05/01.

249. Obst R, van Santen HM, Mathis D, Benoist C. Antigen persistence is required throughout the expansion phase of a CD4(+) T cell response. The Journal of experimental medicine. 2005;201(10):1555-65. Epub 2005/05/18.

250. Ohl L, Mohaupt M, Czeloth N, Hintzen G, Kiafard Z, Zwirner J, et al. CCR7 governs skin dendritic cell migration under inflammatory and steady-state conditions. Immunity. 2004;21(2):279-88. Epub 2004/08/17.

251. O'Neill DW, Adams S, Bhardwaj N. Manipulating dendritic cell biology for the active immunotherapy of cancer. Blood. 2004;104(8):2235-46. Epub 2004/07/03.

252. Orlow SJ. Melanosomes are specialized members of the lysosomal lineage of organelles. The Journal of investigative dermatology. 1995;105(1):3-7. Epub 1995/07/01.

253. Ostrand-Rosenberg S, Sinha P. Myeloid-derived suppressor cells: linking inflammation and cancer. Journal of immunology. 2009;182(8):4499-506. Epub 2009/04/04.

254. Ottaviani S, Zhang Y, Boon T, van der Bruggen P. A MAGE-1 antigenic peptide recognized by human cytolytic T lymphocytes on HLA-A2 tumor cells. Cancer immunology, immunotherapy : CII. 2005;54(12):1214-20. Epub 2005/07/19.

255. Palucka AK, Ueno H, Fay JW, Banchereau J. Taming cancer by inducing immunity via dendritic cells. Immunological reviews. 2007;220:129-50. Epub 2007/11/06.

256. Paludan C, Schmid D, Landthaler M, Vockerodt M, Kube D, Tuschl T, et al. Endogenous MHC class II processing of a viral nuclear antigen after autophagy. Science. 2005;307(5709):593-6. Epub 2004/12/14.

257. Park B, Lee S, Kim E, Cho K, Riddell SR, Cho S, et al. Redox regulation facilitates optimal peptide selection by MHC class I during antigen processing. Cell. 2006;127(2):369-82. Epub 2006/10/24.

258. Parker DC. The functions of antigen recognition in T cell-dependent B cell activation. Seminars in immunology. 1993;5(6):413-20. Epub 1993/12/01.

259. Pecher G, Haring A, Kaiser L, Thiel E. Mucin gene (MUC1) transfected dendritic cells as vaccine: results of a phase

I/II clinical trial. Cancer immunology, immunotherapy : CII. 2002;51(11-12):669-73. Epub 2002/11/20.

260. Pellis NR, Tom BH, Kahan BD. Tumor-specific and allospecific immunogenicity of soluble extracts from chemically induced murine sarcomas. Journal of immunology. 1974;113(2):708-11. Epub 1974/08/01.

261. Penn I, Brunson ME. Cancers after cyclosporine therapy. Transplantation proceedings. 1988;20(3 Suppl 3):885-92. Epub 1988/06/01.

262. Perez-Diez A, Butterfield LH, Li L, Chakraborty NG, Economou JS, Mukherji B. Generation of CD8+ and CD4+ T-cell response to dendritic cells genetically engineered to express the MART-1/Melan-A gene. Cancer research. 1998;58(23):5305-9. Epub 1998/12/16.

263. Perillo NL, Pace KE, Seilhamer JJ, Baum LG. Apoptosis of T cells mediated by galectin-1. Nature. 1995;378(6558):736-9. Epub 1995/12/14.

264. Peters PJ, Neefjes JJ, Oorschot V, Ploegh HL, Geuze HJ. Segregation of MHC class II molecules from MHC class I molecules in the Golgi complex for transport to lysosomal compartments. Nature. 1991;349(6311):669-76. Epub 1991/02/21.

265. Phan GQ, Yang JC, Sherry RM, Hwu P, Topalian SL, Schwartzentruber DJ, et al. Cancer regression and autoimmunity induced by cytotoxic T lymphocyte-associated antigen 4 blockade in patients with metastatic melanoma. Proceedings of the National Academy of Sciences of the United States of America. 2003;100(14):8372-7. Epub 2003/06/27.

266. Pierre P. Dendritic cells, DRiPs, and DALIS in the control of antigen processing. Immunological reviews. 2005;207:184-90. Epub 2005/09/27.

267. Pierre P, Mellman I. Developmental regulation of invariant chain proteolysis controls MHC class II trafficking in mouse dendritic cells. Cell. 1998;93(7):1135-45. Epub 1998/07/10.

268. Pittet MJ, Valmori D, Dunbar PR, Speiser DE, Lienard D, Lejeune F, et al. High frequencies of naive Melan-A/MART-1-specific CD8(+) T cells in a large proportion of human histocompatibility leukocyte antigen (HLA)-A2 individuals. The Journal of experimental medicine. 1999;190(5):705-15. Epub 1999/09/08.

269. Ponsaerts P, Van Tendeloo VF, Berneman ZN. Cancer immunotherapy using RNA-loaded dendritic cells. Clinical and experimental immunology. 2003;134(3):378-84. Epub 2003/11/25.

270. Popov A, Schultze JL. IDO-expressing regulatory dendritic cells in cancer and chronic infection. Journal of molecular medicine. 2008;86(2):145-60. Epub 2007/09/19.

271. Posner JB. Immunology of paraneoplastic syndromes: overview. Annals of the New York Academy of Sciences. 2003;998:178-86. Epub 2003/11/01.

272. Prabakaran I, Menon C, Xu S, Gomez-Yafal A, Czerniecki BJ, Fraker DL. Mature CD83(+) dendritic cells infected with recombinant gp100 vaccinia virus stimulate potent antimelanoma T cells. Annals of surgical oncology. 2002;9(4):411-8. Epub 2002/05/03.

273. Pretscher D, Distel LV, Grabenbauer GG, Wittlinger M, Buettner M, Niedobitek G. Distribution of immune cells in head and neck cancer: CD8+ T-cells and CD20+ B-cells in metastatic lymph nodes are associated with favourable outcome in patients with oro- and hypopharyngeal carcinoma. BMC cancer. 2009;9:292. Epub 2009/08/25.

274. Prlic M, Williams MA, Bevan MJ. Requirements for CD8 T-cell priming, memory generation and maintenance. Current opinion in immunology. 2007;19(3):315-9. Epub 2007/04/17.

275. Pulendran B, Banchereau J, Burkeholder S, Kraus E, Guinet E, Chalouni C, et al. Flt3-ligand and granulocyte colony-stimulating factor mobilize distinct human dendritic cell subsets in vivo. Journal of immunology. 2000;165(1):566-72. Epub 2000/06/22.

276. Purbhoo MA, Irvine DJ, Huppa JB, Davis MM. T cell killing does not require the formation of a stable mature immunological synapse. Nature immunology. 2004;5(5):524-30. Epub 2004/03/30.

277. Purbhoo MA, Li Y, Sutton DH, Brewer JE, Gostick E, Bossi G, et al. The HLA A*0201-restricted hTERT(540-548) peptide is not detected on tumor cells by a CTL clone or a high-affinity T-cell receptor. Molecular cancer therapeutics. 2007;6(7):2081-91. Epub 2007/07/11.

278. Purbhoo MA, Sutton DH, Brewer JE, Mullings RE, Hill ME, Mahon TM, et al. Quantifying and imaging NY-ESO-1/LAGE-1-derived epitopes on tumor cells using high affinity T cell receptors. Journal of immunology. 2006;176(12):7308-16. Epub 2006/06/06.

279. Qi H, Egen JG, Huang AY, Germain RN. Extrafollicular activation of lymph node B cells by antigen-bearing dendritic cells. Science. 2006;312(5780):1672-6. Epub 2006/06/17.

280. Qian SB, Reits E, Neefjes J, Deslich JM, Bennink JR, Yewdell JW. Tight linkage between translation and MHC class I peptide ligand generation implies specialized antigen processing for defective ribosomal products. Journal of immunology. 2006;177(1):227-33. Epub 2006/06/21.

281. Quillien V, Moisan A, Carsin A, Lesimple T, Lefeuvre C, Adamski H, et al. Biodistribution of radiolabelled human dendritic cells injected by various routes. European journal of nuclear medicine and molecular imaging. 2005;32(7):731-41. Epub 2005/06/01.

282. Randolph GJ, Angeli V, Swartz MA. Dendritic-cell trafficking to lymph nodes through lymphatic vessels. Nature reviews Immunology. 2005;5(8):617-28. Epub 2005/08/02.

283. Ranieri E, Kierstead LS, Zarour H, Kirkwood JM, Lotze MT, Whiteside T, et al. Dendritic cell/peptide cancer vaccines: clinical responsiveness and epitope spreading. Immunological investigations. 2000;29(2):121-5. Epub 2000/06/15.

284. Raposo G, Tenza D, Murphy DM, Berson JF, Marks MS. Distinct protein sorting and localization to premelanosomes, melanosomes, and lysosomes in pigmented melanocytic cells. The Journal of cell biology. 2001;152(4):809-24. Epub 2001/03/27.

285. Ratzinger G, Stoitzner P, Ebner S, Lutz MB, Layton GT, Rainer C, et al. Matrix metalloproteinases 9 and 2 are necessary for the migration of Langerhans cells and dermal dendritic cells from human and murine skin. Journal of immunology. 2002;168(9):4361-71. Epub 2002/04/24.

286. Reis e Sousa C, Germain RN. Major histocompatibility complex class I presentation of peptides derived from soluble exogenous antigen by a subset of cells engaged in phagocytosis. The Journal of experimental medicine. 1995;182(3):841-51. Epub 1995/09/01.

287. Reits E, Neijssen J, Herberts C, Benckhuijsen W, Janssen L, Drijfhout JW, et al. A major role for TPPII in trimming proteasomal degradation products for MHC class I antigen presentation. Immunity. 2004;20(4):495-506. Epub 2004/04/16.

288. Restifo NP, Marincola FM, Kawakami Y, Taubenberger J, Yannelli JR, Rosenberg SA. Loss of functional beta 2-microglobulin in metastatic melanomas from five patients receiving immunotherapy. Journal of the National Cancer Institute. 1996;88(2):100-8. Epub 1996/01/17.

289. Reuschenbach M, Waterboer T, Wallin KL, Einenkel J, Dillner J, Hamsikova E, et al. Characterization of humoral immune responses against p16, p53, HPV16 E6 and HPV16 E7 in patients with HPV-associated cancers. International journal of cancer Journal international du cancer. 2008;123(11):2626-31. Epub 2008/09/12.

290. Ridge JP, Di Rosa F, Matzinger P. A conditioned dendritic cell can be a temporal bridge between a CD4+ T-helper and a T-killer cell. Nature. 1998;393(6684):474-8. Epub 1998/06/12.

291. Riese RJ, Chapman HA. Cathepsins and compartmentalization in antigen presentation. Current opinion in immunology. 2000;12(1):107-13. Epub 2000/02/19.

292. Riese RJ, Shi GP, Villadangos J, Stetson D, Driessen C, Lennon-Dumenil AM, et al. Regulation of CD1 function and NK1.1(+) T cell selection and maturation by cathepsin S. Immunity. 2001;15(6):909-19. Epub 2002/01/05.

293. Riley JP, Rosenberg SA, Parkhurst MR. Identification of a new shared HLA-A2.1 restricted epitope from the melanoma antigen tyrosinase. Journal of immunotherapy. 2001;24(3):212-20. Epub 2001/06/08.

294. Rimoldi D, Muehlethaler K, Salvi S, Valmori D, Romero P, Cerottini JC, et al. Subcellular localization of the melanoma-associated protein Melan-AMART-1 influences the processing of its HLA-A2-restricted epitope. The Journal of biological chemistry. 2001;276(46):43189-96. Epub 2001/09/12.

295. Robbiani DF, Finch RA, Jager D, Muller WA, Sartorelli AC, Randolph GJ. The leukotriene C(4) transporter MRP1 regulates CCL19 (MIP-3beta, ELC)-dependent mobilization of dendritic cells to lymph nodes. Cell. 2000;103(5):757-68. Epub 2000/12/15.

296. Robila V, Ostankovitch M, Altrich-Vanlith ML, Theos AC, Drover S, Marks MS, et al. MHC class II presentation of gp100 epitopes in melanoma cells requires the function of conventional endosomes and is influenced by melanosomes. Journal of immunology. 2008;181(11):7843-52. Epub 2008/11/20.

297. Rock KL, Goldberg AL. Degradation of cell proteins and the generation of MHC class I-presented peptides. Annual review of immunology. 1999;17:739-79. Epub 1999/06/08.

298. Rock KL, Rothstein L, Gamble S, Fleischacker C. Characterization of antigen-presenting cells that present exogenous antigens in association with class I MHC molecules. Journal of immunology. 1993;150(2):438-46. Epub 1993/01/15.

299. Rock KL, York IA, Goldberg AL. Post-proteasomal antigen processing for major histocompatibility complex class I presentation. Nature immunology. 2004;5(7):670-7. Epub 2004/06/30.

300. Romero P, Dunbar PR, Valmori D, Pittet M, Ogg GS, Rimoldi D, et al. Ex vivo staining of metastatic lymph nodes by class I major histocompatibility complex tetramers reveals high numbers of antigen-experienced tumor-specific cytolytic T lymphocytes. The Journal of experimental medicine. 1998;188(9):1641-50. Epub 1998/11/06.

301. Rosenberg SA, Yang JC, Restifo NP. Cancer immunotherapy: moving beyond current vaccines. Nature medicine. 2004;10(9):909-15. Epub 2004/09/02.

302. Rouas R, Lewalle P, El Ouriaghli F, Nowak B, Duvillier H, Martiat P. Poly(I:C) used for human dendritic cell maturation preserves their ability to secondarily secrete bioactive IL-12. International immunology. 2004;16(5):767-73. Epub 2004/04/21.

303. Rovere P, Zimmermann VS, Forquet F, Demandolx D, Trucy J, Ricciardi-Castagnoli P, et al. Dendritic cell maturation and antigen presentation in the absence of invariant chain. Proceedings of the National Academy of Sciences of the United States of America. 1998;95(3):1067-72. Epub 1998/03/14.

304. Rubio MT, Means TK, Chakraverty R, Shaffer J, Fudaba Y, Chittenden M, et al. Maturation of human monocyte-derived dendritic cells (MoDCs) in the presence of prostaglandin E2 optimizes CD4 and CD8 T cell-mediated responses to protein antigens: role of PGE2 in chemokine and cytokine expression by MoDCs. International immunology. 2005;17(12):1561-72. Epub 2005/11/24.

305. Rughetti A, Biffoni M, Sabbatucci M, Rahimi H, Pellicciotta I, Fattorossi A, et al. Transfected human dendritic cells to induce antitumor immunity. Gene therapy. 2000;7(17):1458-66. Epub 2000/09/23.

306. Rygaard J, Povlsen CO. The mouse mutant nude does not develop spontaneous tumours. An argument against immunological surveillance. Acta pathologica et microbiologica Scandinavica Section B: Microbiology and immunology. 1974;82(1):99-106. Epub 1974/02/01.

307. Sahin U, Tureci O, Schmitt H, Cochlovius B, Johannes T, Schmits R, et al. Human neoplasms elicit multiple specific immune responses in the autologous host. Proceedings of the National Academy of Sciences of the United States of America. 1995;92(25):11810-3. Epub 1995/12/05.

308. Sallusto F, Lanzavecchia A. Efficient presentation of soluble antigen by cultured human dendritic cells is maintained by granulocyte/macrophage colony-stimulating factor plus interleukin 4 and downregulated by tumor necrosis factor alpha. The Journal of experimental medicine. 1994;179(4):1109-18. Epub 1994/04/01.

309. Sallusto F, Schaerli P, Loetscher P, Schaniel C, Lenig D, Mackay CR, et al. Rapid and coordinated switch in chemokine receptor expression during dendritic cell maturation. European journal of immunology. 1998;28(9):2760-9. Epub 1998/10/01.

310. Sanjabi S, Mosaheb MM, Flavell RA. Opposing effects of TGF-beta and IL-15 cytokines control the number of short-lived effector CD8+ T cells. Immunity. 2009;31(1):131-44. Epub 2009/07/17.

311. Santambrogio L, Sato AK, Carven GJ, Belyanskaya SL, Strominger JL, Stern LJ. Extracellular antigen processing and presentation by immature dendritic cells. Proceedings of the National Academy of Sciences of the United States of America. 1999;96(26):15056-61. Epub 1999/12/28.

312. Santambrogio L, Sato AK, Fischer FR, Dorf ME, Stern LJ. Abundant empty class II MHC molecules on the surface of immature dendritic cells. Proceedings of the National Academy of Sciences of the United States of America. 1999;96(26):15050-5. Epub 1999/12/28.

313. Saric T, Chang SC, Hattori A, York IA, Markant S, Rock KL, et al. An IFN-gamma-induced aminopeptidase in the ER, ERAP1, trims precursors to MHC class I-presented peptides. Nature immunology. 2002;3(12):1169-76. Epub 2002/11/19.

314. Savina A, Amigorena S. Phagocytosis and antigen presentation in dendritic cells. Immunological reviews. 2007;219:143-56. Epub 2007/09/14.

315. Scandella E, Men Y, Gillessen S, Forster R, Groettrup M. Prostaglandin E2 is a key factor for CCR7 surface expression and migration of monocyte-derived dendritic cells. Blood. 2002;100(4):1354-61. Epub 2002/08/01.

316. Scantlebury V, Gjertson D, Eliasziw M, Terasaki P, Fung J, Shapiro R, et al. Influence of HLA and CREG matching in African-American primary cadaver kidney recipients: UNOS 1991-1995. Transplantation proceedings. 1997;29(8):3733-6. Epub 1998/01/01.

317. Schmid D, Pypaert M, Munz C. Antigen-loading compartments for major histocompatibility complex class II molecules continuously receive input from autophagosomes. Immunity. 2007;26(1):79-92. Epub 2006/12/22.

318. Schnurr M, Chen Q, Shin A, Chen W, Toy T, Jenderek C, et al. Tumor antigen processing and presentation depend critically on dendritic cell type and the mode of antigen delivery. Blood. 2005;105(6):2465-72. Epub 2004/11/18.

319. Schubert U, Anton LC, Gibbs J, Norbury CC, Yewdell JW, Bennink JR. Rapid degradation of a large fraction of newly synthesized proteins by proteasomes. Nature. 2000;404(6779):770-4. Epub 2000/04/28.

320. Schumacher K, Haensch W, Roefzaad C, Schlag PM. Prognostic significance of activated CD8(+) T cell infiltrations within esophageal carcinomas. Cancer research. 2001;61(10):3932-6. Epub 2001/05/19.

321. Schuurhuis DH, Lesterhuis WJ, Kramer M, Looman MG, van Hout-Kuijer M, Schreibelt G, et al. Polyinosinic polycytidylic acid prevents efficient antigen expression after mRNA electroporation of clinical grade dendritic cells. Cancer immunology, immunotherapy : CII. 2009;58(7):1109-15. Epub 2008/11/20.

322. Schuurhuis DH, Verdijk P, Schreibelt G, Aarntzen EH, Scharenborg N, de Boer A, et al. In situ expression of tumor antigens by messenger RNA-electroporated dendritic cells in lymph nodes of melanoma patients. Cancer research. 2009;69(7):2927-34. Epub 2009/03/26.

323. Schwab SR, Shugart JA, Horng T, Malarkannan S, Shastri N. Unanticipated antigens: translation initiation at CUG with leucine. PLoS biology. 2004;2(11):e366. Epub 2004/10/29.

324. Schwarz K, van den Broek M, de Giuli R, Seelentag WW, Shastri N, Groettrup M. The use of LCMV-specific T cell hybridomas for the quantitative analysis of MHC class I restricted antigen presentation. Journal of immunological methods. 2000;237(1-2):199-202. Epub 2000/03/22.

325. Seiji M, Kikuchi A. Acid phosphatase activity in melanosomes. The Journal of investigative dermatology. 1969;52(2):212-6. Epub 1969/02/01.

326. Shankaran V, Ikeda H, Bruce AT, White JM, Swanson PE, Old LJ, et al. IFNgamma and lymphocytes prevent primary tumour development and shape tumour immunogenicity. Nature. 2001;410(6832):1107-11. Epub 2001/04/27.

327. Shedlock DJ, Shen H. Requirement for CD4 T cell help in generating functional CD8 T cell memory. Science. 2003;300(5617):337-9. Epub 2003/04/12.

328. Shen L, Rock KL. Priming of T cells by exogenous antigen cross-presented on MHC class I molecules. Current opinion in immunology. 2006;18(1):85-91. Epub 2005/12/06.

329. Shen X, Li N, Li H, Zhang T, Wang F, Li Q. Increased prevalence of regulatory T cells in the tumor microenvironment and its correlation with TNM stage of hepatocellular carcinoma. Journal of cancer research and clinical oncology. 2010;136(11):1745-54. Epub 2010/03/12.

330. Shi GP, Villadangos JA, Dranoff G, Small C, Gu L, Haley KJ, et al. Cathepsin S required for normal MHC class II peptide loading and germinal center development. Immunity. 1999;10(2):197-206. Epub 1999/03/11.

331. Shortman K, Liu YJ. Mouse and human dendritic cell subtypes. Nature reviews Immunology. 2002;2(3):151-61. Epub 2002/03/27.

332. Silk AW, Schoen RE, Potter DM, Finn OJ. Humoral immune response to abnormal MUC1 in subjects with colorectal adenoma and cancer. Molecular immunology. 2009;47(1):52-6. Epub 2009/02/17.

333. Small EJ, Fratesi P, Reese DM, Strang G, Laus R, Peshwa MV, et al. Immunotherapy of hormone-refractory prostate cancer with antigen-loaded dendritic cells. Journal of clinical oncology : official journal of the American Society of Clinical Oncology. 2000;18(23):3894-903. Epub 2000/12/01.

334. Small EJ, Schellhammer PF, Higano CS, Redfern CH, Nemunaitis JJ, Valone FH, et al. Placebo-controlled phase III trial of immunologic therapy with sipuleucel-T (APC8015) in patients with metastatic, asymptomatic hormone refractory prostate cancer. Journal of clinical oncology : official journal of the American Society of Clinical Oncology. 2006;24(19):3089-94. Epub 2006/07/01.

335. Somersan S, Larsson M, Fonteneau JF, Basu S, Srivastava P, Bhardwaj N. Primary tumor tissue lysates are enriched in heat shock proteins and induce the maturation of human dendritic cells. Journal of immunology. 2001;167(9):4844-52. Epub 2001/10/24.

336. Sporri R, Reis e Sousa C. Inflammatory mediators are insufficient for full dendritic cell activation and promote

expansion of CD4+ T cell populations lacking helper function. Nature immunology. 2005;6(2):163-70. Epub 2005/01/18.

337. Starzl TE, Eliasziw M, Gjertson D, Terasaki PI, Fung JJ, Trucco M, et al. HLA and cross-reactive antigen group matching for cadaver kidney allocation. Transplantation. 1997;64(7):983-91. Epub 1997/11/05.

338. Steele JC, Rao A, Marsden JR, Armstrong CJ, Berhane S, Billingham LJ, et al. Phase I/II trial of a dendritic cell vaccine transfected with DNA encoding melan A and gp100 for patients with metastatic melanoma. Gene therapy. 2011;18(6):584-93. Epub 2011/02/11.

339. Steinman RM. The dendritic cell advantage: New focus for immune-based therapies. Drug news & perspectives. 2000;13(10):581-6. Epub 2003/07/25.

340. Steinman RM, Pack M, Inaba K. Dendritic cell development and maturation. Advances in experimental medicine and biology. 1997;417:1-6. Epub 1997/01/01.

341. Steinman RM, Swanson J. The endocytic activity of dendritic cells. The Journal of experimental medicine. 1995;182(2):283-8. Epub 1995/08/01.

342. Stockert E, Jager E, Chen YT, Scanlan MJ, Gout I, Karbach J, et al. A survey of the humoral immune response of cancer patients to a panel of human tumor antigens. The Journal of experimental medicine. 1998;187(8):1349-54. Epub 1998/05/23.

343. Stone AA, Neale JM, Cox DS, Napoli A, Valdimarsdottir H, Kennedy-Moore E. Daily events are associated with a secretory immune response to an oral antigen in men. Health psychology : official journal of the Division of Health Psychology, American Psychological Association. 1994;13(5):440-6. Epub 1994/09/01.

344. Strawbridge AB, Blum JS. Autophagy in MHC class II antigen processing. Current opinion in immunology. 2007;19(1):87-92. Epub 2006/11/30.

345. Stutman O. Tumor development after 3-methylcholanthrene in immunologically deficient athymic-nude mice. Science. 1974;183(4124):534-6. Epub 1974/02/08.

346. Su Z, Dannull J, Yang BK, Dahm P, Coleman D, Yancey D, et al. Telomerase mRNA-transfected dendritic cells stimulate antigen-specific CD8+ and CD4+ T cell responses in patients with metastatic prostate cancer. Journal of immunology. 2005;174(6):3798-807. Epub 2005/03/08.

347. Subklewe M. Dendritic cells for the induction of EBV immunity. Recent results in cancer research Fortschritte der Krebsforschung Progres dans les recherches sur le cancer. 2002;159:38-43. Epub 2002/01/12.

348. Sun JC, Bevan MJ. Defective CD8 T cell memory following acute infection without CD4 T cell help. Science. 2003;300(5617):339-42. Epub 2003/04/12.

349. Sun JC, Williams MA, Bevan MJ. CD4+ T cells are required for the maintenance, not programming, of memory CD8+ T cells after acute infection. Nature immunology. 2004;5(9):927-33. Epub 2004/08/10.

350. Tacken PJ, de Vries IJ, Torensma R, Figdor CG. Dendritic-cell immunotherapy: from ex vivo loading to in vivo targeting. Nature reviews Immunology. 2007;7(10):790-802. Epub 2007/09/15.

351. Taylor GS, Long HM, Haigh TA, Larsen M, Brooks J, Rickinson AB. A role for intercellular antigen transfer in the recognition of EBV-transformed B cell lines by EBV nuclear antigen-specific CD4+ T cells. Journal of immunology. 2006;177(6):3746-56. Epub 2006/09/05.

352. Taylor RC, Patel A, Panageas KS, Busam KJ, Brady MS. Tumor-infiltrating lymphocytes predict sentinel lymph node positivity in patients with cutaneous melanoma. Journal of clinical oncology : official journal of the American Society of Clinical Oncology. 2007;25(7):869-75. Epub 2007/03/01.

353. Tellam J, Fogg MH, Rist M, Connolly G, Tscharke D, Webb N, et al. Influence of translation efficiency of homologous viral proteins on the endogenous presentation of CD8+ T cell epitopes. The Journal of experimental medicine. 2007;204(3):525-32. Epub 2007/02/22.

354. Tellam J, Sherritt M, Thomson S, Tellam R, Moss DJ, Burrows SR, et al. Targeting of EBNA1 for rapid intracellular degradation overrides the inhibitory effects of the Gly-Ala repeat domain and restores CD8+ T cell recognition. The Journal of biological chemistry. 2001;276(36):33353-60. Epub 2001/07/04.

355. Terasaki PI, Cecka JM, Gjertson DW, Cho YW. Spousal and other living renal donor transplants. Clinical transplants. 1997:269-84. Epub 1997/01/01.

356. Terasaki PI, Gjertson DW, Cecka JM, Takemoto S, Cho YW. Significance of the donor age effect on kidney transplants. Clinical transplantation. 1997;11(5 Pt 1):366-72. Epub 1997/11/15.

357. Thery C, Amigorena S. The cell biology of antigen presentation in dendritic cells. Current opinion in immunology. 2001;13(1):45-51. Epub 2001/01/13.

358. Thery C, Duban L, Segura E, Veron P, Lantz O, Amigorena S. Indirect activation of naive CD4+ T cells by dendritic cell-derived exosomes. Nature immunology. 2002;3(12):1156-62. Epub 2002/11/12.

359. Tomsova M, Melichar B, Sedlakova I, Steiner I. Prognostic significance of CD3+ tumor-infiltrating lymphocytes in ovarian carcinoma. Gynecologic oncology. 2008;108(2):415-20. Epub 2007/11/27.

360. Trinchieri G. Interleukin-12 and the regulation of innate resistance and adaptive immunity. Nature reviews Immunology. 2003;3(2):133-46. Epub 2003/02/04.

361. Trombetta ES, Ebersold M, Garrett W, Pypaert M, Mellman I. Activation of lysosomal function during dendritic cell maturation. Science. 2003;299(5611):1400-3. Epub 2003/03/01.

362. Tudor D, Dubuquoy C, Gaboriau V, Lefevre F, Charley B, Riffault S. TLR9 pathway is involved in adjuvant effects of plasmid DNA-based vaccines. Vaccine. 2005;23(10):1258-64. Epub 2005/01/18.

363. Turk D, Janjic V, Stern I, Podobnik M, Lamba D, Dahl SW, et al. Structure of human dipeptidyl peptidase I (cathepsin C): exclusion domain added to an endopeptidase framework creates the machine for activation of granular serine proteases. The EMBO journal. 2001;20(23):6570-82. Epub 2001/12/01.

364. Turley SJ, Inaba K, Garrett WS, Ebersold M, Unternaehrer J, Steinman RM, et al. Transport of peptide-MHC class II complexes in developing dendritic cells. Science. 2000;288(5465):522-7. Epub 2000/04/25.

365. Tuting T, Storkus WJ, Falo LD, Jr. DNA immunization targeting the skin: molecular control of adaptive immunity. The Journal of investigative dermatology. 1998;111(2):183-8. Epub 1998/08/12.

366. Tuyaerts S, Aerts JL, Corthals J, Neyns B, Heirman C, Breckpot K, et al. Current approaches in dendritic cell generation and future implications for cancer immunotherapy.

Cancer immunology, immunotherapy : CII. 2007;56(10):1513-37. Epub 2007/05/16.

367. Ueno H, Klechevsky E, Morita R, Aspord C, Cao T, Matsui T, et al. Dendritic cell subsets in health and disease. Immunological reviews. 2007;219:118-42. Epub 2007/09/14.

368. Valitutti S, Lanzavecchia A. Serial triggering of TCRs: a basis for the sensitivity and specificity of antigen recognition. Immunology today. 1997;18(6):299-304. Epub 1997/06/01.

369. Valmori D, Fonteneau JF, Lizana CM, Gervois N, Lienard D, Rimoldi D, et al. Enhanced generation of specific tumor-reactive CTL in vitro by selected Melan-A/MART-1 immunodominant peptide analogues. Journal of immunology. 1998;160(4):1750-8. Epub 1998/02/20.

370. Van den Eynde BJ, Morel S. Differential processing of class-I-restricted epitopes by the standard proteasome and the immunoproteasome. Current opinion in immunology. 2001;13(2):147-53. Epub 2001/03/03.

371. van Elsas A, van der Burg SH, van der Minne CE, Borghi M, Mourer JS, Melief CJ, et al. Peptide-pulsed dendritic cells induce tumoricidal cytotoxic T lymphocytes from healthy donors against stably HLA-A*0201-binding peptides from the Melan-A/MART-1 self antigen. European journal of immunology. 1996;26(8):1683-9. Epub 1996/08/01.

372. van Houdt IS, Sluijter BJ, Moesbergen LM, Vos WM, de Gruijl TD, Molenkamp BG, et al. Favorable outcome in clinically stage II melanoma patients is associated with the presence of activated tumor infiltrating T-lymphocytes and preserved MHC class I antigen expression. International journal of cancer Journal international du cancer. 2008;123(3):609-15. Epub 2008/05/24.

373. van Kooten C, Gaillard C, Galizzi JP, Hermann P, Fossiez F, Banchereau J, et al. B cells regulate expression of CD40 ligand on activated T cells by lowering the mRNA level and through the release of soluble CD40. European journal of immunology. 1994;24(4):787-92. Epub 1994/04/01.

374. Van Tendeloo VF, Ponsaerts P, Lardon F, Nijs G, Lenjou M, Van Broeckhoven C, et al. Highly efficient gene delivery by mRNA electroporation in human hematopoietic cells: superiority to lipofection and passive pulsing of mRNA and to electroporation of plasmid cDNA for tumor antigen loading of dendritic cells. Blood. 2001;98(1):49-56. Epub 2001/06/22.

375. Van Tendeloo VF, Snoeck HW, Lardon F, Vanham GL, Nijs G, Lenjou M, et al. Nonviral transfection of distinct types of human dendritic cells: high-efficiency gene transfer by electroporation into hematopoietic progenitor- but not monocyte-derived dendritic cells. Gene therapy. 1998;5(5):700-7. Epub 1998/11/03.

376. Van Tendeloo VF, Van de Velde A, Van Driessche A, Cools N, Anguille S, Ladell K, et al. Induction of complete and molecular remissions in acute myeloid leukemia by Wilms' tumor 1 antigen-targeted dendritic cell vaccination. Proceedings of the National Academy of Sciences of the United States of America. 2010;107(31):13824-9. Epub 2010/07/16.

377. Varela-Rohena A, Molloy PE, Dunn SM, Li Y, Suhoski MM, Carroll RG, et al. Control of HIV-1 immune escape by CD8 T cells expressing enhanced T-cell receptor. Nature medicine. 2008;14(12):1390-5. Epub 2008/11/11.

378. Voelter V, Rufer N, Reynard S, Greub G, Brookes R, Guillaume P, et al. Characterization of Melan-A reactive memory CD8+ T cells in a healthy donor. International immunology. 2008;20(8):1087-96. Epub 2008/06/25.

379. von Bergwelt-Baildon MS, Popov A, Saric T, Chemnitz J, Classen S, Stoffel MS, et al. CD25 and indoleamine 2,3-dioxygenase are up-regulated by prostaglandin E2 and expressed by tumor-associated dendritic cells in vivo: additional mechanisms of T-cell inhibition. Blood. 2006;108(1):228-37. Epub 2006/03/09.

380. Vyas JM, Van der Veen AG, Ploegh HL. The known unknowns of antigen processing and presentation. Nature reviews Immunology. 2008;8(8):607-18. Epub 2008/07/22.

381. Waldmann H, Cobbold S. Regulatory T cells: context matters. Immunity. 2009;30(5):613-5. Epub 2009/05/26.

382. Warger T, Osterloh P, Rechtsteiner G, Fassbender M, Heib V, Schmid B, et al. Synergistic activation of dendritic cells by combined Toll-like receptor ligation induces superior CTL responses in vivo. Blood. 2006;108(2):544-50. Epub 2006/03/16.

383. Watts C. The exogenous pathway for antigen presentation on major histocompatibility complex class II and CD1 molecules. Nature immunology. 2004;5(7):685-92. Epub 2004/06/30.

384. Welters MJ, van der Logt P, van den Eeden SJ, Kwappenberg KM, Drijfhout JW, Fleuren GJ, et al. Detection of human papillomavirus type 18 E6 and E7-specific CD4+ T-helper 1 immunity in relation to health versus disease. International journal of cancer Journal international du cancer. 2006;118(4):950-6. Epub 2005/09/10.

385. Wilgenhof S, Van Nuffel AM, Corthals J, Heirman C, Tuyaerts S, Benteyn D, et al. Therapeutic vaccination with an autologous mRNA electroporated dendritic cell vaccine in patients with advanced melanoma. Journal of immunotherapy. 2011;34(5):448-56. Epub 2011/05/18.

386. Williams MA, Tyznik AJ, Bevan MJ. Interleukin-2 signals during priming are required for secondary expansion of CD8+ memory T cells. Nature. 2006;441(7095):890-3. Epub 2006/06/17.

387. Wubbolts R, Fernandez-Borja M, Oomen L, Verwoerd D, Janssen H, Calafat J, et al. Direct vesicular transport of MHC class II molecules from lysosomal structures to the cell surface. The Journal of cell biology. 1996;135(3):611-22. Epub 1996/11/01.

388. Yang S, Vervaert CE, Burch J, Jr., Grichnik J, Seigler HF, Darrow TL. Murine dendritic cells transfected with human GP100 elicit both antigen-specific CD8(+) and CD4(+) T-cell responses and are more effective than DNA vaccines at generating anti-tumor immunity. International journal of cancer Journal international du cancer. 1999;83(4):532-40. Epub 1999/10/03.

389. Yewdell JW, Reits E, Neefjes J. Making sense of mass destruction: quantitating MHC class I antigen presentation. Nature reviews Immunology. 2003;3(12):952-61. Epub 2003/12/04.

390. Yewdell JW, Schubert U, Bennink JR. At the crossroads of cell biology and immunology: DRiPs and other sources of peptide ligands for MHC class I molecules. Journal of cell science. 2001;114(Pt 5):845-51. Epub 2001/02/22.

391. York IA, Mo AX, Lemerise K, Zeng W, Shen Y, Abraham CR, et al. The cytosolic endopeptidase, thimet oligopeptidase, destroys antigenic peptides and limits the extent of MHC class I antigen presentation. Immunity. 2003;18(3):429-40. Epub 2003/03/22.

392. Yoshimori T, Yamamoto A, Moriyama Y, Futai M, Tashiro Y. Bafilomycin A1, a specific inhibitor of vacuolar-type H(+)-ATPase, inhibits acidification and protein degradation in

lysosomes of cultured cells. The Journal of biological chemistry. 1991;266(26):17707-12. Epub 1991/09/15.

393. Young LS, Dawson CW, Clark D, Rupani H, Busson P, Tursz T, et al. Epstein-Barr virus gene expression in nasopharyngeal carcinoma. The Journal of general virology. 1988;69 (Pt 5):1051-65. Epub 1988/05/01.

394. Zammit DJ, Cauley LS, Pham QM, Lefrancois L. Dendritic cells maximize the memory CD8 T cell response to infection. Immunity. 2005;22(5):561-70. Epub 2005/05/17.

395. Zarour HM, Kirkwood JM, Kierstead LS, Herr W, Brusic V, Slingluff CL, Jr., et al. Melan-A/MART-1(51-73) represents an immunogenic HLA-DR4-restricted epitope recognized by melanoma-reactive CD4(+) T cells. Proceedings of the National Academy of Sciences of the United States of America. 2000;97(1):400-5. Epub 2000/01/05.

396. Zarutskie JA, Busch R, Zavala-Ruiz Z, Rushe M, Mellins ED, Stern LJ. The kinetic basis of peptide exchange catalysis by HLA-DM. Proceedings of the National Academy of Sciences of the United States of America. 2001;98(22):12450-5. Epub 2001/10/19.

397. Zehn D, Cohen CJ, Reiter Y, Walden P. Extended presentation of specific MHC-peptide complexes by mature dendritic cells compared to other types of antigen-presenting cells. European journal of immunology. 2004;34(6):1551-60. Epub 2004/05/27.

398. Zhao Y, Boczkowski D, Nair SK, Gilboa E. Inhibition of invariant chain expression in dendritic cells presenting endogenous antigens stimulates CD4+ T-cell responses and tumor immunity. Blood. 2003;102(12):4137-42. Epub 2003/08/16.

399. Zhou BK, Boissy RE, Pifko-Hirst S, Moran DJ, Orlow SJ. Lysosome-associated membrane protein-1 (LAMP-1) is the

melanocyte vesicular membrane glycoprotein band II. The Journal of investigative dermatology. 1993;100(2):110-4. Epub 1993/02/01.

400. Zhou LJ, Tedder TF. CD14+ blood monocytes can differentiate into functionally mature CD83+ dendritic cells. Proceedings of the National Academy of Sciences of the United States of America. 1996;93(6):2588-92. Epub 1996/03/19.

401. Zhou R, Norton JE, Zhang N, Dean DA. Electroporation-mediated transfer of plasmids to the lung results in reduced TLR9 signaling and inflammation. Gene therapy. 2007;14(9):775-80. Epub 2007/03/09.

402. Zippelius A, Batard P, Rubio-Godoy V, Bioley G, Lienard D, Lejeune F, et al. Effector function of human tumor-specific CD8 T cells in melanoma lesions: a state of local functional tolerance. Cancer research. 2004;64(8):2865-73. Epub 2004/04/17.